DESIGN, SYNTHESIS, AND CHARACTERIZATION OF MELANOCORTIN RECEPTOR LIGANDS

By

JERRY RYAN HOLDER

A DISSERTATION PRESENTED TO THE GRADUATE SCHOOL
OF THE UNIVERSITY OF FLORIDA IN PARTIAL FULFILLMENT
OF THE REQUIREMENTS FOR THE DEGREE OF
DOCTOR OF PHILOSOPHY

UNIVERSITY OF FLORIDA

2003

ACKNOWLEDGMENTS

It goes without saying that my graduate career, in particular this dissertation, would not have been possible without the contributions of many people. The first and foremost person deserving recognition is my research advisor Dr. Carrie Haskell-Luevano. The opportunity of working side-by-side with Dr. Haskell-Luevano has afforded me a relationship between student and mentor that is normally not readily available. I am forever thankful for her advice, support, and for instilling in me many of her great scientific qualities. I am also thankful to the remaining members of my research committee, Drs. Kenneth B. Sloan, Margaret O. James, Dong-Hai Wu, and Arthur S. Edison, for their patience, advice and guidance. I would like to give additional thanks to Dr. Arthur Edison, for without his gracious contributions to the project the NMR and molecular dynamics portion of this dissertation surely would not have developed. I owe a great deal of gratitude to Mr. James Rocca for his extensive technical assistance in the acquisition and analysis of NMR data. I would also like to acknowledge all of the members of the Haskell-Luevano lab group, both past and present, for the friendship and support they have given me. I especially am grateful to Rayna M. Bauzo, Dr. Zhimin Xiang, and Joseph Scott for performing the enormous amount of bioassays that were required to make the SAR project successful. I also need to acknowledge all of my close and dear friends, you know who you are, whose humor and encouragement have always been a means of support. I definitely have to thank my parents for all of their love and support throughout these many years of being a student. I also give thanks to my sister,

Maryann, who has been in Iraq for such a long time fighting for this great country. I am also grateful to the newest additions to my family, my in-laws, who have always provided support and kindness. Finally, I will always be grateful to my wife and best friend, Carmen, for being an unwavering source of love and support over the last 4.5 years and especially for the restraint and patience she has shown over the past few months of dissertation writing, defense preparation, and job interviewing. This dissertation has been supported by NIH Grant RO1-DK57080.

TABLE OF CONTENTS

APPENDIX

LIST OF TABLES

LIST OF FIGURES

ABBREVIATIONS

Aaa	aminoadipic acid
ACTH	adrenocorticotropic hormone
AGRP	agouti related protein
Anc	3-Amino-naphthalene-2-carboxylic acid
Atc	2-Amino-1,2,3,4-tetrahydro-naphthalene-2-carboxylic acid
Bal	3-benzothienylalanine
Bip	biphenylalanine
Boc	t-butyloxycarbonyl
Bom	benzyloxymethyl ethers
BOP	benzotriazole-1-yl-oxy-tris-(dimethylamino)-phosphonium hexafluorophosphate
cAMP	cyclic adenosine monophosphate
Cit	cituline
Dab	2,4-diaminobutyric acid
DCC	dicyclohexylcarbodiimide
DCM	dichloromethane
DIC	diisopropylcarbodiimide
DIEA	diisopropylethylamine
Dip	diphenylalanine
DMF	dimethylformamide
Fmoc	9-fluorenylmethoxycarbonyl
For	formyl
GPCR	G-protein coupled receptor
HBTU	2-(1-H-Benzotriazol-1-yl)-1,1,3,3-tetramethyluronium hexafluorophosphate
HF	hydrofluoric acid
HOAc	acetic acid
HOBt	1-hydroxybenzotriazole
MBHA resin	methylbenzhydrylamine
MCR	melanocortin receptor
MeOH	methanol
MSH	melanocyte stimulating hormone
Nal	naphthylalanine
Nle	norleucine
NMR	nuclear magnetic resonance
NPY	neuropeptide Y
OFm	9-fluorenylmethyl ester
Orn	ornithine

Pbf	2,2,4,6,7-pentamethyldihydro-benzofuran-5-sulfonyl
Phg	phenylglycine
(pI)DPhe	para-iodo-D-phenylalanine
POMC	proopiomelanocortin
PYY	peptide YY
RP-HPLC	high performance liquid chromatography
tBu	t-butyl
TFA	trifluoroacetic acid
Thi	2-thienylalanine
Tic	1,2,3,4-tetrahydroisoquinoline-3-carboxylic acid
Tis	triisopropylsilane
Tos	tosyl or para-toluenesulfonate
Trt	trityl
3Pal	3-pyridinylalanine
4Pal	4-pyridinylalanine

Abstract of Dissertation Presented to the Graduate School
of the University of Florida in Partial Fulfillment of the
Requirements for the Degree of Doctor of Philosophy

DESIGN, SYNTHESIS, AND CHARACTERIZATION OF MELANOCORTIN RECEPTOR LIGANDS

By

Jerry Ryan Holder

December 2003

Chair: Carrie Haskell-Luevano
Major Department: Medicinal Chemistry

In the United States the prevalence of obesity has risen at an epidemic rate over the past decade. Currently more than 44 million American adults are considered obese by Body Mass Index (BMI), that is, have a (Kg/m^2) greater ≥30. Although still viewed more as a cosmetic rather than a health issue by the general public, there are a variety of health problems directly associated with being overweight and obese. Successful treatment of obesity and obesity related diseases dictates that the complex pathways involved in weight homeostasis and feeding behavior must be understood.

Remarkable new insights into the mechanisms that control body weight are providing an increasingly detailed framework for a better understanding of obesity pathogenesis. Over the last ten years compelling genetic and pharmacological evidence has emerged that supports a role of the melanocortin (MC) receptor system in weight homeostasis. The current data suggest that central MC3 and MC4 receptors, along with

their endogenous agonists and antagonist, are key components responsible for the regulation of body weight via the modulation of both food intake and energy expenditure.

The melanocortin agonists contain the conserved "His-Phe-Arg-Trp" tetrapeptidyl sequence that has been attributed to melanocortin receptor selectivity and functional activity. To better understand the types of molecular interactions that occur between melanocortin ligands and receptors, we have carried out an extensive set of structure-activity relationship (SAR) studies and conformational analyses of several melanocortin peptides. We have designed and synthesized a tetrapeptide library based on the Ac-His-DPhe-Arg-Trp-NH_2 template consisting of 75 members modified at each amino acid position. Each peptide was pharmacologically characterized for functional activity at the mouse melanocortin MC1, MC3-MC5 receptors. A set of NMR measurements and molecular modeling studies was carried out to delineate the structural features that mediate the biological properties of a series of five cyclic melanocortin ligands, each with variations in mouse MC4 receptor functional activity. The results of these studies include the identification of several key structure-activity trends, receptor subtype selectivity properties, conformational properties, and novel ligands with highly desirable pharmacological activities. The details of these studies are discussed in this dissertation.

CHAPTER 1
INTRODUCTION

The Obesity Epidemic

In the United States the prevalence of obesity has risen at an epidemic rate over the past decade.[1-4] Currently, more than 44 million American adults are considered obese by Body Mass Index (BMI), that is, have a (Kg/m^2) greater ≥30. This reflects an increase of 74% since 1991. Recent studies by the Centers for Disease Control and Prevention (CDC) and the National Health and Nutrition Examination Survey (NHANES) have estimated that more than 60% of U.S. adults are overweight and 20-30% are considered obese.[1,5] United States obesity trends from 1991 to 2001 are shown in Figure 1-1, illustrating both the high prevalence of obesity and the rate of increase.

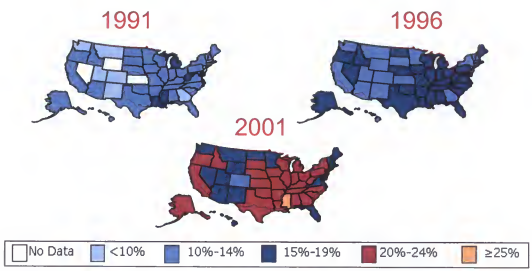

Figure1-1. United States obesity trends by state from 1991 to 2001.[1] Maps are reproduced with permission from the CDC.

The prevalence of overweight children and adolescents has also increased significantly over the last 30 years (Figure 1-2). Childhood obesity can have longstanding

consequences, considering overweight adolescents have a 70% chance of becoming overweight or obese adults.[6] This increases to 80% if one or more parent is overweight or obese.[6] The most immediate consequence of overweight, as perceived by children themselves, is social discrimination associated with poor self-esteem and depression.[7]

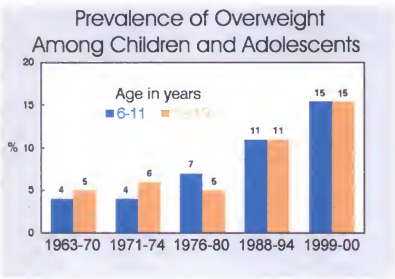

Figure 1-2. Prevalence of Overweight among children (blue) and adolescents (orange) in the United States between 1963 and 2000.[8] Graph reproduced in part with permission from the CDC.

Although still viewed more as a cosmetic rather than a health problem by the general public, excess weight is a major risk factor for a variety of health problems directly associated with excessive weight gain. Diabetes is considered the "twin epidemic" and is a major health concern among the overweight and obese. A recent CDC study found a 61% increase in cases of diagnosed diabetes in Americans from 1991 to 2001, reflecting the strong correlation between obesity and the development of diabetes.[1,2,9] Several recent studies have indicated that many Americans exhibit a cluster of medical conditions that has been termed the "metabolic syndrome," characterized by insulin resistance and the presence of obesity, high levels of abdominal fat, high blood

sugar and triglycerides, high blood cholesterol, and high blood pressure.[10] Overweight and obese individuals are at increased risk for physical ailments such as

- High blood pressure, hypertension
- High blood cholesterol, dyslipidemia
- Type 2 (non-insulin dependent) diabetes
- Insulin resistance, glucose intolerance
- Hyperinsulinemia
- Coronary heart disease
- Angina pectoris
- Congestive heart failure
- Stroke
- Gallstones
- Cholescystitis and cholelithiasis
- Gout
- Osteoarthritis
- Obstructive sleep apnea and respiratory problems
- Some types of cancer (such as endometrial, breast, prostate, and colon)
- Complications of pregnancy
- Poor female reproductive health (such as menstrual irregularities, infertility)
- Bladder control problems (such as stress incontinence)
- Uric acid nephrolithiasis
- Psychological disorders (such as depression, low self esteem)

As the prevalence of overweight and obesity has increased in the United States, so have related health care costs–both direct and indirect. In 1995, the total (direct and indirect) costs attributable to obesity amounted to an estimated $99 billion.[11] In 2000, the total cost of obesity was estimated to be $117 billion ($61 billion direct and $56 billion indirect).[7] Direct health care costs refer to preventive, diagnostic, and treatment services (for example, physician visits, medications, and hospital and nursing home care).[12] Indirect costs are the value of wages lost by people unable to work because of illness or disability, as well as the value of future earnings lost by premature death.

The high prevalence of the obesity metabolic syndrome combined with the enormous socio-economic costs underscores an urgent need to develop comprehensive

efforts directed at controlling the U.S. obesity epidemic. Indeed, one of the national health objectives for the year 2010 is to reduce the prevalence of obesity among adults to less than 15%. However, recent research indicates that the situation is worsening rather than improving. Overweight and obesity are a result of energy imbalance over a long period of time. The cause of energy imbalance for each individual may be due to a combination of several factors. Individual behaviors, environmental factors, and genetics all contribute to the complexity of the obesity epidemic. Successful treatment of obesity and the obesity syndrome dictates that the complex pathways involved in weight homeostasis and feeding behavior must be identified and understood.

Remarkable new insights into the mechanisms that control body weight are providing an increasingly detailed framework for a better understanding of obesity pathogenesis. The central (located in the brain) regulators of food intake and body weight, such as POMC, AGRP, Leptin, Grehlin, PYY and NPY receptors have been identified.[13-21] Key peripheral signals, such as leptin, insulin, and ghrelin, have been linked to these hypothalamic neuropeptide systems, and the networks that integrate these systems have begun to be elucidated.[14]

Over the last ten years compelling genetic and pharmacological evidence has emerged that supports a role of the melanocortin receptor system in weight homeostasis.[22,23] The current data suggest that central MC3 and MC4 receptors, along with their endogenous agonists and antagonist, are key components responsible for the regulation of body weight via the modulation of both food intake and energy expenditure.[23] Below is an overview of the melanocortin system, which includes the known receptors and their endogenous ligands. This is followed by a discussion of the

experimental evidence that warrants further investigations of this important system and justifies the pursuit of the development of melanocortin receptor ligands.

The Melanocortin Receptor System

As mentioned above, the melanocortin system is intricately linked in the complex pathways of feeding behavior and weight homeostasis. The melanocortin receptor family belongs to the G-protein coupled receptor (GPCR) superfamily. The GPCR superfamily is a very large and diverse collection of membrane proteins involved in a vast array of biological activities. It is estimated that 60% of currently marketed drugs target GPCRs.[24] GPCRs are comprised of seven hydrophobic transmembrane spanning regions, three extracellular loop regions, three intracellular loop regions, a periplasmic N-terminal domain and a cytosolic C-terminal domain.[25] GPCRs exert their mechanism of action through a series of events accumulating in communication (signal transduction) across the cellular membrane. These events are believed to consist of molecular recognition of external stimuli, such as neurotransmitters and peptide and protein hormones; binding of stimuli to the receptor; conformation change of the receptor; receptor interaction with a G-protein, followed by either activation or inhibition of a second messenger signal. Compounds that bind to a receptor, referred to as ligands, are said to have affinity to the receptor. Ligands with affinity to a receptor can either initiate a functional response (agonist action) or inhibit functional activity (antagonist action).

The melanocortin receptor family consists of five receptor isoforms identified to date (MC1R-MC5R), named according to the order in which they were discovered.[26-33] The five melanocortin receptors are about 42–67% identical to each other at the amino acid level.[23] Interspecies homology among mammals for each receptor is in the range of 75–94%, with the melanocortin MC4 receptor being the most conserved. When

stimulated the melanocortin receptors activate the cyclic adenosine monophosphate (cAMP) signal transduction pathway. Melanocortin receptor isoforms appear to have developed very early in vertebrate evolution, indicating that these receptors play a vital role in physiological functions.[34] The endogenous agonists for the melanocortin receptors are derived from post-translational modification of the proopiomelanocortin (POMC) gene transcript. Unique to GPCRs, the melanocortin receptors are also regulated by the only two endogenous antagonists of GPCRs identified to date, agouti and agouti related protein (AGRP). Figure 1-3 summarizes the melanocortin receptor system.

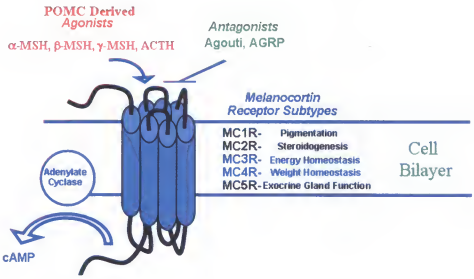

Figure 1-3. Pictorial summary of the melanocortin receptor system.

Melanocortin Receptors

The MC1R is expressed in melanocytes and is involved in skin pigmentation, animal coat coloration, and melanocyte function.[26,27,35,36] Polymorphisms in the MC1R gene have been attributed to the red hair phenotype, melanoma and non-melanoma skin cancer. Due to the association of the MC1R with melanoma, the MC1R may prove to be beneficial in the prevention and treatment of certain forms of skin cancer.[37,38] Melanocytes appear to have additional functions than simply the production of

melanin.[39-48] They are able to secrete a wide range of signal molecules, including cytokines, POMC peptides, catecholamines, and nitric oxide (NO) in response to UV irradiation and other stimuli.[36] The targets for these melanocyte secretory molecules may serve as regulators of a variety of functions yet to be determined. Recently sebocytes isolated from an immortalized human sebaceous cell line were found to express MC1R that modulated interleukin-8 secretion.[49] Bohm *et al.* suggest that MC1 receptors may act as a modulator of inflammatory responses in the pilosebaceous unit.[49] Herpin *et al.* have used a selective small molecule agonist for the MC1R to demonstrate the role of MC1R in modulation of inflammation.[50]

The MC2R, which only responds to stimulation by ACTH, is expressed in the adrenal cortex and adipocytes and is involved in steriodogenesis.[51-54] Recently, the reverse transcription-polymerase chain reaction (RT-PCR) assay has provided evidence that mRNA for the MC2R is expressed in normal and malignant human skin cells, although the function of the receptors has yet to be determined.[55]

The MC3R is found in the brain, heart, placenta and the gut, and in addition to activating the adenylate cyclase pathway, the MC3R may also activate the inositol phospholipid/calcium signal transduction pathway.[31,32,56] Additionally, the MC3R has been shown to induce phosphorylation (activation) of members of the mitogen-activated protein kinase (MAPK) family of transcription factors.[57] Recent studies have implicated the involvement of the MC3R in the complex pathways of energy homeostasis (see discussion below).[58,59]

The MC4R has been detected in the rat and human penis, the rat spinal cord, hypothalamus, brainstem, and pelvic ganglion (major autonomic relay center to the

penis).[60-62] Several lines of evidence support a role for the MC4R in energy and weight homeostasis, although the regulatory pathways of the MC3 and MC4 receptors are believed to be distinct.[58,59,63] Identification of mutations in the MC4R and POMC genes in obese humans provides further support of the involvement of the MC4R in obesity.[64-68] In addition to the participation of the MC4R in weight homeostasis, it appears to be involved in sexual function.[62]

The MC5R has the widest tissue distribution of all the melanocortin receptors.[69] For example, melanocortin MC5 receptor mRNA is detected in fat cells, kidneys, lung, lymph nodes, leukocytes, mammary glands, ovary, pituitary, testis, uterus, stomach, spleen, skeletal muscle, skin, bone marrow, esophagus, and spinal cord.[33,70-72] High levels of the MC5R have been located in exocrine and endocrine glands, including prostate glands, pancreas, adrenal gland, and thymus.[33,70-72] The major function of the MC5R is believed to be involved in thermoregulation, exocrine gland function, and sebaceous gland lipid production.[23,71]

Melanocortin Ligands

The naturally occurring agonists of the melanocortin receptors are derived from posttranslational modification of the proopiomelanocortin (POMC) gene transcript. POMC processing occurs in a tissue specific manner to produce the melanocortin ligands α-, β- and γ- melanocyte-stimulating hormones (α-, β- and γ-MSH) and adrenocorticotropin hormone (ACTH).[23] POMC-derived peptides are among the most abundant neuropeptides in the brain, indicating the peptides are involved in important physiological activities.[22,73,74] The endogenous agonists (Table 1-1) for the melanocortin receptors all contain a central His-Phe-Arg-Trp sequence that has been attributed to

melanocortin receptor selectivity and stimulation.[75-78] Uniquely, the melanocortin receptor system is comprised of both endogenous agonist and antagonists. The melanocortin antagonists, agouti and agouti-related protein (AGRP), are the only two naturally occurring antagonists of GPCRs identified to date.[79-85]

Table 1-1. Endogenous melanocortin agonists

Agonist	Sequence
α-MSH	Ac-SYSME**HFRW**GKPV-NH_2
β-MSH	DEGPYKME**HFRW**GSPPKD
γ-MSH	YVMG**HFRW**DRFG
ACTH	SYSME**HFRW**GKPVGKKRRPVKVYPNGAEDESAEAFPLEF

The endogenous melanocortin agonists derived from post-translational processing of the POMC precursor protein. The core tetrapeptidyl sequence required for activity is shown in boldface.

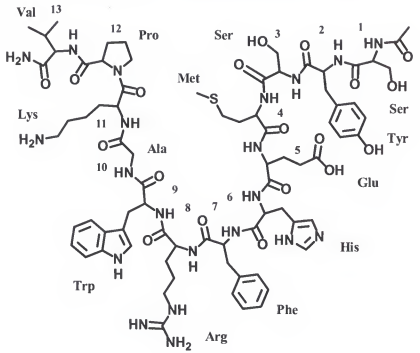

Figure 1-4. Primary chemical strucuture of the endogenous melanocortin agonist α–MSH.

α-MSH is a 13-amino acid peptide (Figure 1-4) that is a non-selective agonist of the MC1R, MC3R-MC5R. This peptide hormone has been studied extensively over the past 50 years, which has led to the identification of many potent synthetic analogues. Table 1-

2 lists the common synthetic melanocortin ligands used to characterize the melanocortin receptors. NDP-MSH, which contains a DPhe substitution at position seven (α-MSH numbering), was one of the first potent and enzymatically stable analogues of α-MSH identified.[86] Although NDP-MSH is a non-selective melanocortin agonist, the iodinated analogue became a very useful ligand for both *in vivo* and *in vitro* characterization of melanocortin receptors. MTII is a highly potent lactam derivative of NDP-MSH.[87] The lactam bridge is believed to hinder conformational flexibility of the non-selective agonist, thereby constricting the peptide in a conformation conducive to high affinity binding to the receptors. Substitution of the DPhe residue of MTII by that of a D-naphthylalanine residue [DNal(2')] resulted in the melanocortin antagonist SHU9119.[88] SHU9119 is a high affinity antagonist for the centrally located MC3R and MC4R, but a high affinity agonist for the MC1R and MC5R. These analogues often referred to as "benchmark" melanocortin ligands, have become the most widely used peptides to characterize the melanocortin receptors.

Table 1-2. Common synthetic melanocortin ligands.

Ligand	Sequence
NDP-MSH	Ac-Ser-Tyr-Ser-**Nle**-Glu-His-**DPhe**-Arg-Trp-Gly-Lys-Pro-Val-NH_2
MTII	Ac-**Nle**-cyclo[Asp-His-**DPhe**-Arg-Trp-Lys]-NH_2
SHU9119	Ac-**Nle**-cyclo[Asp-His-**DNal(2')**-Arg-Trp-Lys]-NH_2

Often referred to as the "benchmark" melanocortin ligands, which have been the most widely used peptides for *in vitro* and *in vivo* characterization of the melanocortin receptor system. Unusual amino acids are shown in boldface.

The Melanocortin System and Body Weight Regulation

A remarkable surge of information on the melanocortin receptors has emerged since the receptor genes were first identified just over ten years ago. This receptor system is now believed to be involved in a wide range of systems, such as pigmentation, coat

coloration, sexual behavior and weight regulation. The role of the melanocortins in weight regulation has received much attention recently due to the therapeutic potential in treatment of obesity and cachexia. Several lines of evidence discussed below converge to indicate that the central melanocortin system, particularly the MC4R, plays a significant role in regulating body weight.

Genetic Evidence

Some of the first genetic evidence to implicate the melanocortin receptors in the complex pathways of weight homeostasis came from investigations of the obese Agouti mouse.[79] The mouse has atypical yellow coat coloration and is significantly obese. A mutation in the promoter region of the agouti gene results in ectopic expression of the agouti protein, the endogenous antagonist of the peripheral MC1R. The yellow coloration of the Agouti mouse has been attributed to antagonism of the MC1R and the obesity attributed to chronic antagonism of the central MC4R.[89,90] A protein similar to agouti, the agouti related protein (AGRP), was latter identified to be an endogenous antagonist of the MC3R and MC4R.[81,83] Mice that were genetically altered to overexpress AGRP developed an obesity syndrome quite similar to the Agouti mouse, without the yellow phenotype.[83] Additional evidence comes from knock-out mice that have either of the central melanocortin receptors removed from their genome. Deletion of the MC4R resulted in a mouse that develops a maturity onset obesity syndrome associated with hyperphagia and type-2 diabetes, similar to the Agouti mouse.[63] Removal of the MC3R gene from the mouse genome resulted in mice with increased fat mass, reduced lean mass and higher feed efficiency than wild-type littermates, despite being hypophagic.[58,59] Identification of mutations in the MC4R and POMC genes in obese humans provides further support for the involvement of the MC4R in obesity.[64-68]

Pharmacological Evidence

In addition to the genetic evidence discussed above, several studies provide pharmacological data to suggest a role of the MC4R, and possibly the MC3R, in energy and weight homeostasis. These studies have utilized various melanocortin ligands to regulate feeding behavior in rodents. Intracerebroventricular (i.c.v.) infusion of the MC3R/MC4R antagonist AGRP increases food intake for a surprisingly long time period.[91,92] Similar results were seen when the synthetic MC3R/MC4R antagonist SHU9119 was administered via i.c.v injection.[90] Conversely to the administration of melanocortin antagonists, the non-selective melanocortin agonist MTII inhibited feeding in wildtype mice, as well as four rodent models of hyperphagia.[90]

The pharmacological and genetic evidence detailed above supports a role of the central MC3 and MC4 receptors in energy and weight homeostasis; thus the receptors have become viable targets for the therapeutic treatment of obesity and related diseases.[23] Identification of potent and selective melanocortin ligands and understanding their structural and conformational characteristics have become focal points of many academic and industrial laboratories. The research presented in this dissertation details our efforts in the design, syntheses, and characterization of melanocortin receptor ligands. There are two main aspects of the work presented herein. The first aspect, presented in chapter 3, details the structure-activity relationship (SAR) studies of a series of 75 analogues based on the His-Phe-Arg-Trp tetrapeptidyl sequence. The His-Phe-Arg-Trp sequence represents the common pharmacophore of all endogenous melanocortin agonists at the MC1R, MC3R-MC5R. We hypothesized that pharmacological characterization of a set of carefully designed analogues based on this sequence could provide useful information for the future development of melanocortin ligands with improved properties. The aim of the

SAR studies presented in chapter 3 was to identify trends that result in an increase or decrease in potency; receptor subtype selectivity; and novel pharmacology at the melanocortin receptors. The second aspect of the dissertation is presented in chapter 4. Chapter 4 herein describes the conformational analysis of a set of five cyclic melanocortin ligands. The ligands are 23 membered peptides based on the melanocortin His-Phe-Arg-Trp tetrapeptidyl pharmacophore described above. Although the five ligands are all similar in primary chemical structure, subtle modifications of only the Phe^7 residue result in significant modulation of activity at the MC4R. It was hypothesized that structural differences exist between the ligands that may be responsible for the variations in MC4R functional activity. The aim of the study presented in chapter 4 of this dissertation was to identify conformational characteristics that can be attributed to the observed MC4R pharmacology.

CHAPTER 2
GENERAL METHODOLOGIES

Solid-Phase Peptide Synthesis

The field of peptide chemistry was revolutionized in 1963 from a publication by R.B. Merrifield.[93] The article described the total synthesis of a tetrapeptide carried out completely while tethered to an insoluble polymeric support. Merrifield had developed a method to attach the C-terminal amino acid of a target peptide to a solid support and then elongate the peptide chain with successive condensation reactions. Although the original synthesis led to several byproducts, improvements on the synthetic scheme quickly followed that allowed for the synthesis of a nine residue peptide in yields and purity far greater than what could be accomplished with solution chemistry.[94-96] Merrifield's method was significantly different than the conventional strategies of peptide synthesis that utilized traditional solution-phase methods. Solution-phase peptide syntheses were time consuming and usually required extensive expertise. The solid-phase approach eliminated the exhaustive isolation, purification, and characterization steps required for each step in solution chemistry. Since the peptide is extended on the solid support, isolation of intermediates is not required and purification between steps is simply accomplished by washing and filtration of the support. Eliminating these steps enhanced both the speed of synthesis and purity that could be achieved, as compared to traditional methods.

The solid-phase synthetic strategy is illustrated in Figure 2-1. The N-termini of amino acids are protected with a "temporary" group that is removed prior to addition of

the next amino acid. Reactive side chain functionalities are blocked with "permanent" protecting groups that are normally not removed until the synthesis is complete.

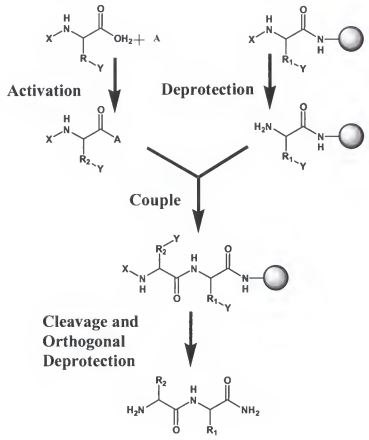

Figure 2-1. The solid-phase peptide synthesis principle. A=carboxy activating agent, X=temporary N-terminal protection group, Y=permanent side chain protection group.

The C-terminal of the amino acid is primed for condensation by activation with a suitable coupling reagent. The first step is attachment of the C-terminal amino acid in the peptide sequence to the polymeric support (referred to as *resin*). Amino acids are generally introduced in excessive concentrations to insure the reaction is driven to completion, which is one of the key characteristics of solid phase synthesis. Once attached to the resin, the reagents and excess amino acid are simply removed by successive filtration and washing steps. Following attachment and washing, the

temporary N-terminal protecting group is removed and introduction of the next amino acid is ready to proceed. The next amino acid is introduced and coupled to the preceding amino acid via amide bond formation. The temporary N-terminal protecting group is removed and the cycle is ready to be repeated with the next amino acid. Once the desired length is reached, the peptide is liberated from the solid support by cleavage of the linker and the permanent orthogonal protecting groups are removed. The process of cleavage and deprotection is normally completed in one step.

The Merrifield Synthetic Strategy

The method of solid-phase peptide synthesis originally developed by Merrifield is still used today in many laboratories across the globe with little modification. The synthetic strategy makes use of amino acids protected primarily with *t*-butyl and benzyl derivatives. Figure 2-2 illustrates the Merrifield synthetic strategy. N-terminal *t*-butyl groups are used for temporary protection and are selectively removed prior to each amino acid coupling cycle. Benzyl-based groups are used for more permanent protection of reactive amino acid side chains and are removed when synthesis of the desired peptide oligomer is complete.

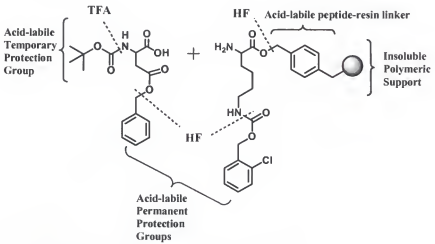

Figure 2-2. The Merrifield solid-phase synthetic strategy.

The most common *t*-butyl protecting moiety used in this strategy is *t*-butyloxycarbonyl (Boc) group, which has led to the Merrifield approach often being referred to as "Boc peptide synthesis." The Boc group is selectively removed from the N-terminus under relatively strong acidic conditions, typically using trifluoroacetic acid (TFA) solutions. Once the Boc group is removed the protonated amino terminus remains as a trifluoroacetate salt that must be neutralized, typically with a tertiary amine such as diisopropylethylamine (DIEA), before condensation with the next amino acid can proceed. A possible mechanism of Boc removal is shown in Figure 2-3 below.

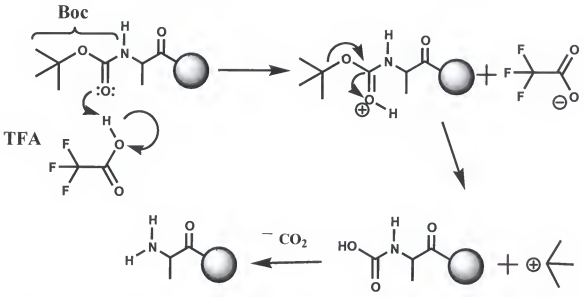

Figure 2-3. Possible mechanism for removal of the acid-labile butyloxycarbonyl (BOC) amino protection group from resin-bound alanine.

Extension of the peptide chain is achieved by introduction of the next protected amino acid with the carboxyl terminus "activated" (see **Coupling Methods** below). Very strong acidic conditions, such as liquid hydrogen fluoride (HF), are required to remove the "permanent" orthogonal protecting groups from reactive amino acid side chains and to liberate the peptide from the solid support. These two steps are typically done simultaneously. The mechanism of deprotection of the reactive side chains precludes the

production of reactive products, often of cationic nature, that can react with the peptide generating unwanted side products. Electron-rich functional groups are particularly prone to modification by the cationic species. This dictates that the appropriate "scavenger" be incorporated into the cleavage solution to quench the reactive intermediates generated in the orthogonal deprotection/cleavage step. Scavengers are nucleophilic reagents such as water, thiols, and silanes. Due to the nature of HF, extreme caution and special equipment must be used during the orthogonal deprotection and cleavage steps of the Merrifield strategy.

Fmoc Synthetic Strategy

Although the Merrifield strategy has significantly increased the speed and purity that can be achieved in peptide synthesis, the method does have shortcomings. Both N^{α} and orthogonal protecting groups are acid labile, resulting in an inherent loss of orthogonal moieties during Boc removal using acids such as TFA. This loss generates two sources of reactive functionalities, the amino acid side chain and the reactive orthogonal protection group, thereby providing a means for side reactions to occur. Some loss of the peptide can be anticipated due to the acid lability of the linker, thus slightly decreasing the yield during each N^{α}-deprotection step. Additionaly, not all sequences are stable to the harsh acidic conditions used during HF cleavage and orthogonal deprotection. As a result of the above stated drawbacks to the Merrifield strategy, several solid phase peptide synthetic methodologies have been developed that utilize milder reaction conditions and do not require special equipment.

The most successful alternative to the Merrifield technique has been the 9-fluorenylmethoxycarbonyl (Fmoc) strategy (Figure 2-4).[97,98] The Fmoc method relies on

the base-labile Fmoc group for temporary N^{α} protection, acid-labile protecting groups for reactive side chains, and acid-labile linkers. Since there is such a large difference between the mechanism of Fmoc removal and that of orthogonal deprotection, much milder reaction conditions can be employed. The large difference also means that Fmoc removal is virtually 100% selective versus side chain deprotection. Additionally, since the linker is acid labile, repeated exposure to basic solutions does not result in loss of peptide from the resin due to premature cleavage.

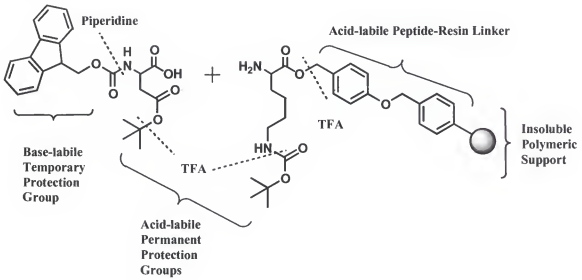

Figure 2-4. The Fmoc solid-phase synthetic strategy

Typically the Fmoc group is removed under basic conditions, such as 20% piperidine in dimethylformamide (DMF). A possible mechanism of Fmoc removal is shown in Figure 2-5. The side chain protecting groups and linker to the polymeric support are generally cleaved together in one step with a TFA solution. Much like the global deprotection and cleavage step in the Merrifield strategy, reactive products are produced at this stage of the Fmoc method, and thus the appropriate scavengers must be utilized to prevent unwanted side reactions.

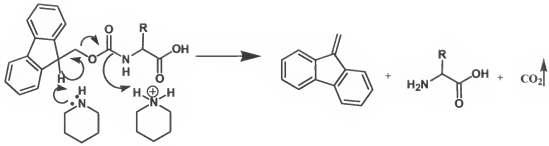

Figure 2-5. Possible mechanism for base-catylized removal of the N-terminal Fmoc protection group.

Coupling Methods

One of the fundamental steps in peptide synthesis is the condensation of two amino acids resulting in amide bond formation. The coupling reaction is accomplished by suitable activation of the carboxyl group of the incoming amino acid and reaction with the free amino portion of the resin bound amino acid. The coupling reaction must be robust and efficient so that the reaction proceeds as close to 100% completion as possible. This requirement necessitates that the activated species be highly reactive. The vast majority of amino acids have a chiral center at the α–carbon, therefore coupling reactions must also proceed with minimal loss of stereostructural integrity. A balance between reactivity and minimal racemization is often difficult to accomplish. The difficulty arises because highly reactive species often have good leaving groups that can increase the acidity of the α–proton. This increase in acidity can have detrimental effects on the chirality of activated amino acids.[99] Figure 2-6 illustrates two possible mechanisms of racemization of activated amino acids.

Presently there are two ways to obtain activated amino acids:1) *in situ* activation of a target amino acid by reaction with suitable activating (coupling) reagent; or 2) using pre-formed activated amino acids (many of which are commercially available). The following sections concentrate on the former and describe the most common methods

used for *in situ* activation. The most widely accepted methods for activation employ either carbodiimides or onium salts.[99]

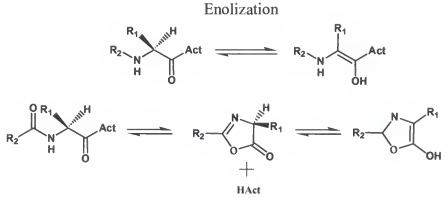

Figure 2-6. Possible mechanisms of racemization of activated amino acids.

Carbodiimides

Carbodiimide activation was the method of choice in the original solid-phase strategies developed by Merrifield, and until recently were the most widely accepted coupling reagents. The two most common carbodiimides N,N-dicyclohexylcarbodiimide (DCC) and N,N-diisopropylcarbodiimide (DIC) are shown in Figure 2-7.[99]

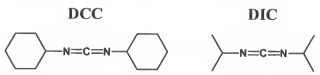

Figure 2-7. Structures of two widely used carbodiimides.

The mechanism of carbodiimide activation is highly solvent dependent and can lead to a variety of active species. Figure 2-8 shows possible mechanisms of carbodiimide activation. Since the first step in the mechanism is protonation of the carbodiimide, addition of a base prior to amino acid activation should be avoided.

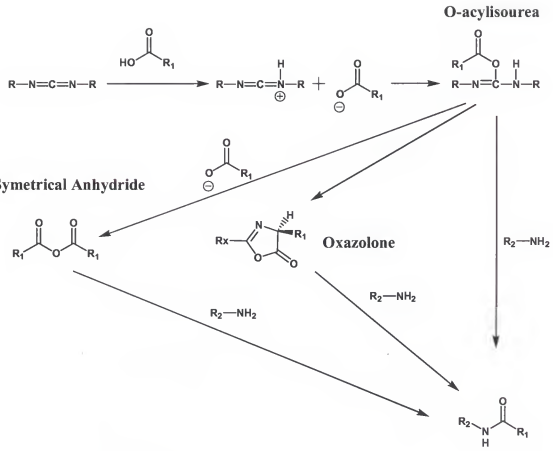

Figure 2-8. Possible mechanisms of amide bond formation via carbodiimide activation.

As illustrated in Figure 2-8, the use of carbodiimides can lead to the formation of O-acylisoureas, symmetrical anhydrides, and 5(4H)-oxazolones (if the amino acid is a N-carboxamide).[99] Each of these possible intermediates are reactive, and thus each can lead to amide bond formation. Oxazolone formation increases the possibility of racemization (see Figure 2-6 above), thereby increasing the possibility of unwanted side products. Oxalone formation can be minimized by addition of a less reactive nucleophile, such as a 1-hydroxybenzotriazole (HOBt), which generates an active ester derivative.[99] Active esters are less reactive than O-acylisoureas, but are far more stable intermediates and significantly reduce the risk of racemization (see below).

Solvents can significantly affect the mechanism of carbodiimide activation and should be carefully selected. For example, it has been shown that only the highly reactive intermediate O-acylisourea is formed when dichloromethane (DCM) is used as the solvent and is stable for hours in the absence of nucleophiles.[100] However when the polar solvent N,N-dimethylformamide (DMF) is used, several intermediates (shown in Figure 2-8) can be detected.[101]

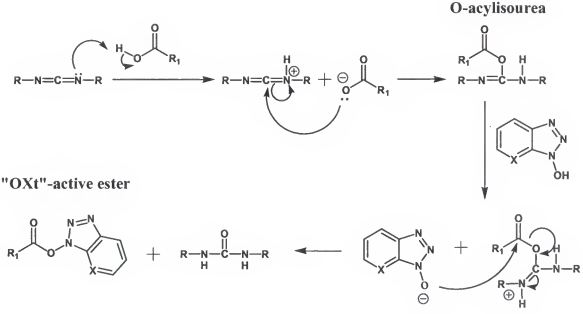

Figure 2-9. A possible mechanism of active ester formation using carbodiimides and hydroxybenzotriazoles. HOBt, X=CH. HOAt, X=N.

When DMF is the solvent, one equivalent of a hydroxylamine should be added to solution so that an active ester is obtained. O-acylisoureas are highly reactive and react readily upon addition of nucleophiles such as hydroxylamines. Figure 2-9 illustrates a possible mechanism of active ester formation using a carbodiimide and either one of the two commonly used hydroxybenzotriazoles, HOBt (X=CH) or 1-hydroxy-7-azabenzotriazole (HOAt, X=N). The esters formed from addition of either HOBt or HOAt are less reactive than O-acylisoureas, however they are more stable and thus can

be stored for short durations during the synthesis. Addition of an equivalent of hydroxylamine serves to concentrate the active ester and reduce the formation of other intermediates, such as oxazolones, thus reducing the possibility of racemization. Once the active ester is added to the peptide-resin, one equivalent of a hindered base such as diisopropylethylamine (DIEA) can be added to accelerate the coupling reaction.[102]

Onium salts

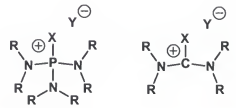

Phosphonium **Aminium**

Figure 2-10. General structure of phosphonium and aminium salts.

Recently phosphonium and aminium salts, generically referred to as "onium" salts (Figure 2-10), have found widespread use in solid-phase peptide synthesis.[99] Common onium salts are listed in Table 2-1 along with their representative structures.

Table 2-1. Common aminium and phosponium coupling reagents.

Name	Abbreviation	Structure
Benzotriazol-l-yl-N-oxy-tris(dimethylamino)phosphonium hexafluorophosphate	BOP	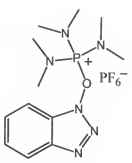

Table 2-1. Continued

Name	Abbreviation	Structure
Benzotriazol-1-yl-N-oxy-tris(pyrrolidino)phosphonium hexafluorophosphate	PyBOP	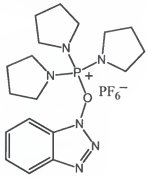
(7-Azabenzotriazol-1-yloxy)-tris(dimethylamino)phosphonium hexafluorophosphate	AOP	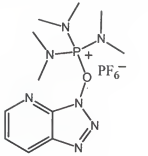
(7-Azabenzotriazol-1-yloxy)-tris(pyrrolidino)phosphonium hexafluorophosphate	PyAOP	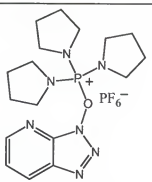
N-[1H-Benzotriazole-1-yl)(dimethylamino)methylene]-N-methylmethanaminium hexafluorphosphate N-oxide	HBTU	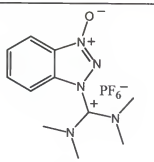

Table 2-1. Continued

Name	Abbreviation	Structure
N-[(Dimethylamino)-lH-l,2,3-triazolo[4,5]pyridino-l-ylmethylene]-N-methylmethanaminium hexafluorphosphate N-oxide	HATU	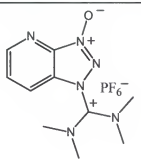
N-[1H-Benzotriazole-1-yl)(dimethylamino)methylene]-N-methylmethanaminium tetrafluoroborate N-oxide	TBTU	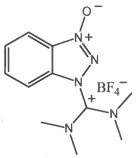
N-[(Dimethylamino)-lH-l,2,3-triazolo[4,5]pyridino-l-ylmethylene]-N-methylmethanaminium tetrafluoroborate N-oxide	TATU	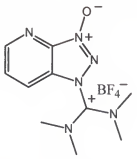

The exact mechanism of phosphonium activation is currently not known, but it is postulated that the mechanism proceeds through a highly reactive acyloxyphosphonium salt to form either an active ester or a symmetrical anhydride.[103-108] The mechanism of aminium activation is believed to proceed through an acyloxy-guanidino intermediate that reacts immediately with the hydroxybenzotriazole base present in the reaction medium. The possible mechanism of aminium salt activation is shown in Figure 2-11A. Aminium reagents can lead to N-terminal guanidino derivatives, and thus terminate chain

elongation (Figure 2-11B). Due to the possibility of guanidation, pre-activation with 0.9 equivalents of aminium reagents per amino acid prior to addition to the peptide-resin is optimal to suppress the unwanted side reaction.[109]

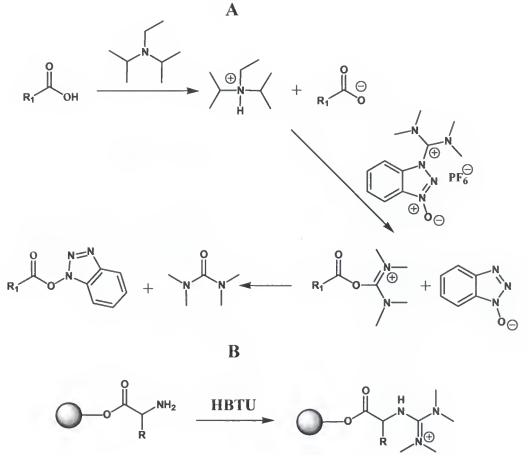

Figure 2-11. Amino acid activiation with the aminium salt coupling reagent HBTU. A) Possible mechanism of active-ester formation; and B) N-terminal guanidation side reaction resulting in peptide chain termination.

Monitoring procedures

It is often convenient to monitor the progression of the coupling reaction, especially during manual synthesis. It should be noted that for short to medium length sequences (approximately 15 residues) the following methods provide a reliable means of monitoring coupling reactions, however the results can be misleading for longer peptide sequences.[99]

The most widely used method of monitoring the coupling reaction is the Kaiser (ninhydrin) test.[110] The method provides a fast and convenient colorimetric test for the detection of free amines. Ninhydrin reacts with free amines to produce the dye Ruhemann's purple, which is readily visible to the naked eye (see Figure 2-14 below). The mechanism of Ruhemann's purple formation is shown in Figure 2-12. The Kaiser test can be adapted for use in both qualitative and quantitative analyses.[111]

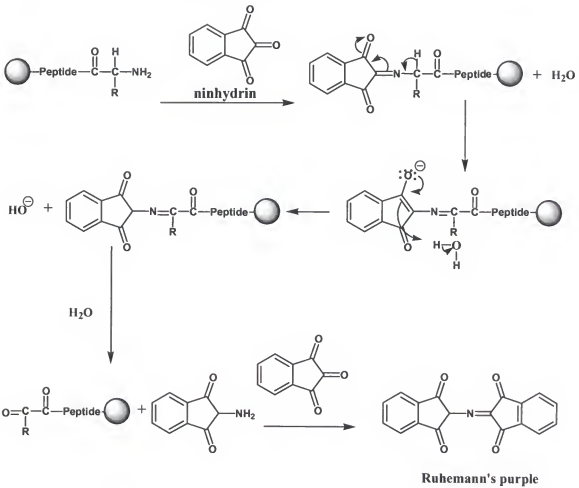

Figure 2-12. Possible mechanism of Ruhemann's purple formation using Kaiser's reagent to monitor the progression peptide synthesis.

Secondary amines, such as proline, do not produce the typical colorimetric response during the Kaiser test, therefore alternative methods must be employed when monitoring proline and other secondary amino acids. The chloranil test is another rapid

and convenient color test that can be used to detect both primary and secondary amines.[112] Chloranil (2,3,5,6-tetrachloro-1,4-benzoquinone) reacts with primary and secondary amines to form the green-blue 2,3,5-Trichloro-6-(2-pyrrolidinyl-vinyl)-[1,4]benzoquinone derivative (Figure 2-13). Since the benzoquinone derivative produces a greenish color visible to the naked eye, the chloranil test provides a rapid test for the presence of secondary amines (Figure 2-14).

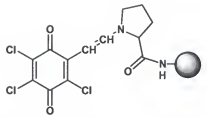

Figure 2-13. Chloranil reacts with the secondary amino acid proline to produce the blue-green benzoquinone derivative. This colorimetric response provides a rapid method to monitor the presence of secondary amines.

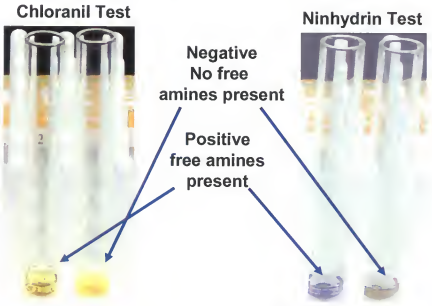

Figure 2-14. The two colorimetric assays used to monitor peptide synthesis. A positive response (color formation) indicates the presence of free amino-termini.

Purification and analysis

Following the cleavage and orthogonal deprotection steps, the crude peptide is generally precipitated by addition of cold (4°C) ethyl ether. Following precipitation, the peptide can be filtered over a course glass frit and washed with additional cold ether to improve purity. The precipitated peptide can then either be extracted (often with neat acetic acid or acidic aqueous solutions) and lyophilized, or simply dried *in vacuo* prior to purification.

Peptide quality is routinely analyzed by using analytical high performance reversed-phase liquid chromatography (RP-HPLC) to access purity and mass spectral analysis to assure the correct molecular weight. The majority of crude peptides can purified to homogeneity with relative ease using semi-preparative HPLC with the appropriate solvent system.

Analytical analysis of the purified sample is accomplished by either analytical HPLC in two diverse solvent systems or thin layer chromatography (TLC) in three solvent systems. Elemental and amino acid analysis can also provide further detail of peptide content. Additionally, data from ^{1}H-NMR can provide reliable information regarding structural integrity.

Nuclear Magnetic Resonance

Nuclear magnetic resonance (NMR) was initially developed by physicists to study the various states of matter, but the technique has made the most profound influence on the field of chemistry. Indeed, organic chemist quickly realized the applicability and power of using NMR as a tool in organic structure analysis. Today NMR has become one of the most widely accepted means of analytical characterization of organic compounds. Moreover, NMR has significantly enhanced the study of biological molecules such as

peptides, proteins, and nucleic acids.[113] The first publication to reveal the potential of NMR in the field of protein research was in 1957 with the NMR spectrum of ribonuclease.[114] Inadequate instrumentation and lack of homogenous samples initially hindered the progress of NMR analysis of peptides and proteins, however, NMR is now considered one of the principle methods to examine the structural properties of biological macromolecules.[113] NMR is often complementary to X-ray crystallography as a method of structure determination of biological macromolecules, although NMR examination is in solution rather than in crystalline form. Additional information can be gained from NMR analysis versus X-ray crystallography since experimental conditions, such as temperature and pH, can easily be manipulated in solution. Additionally, NMR is unique in that direct and quantitative dynamical information can be obtained for biological macromolecules over a large timescale.

Basics of the NMR Phenomenon

The basis for the NMR phenomenon is the property called nuclear spin.[115] Atomic nuclei are comprised of protons and neutrons and are associated with a charge, and thus a spin state. Protons, neutrons, and electrons possess a spin of ½, each with two possible spin orientations. Another important property of nuclei with spin is *spin angular momentum*, ω. A magnetic dipole is generated as a result of ω and the magnitude of this dipole is the property of *nuclear magnetic moment*, μ. When particles with spin are paired the magnetic moments cancel and there is no bulk magnetization, therefore only nuclei with unpaired spins, such as ^{1}H, ^{13}C, ^{15}N, and ^{19}F, can by observed by NMR. The ratio of *nuclear magnetic moment* to the *spin angular momentum* is called the gyromagnetic ratio (γ).

$$\gamma = \mu/\omega$$

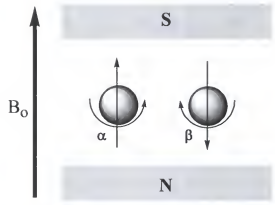

Figure 2-15. The spin states important in the NMR phenomenon.

When nuclei that have a nuclear magnetic moment are placed into an externally applied static magnetic field (B_o) the spins behave like tiny magnets and will orient themselves either parallel (α state) or antiparallel (β state) to the magnetic field (Figure 2-15). The α state is slightly lower in energy than the β state and thus is slightly more populated. The spinning nuclei align with B_o and there is bulk magnetization parallel to B_o. The rotational axis of the spinning nuclei begin to precess with a frequency υ_o (Figure 2-16). This is often referred to as the Lamor frequency, which can be related to γ and B_o by the equation $\upsilon_o=\gamma B_o$.

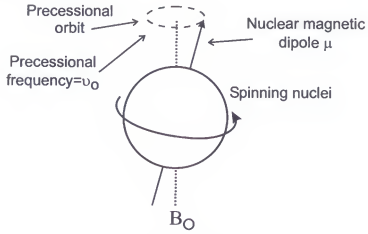

Figure 2-16. Behavior of nuclei with spin in a homogeneous magnetic field B_o.

If an additional external magnetic field (B_1) is applied perpendicular to B_o at the exact frequency as υ_o the spinning nuclei can absorb a photon. When the frequency of B_1 is equal to υ_o this is referred to as "on resonance" and is where the term nuclear magnetic resonance originates. When resonance occurs a photon can be absorbed and transitions from the α to β spin states can occur. In NMR experiments, the photon is in the radio frequency range. The energy difference between the two states can be related by

$$\Delta E = h\upsilon_o$$

where h is Planck's constant (6.626×10^{-34} J s). This energy difference is the basis for the NMR phenomenon and is illustrated in Figure 2-17.

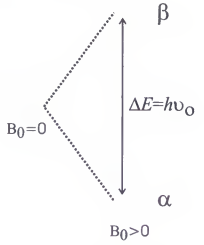

Figure 2-17. The two energy states of a spin ½ nuclei (i.e. proton, electron or ^{13}C) and the relationships between ΔE, Lamor frequency υ_o, and the external magnetic field B_o.

The NMR phenomenon is observed at the resonance frequency (υ_o) required for the transitions to take place. As previously mentioned, when nuclei with spin are placed into B_o there is bulk magnetization (M_o) parallel to B_o, illustrated in Figure 2-18A (the Z axis). When B_1 is applied perpendicular to B_o the magnetization vector is tipped into the X-Y plane to a new value M. The transverse magnetization M then precesses in the X-Y plane at a frequency equal to υ_o (Figure 2-18B). The magnetization in the X-Y plane produces a

new non-zero magnetization component in the X-Y plane which did not exist before $B1$ was applied, which can be recorded by a detection coil. The transverse magnetization M decays over time and the decay is recorded by the detection coils. The motion of the transverse magnetization vector can be described by the Bloch equations.[116] The recorded magnetization is then Fourier transformed (FT) to produce the frequency spectrum.

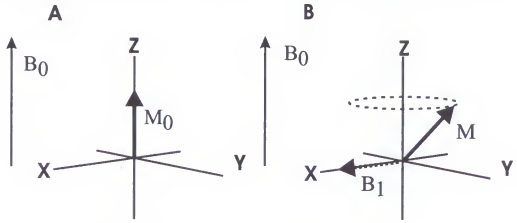

Figure 2-18. The behavior of nuclei with spin in a homogeneous magnetic field (B_o). A) At equilibrium, the net magnetization vector lies along the direction of the applied magnetic field B_o. B) The net magnetization is tipped in the X-Y plane by an external electromagnetic field B_1 applied perpendicular to B_o. The new magnetization vector M now precesses about the Z axis at a frequency equal to the frequency of the photon (υ_o)which would cause a transition between the two energy levels of the spin and produces a new non-zero magnetization component in the X-Y plane which did not exist before B_1 was applied.

Since nuclei are charged and have spin they generate there own nuclear magnetic fields. This magnetic field will affect the observed B_o at the nuclei and thus will dictate the υ_o. The nuclear magnetic field will also affect the observed B_o of other nuclei in close proximity and thus change their υ_o. Because υ_o is not the same for nuclei in different magnetic environments, the frequency of B_1 required for the transition between energy levels will also be slightly different. This frequency difference, required for the transition from α to β spin states, is the origin of the chemical shift and the underlying basis for NMR analysis.

Two-Dimensional (2D) NMR

Information obtained from 1D-NMR data is often limited and may not provide enough detail for complete structural analysis, especially when studying large and complex macromolecules. Due to the limitations of 1D-NMR experiments, researchers began to develop multipulse NMR methodologies in the 1980s that would become the foundation of multidimensional NMR.[115,117] Indeed, 2D-NMR experiments have become routine in the examination of molecules such as peptides and proteins. The power of 2D-NMR strategies lies in the ability to determine covalent connectivities (using correlation spectroscopy) as well as through-space interactions [using nuclear Overhauser enhancement (NOE) spectroscopy]. Typically all resonance assignments can be made for a polypeptide by using a combination of correlation and NOE spectroscopic techniques.[113] Although a detailed mathematical description of the fundamental principles of multidimensional NMR techniques is beyond this discussion, a brief summary of NMR in two dimensions is warranted.

All 2D-NMR experiments comprise the same basic scheme (Figure 2-19):a preparation period, an evolution period (t_1) during which time the spins are labeled according to their chemical shift, a mixing period (τ) during which time the spins are correlated with each other, and finally a detection period (t_2).[117] Multiple experiments are recorded for each sample with incremental values of the evolution time period. The recorded data is Fourier transformed in two dimensions to produce the 2D frequency spectrum. The 1D frequency spectrum is placed along each of the two frequency axes and once as a contour projection along the diagonal in the majority of 2D-NMR spectrum and cross peaks that occur on either side of the diagonal indicate a correlation between nuclei

that have different resonance frequencies. The type of experiment (correlation or NOE spectroscopy) will dictate the nature of the cross peak correlation.

Figure 2-19. Basic scheme of 2D-NMR experiments.

As previously mentioned, complete resonance assignments can be made for polypeptides using a combination of correlation and NOE spectroscopy. For example, 2D Total Correlation Spectroscopy (TOCSY)[118] can be used to determine intraresidue connectivity by three bond ^{1}H-^{1}H *J* couplings and 2D Nuclear Overhauser Enhancement Spectroscopy (NOESY)[119] can be used to determine through space interactions $\leq$5Å (Figure 2-20).

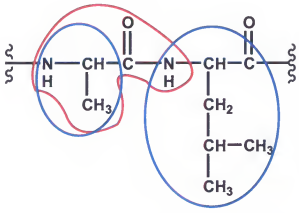

Figure 2-20. Illustration of the types of interactions that can be detected in typical 2D-NMR experiments. Proton interactions detected in a TOCSY experiment are circled in blue. In addition to the protons circled in blue, a NOE experiment will provide a correlation to the protons circled in red.

Cross peaks in a TOCSY spectrum indicate that the nuclei are connected covalently within a residue, and thus allow one to assign the chemical shift of each intraresidue proton. Cross peaks in a NOESY spectrum indicate that the nuclei are within 5Å of each other. Given that amide protons and the preceding αH proton of amino acid residues are within the NOE distance limit of 5Å, a correlation can be made between neighboring

residues. This interresidue correlation provides the information needed to determine sequence specific residue assignments.[113] NOE crosspeaks that are not between neighboring residues indicate that the two nuclei are within a proximity of 5Å of one another in three dimensional space. Sequence specific residue assignments in conjunction with through-space NOE correlations are the basis for structural studies of peptides and proteins. Figure 2-21 illustrates how TOCSY and NOESY spectra can be used to completely assign proton chemical shifts using an alanine-serine dipeptide sequence as an example.

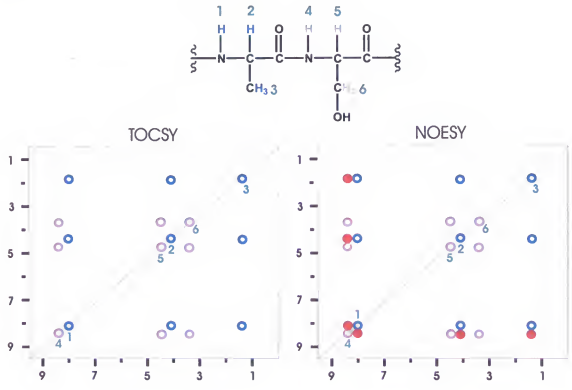

Figure 2-21. Illustration of TOCSY and NOESY spectra for a Ala-Ser sequence.

Protons have been assigned numbers for identification in the spectra. The colored circles along the diagonal represent all of the chemical shifts of the dipeptide. Blue (alanine) and pink (serine) cross peaks in the TOCSY spectrum correlate the protons within

a residue but provide no correlation between residues. The blue and pink cross peaks in the NOESY spectrum also correlate protons within a residue but the red cross peaks provide the correlations between residues and the mechanism for sequential assignments.

Multidimensional NMR techniques have provided us with powerful tools to discern structural characteristics of peptides and proteins. Structural studies have proven to be invaluable in the analysis of protein function and ligand-receptor interactions. The basic principles of structure determination by NMR are summarized in Figure 2-21.[117] Assignment of sequence specific resonances is the first step in the process; followed by using scalar J coupling values, or intraresidue and interresidue NOE data to determine torsional angle restraints; the next step is to use NOE data to assign through-space interactions between protons within 5Å of each other; and the final step is to implement the NMR derived data as torsional and distance restraints to calculate a three-dimensional structure using computer assisted molecular modeling.

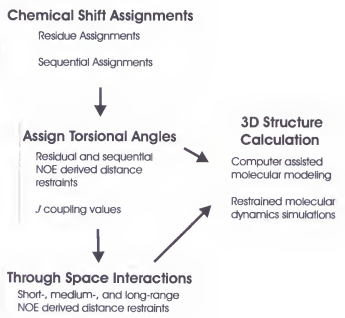

Figure 2-22. Summary of the general strategy employed to solve 3D structures of macromolecules using NMR.

Molecular Modeling and Molecular Dynamics Simulations

It is often useful for the medicinal chemist to have an accurate structural model of a compound of interest. Molecular models provide a three-dimensional structural representation of all the atoms and their connectivity in small molecules, peptides, and even large macromolecules such as proteins. Molecular models can aid in understanding some of the fundamental problems of drug design, such as the interaction of a ligand with a receptor. There are two main methods used to predict the structure of a compound: 1) computational methods based on theoretical structure calculations; and 2) analytical methods where the structure is derived from experimentally derived data.[120] Often the most accurate way to determine structure is to use a combination of the above two methods.

Computational Methods

Two of the most widely used computational methods for biological organic compounds are molecular dynamics simulations and molecular mechanics. Many biological compounds, such as peptides and proteins, are considerably flexible. This flexibility permits motion in the biological molecule and thus allows the possibility of several three-dimensional conformations to exist. Molecular dynamics simulations are used to calculate the motions of atoms in a chemical system and can be used to describe graphically the chemical behavior of a flexible molecule, and thus approximate the structure and motions of the compound. Molecular systems will often exhibit many energy minima due to this molecular flexibility. Molecular mechanics are used to calculate the geometry of the energy minima through a process called energy minimization. Energy minimized conformations can be accurately approximated when molecular simulations are used in conjunction with molecular mechanics.

Molecular dynamics simulations are used to calculate and describe the motion of atoms in a molecule using the laws of classical mechanics. For example: if the atoms in a molecule were considered to be balls and the bonds considered to be springs, the energy could be calculated knowing the mass of the balls and the spring constants of the springs.[120] The laws of classical mechanics can thus be used to calculate the motions of the balls, the lowest energy arrangement of the balls, and the dynamic behavior due to electronic perturbations in the system. The energy expression used to calculate these motions is called the force field. In simplest terms, the force field can be considered an energy expression (see below) encompassing all the energies of the system.[120] This equation can be used to calculate all of the forces on the molecular system.

E(total) = E(bond) + E(Coulomb) + E(VdW) + E(torsion) + E(angle) + ...

The force field must contain a mathematical function to describe every possible energy component of the system. Every atom, and groups of atoms, described in this function must contain all necessary parameters (for example, C-O bonds will have a different parameter than a C-N bond). If we consider the ball and spring analogy, an energy function can be used to describe the bond energy and a parameter used to describe the spring constant. Due to the complexity of the functions and parameters used to describe dynamic properties of molecular compounds, any given force field will consist of an extremely large collection of mathematical expressions.

Biophysical Methods

Biophysical methods can be used in a similar fashion as computational methods to determine the structural properties of a compound. Unlike computational methods, which use mathematical calculations to derive the theoretical structure, biophysical methods use data derived from experimental procedures using analytical instruments. Some of the

most common biophysical methods include: X-ray crystallography, high resolution mass spectrometry, infrared (IR) spectroscopy, electron microscopy, and nuclear magnetic resonance (NMR). As mentioned previously, the most reliable means of structure determination often employs a combination of biophysical and computational methodologies.

CHAPTER 3
STRUCTURE-ACTIVITY RELATIONSHIPS OF THE MELANOCORTIN TETRAPEPTIDE Ac-His-DPhe-Arg-Trp-NH_2 AT THE MOUSE MELANOCORTIN RECEPTORS

Portions of the study presented in this chapter have been previously published and have been reproduced in part with permission from: 1) Holder, J.R.;Bauzo, R.M.;Xiang, Z.;Haskell-Luevano, C. *J. Med. Chem.,* **2002**, *45*, 2801, Copyright (2002) American Chemical Society; 2) Holder, J.R.;Bauzo, R.M.;Xiang, Z.;Haskell-Luevano, C. *J. Med. Chem.,* **2002**, *45*, 3073, Copyright (2002) American Chemical Society; 3) Holder, J.R.;Bauzo, R.M.;Xiang, Z.;Haskell-Luevano, C. *J. Med. Chem.,* **2002**, *45*, 5736, Copyright (2002) American Chemical Society; and 4) Holder, J.R.;Bauzo, R.M.;Xiang, Z.;Haskell-Luevano, C. *Peptides,* **2003**, *24*, 73, Copyright (2003) Elsevier. All peptides were designed, synthesized, purified, and analytically characterized by Jerry Ryan Holder under the supervision of Dr. Carrie Haskell-Luevano. The pharmacology studies were carried out by Rayna Bauzo and Dr. Zhimin Xiang, both members of the Haskell-Luevano lab group. Pharmacology data calculations were performed by Dr. Carrie Haskell-Luevano. NMR data was obtained by Jerry Ryan Holder at the Advanced Magnetic Resonance Imaging and Spectroscopy (AMRIS) facility in the McKnight Brain Institute of the University of Florida with guidance from Mr. Jim Rocca and Dr. Arthur Edison.

Introduction

There are two primary methods of drug discovery: random screening of diverse collections of compounds, such as natural products mainly derived from plants and

microorganisms; and rational drug design.[121] Rather than screening random compounds against a variety of disease states, the rational design approach relies on knowledge of the mechanistic basis for the disease and the molecular characteristics of compounds that interact with the disease target.[121] The costs associated with random screening combined with the low yield of new and useful lead compounds have led to a decrease in popularity of the former method.

The rational design approach relies on identification of a disease target and understanding the fundamental physiologic and biochemical processes involved in the disease state. Once a disease target has been selected, a lead compound needs to be established. Lead compounds serve as a starting point in the rational drug design process. Often these compounds are the natural ligand for a receptor or a substrate for an enzyme. Once a lead is identified, it is necessary to determine what key structural features of the compound are responsible for activity. In the case of a peptide ligand, this information can be obtained by a set of experiments carefully designed to provide information regarding ligand-receptor interactions. These experiments are referred to as structure-activity relationship studies, and in the case of peptides and proteins often begin with two important experiments: 1) an alanine scan to determine the specific side chains involved in binding and functional activity; and 2) truncation studies to determine the minimal fragments needed to retain activity and binding, as well as potency equal to that of the lead peptide. Once the above studies are completed, one can generally determine the pharmacophore of the lead compound. Following the establishment of the peptidic pharmacophore, one can begin to assess how structural changes will affect activity. This structural knowledge is then used in the design of new ligands with improved properties.

Structure-activity studies are designed to provide insight into the types of interactions that occur in the formation of the ligand-receptor complex. One would like to know both the favorable and unfavorable processes that occur in ligand-receptor interactions that result in receptor stimulation (or inhibition). One objective of structure-activity studies is to aid in the design of ligands, with specific function, *a priori* for a given receptor or receptor system.

Previous Melanocortin SAR Studies

Due to the participation of the melanocortin receptor family in a vast array of physiological functions, and particularly the involvement of the MC3R and MC4R in energy and weight homeostasis,[58,59,63] these receptors have been the center of a large amount of research by both academic and industrial laboratories. The melanocortin ligands, both endogenous and synthetic, have been lead compounds in many structure-activity (SAR) studies. The studies discussed below exemplify the rational design processes of peptide research and reveal the insight these studies have provided to the melanocortin field. Amino acid numbering throughout this dissertation refers to the corresponding position of the amino acid residue in the sequence of α-MSH (Ac-Ser^{1}-Tyr^{2}-Ser^{3}-Met^{4}-Glu^{5}-His^{6}-Phe^{7}-Arg^{8}-Trp^{9}-Gly^{10}-Lys^{11}-Pro^{12}-Val^{13}-NH_2).

Truncation Studies

Once a peptide lead has been established, it is important to know which of the amino acid residues contribute to molecular recognition and receptor stimulation. Studies have been undertaken to determine the minimal sequence required to illicit a pharmacological response from α-MSH and the highly-potent analogue NDP-MSH (Ac-Ser^{1}-Tyr^{2}-Ser^{3}-*Nle*^{4}-Glu^{5}-His^{6}-*DPhe*^{7}-Arg^{8}-Trp^{9}-Gly^{10}-Lys^{11}-Pro^{12}-Val^{13}-NH_2).[75-77,122-124]

These studies involved selective removal (truncation) of N- and C-terminal residues, followed by evaluation of the truncated analogues for binding and/or functional activity. Figure 3-1 illustrates the truncation process for NDP-MSH and the results of truncation at the MC4R. In the classical frog (*Rana pipiens*) and lizard (*Anolis carolinensis*) skin bioassays, peptide activity was monitored by quantifying the amount of skin darkening that occurs in response to exposure to the peptide. The minimal sequence required for biological activity was determined to be Ac-His^{6}-Phe^{7}-Arg^{8}-Trp^{9}-NH_2 for α–MSH$^{75-77}$ and Ac-DPhe^{7}-Arg^{8}-Trp^{9}-NH_2 for NDP-MSH using these bioassays.[77,123] Our lab has recently utilized the cloned mouse receptors (MC1R, MC3R-MC5R) to characterize truncated NDP-MSH peptides to determine if results from the cloned receptors correlate with the previous results using the classical skin bioassays.[78,125] It should be noted that although the minimal NDP-MSH sequence required for activity was determined to be Ac-DPhe-Arg-Trp-NH_2, addition of histidine significantly increases potency at each of the four receptors. Truncation studies of α–MSH using the frog skin bioassay revealed that residues 4,10, and 12 contribute to the potency of the peptide and that residues 1-3, 5, 11, and 13 negligibly effect potency.[75] Likewise, in the lizard skin bioassay residues 1-3, 5, and 13 were not important for potency.[76] These data suggest that residues 4-12 of α-MSH and residues 4-9 of NDP-MSH are the minimal residues required to retain potency equivalent to the lead peptides. Three conclusions regarding the importance of α-MSH and NDP-MSH amino acids can be made from the truncation studies: 1) the melanocortin peptides contain an essential core sequence that is required to elicit measurable biological activity, 2) the peptides contain important potentiating amino acids that are required to

retain equipotency to the parent peptide and 3) the peptides contain amino acids that contribute minimally to the potency of the ligands.

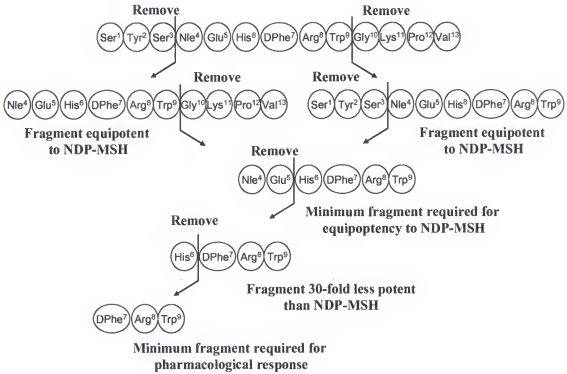

Figure 3-1. Illustration of the peptide truncation strategy. Truncation of NDP-MSH is shown as an example. The results shown are for the MC4R.

Alanine Scans

Specific interactions must take place between ligand and receptor in order for: 1) molecular recognition/ ligand binding; and 2) receptor stimulation to occur. It is important to determine which residues of the lead peptide are required for these processes to occur, especially if one desires to design a ligand with specific activity at a particular receptor system. One such method used to determine the amino acid residues involved in these processes is the alanine scan method. Alanine scanning studies can complement truncation studies and aid in the identification of the residues responsible for, or contributing to, the biological properties of the native peptide.[126,127] There has been a complete alanine scan of α-MSH utilizing B16 murine melanoma cells (putative

MC1R),[128] and more recently a complete alanine scan of γ-MSH characterized at the cloned human MC3R-MC5R.[129] The essential role that the core His-Phe-Arg-Trp sequence plays in peptide-receptor interactions was illustrated in both of these alanine scan studies. The results of an alanine scan study of the endogenous melanocortin agonist α-MSH are illustrated in Figure 3-2 below.

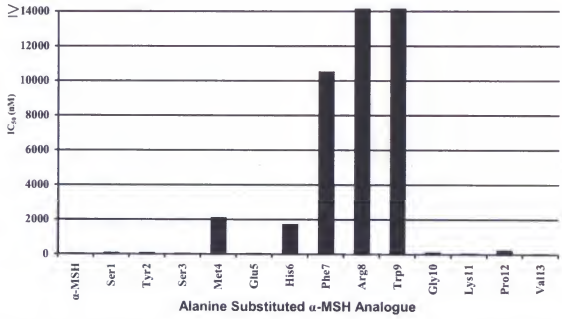

Figure 3-2. Graphical representation summarizing the effect that alanine substitution of each residue in α-MSH has on binding affinity. α-MSH and alanine substituted analogues were characterized using B16 murine melanoma cells (putative MC1R). IC_{50} values taken from reference 121.

Melanocortin Core Tetrapeptidyl Sequence

The SAR studies discussed above support the hypothesis that the His-Phe-Arg-Trp sequence represents the key structural features required for functional activity at the melanocortin receptors. It was *hypothesized* that pharmacological characterization of a set of carefully designed analogues based on this sequence could provide useful information for the future development of melanocortin ligands with improved properties. The aim of the SAR studies was to identify trends that result in: an increase or decrease in potency,

receptor subtype selectivity, and novel pharmacology at the melanocortin receptors. The studies presented below were undertaken to examine the role of various aromatic, natural, and unnatural amino acids in each amino acid position of the tetrapeptide Ac-His-DPhe-Arg-Trp-NH_2 for structure-activity-relationships and selectivity properties at the mouse melanocortin receptors.

Modification of the His^6 Position

The role of the His amino acid at the 6 position of α-MSH derivatives has not been previously explored in extensive detail throughout the literature, although an invention disclosure has been issued detailing modifications at the His^6 position.[130] A Peptide modified at the His position of the SHU9119 template (Ac-Nle-c[Asp-His-DNal(2')-Arg-Trp-Lys]-NH_2)[88] with (1-Me)His resulted in conversion of the SHU9119 mMC5R agonist into an antagonist.[131] Modification of the His^6 by Pro in the MTII peptide template (Ac-Nle-c[Asp-His-DPhe-Arg-Trp-Lys]-NH_2),[132] resulted in the identification of modifications that might lead to increased MC4R selectivity versus the MC3R.[133,134] More recently, modification of the MTII lactam cyclization ring size of peptides containing the His-DPhe-Arg-Trp sequence resulted in the identification of 50-fold[135,136] and 90-fold[137] MC4 versus MC3 receptor selective peptides. Incorporation of the unusual amino acid, Atc in its racemic form (Figure 3-3) at the 6 position in the peptide c[Asp-(racemic)Atc-DPhe-Arg-Trp-Lys]-NH_2, resulted in a peptide possessing 65nM agonist activity at the human MC4R while possessing only slight agonist activity at the hMC3R, resulting in one of the most MC4R versus MC3R selective compound disclosed to date.[138] This latter report also made several other amino acid substitutions and Atc derivatives at the His position resulting in interesting pharmacological properties at the

melanocortin receptors.[138] Substitution of the His amino acid by Pro, DPro, Glu, Gly, Ala, in various cyclic peptide templates has been reported by different research laboratories, generally resulting in decreased peptide potency for the melanocortin receptors.[133,134,137,139,140] Interestingly, upon deletion of the His amino acid in the Ac-His-DPhe-Arg-Trp-NH_2 tetrapeptide, only 2-fold decreased potency was observed at the human MC4R,[141] while at the mouse MC4R 220-fold decreased potency was observed,[78] with a loss of full agonist activity at the mMC3R and 170- to 480-fold decreased potency at the mMC1R and mMC5R, respectively.[78] These latter results demonstrate that the 6 position of the melanocortin peptides (α-MSH numbering) may be important for receptor selectivity and potency in the Ac-His-DPhe-Arg-Trp-NH_2 tetrapeptide template. This study was undertaken to examine the role of various aromatic, natural, and unnatural amino acids in the His position of the tetrapeptide Ac-Xaa-DPhe-Arg-Trp-NH_2 for structure-activity-relationships and selectivity properties at the mouse melanocortin receptors. The amino acids used in the His^6 position in this study are shown in Figure 3-3.

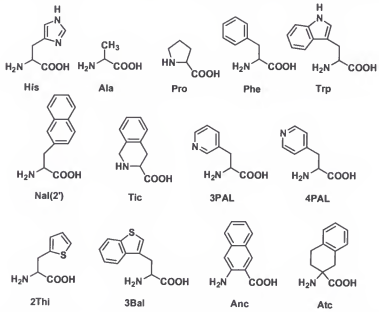

Figure 3-3. Structures of the amino acids used to replace His in the tetrapeptide template.

Results

Chemical synthesis and characterization

The peptides reported herein were synthesized using standard fluorenylmethyloxycarbonyl (Fmoc)[97,98] chemistry and a parallel synthesis strategy on an automated synthesizer (Advanced ChemTech 440MOS, Louisville, KY). The peptides were purified to homogeneity using semi-preparative reversed-phase high pressure liquid chromatography (RP-HPLC). The purity of these peptides was assessed by mass spectrometry (Table 3-1), analytical RP-HPLC in two diverse solvent systems (Table 3-1), and one-dimensional ^{1}H NMR (Appendix A).

Table 3-1. Analytical data for the His[6] modified tetrapeptides synthesized in this study.

Peptide	Structure	HPLC k' (System 1)	HPLC k' (System 2)	M+1 (Calculated)	(M+1) (Experimental)	Purity
1	Ac-**His**-DPhe-Arg-Trp-NH_2	3.9	6.9	686.8	686.3	>98%
2	Ac-**Ala**-DPhe-Arg-Trp-NH_2	4.9	8.2	620.7	620.3	>97%
3	Ac-**Pro**-DPhe-Arg-Trp-NH_2	8.1	9.0	646.8	646.1	>99%
4	Ac-**Phe**-DPhe-Arg-Trp-NH_2	6.8	10.6	696.8	696.3	>99%
5	Ac-**DPhe**-DPhe-Arg-Trp-NH_2	6.5	9.9	696.8	696.4	>99%
6	Ac-**Trp**-DPhe-Arg-Trp-NH_2	6.7	10.5	735.9	735.9	>99%
7	Ac-**DTrp**-DPhe-Arg-Trp-NH_2	6.5	10.0	735.9	735.1	>99%
8	Ac-**Nal(2')**-DPhe-Arg-Trp-NH_2	7.7	12.0	746.9	746.2	>99%
9	Ac-**DNal(2')**-DPhe-Arg-Trp-NH_2	7.5	11.4	746.9	746.1	>97%
10	Ac-**Tic**-DPhe-Arg-Trp-NH_2	6.9	10.3	708.8	708.2	>99%
11	Ac-**DTic**-DPhe-Arg-Trp-NH_2	6.9	10.3	708.8	708.3	>99%
12	Ac-**3PAL**-DPhe-Arg-Trp-NH_2	4.0	6.7	697.8	697.3	>99%
13	Ac-**4PAL**-DPhe-Arg-Trp-NH_2	3.9	6.6	697.8	697.3	>99%
14	Ac-**2Thi**-DPhe-Arg-Trp-NH_2	6.4	10.4	702.8	702.3	>99%
15	Ac-**3Bal**-DPhe-Arg-Trp-NH_2	5.3	12.1	752.9	752.1	>99%
16	Ac-**Anc**-DPhe-Arg-Trp-NH_2	7.3	11.1	717.8	717.7	>99%
17	Ac-**Atc**-DPhe-Arg-Trp-NH_2	7.2, 7.3	11.2, 11.4	721.9	722.2	>99%
18	Ac-**DHis**-DPhe-Arg-Trp-NH_2	4.1	6.7	685.8	686.0	>99%

HPLC k' = [(peptide retention time - sovent retention time) / solvent retention time] in solvent system 1 (10% acetonitrile in 0.1% trifluoroacetic acid/ water and a gradient to 90% acetonitrile over 35 min) or solvent system 2 (10% methanol in 0.1% trifluoroacetic acid/ water and a gradient to 90% methanol over 35 min). An analytical Vydac C18 column (Vydac 218TP104) was used with a flow rate of 1.5mL/min. The peptide purity was determined by HPLC at a wavelength of 214nM.

Biological evaluation

Table 3-2 summarizes the His[6] substituted tetrapeptide agonist pharmacology at the cloned mouse melanocortin MC1, MC3, MC4, and MC5 receptors.

Table 3-2. Functional activity of the His[6] modified tetrapeptides at the mouse melanocortin receptors.

Peptide	Structure	mMC1R		mMC3R		mMC4R		mMC5R	
		EC_{50} (nM)	Fold Difference	EC_{50} (nM)	Fold Difference	EC_{50} (nM)	Fold Difference	EC_{50} (nM)	Fold Difference
α-MSH	Ac-Ser-Tyr-Ser-Met-Glu-His-Phe-Arg-Trp-Gly-Lys-Pro-Val-NH_2	0.55±0.09		0.79±0.14		5.37±0.62		0.44±0.09	
NDP-MSH	Ac-Ser-Tyr-Ser-Nle-Glu-His-DPhe-Arg-Trp-Gly-Lys-Pro-Val-NH_2	0.038±0.012		0.098±0.013		0.21±0.03		0.071±0.012	
MTII	Ac-Nle-c[Asp-His-DPhe-Arg-Trp-Lys]-NH_2	0.020±0.003		0.16±0.03		0.087±0.008		0.16±0.03	
1	Ac-His-DPhe-Arg-Trp-NH_2	20.1±0.57	1	156±9.2	1	17.2±2.80	1	3.96±0.94	1
2	Ac-**Ala**-DPhe-Arg-Trp-NH_2	1,800±370	90	9,000±2,500	58	1,000±280	58	300±7	76
3	Ac-**Pro**-DPhe-Arg-Trp-NH_2	4,250±1,400	211	15,000±1,600	96	1,500±660	87	684±142	173
4	Ac-**Phe**-DPhe-Arg-Trp-NH_2	503±100	25	11,900±1,800	76	70.6±13.8	4	143±5	36
5	Ac-**DPhe**-DPhe-Arg-Trp-NH_2	11,500±1,800	57	>100,000		2,170±390	126	2,980±1,800	753
6	Ac-**Trp**-DPhe-Arg-Trp-NH_2	5,400±1,800	269	10,300±1,500	66	528±150	31	507±96	128
7	Ac-**DTrp**-DPhe-Arg-Trp-NH_2	6,600±1,200	328	>100,000		6,200±2,00	260	1,260±300	319
8	Ac-**Nal(2')**-DPhe-Arg-Trp-NH_2	9,500±5,100	473	14,700±2,000	94	2,900±2,400	169	606±360	153
9	Ac-**DNal(2')**-DPhe-Arg-Trp-NH_2	7,100±980	353	>100,000		1,500±300	87	2,240±900	566
10	Ac-**Tic**-DPhe-Arg-Trp-NH_2	2,600±600	129	11,800±1,600	76	2,900±1,600	169	369±140	93
11	Ac-**DTic**-DPhe-Arg-Trp-NH_2	11,300±3,100	562	>100,000		11,700±420	680	12,000±500	3,030
12	Ac-**3PAL**-DPhe-Arg-Trp-NH_2	1,150±240	57	Slight agonist		887±99	52	400±147	101
13	Ac-**4PAL**-DPhe-Arg-Trp-NH_2	176±80	9	2,270±770	15	128±33	7	92.5±22.3	23
14	Ac-**2Thi**-DPhe-Arg-Trp-NH_2	203±40	10	2,950±250	19	91.2±39	5	40.5±13	10
15	Ac-**3Bal**-DPhe-Arg-Trp-NH_2	4,400±3,000	219	19,800±3,200	127	211±62	12	381±123	96
16	Ac-**Anc**-DPhe-Arg-Trp-NH_2	7,900±4,200	393	Slight agonist	**Antagonist**	21.1±6.0	1	45.6±6.9	12
				pA_2=5.60±0.11	Ki=2,500nM				
17	Ac-**rac(Atc)**-DPhe-Arg-Trp-NH_2	7,730±1,200	384	Slight agonist		714±150	42	2,400±1,030	606
18	Ac-**DHis**-DPhe-Arg-Trp-NH_2	289±107	14	6,190±2,460	40	506±58	29	138±24	35

The indicated errors represent the standard error of the mean determined from at least four independent experiments. Slight agonist denotes that some stimulatory response was observed but not enough to determine an EC_{50} value. The compounds not demonstrating full agonism were assayed for antagonism using the Schild pA_2 analysis and the MTII peptide as the agonist, Ki = -Log pA_2.

Mouse melanocortin-1 receptor. The peripheral skin melanocortin receptor, MC1R, is involved in human skin pigmentation[26,27] and animal coat coloration.[142] Our laboratory has previously reported the lead tetrapeptide **1**, Ac-His-DPhe-Arg-Trp-NH_2, to possess 25nM stimulatory activity at the mMC1R,[78] an EC_{50} value of 200nM in the classical *Rana pipiens* frog skin assay (putative MC1R),[77] and was determined to possess a mMC1R EC_{50} =20nM herein. Substitution at the His^6 position within this tetrapeptide by Pro, Phe, DPhe, Trp, DTrp, Nal(2'), DNal(2'), Tic, DTic, 3PAL, 4PAL, 2Thi, 3Bal, Anc, Atc, and DHis all resulted in 9- to 562-fold decreased agonist activity at the mMC1R. Removal of the imidazole His side chain and replacement by the methyl side chain of Ala (**2**) resulted in 90-fold decreased potency. The Pro^6 containing tetrapeptide **3**, resulted in 211-fold decreased potency, while the Phe^6 and $DPhe^6$ containing tetrapeptides **4 and 5**, respectively possessed 25- and 57-fold decreased potencies, respectively, compared with the His^6 peptide **1**. Substitution of the imidazole His^6 side chain with the Trp^6 indole in either the L or D stereochemical configurations resulted in 269- and 328-fold decreased potencies of peptides **6** and **7**, respectively. In tetrapeptides **8** and **9**, containing $Nal(2')^6$ and $DNal(2')^6$, 473- and 353-fold decreased potencies were observed at the mMC1R, respectively, as compared with peptide **1**. Replacement of the imidazole side chain at the 6 position with the topographically constrained chi (χ) side chain derivative of the Phe amino acid, Tic and DTic, (**10** and **11**) resulted in 129- and 562-fold decreased potencies at the mMC1R, respectively. Substitution at the 6 position with phenyl derivatives containing nitrogen at either the 3 or 4 positions of the phenyl ring, 3PAL peptide **12** and 4PAL peptide **13**, resulted in 57- and 9-fold decreased potencies at the mMC1R, as compared with the His^6 containing peptide **1**. Interestingly,

substitution of the imidazole ring with the sulfur containing 2Thi amino acid (peptide **14**) resulted in a 10-fold decrease in potency at the mMC1R. Incorporation of an additional benzyl ring (3Bal, **15**) onto the peptide **14** position 6 side chain resulted in 219-fold decreased potency as compared with the imidazole side chain (**1**) and a 22-fold decreased potency compared to peptide **14** at the mMC1R. The Anc and racemic Atc containing peptides **16** and **17**, respectively, are equipotent to each other, and resulted in 393- and 384-fold decreased potency compared with peptide **1** at the mMC1R. Stereochemical inversion of His^6 to $DHis^6$ (**18**) resulted in 18-fold decreased potency at the mMC1R.

Mouse Melanocortin-3 Receptor. The MC3R is expressed both peripherally and centrally and appears to be involved in metabolism and energy homeostasis.[29,32,58,59] The lead tetrapeptide **1**, Ac-His-DPhe-Arg-Trp-NH_2, has been previously reported to possess a 195nM agonist EC_{50} at the mMC3R[78], a 1000nM EC_{50} at the hMC3R,[143] and was determined to possess a 156nM EC_{50} herein. Substitution at the His^6 position within this tetrapeptide by Pro, Phe, DPhe, Trp, DTrp, Nal(2'), DNal(2'), Tic, DTic, 3PAL, 4PAL, 2Thi, 3Bal, Anc, Atc, and DHis all resulted in 15-fold decreased potency, slight agonism at 100μM concentrations but not enough to determine an EC_{50} value (Figure 3-4), a complete loss of agonist activity (up to 100μM concentrations), or for a single peptide (**16**) a weak μM antagonist (Figure 3-5) at the mMC3R. The peptides that did not demonstrate agonist activities were tested for antagonism at up to 10μM concentrations and did not result in any observable antagonistic properties (data not shown). Peptides **2** and **3**, containing Ala^6 and Pro^6, resulted in 58- and 96-fold decrease mMC3R potency, respectively, compared with the His^6 lead peptide **1**. Phenyl side chain substitution of the imidazole at the 6 position with Phe or DPhe containing peptides, **4** and **5**, resulted in 76-

fold decreased potency and a loss of stimulatory activity at up to 100μM, respectively, at the mMC3R. Substitution of the His^6 imidazole side chain with the Trp indole in either the L- or D- stereochemical configuration resulted in 66-fold decreased potency for the Trp^6 containing peptide **6** and loss of stimulatory activity at up to 100μM for the $DTrp^6$ containing tetrapeptide **7** at the mMC3R. Tetrapeptide **8**, containing $Nal(2')^6$, resulted in 94-fold decreased potency compared with the His^6 **peptide 1**, while the $DNal(2')^6$ tetrapeptide **9** resulted in a loss of stimulatory activity at up to 100μM at the mMC3R. Replacement of the imidazole side chain at the 6 position with Tic^6 (**10**) resulted in 76-fold decreased potency, compared with **1**, while the $DTic^6$ containing tetrapeptide **11** resulted in loss of stimulatory activity at up to 100μM concentrations at the mMC3R. At the mMC3R, substitution at the 6 position with phenyl derivatives containing nitrogen at either the 3 or 4 positions of the phenyl ring gave either 3PAL or 4PAL derivatives. $3PAL^6$ peptide **12** possessed agonist activity (at 100μM, Figure 3-4) but not enough to determine an EC_{50} value, whereas $4PAL^6$ peptide **13** resulted in only 15-fold decreased potency compared with peptide **1**. Tetrapeptide **14**, containing 2Thi at the 6 position, resulted in 19-fold decreased mMC3R potency, whereas the $3Bal^6$ containing tetrapeptide **15** resulted in 127-fold decreased potency at the mMC3R compared with the His^6 peptide **1**. The Anc^6 containing tetrapeptide **16** possessed only slight agonist activity and when tested for antagonism resulted in a weak μM antagonist with a pA_2=5.6 (Ki=2.5μM= -Log pA_2). The dose response curves of **16** at the MC3R are shown in Figure 3-5. Interestingly, peptides **17** and **18** possessed only slight agonist activity at the mMC3R at up to 100μM concentrations (Figure 3-4). Finally, inversion of chirality from His^6 to $DHis^6$, peptide **18**, resulted in 40-fold decreased potency at the mMC3R.

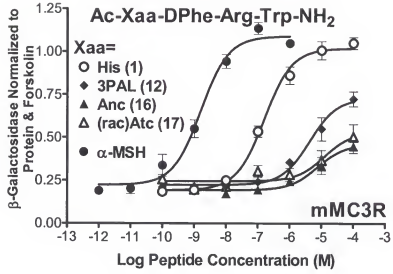

Figure 3-4. Illustration of the tetrapeptides possessing slight agonist activity at the mMC3R. The amino acid in the Xaa position is listed, and the number in parentheses represents the compound number. The peptides α-MSH and peptide **1** are included as controls to illustrate the maximal response observed for full agonists using this assay.

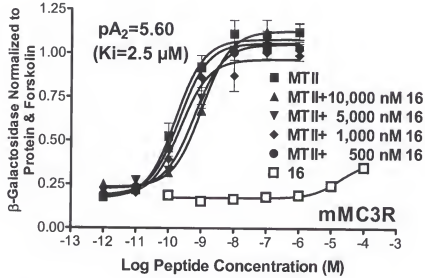

Figure 3-5. Illustration of weak antagonism of tetrapeptide **16**, Ac-Anc-DPhe-Arg-Trp-NH_2, at the mouse MC3R.

Mouse Melanocortin-4 Receptor. The central MC4R has been identified as physiologically participating in food consumption[90] and obesity in mice.[63] Several

polymorphisms of the MC4R have been observed in obese humans.[67,144-148] The lead tetrapeptide in this study, Ac-His-DPhe-Arg-Trp-NH_2 (**1**), was previously reported to possess a 10nM agonist EC_{50} values at the mMC4R,[78] a 8nM[141] and 47nM[143] agonist EC_{50} values at the hMC4R, and was determined to have a potency at the mMC4R of 17nM herein. Substitution at the His^6 position within this tetrapeptide by Pro, Phe, DPhe, Trp, DTrp, Nal(2'), DNal(2'), Tic, DTic, 3PAL, 4PAL, 2Thi, 3Bal, Anc, Atc, and DHis resulted in 4- to 680-fold decreased potency at the mMC4R. Tetrapeptides **2** (Ala^6) and **3** (Pro^6) resulted in 58- and 87-fold decreased potencies, respectively, compared to the His^6 containing tetrapeptide **1** at the mMC4R. Substitution of the His^6 imidazole with either Phe (**4**) or DPhe (**5**) resulted in 4- and 126-fold decreased potencies, respectively, at the mMC4R. The Trp substitution of the His at the 6 position resulted in 31-fold (**6**, Trp^6) and 260-fold (**7**, $DTrp^6$) decreased potencies at the mMC4R. The $Nal(2')^6$ containing peptide **8** possessed 169-fold decreased potency and the $DNal(2')^6$ containing peptide **9** resulted in 87-fold decreased potency at the mMC4R compared with the His^6 containing peptide **1**. Substitution of the imidazole amino acid with the Phe derivatives, Tic^6 (**10**) and $DTic^6$ (**11**), resulted in 169- and 680-fold decreased potencies at the mMC4R, respectively. Insertion of a nitrogen into the phenyl side chain of Phe in peptide **12** ($3PAL^6$) and peptide **13** ($4PAL^6$) resulted in 52- and 7-fold decreased potencies, respectively, at the mMC4R compared with peptide **1**. Finally, peptide **14** ($2Thi^6$) resulted in 5-fold decreased potency whereas the $3Bal^6$ containing tetrapeptide **15** resulted in 12-fold decreased potency at the mMC4R compared with the His^6 containing tetrapeptide **1**. Peptide **16**, containing Anc in the 6 position, resulted in equipotency with the His^6 peptide **1** at the mMC4R. Peptide **17** (racemic Atc) resulted in 42-fold decreased

potency while the DHis^6 peptide **18**, resulted in 29-fold decreased potency at the mMC4R compared with **1**.

Melanocortin-5 Receptor. The peripheral MC5R is expressed in a variety of tissues and has been implicated as physiologically participating in the role of exocrine gland function.[71,149,150] The lead tetrapeptide **1**, Ac-His-DPhe-Arg-Trp-NH_2, has been previously reported to possess a 3.4nM agonist EC_{50} at the mMC5R,[78] a 17% response at a 5μM concentration at the hMC5R,[143] and was determined to possess a 3.9nM EC_{50} at the mMC5R herein. Substitution at the His^6 position within this tetrapeptide by Pro, Phe, DPhe, Trp, DTrp, Nal(2'), DNal(2'), Tic, DTic, 3PAL, 4PAL, 2Thi, 3Bal, Anc, Atc, and DHis resulted in 10- to 3,030-fold decreased potency at the mMC5R. Replacement of the His side chain at the 6 position with Ala (**2**) or Pro (**3**) resulted in a 76- and 173-fold decrease in potency, respectively, at the mMC5R. Substitution of the His imidazole side chain with Phe (**4**) or DPhe (**5**) resulted in 36- and 753-fold decreased potencies, respectively, at the mMC5R. The indole Trp substitution of the His imidazole at the 6 position in peptides **6** (Trp) and **7** (DTrp) resulted in 128- and 319-fold decreased potencies, respectively, at the mMC5R. The Nal(2')^6 containing peptide **8** possessed 153-fold decreased potency compared to peptide **1**, while the DNal(2')^6 peptide **9** possessed 566-fold decreased potency compared to peptide **1** at the mMC5R. Substitution of the His^6 amino acid by Tic (**10**) or DTic (**11**) resulted in 93- and 3,030-fold decreased potencies, respectively, at the mMC5R compared to peptide **1**. Peptides **12** (3PAL^6) and **13** (4PAL^6) possessed 101- and 23-fold decreased potencies, respectively, compared with the His^6 peptide **1** at the mMC5R. Peptides **14** (2Thi^6) and **15** (3Bal^6) resulted in 10- and 96-fold decreased potencies, respectively, compared with peptide **1** at the mMC5R. The

Anc[6] containing peptide **16** resulted in 12-fold decreased mMC5R potency, the racemic Atc[6] containing peptide **17** resulted in 600-fold decreased mMC5R potency, while the DHis[6] peptide **18** resulted in 35-fold decreased mMC5R potency compared with peptide **1**.

Discussion

Substitution of the His[6] side chain imidazole for other functional groups.

Figure 3-6 summarizes the effect that modifying the His side chain of the template peptide Ac-Xaa-DPhe-Arg-Trp-NH_2 with the amino acids examined in this study has on potency at the melanocortin receptors. Substitution of the His[6] side chain (α-MSH numbering) with Ala (**2**) in the lead tetrapeptide, Ac-His-DPhe-Arg-Trp-NH_2 (**1**), resulted in decreased receptor potencies in the order of mMC5R > mMC4R > mMC1R >> mMC3R. Replacement of the His[6] residue of MTII with Ala resulted in a 1- to 5-fold decreased potencies at the hMC3, hMC4, and hMC5 receptors,[139] and His[6] to Ala in NDP-MSH resulted in only a 4-fold decreased potency at the hMC4R.[141] Interestingly, substitution of His[6] with Ala in a 23-membered lactam cyclic agonist peptide template (c[$COCH_2CH_2CO$-His[6]-DPhe-Arg-Trp-Lys]-NH_2) resulted in a lack of cAMP response (up to 5000nM) at the hMC3R and hMC5R, while resulting in only a 48-fold decreased potency at the hMC4R.[137] These data suggest that in the tetrapeptide template the peptide backbone at the six position is less important for biological activity than the presence of the imidazole side chain, while in longer, more potent peptides such as MTII and NDP-MSH the His side chain appears to be less important for agonist potency.

When His is replaced by Pro at the six position in the tetrapeptide, a 87- to 211-fold decrease in ligand potency is observed at the mMC1 and mMC3-5 receptors, which results in approximately the same order of magnitude (within experiment error) reduction in ligand potency at these receptors, compared with **1**, and results in the same trend in

potency as the Ala at these receptors (mMC5R > mMC4R > mMC1R > mMC3R). When Pro is substituted for His^6 in MTII, a 2- to 4-fold decreased potency is observed at the hMC4R and hMC3R, while a 2.5-fold increased potency is observed for the Pro^6-MTII peptide at the hMC5R.[133] Interestingly, substitution of His^6 with Pro in the cyclic agonist peptide template, c[$COCH_2CH_2CO$-His^6-DPhe-Arg-Trp-Lys]-NH_2, resulted in 10- and 76-fold decreased potency at the hMC3R and hMC4R while 2-fold increased potency resulted at the hMC5R.[137] In this latter study by Bednarek et al., inverting the stereochemistry of the Pro^6 to $DPro^6$ in their peptide template resulted in 3-5% agonist stimulation at 10μM concentrations. Modification of the His in the six position by Pro in the MTII peptide template resulted in the identification of modifications that might lead to increased MC4R selectivity versus the MC3R.[133,134]

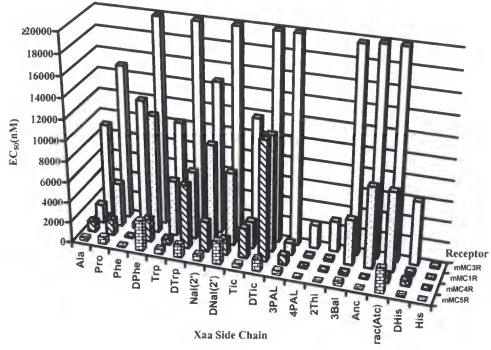

Figure 3-6. Graphical representation summarizing the effect on melanocortin receptor (Y axis) agonist EC_{50} values (Z axis) of the indicated amino acid substitution (X axis) of the His residue in the tetrapeptide template.

Replacement of the His^6 imidazole by the phenyl side chain of Phe (**4**) resulted in only a 4-fold decrease in potency at the mMC4R while 25-, 76-, and 36-fold decreased potencies at the mMC1R, mMC3R, and mMC5R resulted, respectively, compared with **1**. This information suggests that substitution of a His by Phe for the design of non-peptide MC4R selective small molecule agonists may be a viable option. By using this Phe amino acid for the development of non-peptide molecules, the side chain does not need to possess a protecting group like the His residue may during synthesis, facilitating an easier synthetic chemistry strategy. Inversion of stereochemistry to the $DPhe^6$ containing tetrapeptide **5** resulted in decreased potencies compared to the His^6 peptide **1** (mMC4R > mMC5R >mMC1R), while losing ability to stimulate the mMC3R at up to 100μM concentrations. Comparing tetrapeptides **4** (Phe^6) and **5** ($DPhe^6$) a 2-, 31- and 21-fold decrease in potency of the $DPhe^6$ peptide compared with the Phe^6 tetrapeptide was observed at the mMC1R, mMC4R, and mMC5R, respectively (Figure 3-6).

The Tic amino acid (Figure 3-3) is a topographically constrained derivative of Phe which severely restricts rotation about the chi $(\chi)_1$ and χ_2 side chain torsional angles and has been previously reported to result in increased biological activities and potencies.[151,152] In the tetrapeptides **10** (Tic^6) and **11** ($DTic^6$), the L-configured compound possessed full agonism at the melanocortin receptors with 76- to 169-fold decreased potencies compared with the His^6 tetrapeptide **1**, while the D-configured molecule (**11**) lacked any observable mMC3R stimulation at up to 100μM(was not an mMC3R antagonist), and resulted in 562- to 3000-fold decreased potencies at the mMC1R, mMC4R, and mMC5R. Comparing the Tic^6 tetrapeptide (**10**) with their corresponding Phe^6 (**4**) peptide, the L-configuration resulted in 5-, equipotency, 41- and 3-fold

(equipotent within experimental error) at the mMC1R, mMC3R, mMC4R, and mMC5R, respectively. Comparing the DTic[6] tetrapeptide (**11**) with their corresponding DPhe[6] (**5**) peptide, the D-configuration resulted in equipotency at the mMC1R, lack of stimulation at up to 100μM at the mMC3R, 5- and 4-fold decreased potency at the mMC4R and mMC5R, respectively.

Modification of the Phe[6] benzyl ring by the insertion of a nitrogen in either the meta (3PAL, **12**) or para (4 PAL, **13**) positions generally resulted in decreased melanocortin receptor potency compared with peptide **1**. Tetrapeptide Ac-4PAL-DPhe-Arg-Trp-NH_2 (**13**) resulted in only 7- to 23-fold decreased melanocortin receptor potencies compared with **1**, and was equipotent at the mMC1R, mMC4R, and mMC5R, within experimental error, but was 5-fold more potent at the mMC3R than the Phe[6] containing tetrapeptide **4**. Thus, incorporation of a nitrogen into the Phe side chain at the *m* or *p* positions generally resulted in decreased melanocortin receptor potency except for the 4PAL derivative at the mMC3R.

Naphthyl(2') side chain replacement of the His[6] (**1**), tetrapeptide **8**, resulted in decreased potencies at the melanocortin receptors compared with **1**. Inversion of stereochemistry to DNal(2')[6] in tetrapeptide **9** resulted in a loss of agonist activity at the mMC3R (up to 100μM concentrations) and 87- to 566-fold decreased potencies at the mMC1R, mMC4R, and mMC5R compared with **1**. Comparison of the Nal(2')[6] peptide **8** with the DNal(2')[6] peptide **9** resulted in nearly equipotent activities at the mMC1R, mMC4R, and mMC5R.

Substitution of the imidazole by an indole to give Trp (**6**) at the six position resulted in decreased potencies at the mMC1 and mMC3-5 receptors compared with

tetrapeptide **1**. Converting Trp to the DTrp (**7**) stereochemistry at the six position resulted in a loss of agonist activity at the mMC3R (up to 100μM), and 260- to 328-fold decreased potencies at the mMC1 and mMC4-5 receptors compared with **1**. Comparing tetrapeptides **6** (Trp^6) and **7** ($DTrp^6$) resulted in equipotent activities at the mMC1R and mMC5R (within experimental error) and an 8-fold decreased potency for the $DTrp^6$ analogue at the mMC4R. Upon substitution of His^6 with Trp in the SHU9119 peptide, Ac-Nle-c[Asp-His-DNal(2')-Arg-Trp-Lys]-NH_2, 51-, 25-, and 16-fold decreased potencies were observed at the mMC1R (agonist), the mMC3R (antagonist) and mMC4R (antagonist), respectively, while the compound was converted from a full agonist (His^6 EC_{50}=2.3nM) to a compound resulting in only slight agonist activity up to 1μM at the mMC5R.[131] Upon substitution of the indole nitrogen of Trp^6 (**6**) with a sulfur ($3Bal^6$, **15**) nearly equipotency was observed at all the melanocortin receptors examined, suggesting that the heteroatom of the indole ring at the 6 position may not be particularly important for ligand potency. However, comparison of the $2Thi^6$ (**14**) and $3Bal^6$ (**15**) peptides resulted in 22-, 7-, equipotency, and 10-fold decreased potency at the mMC1R, mMC3R, mMC4R, and mMC5R, respectively, suggesting that the three-dimensional location of the benzyl portion of the indole like structure does not effect the mMC4R ligand-receptor interactions as much as the other receptor isoforms.

Comparison of the $2Thi^6$ amino acid derivative (Figure 3-3) with the His^6 containing tetrapeptides resulted in 5- to 19-fold decreased melanocortin receptor potencies, suggesting that the electronic and basic features of the imidazole ring may be important for receptor potency, perhaps through salt bridge or hydrogen bonding interactions.

MC4 versus MC3 receptor selectivity

Identification of ligands selective for either of the centrally located melanocortin receptors, MC3R or MC4R, are highly sought after since both these receptors have been identified as physiologically participating in the neuroendocrine process of energy homeostasis using a combination of non-specific melanocortin agonists and antagonists and knockout mice.[58,59,63,78,90,153-155] As mentioned previously, substitution of His with Pro in the MTII agonist template resulted in the identification of this position contributing to MC4 versus MC3 receptor selectivity.[133,134] The recent public disclosure by Hoffmann-La Roche Inc. indicated the His position as the most critical position for the identification of MC4 versus MC3 receptor compounds, as demonstrated by the peptide c[Asp-(D,L)Atc-DPhe-Arg-Trp-Lys]-NH_2 possessing 65nM hMC4R potency and only possessing slight agonist activity at the hMC3R at μM concentrations.[138] The studies presented herein support this hypothesis by the identification of compounds that possess full agonist activity at the mMC4R while lacking mMC3R full agonist activity at up to 100μM concentrations (Figure 3-4). The most potent and mMC4R selective (versus mMC3R) tetrapeptide is Ac-Anc-DPhe-Arg-Trp-NH_2 (**16**), which is equipotent to the His containing tetrapeptide **1** and only 4-fold less potent than the endogenous agonist α-MSH at the mMC4R (Table 3-1), while only possessing slight agonist activity (<50% maximal stimulation at 100μM) at the mMC3R (Figure 3-4). Unexpectantly, Ac-Anc-DPhe-Arg-Trp-NH_2 (**16**) resulted in a μM mMC3R antagonist (Figure 3-5).Even with this pharmacological profile, if the compound is administered in the high nM range, stimulation of the MC4R should result with a postulated absence of activity at the mMC3R. The tetrapeptide containing Atc^6, Ac-(racemic)Atc-DPhe-Arg-Trp-NH_2 (**17**),

has incorporated the same amino acid reported by Danho and colleagues.[138] Peptide **17** was 34-fold less potent than peptide **16** at the mMC4R and only 11-fold less potent that the previously identified cyclic hexapeptide.[138] Similarl to the Hoffmann-La Roche cyclic hexapeptide (although it was not mentioned if it was tested for MC3R antagonist activity), the Atc[6] containing peptide **17** only possessed slight agonist activity (<50% maximal stimulation at 100μM) at the mMC3R. Interestingly, the aromatic side chains in the D-configuration at the 6 position resulted in decreased μM potencies at the mMC4R but did not stimulate the mMC3R at up to 100μM concentrations. These data, and the fact that the Atc peptide **17** is actually a racemic mixture, suggest that the DAtc[6] containing tetrapeptide might be more potent and selective for the MC4R than the Anc peptide reported herein. Thus, these data support the hypothesis that the His[6] position is important for MC4 versus MC3 receptor selectivity[134,138] and extends this hypothesis to include an aromatic benzyl ring in the proper topographical three-dimensional space as an additional consideration. Peptides modified at the His[6] position that are selective for the mMC4R versus the mMC3R are listed in Table 3-3. The information gained by the His[6] SAR studies reported herein are extremely valuable and applicable for the design of small molecule non-peptide MC4R selective agonists.

Table 3-3. Central melanocortin receptor selective His[6] modified tetrapeptides.

Peptide	Structure	mMC3R EC_{50} (nM)	mMC4R EC_{50} (nM)	Selectivity Ratio mMC3R EC_{50}/mMC4R EC_{50}
16	Ac-**Anc**-DPhe-Arg-Trp-NH_2	>100,000	21.1	>4700
17	Ac-**rac(Atc)**-DPhe-Arg-Trp-NH_2	>100,000	714	>140
12	Ac-**3PAL**-DPhe-Arg-Trp-NH_2	>100,000	887	>113
4	Ac-**Phe**-DPhe-Arg-Trp-NH_2	11,900	70.6	169
15	Ac-**3Bal**-DPhe-Arg-Trp-NH_2	19,800	211	94
9	Ac-**DNal(2')**-DPhe-Arg-Trp-NH_2	>100,000	1,500	>67
5	Ac-**DPhe**-DPhe-Arg-Trp-NH_2	>100,000	2,170	>46
7	Ac-**DTrp**-DPhe-Arg-Trp-NH_2	>100,000	6,200	>16
11	Ac-**DTic**-DPhe-Arg-Trp-NH_2	>100,000	11,700	>9

Modification of the Phe^7 Position

The Phe residue at the seven position (α-MSH numbering) has previously been modified and resulted in the discovery of antagonists for the central MC3 and MC4 receptors.[88] The DNal(2') and (pI)DPhe substitutions of the Phe amino acid in the MTII cyclic peptide template (Ac-Nle-c[Asp-His-DPhe-Arg-Trp-Lys]-NH_2) resulted in the MC3R and MC4R partial agonists and antagonists SHU9119 and SHU8914.[88] The (pI)DPhe substitution of the DPhe amino acid in the NDP-MSH linear peptide template (Ac-Ser-Tyr-Ser-Nle-Glu-His-DPhe-Arg-Trp-Gly-Lys-Pro-Val-NH_2) resulted in the SHU9005 partial agonist and antagonist activity at the MC3R and MC4R.[124] The MTII (agonist) and SHU9119 (antagonist) ligands were further utilized in rodent feeding studies to demonstrate that the central melanocortin pathway could modify feeding behavior by increasing food intake upon antagonist administration, and decreasing food intake upon agonist administration into the brain.[90] Subsequent studies substituting the DNal(2') amino acid into various melanocortin agonist peptide templates at the Phe position resulted in MC3 and/or MC4 receptor antagonists.[131,136,137,156-158] Computer GPCR homology molecular modeling of the MC1R,[159] and receptor mutagenesis studies of the peripheral MC1R[160] and the central MC4R[131,141] resulted in the identification of the melanocortin ligand DPhe residue as putatively interacting with a hydrophobic receptor pocket consisting of several aromatic receptor side chains.[161] The study presented herein utilizes the tetrapeptide template Ac-His-Xaa-Arg-Trp-NH_2, where Xaa is substituted with natural, unnatural, and aromatic amino acids (Figure 3-7) to examine the melanocortin ligand side chain properties important for melanocortin receptor selectivity,

potency, structure-activity relationship trends, and differentiation of agonist versus antagonist activities at the mouse MC1, MC3, MC4 and MC5 receptors.

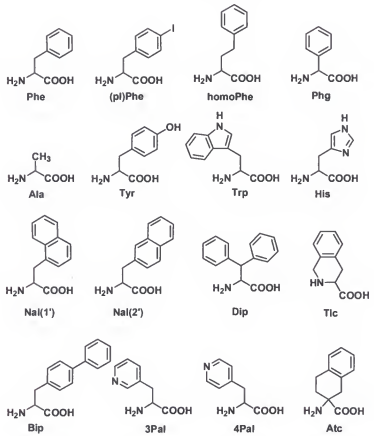

Figure 3-7. Structures of the amino acids used to replace Phe in the tetrapeptide template.

Results

Chemical synthesis and characterization

The peptides reported herein were synthesized using standard fluorenylmethyloxycarbonyl (Fmoc)[97,98] chemistry and a parallel synthesis strategy on an automated synthesizer (Advanced ChemTech 440MOS, Louisville, KY). The peptides were purified to homogeneity using semi-preparative reversed-phase high pressure liquid chromatography (RP-HPLC). The purity of these peptides was assessed by mass spectrometry (Table 3-4) and analytical RP-HPLC in two diverse solvent systems (Table 3-4).

Table 3-4. Analytical data for the Phe[7] modified tetrapeptides synthesized in this study

Peptide	Structure	HPLC k' (System 1)	HPLC k' (System 2)	M+1 (Calculated)	(M+1) (Experimental)	Purity
1	Ac-His-DPhe-Arg-Trp-NH_2	3.9	6.9	686.8	686.3	>98%
19	Ac-His-**Ala**-Arg-Trp-NH_2	3.1	4.9	610.7	610.3	>98%
20	Ac-His-**(pI)DPhe**-Arg-Trp-NH_2	5	8.3	812.7	812	>98%
21	Ac-His-**homoPhe**-Arg-Trp-NH_2	5.3	8.4	700.8	700.3	>97%
22	Ac-His-**homoDPhe**-Arg-Trp-NH_2	4.6	7.6	700.8	700	>96%
23	Ac-His-**Tyr**-Arg-Trp-NH_2	3.8	6.2	702.8	702.2	>99%
24	Ac-His-**DTyr**-Arg-Trp-NH_2	3.6	5.7	702.8	702.1	>99%
25	Ac-His-**Trp**-Arg-Trp-NH_2	4.9	7.7	725.8	725.3	>99%
26	Ac-His-**DTrp**-Arg-Trp-NH_2	4.2	6.9	725.8	725.3	>96%
27	Ac-His-**Phg**-Arg-Trp-NH_2	4.3	6.9	672.8	672.3	>97%
28	Ac-His-**DPhg**-Arg-Trp-NH_2	3.8	5.8	672.8	672.4	>98%
29	Ac-His-**Nal(1')**-Arg-Trp-NH_2	5.6	9.5	736.8	737.2	>98%
30	Ac-His-**DNal(1')**-Arg-Trp-NH_2	4.8	8.1	736.8	736	>97%
31	Ac-His-**Nal(2')**-Arg-Trp-NH_2	5.6	9.4	736.8	736.4	>98%
32	Ac-His-**DNal(2')**-Arg-Trp-NH_2	5	8.3	736.8	736.3	>98%
33	Ac-His-**Dip**-Arg-Trp-NH_2	5.7	9.9	762.9	762.3	>98%
34	Ac-His-**DDip**-Arg-Trp-NH_2	4.8	8.1	762.9	762.2	>98%
35	Ac-His-**Tic**-Arg-Trp-NH_2	4.5	7.4	698.8	698.1	>96%
36	Ac-His-**DTic**-Arg-Trp-NH_2	4.1	6.8	698.8	698.1	>98%
37	Ac-His-**Bip**-Arg-Trp-NH_2	6.2	10.2	762.9	761.8	>98%
38	Ac-His-**DBip**-Arg-Trp-NH_2	5.6	9.3	762.9	762.1	>98%
39	Ac-His-**His**-Arg-Trp-NH_2	3.1	4.7	676.7	676.3	>99%
40	Ac-His-**3Pal**-Arg-Trp-NH_2	3.1	4.9	687.8	687.3	>98%
41	Ac-His-**4Pal**-Arg-Trp-NH_2	3.1	4.9	687.8	687.2	>98%
42	Ac-His-**Atc**-Arg-Trp-NH_2	4.7	7.9	712.8	712.3	>98%
43	Ac-His-**Atc**-Arg-Trp-NH_2	4.8	8.2	712.8	712.3	>96%
44	Ac-His-**Phe**-Arg-Trp-NH_2					

HPLC k' = [(peptide retention time - sovent retention time) / solvent retention time] in solvent system 1 (10% acetonitrile in 0.1% trifluoroacetic acid/ water and a gradient to 90% acetonitrile over 35 min) or solvent system 2 (10% methanol in 0.1% trifluoroacetic acid/ water and a gradient to 90% methanol over 35 min). An analytical Vydac C18 column (Vydac 218TP104) was used with a flow rate of 1.5 mL/min. The peptide purity was determined by HPLC at a wavelength of 214nM.

Biological evaluation

Table 3-5 summarizes the pharmacology at the mouse melanocortin receptors, mMC1R, mMC3R, mMC4R, and mMC5R of the 27 tetrapeptides modified at the Phe seven position (α-MSH numbering) of the tetrapeptide template, Ac-His-Xaa-Arg-Trp-NH_2, prepared in this study. The compounds that did not show agonist activity, >100,000nM EC_{50} values in Table 3-4, were tested for antagonism at up to 10μM concentrations (data not shown).

Table 3-5. Functional activity of the Phe[7] modified tetrapeptides at the mouse melanocortin receptors

		mMC1R		mMC3R		mMC4R		mMC5R	
Peptide	**Structure**	EC_{50} (nM)	Fold Difference	EC_{50} (nM)	Fold Difference	EC_{50} (nM)	Fold Difference	EC_{50} (nM)	Fold Difference
α-MSH	Ac-Ser-Tyr-Ser-Met-Glu-His-Phe-Arg-Trp-Gly-Lys-Pro-Val-NH_2	0.55±0.09		0.79±0.14		5.37±0.62		0.44±0.09	
NDP-MSH	Ac-Ser-Tyr-Ser-Nle-Glu-His-DPhe-Arg-Trp-Gly-Lys-Pro-Val-NH_2	0.038±0.012		0.098±0.013		0.21±0.03		0.071±0.012	
MTII	Ac-Nle-c[Asp-His-DPhe-Arg-Trp-Lys]-NH_2	0.020±0.003		0.16±0.03		0.087±0.008		0.16±0.03	
1	Ac-His-DPhe-Arg-Trp-NH_2	20.1±0.57	1	156±9.2	1	17.2±2.80	1	3.96±0.94	1
19	Ac-His-**Ala**-Arg-Trp-NH_2	30,000±6,100	1,490	>100,000		>100,000		>100,000	
20	Ac-His-**(pI)DPhe**-Arg-Trp-NH_2	60.4±13.4	3	Partial Agonist pA_2=7.25±0.18	**Antagonist**	25.0±9.78	1	1.60±0.35	-2
21	Ac-His-**homoPhe**-Arg-Trp-NH_2	33,100±8,300	1,650	>100,000		>100,000		11,800±4,700	2,980
22	Ac-His-**homoDPhe**-Arg-Trp-NH_2	6,250±2,000	310	>100,000		11,100±2,000	645	2,800±780	700
23	Ac-His-**Tyr**-Arg-Trp-NH_2	61,400±17,10	3,050	>100,000		>100,000		32,700±9,400	8,260
24	Ac-His-**DTyr**-Arg-Trp-NH_2	3,200±1,300	159	34,000±5,000	218	2,400±690	140	631±97	159
25	Ac-His-**Trp**-Arg-Trp-NH_2	33,400±10,70	1,660	>100,000		34,300±7,900	1,990	18,400±6,800	4,650
26	Ac-His-**DTrp**-Arg-Trp-NH_2	25,100±15,00	1,250	>100,000		>100,000		6,950±1,780	1,760
27	Ac-His-**Phg**-Arg-Trp-NH_2	14,700±2,000	731	44,000±13,700	282	40,500±9,300	2,360	4,000±1,300	1,010
28	Ac-His-**DPhg**-Arg-Trp-NH_2	16,900±3,200	841	>100,000		>100,000		Slight Agonist @ 100 μM	
29	Ac-His-**Nal(1')**-Arg-Trp-NH_2	15,200±3,100	756	>100,000		>100,000		11,200±2,300	2,830
30	Ac-His-**DNal(1')**-Arg-Trp-NH_2	356±64	18	4,100±1,000	26	303±65	18	51.4±4.07	13
31	Ac-His-**Nal(2')**-Arg-Trp-NH_2	22,000±5,600	1,100	>100,000		>100,000		7,400±1,800	1,870
32	Ac-His-**DNal(2')**-Arg-Trp-NH_2	167±41	8	Partial Agonist pA_2=6.53±0.09	**Antagonist**	pA_2=7.78±0.18	**Antagonist**	34.7±6.75	9
33	Ac-His-**Dip**-Arg-Trp-NH_2	19,000±7,100	945	>100,000		>100,000		>100,000	
34	Ac-His-**DDip**-Arg-Trp-NH_2	1,500±280	75	>100,000		5,000±750	291	4,300±695	1,090
35	Ac-His-**Tic**-Arg-Trp-NH_2	53,600±13,60	2,670	>100,000		>100,000		21,300±9,700	5,380
36	Ac-His-**DTic**-Arg-Trp-NH_2	40,800±19,90	2,030	>100,000		>100,000		>100,000	
37	Ac-His-**Bip**-Arg-Trp-NH_2	10,600±3,700	527	>100,000		Slight Agonist @ 100 μM		5,500±2,300	1,390
38	Ac-His-**DBip**-Arg-Trp-NH_2	28.4±11.4	1	2,050±734	13	68.4±15.8	4	11.6±3.92	3
39	Ac-His-**His**-Arg-Trp-NH_2	41,700±19,20	2,080	>100,000		>100,000		41,200±14,40	10,400
40	Ac-His-**3Pal**-Arg-Trp-NH_2	22,900±1,200	1,140	>100,000		>100,000		36,100±9,300	9,100
41	Ac-His-**4Pal**-Arg-Trp-NH_2	36,700±10,10	1,830	>100,000		24,400±2,000	1,420	9,700±1,500	2,450
42	Ac-His-**Atc**-Arg-Trp-NH_2	2,350±930	117	9,900±2,900	63	1,780±163	103	263±81	66
43	Ac-His-**Atc**-Arg-Trp-NH_2	5,800±2,070	289	7,800±1,300	50	7,130±1,400	415	2,070±657	523
44	Ac-His-**Phe**-Arg-Trp-NH_2	5,190±2320	258	16600±5780	106	513±78.9	30	596±137	151

The indicated errors represent the standard error of the mean determined from at least four independent experiments. Slight agonist denotes that some stimulatory response was observed but not enough to determine an EC_{50} value. Compounds possessing >100,000 EC_{50} values were not found to possess antagonist properties at up to 10μM concentrations.

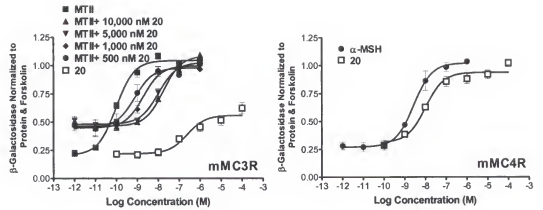

Figure 3-8. Illustration of the tetrapeptide **20** possessing partial agonist and antagonist pharmacology at the mouse MC3R and agonist pharmacology at the mouse MC4R. The endogenous agonist for the melanocortin receptors, α-MSH, is only 5-fold more potent at the mMC4R than tetrapeptide **20**, Ac-His-(pI)DPhe-Arg-Trp-NH_2.

Tetrapeptide **1**, Ac-His-DPhe-Arg-Trp-NH_2, is the lead peptide for this study. Substitution of DPhe for the L-stereoisomer (peptide **44**) resulted in 258-, 106, 30-, and 151-fold decreased potency at the mMC1R, mMC3R, mMC4R, and mMC5R, respectively. Replacement of DPhe with Ala in peptide **19** resulted in the inability to stimulate the MC3, MC4, and MC5 receptors and a 1500-fold decreased potency at the MC1R. The (pI)DPhe[7] containing tetrapeptide **20** maintained equipotency at the mMC1R, mMC4R, and mMC5R (within the inherent 3-fold experimental error) with DPhe[7] (**1**), but was a partial agonist possessing potent antagonist activity (pA_2=7.25, Ki=56nM] at the MC3R (Figure 3-8). The homoPhe[7] tetrapeptide **21** resulted in 1650- and 2980-fold decreased potencies at the mMC1R and mMC5R, respectively, compared with **1**, but were not able to stimulate the mMC3 and mMC4 receptors at up to 100μM concentrations. The homoDPhe[7] tetrapeptide **22** resulted in only 310-, 645, and 700-fold decreased potency at the mMC1R, mMC4R, and mMC5R, respectively, compared with **1**, and similar to the homoPhe containing tetrapeptide **21** was unable to stimulate the

mMC3R at up to 100μM concentrations. The Phg^7 tetrapeptide **27**, which contains one less CH_2 in the side chain length than Phe, resulted in 731-, 282-, 2360-, and 1010-fold decreased potency compared with the Phe^7 tetrapeptide **1** at the mMC1R, mMC3R, mMC4R, and mMC5R, respectively. Tetrapeptide **28** ($DPhg^7$) resulted in 841-fold decreased mMC1R potency compared with **1**, and possessed only slight agonist activity (at 100μM) at the mMC5R, and was unable to stimulate either the mMC3 or mMC4 receptors. The Nal(1')7 containing tetrapeptide **29** possessed 756-fold decreased potency at the mMC1R and 2830-fold decreased mMC5R potency compared with $DPhe^7$ (**1**), and did not stimulate the mMC3R or mMC4R. However, the $DNal(1')^7$ tetrapeptide **30** resulted in only slightly decreased potency (13- to 26-fold) compared with **1**, at the mMC1-5 receptors. Tetrapeptide **31**, containing Nal(2') at the Phe position, resulted in an equipotent decreased potency at the mMC1R (1100-fold) and mMC5R (1870-fold) compared with **1**, and was also unable to stimulate the mMC3 and mMC4 receptors. The tetrapeptide Ac-His-DNal(2')-Arg-Trp-NH_2 (**32**) resulted in 8- and 9-fold decreased agonist potency at the mMC1R and mMC5R, respectively, compared with **1**; and was a partial agonist with antagonist activity at the mMC3R (pA_2=6.5, Ki=295nM) and a mMC4R antagonist (pA_2=7.78, Ki=17nM), see Figure 3-9 below. The Tic^7 containing tetrapeptide **35** resulted in 2670-fold decreased mMC1R potency and 5380-fold decreased mMC5R potency compared with **1,** and was unable to stimulate the mMC3 and mMC4 receptors. Tetrapeptide **36** ($DTic^7$) possessed 2030-fold decreased mMC1R potency compared with the $DPhe^7$ tetrapeptide **1**, and did not stimulate the mMC3-5 receptors at up to 100μM concentrations. Tetrapeptide **37**, containing the Bip amino acid in the Phe position, resulted in 527-fold decreased mMC1R potency and 1390-fold

decreased mMC5R potency compared with **1**; and possessed slight agonist activity at the mMC4R (100μM) but was unable to stimulate the mMC3R. Interestingly, DBip[7] (**38**) was equipotent with **1** at the mMC1R, mMC4R, and mMC5R (within experimental error), but was 13-fold less potent at the mMC3R. Incorporation of the racemic Atc amino acid into the tetrapeptide template resulted in the separation of two separate peaks by RP-HPLC, designated peptides **42** and **43**. Tetrapeptide **42**, the first Atc containing peptide eluted by RP-HPLC resulted in 63-fold decreased potency at both the mMC3R and mMC5R, and 103-fold decreased potency at the mMC1R and mMC4R compared with **1**. Tetrapeptide **43**, the second Atc[7] peptide eluted from the column, resulted in 50-fold decreased mMC3R potency, 289-fold decreased mMC1R potency, 415-fold decreased mMC4R potency, and 523-fold decreased mMC5R potency, compared with the DPhe[7] containing tetrapeptide **1**.

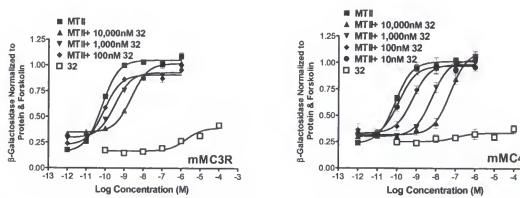

Figure 3-9. Illustration of tetrapeptide **32**, Ac-His-DNal(2')-Arg-Trp-NH_2, antagonist pharmacology at the mMC3 and mMC4 receptors. Slight agonism is observed for **32** at the mMC3R at greater than 1μM concentrations.

Discussion

Mouse melanocortin-1 receptor

The peripheral skin melanocortin receptor, MC1R, is involved in human skin pigmentation[26,27] and animal coat coloration.[27] Interestingly, all the substitutions at the

DPhe position of the tetrapeptide Ac-His-DPhe-Arg-Trp-NH_2 (**1**) were tolerated by the mMC1R (Table 3-5), unlike the pharmacology of these compounds at the mMC3R and mMC4R. As expected, peptide **1** with the D-isomer of Phe was 260-fold more potent than the L-isomer in peptide **44**. Interestingly, the Ala^7 tetrapeptide **19** retained functional activity at the MC1R, albeit with a 1500-fold drop in potency, suggesting that the aromatic phenyl ring is not critical for mMC1 receptor stimulation. Incorporation of homoPhe (**21**), Tyr (**23**), Trp (**25**), DTrp(**26**), Nal(2') (**31**), Tic (**35**), DTic (**36**), His (**39**), 3Pal (**40**), and 4Pal (**41**) at the Phe position in the tetrapeptides resulted in approximately the same fold decreased potency as the Ala containing tetrapeptide **19.** The most potent Phe substitution (peptide **38**) in the tetrapeptide template is the DBip amino acid (Figure 3-7), and resulted in equipotent mMC1R activity compared with the lead tetrapeptide **1**. Tetrapeptides possessing nM mMC1R agonist activity include the (pI)DPhe (**20**), DNal(2') (**32**), and DNal(1') (**30**) amino acid substitutions at the Phe position. Interestingly, melanocortin peptides that possess the $(pI)DPhe^7$ substitution have been reported as melanocortin antagonists at putative MC1 receptors. For example, SHU8914 [$(pI)DPhe^7$] was a potent (pA_2=10.3) antagonist in the frog skin bioassay (putative MC1R), but was a potent agonist at both the mouse and human MC1 receptors.[88]

Receptor mutagenesis and GPCR homology molecular modeling studies of the MC1R have identified a putative hydrophobic receptor pocket consisting of multiple Phe receptor residues that are proposed to interact with the melanocortin ligand Phe amino acid.[124,141,159] The tetrapeptides reported herein that possessed nM agonist pharmacology (**1, 20, 31, 32,** and **38**) consisted of a D-configured amino acid derivative with either a phenyl, bi-phenyl, or naphthyl moiety. These data are consistent with the receptor

mutagenesis and modeling studies, suggesting that an aromatic network of interactions is formed between the melanocortin agonist DPhe amino acid and multiple Phe residues of the MC1 receptor.

Mouse melanocortin-3 receptor

The MC3R is expressed both peripherally and centrally and appears to be involved in metabolism and energy homeostasis.[31,32,58,59] Substitution of the Phe^7 residue of the lead tetrapeptide by Ala resulted in loss of agonist activity at up to 100μM concentrations. This result is similar to the result of replacement of DPhe with Ala at the seven position of the cyclic MTII template, which only had 19% total binding at 10μM and 2% agonist stimulation at 20μM concentrations at the human MC3R.[139] Additionally, substitution of the Phe^7 residue with either homoPhe, DhomoPhe, Tyr, Trp, DTrp, DPhg, Nal(1'), Nal(2'), Dip, DDip, Tic, DTic, Bip, His, 3Pal, and 4Pal (Figure 3-7) resulted in loss of agonist activity at up to 100μM concentrations (Table 3-4). These data suggest that the aromatic ring is required in the correct size and orientation for functional activity at the mMC3R. Incorporation of the (pI)DPhe amino acid in tetrapeptide **20** resulted in a partial mMC3R agonist with potent antagonist activity (pA_2=7.25), which corresponded to a K_i value of 56nM (Figure 3-8). This result is similar to previous studies that incorporated the (pI)DPhe substitution in either the cyclic MTII template (SHU8914, hMC3R pA_2=8.3, K_i =5nM)[88] or the linear NDP-MSH template (SHU9005, mMC3R pA_2 ca 9.0, unpublished results C. Haskell-Luevano, V.J. Hruby, and R.D. Cone), which led to partial agonistic in addition to MC3R antagonistic pharmacology. The tetrapeptide Ac-His-DNal(2')-Arg-Trp-NH_2 (**32**) is also a mMC3R antagonist (pA_2=6.53, K_i =295nM) that possessed slight agonist activity, albeit much less than the agonist response of peptide **20**, at concentrations greater than 1μM (Figure 3-9). The DNal(2') substitution

for that of Phe in the cyclic MTII template resulted in the identification of the first MC3R antagonist (slight partial agonist activity).[88] Subsequently, this DNal(2') substitution in several other cyclic melanocortin templates also resulted in antagonists of the MC3 receptor.[131,136,156,162] The most potent agonist tetrapeptides substituted at the Phe position reported herein include the DBip[7] (**38**) and the DNal(1')[7] (**30**) containing molecules that are only 13- and 26-fold less potent that the DPhe tetrapeptide **1** at the mMC3R.

Mouse melanocortin-4 receptor

The central MC4R has been identified as physiologically participating in food consumption and obesity in mice[63,90] with several polymorphisms of the MC4R observed in obese humans.[66,67,144,145,147,163,164] Similar to activity at the mMC3R, substitution of the Phe benzyl side chain with a methyl group of Ala (**19**) resulted in a loss of a functional response at the mMC4R. Interestingly, when the DPhe of the linear thirteen amino acid NDP-MSH peptide was replaced with a DAla, only ca 1200-fold decreased binding and agonist potency was reported at the human MC4R.[141] In a separate report, replacement of DPhe with Ala at the seven position of the cyclic MTII template resulted in only 13% total binding at 10μM and 32% agonist stimulation at 20μM concentrations at the human MC4R.[139] Substitution of the Phe amino acid with homoPhe (**21**), Tyr (**23**), DTrp (**26**), DPhg (**28**), Nal(1') (**29**), Nal(2') (**31**), Dip (**33**), Tic (**35**), DTic (**36**), His (**39**), and 3Pal (**40**) resulted in a loss of agonist activity at up to 100μM concentrations. Tetrapeptide **37** containing the Bip amino acid instead of DPhe (**1**) possessed slight agonist activity at up to 100μM concentrations at the mMC4R, but not enough agonist response to determine an EC_{50} value. Substitutions of the DPhe (**1**) residue in the tetrapeptide template resulting in nM mMC4R agonist potency include the (pI)DPhe (**20**), DBip (**38**), and DNal(1') (**30**) amino acids. These later results suggest that substitution of the DPhe residue in

melanocortin small molecules by either the (pI)DPhe, DNal(1') or DBip amino acids may result in non-peptide compounds possessing similar MC4R agonist potency as homologous compounds containing the DPhe moiety. Surprisingly, tetrapeptide **20** containing the (pI)DPhe^7 amino acid resulted in a potent mMC4R agonist (EC_{50}=25nM) that is only 5-fold less potent than α-MSH (Table 3-5). This is an unexpected result, as antagonist pharmacology was predicted based on previous results reported in the literature. Previous studies incorporating a para-iodo-Phe at the seven position in both the seven amino acid MTII cyclic template, SHU8914,[88] and the linear thirteen amino acid NDP-MSH template, SHU9005,[124] resulted in potent antagonism (pA_2=9.7, Ki=0.2nM) at the human and mouse MC4 receptors. Since the tetrapeptide (**20**) containing the (pI)DPhe^7 residue is a potent MC4R agonist at the mouse receptor, we further examined this peptide using the human MC4R clone. Full agonist activity with 4nM potency (data not shown) was observed at the human MC4R. Thus, the agonist pharmacology for compound **20** does not appear to be species specific (human versus mouse). It is therefore interesting to speculate that differences in antagonist activity of the larger (pI)DPhe^7 containing peptides, versus agonist activity of the tetrapeptide reported herein, may be attributed to the additional amino acids at the N- and C-terminal. Presumably, the additional residues may be modifying the secondary structure and/or topography of how these ligands interact with the putative MC4 receptor binding pocket. The first MC4R antagonist, named SHU9119, was discovered by the subtle substitution of the Phe^7 residue by that of a DNal(2') amino acid.[88] As predicted, tetrapeptide **32** containing DNal(2')^7 resulted in a mMC4R antagonist (pA_2=7.8, K_i=17nM). The antagonist dose response curves are shown in Figure 3-9.

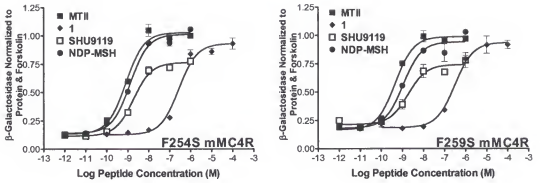

Figure 3-10. Comparison of the mMC4R agonist peptides MTII, NDP-MSH and **1** (Ac-His-DPhe-Arg-Trp-NH_2) and the mMC4R antagonist SHU9119 at the mutant F254S and F259S mMC4 receptors. The SHU9119 peptide possesses partial agonist activity at these mutant receptors versus possessing competitive antagonist pharmacology at the wild-type mMC4R.

Receptor mutagenesis studies of the mouse MC4R identified mutations in the putative TM6 domain that converted the SHU9119 and SHU9005 MC4R antagonists into agonists.[124] Interestingly, these two mutant receptors, F254S mMC4R and F259S mMC4R, did not result in conversion of the endogenous antagonist hAGRP(83-132) into a ligand possessing agonist activity, nor did the hAGRP(109-118) decapeptide result in any agonist activity at these two mutant receptors. Figure 3-10 shows the agonist pharmacology of the MTII, NDP-MSH, tetrapeptide **1** presented herein, and the partial agonist activity of the SHU9119 MC4R antagonist at these F254S and F259S mutant mMC4 receptors. Based on these results, we hypothesized that the F254 and F259 residues are responsible for differentiating agonists versus antagonist activity of melanocortin sequence based ligands (i.e., SHU9119 and SHU9005) versus the endogenous antagonist AGRP(83-132). To further test this hypothesis, we tested the tetrapeptide **32**, Ac-His-DNal(2')-Arg-Trp-NH_2, at these F254S and F259S mutant mMC4 receptors to determine if the ligand would possess pharmacology similar to the

melanocortin based antagonist SHU9119. Figure 3-11 summarizes the pharmacology of the DNal(2') containing tetrapeptide **32** at the F254S and F259S mMC4Rs, that resulted in agonist activity of the compound **32** that is a competitive antagonist at the wild-type mMC4R (Figure 3-9). These data support our previous hypothesis that the mMC4R Phe 254 and 259 residues in the putative TM6 domain interact with the melanocortin DNal(2') amino acid, which is substituted for the DPhe amino acid in the agonists.[124]

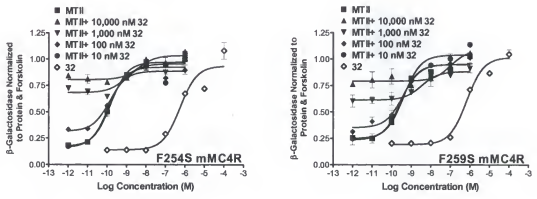

Figure 3-11. Illustration of the tetrapeptide **32**, Ac-His-DNal(2')-Arg-Trp-NH_2, pharmacology at the mutant F254S and F259S mouse MC4 receptors. Similarly to the SHU9119 peptide, this DNal(2')[7] containing tetrapeptide results in agonist pharmacology at these two mutant mMC4 receptors, whereas at the wild-type mMC4R (Figure 3-9) competitive antagonist pharmacology results.

Mouse melanocortin-5 receptor

The peripheral MC5R is expressed in a variety of tissues and has been implicated as physiologically participating in the role of exocrine gland function.[71,149,150] Similarl to results at the mMC3 and mMC4 receptors, tetrapeptide, **19** containing Ala instead of the DPhe amino acid at the seven position, results in a loss of determinable EC_{50} value at up to 100μM concentrations at the mMC5R. Tetrapeptide **36**, containing the DTic[7], was the only compound in addition to **19** that lost agonist activity at up to 100μM concentrations, although **28** (DPhg) resulted in only slight agonist activity at up to 100μM

concentrations. It has been previously reported that replacement of DPhe with Ala at the seven position of the cyclic MTII template resulted in only 14% total binding at 10μM and 5% agonist stimulation at 10μM concentrations at the human MC5R.[139] Tetrapeptides possessing nM mMC5R agonist potencies include the (pI)DPhe (**20**), DTyr (**24**), DNal(1') (**30**), DNal(2') (**32**), DBip (**38**), and Atc (peak 1, **42**) amino acids. These results suggest that modification of the $DPhe^7$ position by the (pI)DPhe, DBip, and possibly the DNal(2') amino acids in small non-peptidic molecules may result in similar mMC5R agonist potency as homologous compounds containing the $DPhe^7$ residue. Substitution of the DPhe with the DNal(2') amino acid in a variety of melanocortin peptide templates resulted in mMC5R agonist activities ranging from nM to μM, depending upon the template used.[131,156,162] Amino acid substitutions of the DPhe in this tetrapeptide template that resulted in significantly decreased mMC5R agonist potencies include the homoPhe, Tyr, Trp, DPhg, Nal(1'), Tic, His, and 3Pal amino acids, all of which appear to be less tolerated in this position at the MC5 receptor than DPhe.

Modification of the Arg^8 Position

The Arg side chain contained within the conserved melanocortin agonist ligand "His-Phe-Arg-Trp" sequence has been previously thought to play an important role in melanocortin receptor stimulation.[35,165,166] Replacement of Arg^8 by Ala^8 in the native α-MSH peptide agonist resulted in 2000-fold decreased binding affinity in mouse B16 melanoma cells (presumably the MC1R).[128] Substitution of Arg^8 by Pro^8 in the MTII peptide template resulted in only 2% to 7% cAMP stimulation at a concentration of 2μM,[133] Upon substituting Glu^8 for Arg^8 in the α-MSH peptide, 4000- and 2500-fold decreased agonist potency was observed at the hMC3R and hMC4R while only a 14%

maximal response was observed at the hMC5R at a concentration of 5μM, clearly indicating the importance of the Arg^8 side chain for melanocortin receptor potency.[143] Substitution of the Arg^8 by Ala in the MTII template resulted in 138- and 282-fold decreased potency, compared with MTII, at the human MC3 and MC4 receptors.[139] Modification of the Arg^8 amino acid by Ala, Gly, and Lys in the tripeptide Ac-DPhe-Xaa-DTrp-NH_2 resulted in ligands that possessed a decrease in the length of prolonged activity (in the absence of ligand) in the classical *Rana pipiens* frog skin bioassay, compared with the Arg^8 containing peptide,[167] further supporting the importance of the Arg side chain for melanocortin receptor pharmacology. Homology molecular modeling of the MC1R resulted in the identification of the putative melanocortin receptor binding pocket including a hydrophobic portion in which the ligand Phe^7 and Trp^9 amino acids were proposed to interacted, and a hydrophilic pocket in which the ligand Arg^8 was proposed to interact (Figure 3-12).[159]

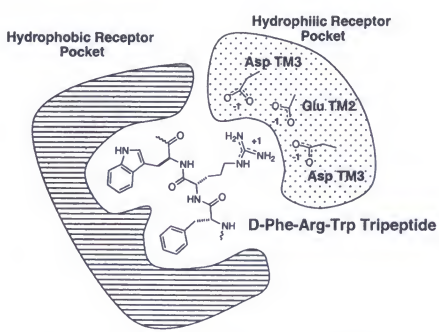

Figure 3-12. Illustration of the melanocortin agonist amino acids DPhe-Arg-Trp in the putative melanocortin receptor binding pocket.

Naturally occurring polymorphisms in the MC1R of several animal species including mice, chicken and fox, were identified that resulted in constitutively active receptors and hence dark animal coat colors.[142] Interestingly, several mutations resulting in constitutively active MC1 receptors occurred in the putative transmembrane spanning domains (TM) 2 and 3 that were postulated to be involved in the melanocortin ligand Arg residue binding to the MC1R (Figure 3-13).[142,159-161] Key evidence in suggesting the hypothesis that the two Asp receptor residues in TM3 and a Glu receptor residue in TM2 (Figure 3-13) are involved in interacting with the melanocortin agonist ligands is that these three amino acids are conserved in all the melanocortin receptors, MC1R-MC5R,[150]. Additionally, genetic analysis of the somber mouse (dark coat color) identified the TM2 Glu was mutated to Lys in the receptor and this resulted in a constitutively active MC1R, providing a possible molecular mechanism for the dark coat color.[168] Interestingly, when the TM2 Glu is mutated to Lys a constitutively active receptor results with a basal cAMP activity of 50% the maximal response; and when this Glu is mutated to an Arg, nearly 100% maximal cAMP activity is observed in the absence of ligand.[142] These compelling MC1R genetic and mutagenesis studies support the hypothesis that upon substitution of the TM2 Glu to amino acids that resemble the Arg residue of melanocortin ligands, constitutively active receptors result, suggesting that these receptor mutations may be mimicking the ligand Arg side chain-receptor interactions important for melanocortin receptor stimulation. Independent melanocortin receptor mutagenesis studies of the MC1R and MC4R also support the concept of a hydrophilic receptor pocket in which the ligand Arg side chain is interacting with the Asp amino acids in TM3 and the Glu residue in TM2 (Figure 3-13).[124,141,142,160]

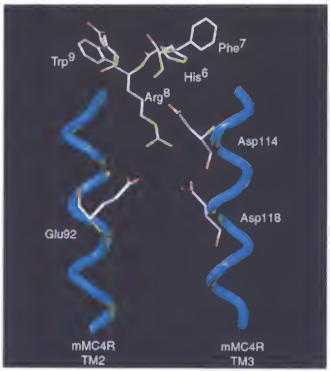

Figure 3-13. Illustration of the putative ionic interactions between the melanocortin agonist Arg^8 residue and the acidic residues of the mouse MC4R transmembrane regions. Oxygen atoms are represented in red and nitrogen atoms are represented in yellow for clarity.

However, other studies of melanocortin ligand substitutions at the Arg position suggest that this side chain may not be as critical for melanocortin receptor activation as previously thought. For example, Glu^8 substitution for Arg^8 in the NDP-MSH peptide template only resulted in 90-fold decreased hMC3R and hMC4R potency compared to NDP-MSH at these receptors that may suggest that, in combination with the $DPhe^7$, the Arg^8 side chain plays a less dramatic role for melanocortin receptor potency.[143] Surprisingly, the non-peptide β-turn MC1R agonist molecules EL1, containing a Pro moiety in the i+2 position, and EL2, with Lys in the i+2 position were nearly equipotent MC1R μM agonists.[169] This study was undertaken to examine the role of chain length, acidic or basic functionalities, and the effect of Ala and Pro modifications at the

melanocortin ligand Arg^8 position and determine if any of these modifications result in melanocortin receptor selectivity at the mouse MC1R, MC3R, MC4R, and MC5R.

Results

Chemical synthesis and characterization

The peptides reported herein were synthesized using standard fluorenylmethyloxycarbonyl (Fmoc)[97,98] chemistry and a parallel synthesis strategy on an automated synthesizer (Advanced ChemTech 440MOS, Louisville, KY). The peptides were purified to homogeneity using semi-preparative reversed-phase high pressure liquid chromatography (RP-HPLC). The purity of these peptides was assessed by mass spectrometry (Table 3-6), analytical RP-HPLC in two diverse solvent systems (Table 3-6), and one-dimensional ^1H NMR (Appendix A).

Table 3-6. Analytical data for the Arg^8 modified tetrapeptides synthesized in this study

Peptide	Structure	HPLC k' (System 1)	HPLC k' (System 2)	M+1 (Calculated)	(M+1) (Experimental)	Purity
1	Ac-His-DPhe-Arg-Trp-NH_2	3.9	6.9	686.8	686.3	>98%
45	Ac-His-DPhe-**DArg**-Trp-NH_2	4.1	6.8	686.8	686.6	>96%
46	Ac-His-DPhe-**Ala**-Trp-NH_2	4.9	7.2	600.7	600.6	>99%
47	Ac-His-DPhe-**Pro**-Trp-NH_2	5.7	7.2	626.7	626.8	>99%
48	Ac-His-DPhe-**homoArg**-Trp-NH_2	4.1	6.6	700.8	700.9	>99%
49	Ac-His-DPhe-**Cit**-Trp-NH_2	4.1	6.8	687.8	686.9	>98%
50	Ac-His-DPhe-**Lys**-Trp-NH_2	3.8	6.5	657.8	658	>99%
51	Ac-His-DPhe-**Orn**-Trp-NH_2	3.9	7.2	643.7	644	>99%
52	Ac-His-DPhe-**Dab**-Trp-NH_2	3.9	7.2	629.7	630	>99%
53	Ac-His-DPhe-**Aaa**-Trp-NH_2	4.5	7.2	672.7	672.9	>99%
54	Ac-His-DPhe-**Asp**-Trp-NH_2	4.3	7.2	644.7	645.1	>99%
55	Ac-His-DPhe-**Glu**-Trp-NH_2	4.3	7.2	658.7	659.1	>99%

HPLC k' = [(peptide retention time - sovent retention time) / solvent retention time] in solvent system 1 (10% acetonitrile in 0.1% trifluoroacetic acid/ water and a gradient to 90% acetonitrile over 35 min) or solvent system 2 (10% methanol in 0.1% trifluoroacetic acid/ water and a gradient to 90% methanol over 35 min). An analytical Vydac C18 column (Vydac 218TP104) was used with a flow rate of 1.5 mL/min. The peptide purity was determined by HPLC at a wavelength of 214nM.

Biological evaluation

Table 3-7 summarizes the pharmacology at the mouse melanocortin receptors, mMC1R, mMC3R, mMC4R, and mMC5R of the tetrapeptides modified at the Arg^8

position (α-MSH numbering) of the tetrapeptide template, Ac-His-DPhe-Xaa-Trp-NH_2, prepared in this study. The compounds that did not show agonist activity, >100,000nM EC_{50} values in Table 3-7, were tested for antagonism at up to 10μM concentrations (data not shown).

Mouse melanocortin-1 receptor. The peripheral skin melanocortin receptor, MC1R, is involved in human skin pigmentation[26,27] and animal coat coloration.[142] The lead tetrapeptide **1**, Ac-His-DPhe-Arg-Trp-NH_2, has been previously reported to possess 25nM stimulatory activity at the mMC1R,[78] an EC_{50} value of 200nM in the classical *Rana pipiens* frog skin assay (putative MC1R),[77] and possesses a mMC1R EC_{50} =20nM reported herein. Substitution at the Arg^8 position within this tetrapeptide by DArg, Ala, Pro, homoArg, Cit, Lys, Orn, Dab, Aaa, Asp, and Glu (Figure 3-14) resulted in derivatives that were equipotent to **1** or exhibited up to 2500-fold decreased mMC1R potency. Inversion of chirality of Arg to DArg (**45**) resulted in 177-fold decreased mMC1R potency compared with **1**. Substitution of the guanidinyl moiety of Arg with the methyl of Ala (**46**) resulted in a 3.4μM mMC1R agonist (170-fold decreased potency compared with **1**). Incorporation of Pro (**47**) into the 8 position resulted in 1.9μM agonist mMC1R potency and only 95-fold decreased potency compared with **1**. Elongation of the Arg side chain by one CH_2 group in the homoArg tetrapeptide **48** resulted in an 8nM agonist with a slight increase in mMC1R potency, compared with **1**. Substitution of the guanidinyl moiety with a urea type moiety in Cit (**49**) resulted in μM agonist activity and was 190-fold less potent than the guanidinyl containing side chain **1**. Upon incorporation of the Lys side chain (**50**) in the eight position, only a 38-fold decrease in mMC1R potency resulted compared with **1**. However, upon decreasing the Lys side chain length

Table 3-7. Functional activity of the Arg^8 modified tetrapeptides at the mouse melanocortin receptors

		mMC1R		mMC3R		mMC4R		mMC5R	
Peptide	**Structure**	EC_{50} (nM)	Fold Difference	EC_{50} (nM)	Fold Difference	EC_{50} (nM)	Fold Difference	EC_{50} (nM)	Fold Difference
α-MSH	Ac-Ser-Tyr-Ser-Met-Glu-His-Phe-Arg-Trp-Gly-Lys-Pro-Val-NH_2	0.55±0.09		0.79±0.14		5.37±0.62		0.44±0.09	
NDP-MSH	Ac-Ser-Tyr-Ser-Nle-Glu-His-DPhe-Arg-Trp-Gly-Lys-Pro-Val-NH_2	0.038±0.012		0.098±0.013		0.21±0.03		0.071±0.012	
MTII	Ac-Nle-c[Asp-His-DPhe-Arg-Trp-Lys]-NH_2	0.020±0.003		0.16±0.03		0.087±0.008		0.16±0.03	
1	Ac-His-DPhe-Arg-Trp-NH_2	20.1±0.57	1	156±9.2	1	17.2±2.80	1	3.96±0.94	1
45	Ac-His-DPhe-**DArg**-Trp-NH_2	3,600±1,600	177	17,400±5,800	112	3,240±880	180	612±190	155
46	Ac-His-DPhe-**Ala**-Trp-NH_2	3,400±1,600	169	42,000±8,900	269	23,000±4,100	1,340	6,900±1,500	1,740
47	Ac-His-DPhe-**Pro**-Trp-NH_2	1,900±1,000	95	>100,000		18,700±4,400	1,090	46,700±11,80	11,800
48	Ac-His-DPhe-**homoArg**-Trp-NH_2	7.80±0.9	-2.5	2,400±200	15	42.7±7.60	2.5	17.2±3.0	4
49	Ac-His-DPhe-**Cit**-Trp-NH_2	3,900±1,500	193	11,200±5,300	72	2,300±760	134	195±7.4	49
50	Ac-His-DPhe-**Lys**-Trp-NH_2	770±500	38	25,500±1,900	163	830±140	48	320±14	80
51	Ac-His-DPhe-**Orn**-Trp-NH_2	6,100±2,200	303	55,600±2,800	356	6,500±1,900	378	540±30	135
52	Ac-His-DPhe-**Dab**-Trp-NH_2	9,300±3,100	463	38,900±5,800	249	3,800±893	221	610±40	154
53	Ac-His-DPhe-**Aaa**-Trp-NH_2	51,900±15,40	2,580	22,300±1,800	143	24,900±7,500	1,450	6,200±1,800	1,570
54	Ac-His-DPhe-**Asp**-Trp-NH_2	43,400±9,700	2,160	>100,000		>100,000		16,400±7,900	4,140
55	Ac-His-DPhe-**Glu**-Trp-NH_2	42,900±9,700	2,130	65,400±9,100	419	15,500±2,200	901	2,000±970	505

The indicated errors represent the standard error of the mean determined from at least four independent experiments. Slight agonist denotes that some stimulatory response was observed but not enough to determine an EC_{50} value. Compounds possessing >100,000nM EC_{50} values were not found to possess antagonist properties at up to 10μM concentrations.

by one CH_2 (Orn, **51**) or two CH_2 groups (Dab, **52**), 300- to 460-fold decreased mMC1R potency resulted compared with **1**, respectively, and only 8- to 12-fold decreased potency resulted compared with Lys (**7**), respectively. Upon incorporation of an acidic side chain, $(CH_2)_nCOOH$, where n=3 (Aaa, **53**), n=1 (Asp, **54**), and n=2 (Glu, **55**) approximately 2100-fold decreased mMC1R potency resulted compared with **1.** Peptides **53-55** are nearly equipotent μM agonists at eh MC1R (Table 3-7).

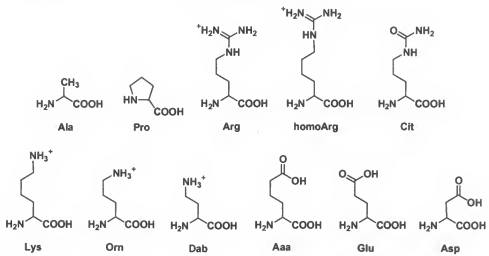

Figure 3-14. Structures of the amino acids used to replace Arg^8 in the tetrapeptide template.

Mouse melanocortin-3 receptor. Substitution at the Arg^8 position within this tetrapeptide by DArg, Ala, Pro, homoArg, Cit, Lys, Orn, Dab, Aaa, Asp, and Glu (Figure 3-14) resulted in 15-fold to a complete loss of stimulatory activity at up to 100μM at the mMC3R. Inversion of chirality from Arg^8 (**1**) to $DArg^8$ (**45**) resulted in a 17μM agonist that has an 112-fold decreased potency at the mMC3R compared with **1**. Removing the guanidinyl side chain functionality of Arg and replacing it with the methyl group of Ala in tetrapeptide **46** resulted in ca 270-fold decreased mMC3R potency, compared with **1**. Substitutions of the Arg in tetrapeptide **1** with Lys (**50**), Orn (**51**), Dab (**52**), Aaa (**53**), and Glu (**55**) resulted in approximately the same μM agonist EC_{50} values at the mMC3R

(within experimental error, Table 3-7), and possessed similar decreased potency as the Ala amino acid (**46**) at the eight position compared to **1**. Incorporation of Pro (**47**) and Asp (**54**) into the Arg position of this Ac-His-DPhe-Xaa-Trp-NH_2 tetrapeptide template resulted in a loss of stimulatory activity at the mMC3R at up to 100μM concentrations. Tetrapeptide **48** containing the homoArg amino acid possessed a 2.4μM mMC3R agonist potency and was only 15-fold less potent than the Arg containing tetrapeptide **1** at this receptor. Incorporation of the Cit side chain (**49**) resulted in 72-fold decreased mMC3R potency compared with **1**.

Mouse melanocortin-4 receptor. The central MC4R has been identified as physiologically contributing to food consumption[90] and obesity in mice[63] with several polymorphisms of the MC4R observed in obese humans. [67,144,145,147,148,164] The lead tetrapeptide in this study, Ac-His-DPhe-Arg-Trp-NH_2 (**1**), was previously reported to possess a 10nM agonist EC_{50} values at the mMC4R,[78] a 8nM[141] and 47nM[143] agonist EC_{50} values at the hMC4R, with a potency at the mMC4R of 17nM reported herein. Substitution at the Arg^8 position within this tetrapeptide by DArg, Ala, Pro, homoArg, Cit, Lys, Orn, Dab, Aaa, Asp, and Glu resulted in derivatives that were equipotent to **1** or had complete loss of stimulatory activity at up to 100μM at the mMC4R. Inversion of chirality at the Cα position of the Arg residue to DArg in tetrapeptide **45** resulted in an 180-fold decrease in mMC4R potency. Substitution of Arg by Cit (**49**), Orn (**51**), and Dab (**52**) resulted in 130- to 380-fold decreased mMC4R potency compared with **1**, which is similar to the result of peptide **45**. Removal of the Arg side chain and incorporation of the Ala amino acid in **46** resulted in 1340-fold decreased mMC4R potency compared with **1**. Similar to **46**, 1000- to 1450-fold decreased mMC4R potency

was observed for the Pro (**47**), Aaa (**53**), and Glu (**55**) containing tetrapeptides compared with **1**. Elongation of the Arg side chain by one CH_2 group in the homoArg containing tetrapeptide **48** resulted in nearly equipotent mMC4R activity with **1** (within experimental error). Substitution of the guanidinyl group by the basic amine of Lys (**50**) resulted in 48-fold decreased potency compared with **1** at the mMC4R. Incorporation of the Asp amino acid in the eight position (**54**) was unable to stimulate the mMC4R at up to 100μM concentrations.

Mouse melanocortin-5 receptor. The peripheral MC5R is expressed in a variety of tissues and has been implicated as physiologically participating in the role of exocrine gland function.[71,149,150] The lead tetrapeptide **1**, Ac-His-DPhe-Arg-Trp-NH_2, has been previously reported to possess a 3.4nM agonist EC_{50} at the mMC5R,[78] a 17% response at a 5μM concentration at the hMC5R,[143] and possesses a 3.9nM EC_{50} at the mMC5R reported herein. Substitution at the Arg^8 position (α-MSH numbering) within this tetrapeptide by DArg, Ala, Pro, homoArg, Cit, Lys, Orn, Dab, Aaa, Asp, and Glu (Figure 3-14) resulted in 4- to 11800-fold decreased mMC5R potency. Conversion of chirality of the Arg amino acid in the tetrapeptide Ac-His-DPhe-Arg-Trp-NH_2 (**1**) to DArg in tetrapeptide **45** resulted in 155-fold decreased mMC5R potency and a 600nM agonist. Substitution in the Arg^8 position by Lys (**50**), Orn (**51**), and Dab (**52**) resulted in similar 300- to 600-fold decreased mMC5R potency compared with **1**.Peptides **50-52** exhibited similar agonist EC_{50} values as the $DArg^8$ containing tetrapeptide **45**, within experimental error. Interestingly, when Ala (**46**) and the acidic Aaa (**53**) side chains were incorporated into the tetrapeptide template, similar 6μM agonist potency resulted, which significanlty decreased mMC5R potency when compared with tetrapeptide **1**. The Pro containing

tetrapeptide **47** resulted in an 11800-fold decreased mMC5R potency compared with **1** and possessed only a 46.7μM EC_{50} value. The homoArg[8] containing tetrapeptide **48** possessed a 17nM agonist potency at the mMC5R and was only 4-fold less potent at this receptor than the lead peptide **1**. Incorporation of the Cit amino acid side chain into the tetrapeptide template at the eight position (**49**) resulted in 50-fold decreased mMC5R potency compared with **1**, and a 195nM agonist EC_{50} value. Substitution of the Arg of tetrapeptide 1 with the acidic amino acids Asp (**54**) and Glu (**55**) resulted in 4140- and 500-fold decreased mMC5R potency, respectively, compared with **1**.

Discussion

Figure 3-15 summarizes the agonist EC_{50} values of the peptides listed in Table 3-7. It has been previously proposed that the primary function of the Arg group of the melanocortin agonist ligands may be to "anchor" the ligand into the receptor in the proper orientation so that the aromatic Phe and Trp ligand residues may make the necessary points of contact with the receptor residues necessary for melanocortin receptor stimulation.[170] In a mMC4 receptor mutagenesis study, ligands based upon the agonist MTII and antagonist SHU9119 templates were substituted with the DNal(1') and Nal(2') amino acids at the Phe seven position (α-MSH numbering), and evaluated at mutant mMC4R receptors where hydrophobic or hydrophilic residues were modified. Surprisingly, the most dramatic differences in pharmacology of these DNal(1')[7], Nal(2')[7] and DNal(2')[7] containing MTII peptide ligands were observed at the hydrophilic TM2 Glu and the two conserved TM3 Asp receptor mutations versus the predicted hydrophobic receptor mutants. These data resulted in the *hypothesis* that the "bulky" aromatic groups at the MTII DPhe[7] position may be affecting the ligand Arg[8] interactions

with the MC4R.[124] A recent report by Yang et al., using chimeric human MC1 and MC4 receptors, identified the TM3 as important for the antagonist activity of SHU9119,[171] further supporting the above hypothesis. Both these hypothesis are consistent with the premise that the melanocortin ligand Arg amino acid is important for melanocortin peptide-receptor molecular recognition and stimulation processes.

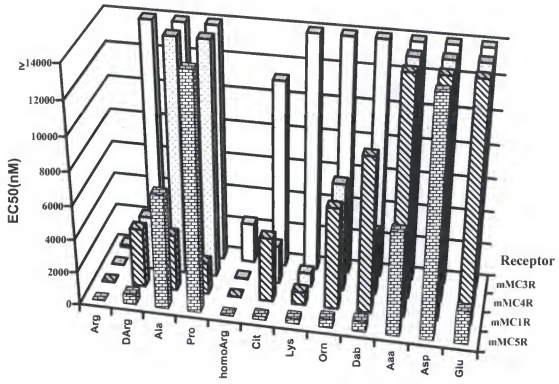

Figure 3-15. Graphical representation summarizing the effect on melanocortin receptor (Y axis) agonist EC_{50} values (Z axis) of the indicated amino acid substitution (X axis) of the Arg residue in the tetrapeptide template.

Proline substitution of the arginine

Previous reports of the melanocortin agonist Arg^8 being replaced by Pro^8 in the MTII peptide template resulted in a dramatic loss of stimulatory activity at melanocortin

receptors.[133] However, in the non-peptide β-turn mimetic molecule EL1, a Pro modification at the homologous peptide Arg position resulted in 42μM MC1R agonist potency (Figure 3-16A).[169] Furthermore, additional non-peptide small molecules based upon a different β-turn template and containing a Pro in the i+2 position resulted in a 4μM MC1R agonist (Figure 3-16B).[172] These data suggested that the Arg side chain may be important for peptide based molecules, where smaller non-peptide molecules may tolerate the loss of the Arg side chain by substituting the constrained Pro residue at the MC1R. To test this hypothesis, the Arg amino acid was replaced by the Pro residue in tetrapeptide **47** (Ac-His-DPhe-Pro-Trp-NH_2). At the mMC1R and MC4R, tetrapeptide **47** was equivalent the Ala substitution (**46**), within experimental error, however **47** was unable to stimulate the mMC3R at up to 100μM concentrations, yet resulted in 7-fold decreased mMC5R potency as compared to **46**. Comparison of tetrapeptide **47** with the non-peptide compound EL1 (EC_{50}= 42μM, Figure 3-16A)[169] at the mMC1R indicate that the tetrapeptide is 22-fold more potent than the EL1 molecule. Comparison of **47** with a second thioether cyclized peptidomimetic molecule containing Pro at the Arg position (EC_{50} = 4.5μM, Figure 3-16B)[172] resulted in nearly equipotent mMC1R agonist ligands. These data support the hypothesis that the Arg side chain is not critical for melanocortin receptor stimulation, but may participate in orientating the aromatic Phe and Trp melanocortin ligand residues into the correct orientation for receptor activation with high potency,[170] at least within the context of small peptidic and non-peptidic MC1R agonists. These data also called into question the importance of the Arg^8 residue in receptor activation, and suggested that the spatial arrangement of hydrophobic side chains may be more important than the presence of an "arginine-like" basic residue.

In addition to the above studies, several groups have recently reported the design and synthesis of novel non-peptide ligands for the melanocortin receptors. Not surprisingly, many of these ligands are based upon recurring structural features found in melanocortin peptides. The Merck research group has reported a potent and receptor selective small molecule agonist for the MC4R.[173] This compound, based on the 4-substituted 4-cyclohexylpiperidine template (Figure 3-16C), is the first literature disclosure of a highly potent non-peptide ligand selective for the MC4R. The compound was found to significantly inhibit food intake[62,173] and increased the erectile response[174] in rodent models, further validating the role of the MC4R in energy homeostasis and erectile activity. This compound does not contain a basic moiety that can mimic the Arg^8 side chain, although the compound is highly potent at the MC4R. This data further suggest that the spatial arrangement of the hydrophobic groups is an important factor in molecular recognition and activation of the melanocortin receptors. The significance of spatial arrangement of the hydrophobic residues may be inferred from a comparison of the low energy conformer of this small molecule with the low energy conformer of MTII. The orientation of the hydrophobic functionalities of this compound is very similar to the orientation of hydrophobic side chains in the low energy conformer of MTII.[173] The scientists at Bristol-Myers Squibb have reported the first highly potent and selective small molecule agonist for the MC1R.[50] This compound is based on a 4-substituted 4-phenylpiperidine template that has many structural features similar to the Merck MC4R selective small molecule (Figure 3-16D), and it also lacks a basic "arginine-like" residue.

Side chain length and charge modifications

Substitution of the Arg^8 melanocortin agonist ligand by amino acids other than Ala, Glu, Nle, and Pro has not been extensively reported at the cloned melanocortin

receptors.[128,133,139,141,143] A previous study at the frog skin melanocortin receptor (presumed to be the MC1R) examined the decreased agonist potency resulting from substituting the Arg residue with Lys, Gln, Ala, and Gly amino acids in the peptide template Ac-DPhe-Xaa-Trp-NH_2.[77] Figure 3-14 shows the amino acid side chain structure for those examined in the Ac-His-DPhe-Xaa-Trp-NH_2 peptide template reported herein. Upon elongation of the Arg^8 side chain by one CH_2 group in the $homoArg^8$ containing tetrapeptide **48**, equipotency was observed at the MC1R and MC4R, a 4-fold decreased potency at the MC5R and a 15-fold decreased potency at the MC3R resulted compared with **1**. Comparison of the chain lengths for the amine containing amino acid substitutions ($-(CH_2)_nNH_3^+$) at the eight position [Lys (**50**) n=4, Orn (**51**) n=3, and Dab (**52**) n=2] resulted in the observation that decreasing the side chain length shorter than the Lys amino acid results in ca 100-fold decreased MC1R potency, equipotency at the MC3R and MC5R, and only 5- to 8-fold decreased MC4R potency. Chain length of the acidic amino acids ($-(CH_2)_nCOO^+$) Aaa (**53**), Asp (**54**) and Glu (**55**) used to replace Arg resulted in nearly equipotent decreased potency for Aaa and Glu at the MC1R, MC3R, and MC4R. The Asp^8 containing tetrapeptide **11** was unable to stimulate the MC3R and MC4R at up to 100μM concentrations, yet was a 43μM MC1R and 16μM MC5R agonist. At the mMC5R, the Asp (n=1) was less potent than the Aaa (n=3) and Glu (n=2) chain lengths. A previous report of the tetrapeptide Ac-His-DPhe-Glu-Trp-NH_2 at the human melanocortin MC3-5 receptors observed slight agonist activities at the hMC3R and hMC5R at 5μM concentrations, and an hMC4R agonist EC_{50} value of 4.3μM which is only 4-fold different than the results reported herein.[143] Generally, the acidic substitutions of the side chains at the eight position appears to be detrimental, and interestingly, more

so than that observed for the Pro and Ala substituted derivatives at the MC1R. This may be a result of charge repulsion effects between the acidic receptor residues in the putative binding pocket and the acidic amino acids of the ligands. The Lys (**50**) substitution of the Arg (**1**) side chain resulted in only 38- and 48-fold decreased potencies at the mMC1R and mMC4R, respectively, and retained high nM potencies at the MC1R, MC4R, and MC5R. Thus, the Lys substitution for the Arg at the eight position appears to be tolerated at the mMC1R, mMC4R, and mMC5R but results in notable decreased receptor agonist potencies. Interestingly, substitution with Cit^8 was reasonably tolerated at each receptor assayed. Cit closely resembles Arg, however it is not charged at physiological pH. These data may indicate that the hydrogen-bonding potential may be more important for receptor stimulation than the positive charge.

Receptor selectivity

Interestingly, nM potencies were observed at the MC1R, MC4R and MC5R while a μM potency resulted at the MC3R (Figure 3-15, Table 3-7) for the homoArg containing compound **48**, suggesting that the addition of the extra CH_2 group in the Arg side chain may be a mechanism for the design of MC4 versus MC3 receptor selectivity. At the mMC3R, the Lys containing tetrapeptide **50** possessed 827nM mMC4R agonist potency while only 25μM agonist mMC3R potency (Figure 3-15. This resulted in 31-fold MC4 versus MC3 receptor selectivity. Comparison of the Orn containing tetrapeptide **51** resulted in ca 120-fold MC5 versus MC4 and MC1 receptor selectivity and ca 100-fold MC5 versus MC3 receptor selectivity.

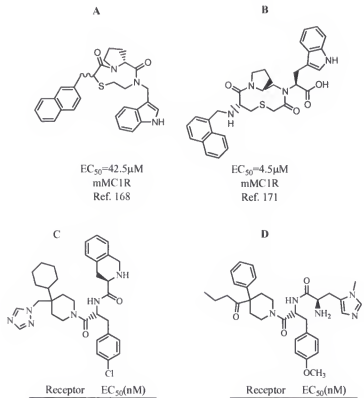

Figure 3-16. Non-peptide melanocortin ligands that do not contain a basic gaunidinyl residue to mimic the Arg^8 peptide residue.

Modification of the Trp^9 Position

The role of the Trp amino acid at the nine position of α-MSH and peptide derivatives has not been previously explored at the cloned melanocortin receptors in extensive detail. Deletion of the Trp residue from the Glu-His-DPhe-Arg-Trp-NH_2 peptide resulted in a ligand that was unable to bind or stimulate the hMC4R.[141] Substitution of the Trp amino acid by Ala or Pro in the cyclic MTII (Ac-Nle-c[Asp-His-DPhe-Arg-Trp-Lys]-NH_2) agonist template resulted in significantly reduced ligand binding affinity and intracellular cAMP stimulation.[133,139] Inversion of chirality at the Trp nine position to the D-configuration in a cyclic melanocortin antagonist template did not

modify potency at the human MC3-5 receptors.[162] Interestingly, substitution of Trp by Nal(2') in a cyclic agonist template resulted in equipotent activity at the hMC3R and hMC4R. This substitution also resulted in the inability to stimulate an agonist response at the hMC5R at up to 5μM,[137] yet resulted in the conversion of a partial agonist to a MC5R antagonist in a different cyclic peptide template.[131] These limited studies implicate an important role of the Trp amino acid for melanocortin receptor binding and functional activity. Putative ligand-receptor interactions involving the ligand Trp amino acid and the melanocortin-1 and -4 receptors have been postulated,[124,159,161] but receptor mutagenesis studies[124,141,160,161] remain inconclusive regarding the specific receptor residues that are interacting with the Trp amino acid of the ligands. This study was undertaken to examine the role of various aromatic, natural, and unnatural amino acids (Figure 3-17) in the Trp position of the tetrapeptide Ac-His-DPhe-Arg-Trp-NH_2 for structure-activity-relationships and selectivity properties at the mouse melanocortin receptors. Furthermore, compounds identified from this study resulting in unique receptor pharmacological properties could potentially be utilized to probe melanocortin ligand-receptor interactions at the Trp position, and could potentially aid in the design of receptor selective small molecules.

Results

Chemical synthesis and characterization

The peptides reported herein were synthesized using standard fluorenylmethyloxycarbonyl (Fmoc)[97,98] chemistry and a parallel synthesis strategy on an automated synthesizer (Advanced ChemTech 440MOS, Louisville, KY). The peptides were purified to homogeneity using semi-preparative reversed-phase high pressure liquid chromatography (RP-HPLC). The purity of these peptides was assessed by mass

spectrometry (table 3-8), analytical RP-HPLC in two diverse solvent systems (table 3-8), and one-dimensional ^{1}H NMR (Appendix A).

Table 3-8. Analytical data for the Trp^9 modified tetrapeptides synthesized in this study.

Peptide	Structure	HPLC k' (System 1)	HPLC k' (System 2)	M+1 (Calculated)	(M+1) (Experimental)	Purity
1	Ac-His-DPhe-Arg-Trp-NH_2	3.9	6.9	686.8	686.3	>98%
56	Ac-His-DPhe-Arg-**Ala**-NH_2	0.9	4	571.6	571.2	>98%
57	Ac-His-DPhe-Arg-**DTrp**-NH_2	4.1	6.3	686.8	686.9	>99%
58	Ac-His-DPhe-Arg-**His**-NH_2	2.7	3.9	637.7	637.2	>96%
59	Ac-His-DPhe-Arg-**Phe**-NH_2	3.9	6.6	647.7	647.6	>98%
60	Ac-His-DPhe-Arg-**DPhe**-NH_2	3.7	6.3	647.7	647	>99%
61	Ac-His-DPhe-Arg-**Nal(1')**-NH_2	5.1	7.1	697.8	698.8	>99%
62	Ac-His-DPhe-Arg-**DNal(1')**-NH_2	5	8.1	697.8	696.7	>98%
63	Ac-His-DPhe-Arg-**Nal(2')**-NH_2	5.2	7.2	697.8	697.9	>98%
64	Ac-His-DPhe-Arg-**DNal(2')**-NH_2	5	8.1	697.8	697.3	>98%
65	Ac-His-DPhe-Arg-**Tic**-NH_2	4.3	7.1	659.8	658.9	>98%
66	Ac-His-DPhe-Arg-**DTic**-NH_2	4.2	7	659.8	659.3	>99%
67	Ac-His-DPhe-Arg-**Dip**-NH_2	5.6	8.9	723.8	723.2	>99%
68	Ac-His-DPhe-Arg-**DDip**-NH_2	5.4	8.6	723.8	722.8	>99%
69	Ac-His-DPhe-Arg-**Bip**-NH_2	6	9.5	723.8	723.1	>99%
70	Ac-His-DPhe-Arg-**DBip**-NH_2	5.9	9.1	723.8	723.8	>98%
71	Ac-His-DPhe-Arg-**4Pal**-NH_2	2.7	3.9	648.7	648.9	>96%
72	Ac-His-DPhe-Arg-**3Bal**-NH_2	5	6.5	703.8	703.9	>99%
73	Ac-His-DPhe-Arg-**2Thi**-NH_2	3.7	6.2	653.8	652.8	>99%
74	Ac-His-DPhe-Arg-**Atc**-NH_2 **(peak 1)**	4.1	7.2	672.8	672.6	>99%
75	Ac-His-DPhe-Arg-**Atc**-NH_2 **(peak 2)**	4.3	7.6	672.8	672.7	>99%

HPLC k' = [(peptide retention time - sovent retention time) / solvent retention time] in solvent system 1 (10% acetonitrile in 0.1% trifluoroacetic acid/ water and a gradient to 90% acetonitrile over 35 min) or solvent system 2 (10% methanol in 0.1% trifluoroacetic acid/ water and a gradient to 90% methanol over 35 min). An analytical Vydac C18 column (Vydac 218TP104) was used with a flow rate of 1.5 mL/min. The peptide purity was determined by HPLC at a wavelength of 214nM.

Biological evaluation.

Table 3-9 summarizes the pharmacology at the mouse melanocortin receptors, mMC1R, mMC3R, mMC4R, and mMC5R of the twenty tetrapeptides modified at the Trp nine position of the tetrapeptide template, Ac-His-DPhe-Arg-Xaa-NH_2, prepared in this study. The amino acids substituted at the Trp^9 position include Ala, DTrp, His, L/DPhe, L/D-Nal(1'), L/D-Nal(2'), L/D-Tic, L/D-Dip, L/D-Bip, 4Pal, 3Bal, 2Thi, and racemic Atc. The compounds that did not show agonist activity, >100,000nM EC_{50} values in Table 3-9, were tested for antagonism at up to 10μM concentrations, but did not possess antagonistic pharmacological profiles (data not shown). Figure 3-17 illustrates

the amino acids used to replace Trp at the nine position in the tetrapeptide template used herein.

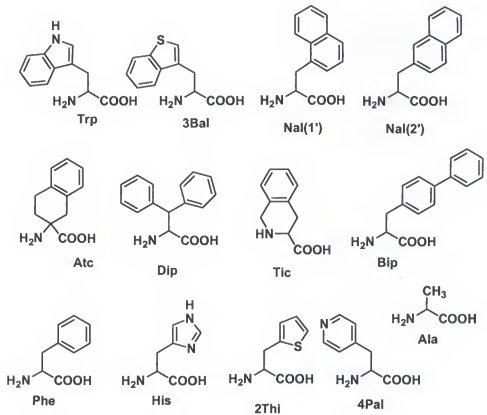

Figure 3-17. Structures of the amino acids used to replace Trp^9 in the tetrapeptide template.

Replacement of the Trp indole moiety with the methyl of Ala (**56**) resulted in 200- to 9700-fold decreased activity at the MC1R, MC4R, and MC5R and was unable to stimulate the MC3R at up to 100μM concentrations. Inversion of stereochemistry from L-Trp to D-Trp (**57**) resulted in 7- to 35-fold decreased MC1R, and MC3-5 R potency, and was 22-fold selective for the MC4R versus the MC3R. Replacement of the indole ring by the imidazole side chain of His (**58**) resulted in a loss of agonist activity at the MC3R at up to 100μM, and 190- to 9000-fold decreased MC1R, MC4R, and MC5R potency compared to **1**, which was similar to the Ala (**56**) substitution.

Table 3-9. Functional activity of the Trp^9 modified tetrapeptides at the mouse melanocortin receptors.

Peptide	Structure	mMC1R EC_{50} (nM)	mMC1R Fold Difference	mMC3R EC_{50} (nM)	mMC3R Fold Difference	mMC4R EC_{50} (nM)	mMC4R Fold Difference	mMC5R EC_{50} (nM)	mMC5R Fold Difference
α-MSH	Ac-Ser-Tyr-Ser-Met-Glu-His-Phe-Arg-Trp-Gly-Lys-Pro-Val-NH_2	0.55±0.09		0.79±0.14				0.44±0.09	
NDP-MSH	Ac-Ser-Tyr-Ser-Nle-Glu-His-DPhe-Arg-Trp-Gly-Lys-Pro-Val-NH_2	0.038±0.012		0.098±0.013				0.071±0.012	
MTII	Ac-Nle-c[Asp-His-DPhe-Arg-Trp-Lys]-NH_2	0.020±0.003		0.16±0.03				0.16±0.03	
1	Ac-His-DPhe-Arg-Trp-NH_2	20.1±0.57	1	156±9.2	1		1	3.96±0.94	1
56	Ac-His-DPhe-Arg-**Ala**-NH_2	4,400±176	219	>100,000		43,700±6,400	2,540	38,400±11,100	9,700
57	Ac-His-DPhe-Arg-**DTrp**-NH_2	140±60	7	5,400±1,100	35	240±30	14	35.3±13	9
58	Ac-His-DPhe-Arg-**His**-NH_2	3,800±1,500	190	>100,000		27,600±4,400	1,600	36,000±10,900	9,090
59	Ac-His-DPhe-Arg-**Phe**-NH_2	530±240	27	27,000±7,000	173	7,800±2,500	453	890±110	224
60	Ac-His-DPhe-Arg-**DPhe**-NH_2	2,500±1,900	124	15,000±2,300	96	1,000±150	58	470±150	118
61	Ac-His-DPhe-Arg-**Nal(1')**-NH_2	730±320	37	3,500±1,300	22	260±30	15	33.1±3.9	8
62	Ac-His-DPhe-Arg-**DNal(1')**-NH_2	750±220	37	21,900±4,900	140	5,400±1,260	314	750±80	189
63	Ac-His-DPhe-Arg-**Nal(2')**-NH_2	17.9±6.0	1	740±160	5	15.8±0.2	1	4.86±1.50	1
64	Ac-His-DPhe-Arg-**DNal(2')**-NH_2	127±27	6	1,620±630	10	46.2±7.9	3	12.1±3.3	3
65	Ac-His-DPhe-Arg-**Tic**-NH_2	43.0±12.5	2	23,200±2,300	149	8,500±930	494	700±99	176
66	Ac-His-DPhe-Arg-**DTic**-NH_2	1,500±210	75	>100,000		39,400±16,500	2,290	24,800±7,300	6,263
67	Ac-His-DPhe-Arg-**Dip**-NH_2	2,300±710	114	53,300±12,300	342	11,600±3,600	674	7,100±1,100	1,790
68	Ac-His-DPhe-Arg-**DDip**-NH_2	680±140	34	16,000±1,300	103	7,800±1,800	453	7,440±1,900	1,880
69	Ac-His-DPhe-Arg-**Bip**-NH_2	51.9±9.9	3	13,400±810	86	2,700±460	157	100±20	26
70	Ac-His-DPhe-Arg-**DBip**-NH_2	310±70	15	16,200±4,800	104	1,500±380	87	150±13	38
71	Ac-His-DPhe-Arg-**4Pal**-NH_2	2,240±770	111	>100,000		30,000±12,300	1,740	14,500±1,400	3,660
72	Ac-His-DPhe-Arg-**3Bal**-NH_2	79.9±8.7	4	3,700±1,400	24	143±24	8	47.7±3.8	12
73	Ac-His-DPhe-Arg-**2Thi**-NH_2	2,780±1,130	138	30,250±4,600	194	8,120±1,100	472	850±90	215
74	Ac-His-DPhe-Arg-**Atc**-NH_2(peak 1)	700±250	35	9,900±1,800	63	3,460±1,260	201	180±70	46
75	Ac-His-DPhe-Arg-**Atc**-NH_2(peak 2)	680±190	34	33,500±12,200	215	8,800±1,340	512	960±90	243

The indicated errors represent the standard error of the mean determined from at least four independent experiments. Slight agonist denotes that some stimulatory response was observed but not enough to determine an EC_{50} value. Compounds possessing >100,000 EC_{50} values were not found to possess antagonist properties at up to 10μM concentrations.

Incorporation of the benzyl moiety in either the Phe (**59**) or DPhe (**60**) configurations resulted in 27- to 450-fold decreased melanocortin receptor potency compared to **1**. The Nal(1') containing tetrapeptide **61** resulted in a 8- to 37-fold decreased melanocortin receptor potency, whereas the DNal(1') tetrapeptide **62** resulted in 37- to 300-fold decreased receptor potency compared with **1**. Interestingly, the Nal(2') (**63**) and DNal(2') (**64**) tetrapeptides were equipotent with the lead tetrapeptide **1** (within the inherent 3-fold experimental error) at the MC4R and MC5R, and were up to a 10-fold less potent at the MC1R and MC3R. Incorporation of the conformationally constrained Tic residue (**65,** Figure 3-17) at the nine position was equipotent with **1** at the MC1R, but possessed 150- to 490-fold decreased potency at the MC3-5Rs. The DTic[9] compound **66** resulted in 75-fold decreased potency at the MC1R, 2290- to 6200-fold decreased potency at the MC4R and MC5R respectively, compared to **1**, and did not posses agonist or antagonist pharmacology at the MC3R. The Dip (**67**) and DDip (**68**) analogues resulted in 34- to 6700-fold decreased melanocortin receptor potency as compared with the Trp amino acid (**1**). The Bip (**69**) containing peptide was equipotent with **1** at the MC1R (within experimental error) and possessed 26- to 150-fold decreased potency at the MC3-5Rs. Tetrapeptide **70**, DBip[9], resulted in 15- to 100-fold decreased potency at the melanocortin receptors compared with **1**. Incorporation of the unusual amino acid 4Pal (**71**) resulted in similar pharmacology as the Ala (**56**) substitution where a loss of activity was observed at the MC3R and 100- to 3600-fold decreased potency resulted at the MC1R, MC4R, and MC5R compared with **1**. The 3Bal compound **72**, with the indole nitrogen replaced by sulfur, was nearly equipotent with the Trp containing homologue **1** at the MC1R, but resulted in 8- to 24-fold decreased MC3-5R potency. The 2Thi[9] moiety

(**73**) closely resembles the His side chain, and resulted in 130- to 470-fold decreased melanocortin receptor potency compared with **1**. Comparison of the His^9 (**58**) and the $2Thi^9$ (**73**) resulted in equipotency at the MC1R and MC4R, μM agonist activity of **73** at the MC3R, and a 42-fold difference in potency at the MC5R. Finally, incorporation of the racemic Atc^9 amino acid resulted in two peptides that eluted at different retention times (Table 3-8), which were designated peak 1 (**74**) and peak 2 (**75**) based upon the order of their elution from the RP-HPLC column. These Atc containing tetrapeptides **74** and **75** resulted in 34- to 510-fold decreased potency at the melanocortin receptors compared with **1**.

Discussion

Figure 3-18 summarizes the effect that each amino acid substitution at the Trp^9 position had on functional activity at the cloned mouse melanocortin receptors.

Melanocortin-1 receptor.

The peripheral skin melanocortin receptor, MC1R, is involved in human skin pigmentation and animal coat coloration.[26,27,79] Substitution of the Trp^9 side chain of **1** with the methyl of Ala (**56**) or the imidazole of His (**58**) resulted in ca 200-fold decreased MC1R potency, suggesting that putative melanocortin ligand Trp^9 side chain-receptor interactions, versus peptide backbone-receptor interactions, are important at this position for MC1R potency. It has been previously reported that, when Trp^9 is replaced with an Ala in the endogenous α-MSH peptide template, a 2000-fold decreased binding was observed in B16 mouse melanoma cells (putative MC1R),[128] consistent with the results presented herein. Substitution of Trp^9 in the tetrapeptide template by DTrp (**57**), Phe (**59**), Nal(1') (**61**), DNal(1') (**62**), Nal(2') (**63**), DNal(2') (**64**), Tic (**65**), DDip (**68**), Bip (**69**),

DBip (**70**), 3Bal (**72**), and Atc (**74,75**) resulted in nM MC1R potency (Table 3-9, Figure 3-18).

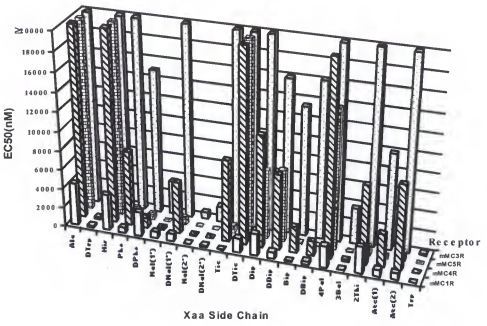

Figure 3-18. Graphical representation summarizing the effect on melanocortin receptor (Y axis) agonist EC_{50} values (Z axis) of the indicated amino acid substitution (X axis) for the Trp residue in the tetrapeptide template

The Nal(2') amino acid substitution for Trp in the tetrapeptide Ac-His-DPhe-Arg-Trp-NH_2 resulted in identical MC1R agonist potency. This observation may be predicted *a priori* based upon scrutiny of the amino acid side chain structures (Figure 3-17), and our previous efforts substituting Nal(2') at the Trp position in the cyclic MTII and SHU9119 templates.[131] Interestingly, the Tic (**65**) and Bip (**69**) amino acid modifications, which possess significantly different biophysical and structural properties compared with the Trp residue (Figure 3-17), are equipotent with the Trp containing tetrapeptide at the MC1R. While very limited structure-activity relationships of the Trp residue at the MC1R have been reported, previous studies examining the incorporation of the four isomers of β-MeTrp at the nine position of the MTII cyclic agonist template resulted

significant differences in MC1R potency, prolonged biological activity, and receptor dissociation kinetics.[175-177] These previous reports, and the data presented herein, suggest that the indole side chain at the nine position of melanocortin ligands is important and warrants further experimental probing to determine if this site can be utilized for the design of receptor selective ligands. Additionally, peptides modified at this position may be used in combination with receptor mutagenesis studies to help probe for receptor residues involved in interaction with the Trp peptide residue.

Melanocortin-3 receptor.

The MC3R is expressed both peripherally and centrally and appears to be involved in metabolism and energy homeostasis.[31,32,58,59] Substitution of the Trp amino acid side chain at the nine position of the lead tetrapeptide by Ala, His, DTic, and 4Pal resulted in a loss of MC3R agonist or antagonist activity at up to 100μM concentrations. Incorporation of the Nal(2'), DNal(2'), Nal(1'), and 3Bal resulted in only up to a 24-fold decreased MC3R potency compared to the Trp indole ring. Previous reports of Trp^9 substitution by Ala^9 and Pro^9 in the cyclic peptide MTII resulted in slight MC3R binding and 2% cAMP stimulation at the hMC3R,[139,143] which are similar to the results presented herein for the tetrapeptide Ac-His-DPhe-Arg-Ala-NH_2. When Trp^9 is modified to the D-Trp configuration, a 35-fold decreased MC3R potency is observed. This is surprising, since inversion of chirality of Trp to DTrp in γ-MSH resulted in ca 20-fold increase in MC3R potency.[178] $Nal(2')^9$ incorporation into the tetrapeptide **63** did not affect potency at the MC3R, which is similar to substitution of Trp^9 with Nal(2') in other melanocortin cyclic peptide templates resulting in a equipotent MC3R agonist[137] or antagonist.[131] Generally, modifications at the Trp^9 position in the tetrapeptide template examined herein resulted in μM agonist MC3R values, suggesting that the MC3R is less tolerant of substitutions at

this position,compared with the MC1, MC4, and MC receptors. This information is useful, given that the low tolerance of Trp modifications at the MC3R may be utilized to develop ligands selective for the other MC receptors as compared to the MC3R.

Melanocortin-4 receptor.

Substitution of the Trp^9 indole side chain with the side chain moieties of Ala, His, DTic, and 4-Pal resulted in >25μM EC_{50} values, demonstrating these modifications are not well tolerated at the MC4R. The substitution of Ala^9 and Pro^9 in the MTII cyclic template also resulted in peptide analogues that did not bind or stimulate the hMC4R.[133,139] Substitution of the Trp^9 residue by Nal(2') and DNal(2') resulted in equipotent MC4R agonists, suggesting that the Nal(2') side chain may be used as a surrogate for Trp to retain equivalent potency at the MC4R. This information is beneficial for the design of future peptide and non-peptide ligands for the MC4R, considering that the reactive indole moiety typically requires temporary protection during synthesis whereas naphthyl derivatives do not. This can simplify the synthetic strategy for future MC4R ligands, reducing both time and costs associated with synthesis. Previous substitution of the Trp^9 with Nal(2') in cyclic templates also resulted in equipotent compounds at the MC4R,[131,137] supporting the use of these substitutions in non-peptide as well as peptide templates. Substitution by the 3Bal amino acid, that contains a sulfur instead of the nitrogen heteroatom in the side chain (Figure 3-17), resulted in only 8-fold decreased MC4R agonist potency. Likewise, Bal derivatives do not require protection during synthesis, therefore this type of derivative may be considered in the design of MC4R ligands in addition to naphthyl amino acids. Incorporation of the hydrophobic amino acids Leu and Phe at the nine position of the NDP-MSH template resulted in 13-fold decreased MC4R potency for the Leu substitution and equipotency for the Phe

substitution at the hMC4R, compared to NDP-MSH.[141] Substitution of the Trp^9 by Phe^9 in the tetrapeptide **59**, however, resulted in 450-fold decreased MC4R potency. This data may suggest that for ligands with reduced size, as compared with the 13 amino acid peptide NDP-MSH, the increased aromatic bulk provided by indole and "indole-like" moieties, compared with Leu and Phe, may be necessary to retain the types of ligand-receptor interactions required for high potency at the MC4R.

Melanocortin-5 receptor.

Incorporation of Ala, His, DTic, Dip, DDip, and 4Pal at the nine position in the tetrapeptide template Ac-His-DPhe-Arg-Xaa^9-NH_2 resulted in less potent peptides (μM EC_{50} values) than lead peptide **1** at the MC5R. Conversely, substitution of the Trp^9 indole with the side chains of Nal(1'), Nal(2'), DNal(2'), and 3Bal resulted in a maximum decrease of 12-fold in MC5R agonist potency. Interestingly, substitution of the Trp^9 with Nal(2') in cyclic peptide templates resulted in a lack of MC5R agonist activity at up to 5μM,[137] or conversion of a MC5R antagonist into a MC5R partial agonist.[131] At the MC5R, tetrapeptides modified at the Trp^9 position resulted from equipotent to 9700-fold decreased potency. These data indicate that the MC5R is less tolerant of Trp^9 modifications, suggesting that this position is important for potent agonist activity. Furthermore, these data provide a theoretic basis for using the MC5 receptor as a tool to putatively identify melanocortin ligand indole interactions with the receptor by using a combination of receptor and ligand complementary mutagenesis experiments.

Stereochemical modifications.

Inversion of chirality from the natural L-configuration to the D-configuration at the Phe seven position of melanocortin peptides generally resulted in enhanced agonist or antagonist potency.[35,86-88,132] Using the tetrapeptide template, Ac-His-DPhe-Arg-Xaa-

NH_2, modification of the stereochemistry at the Trp position did not result in any consistent stereochemical preference, other than the DTrp analogue resulted in 7- to 35-fold decreased melanocortin receptor potency compared with the lead tetrapeptide **1**. Inversion of chirality of the Trp residue in γ-MSH resulted in ca 20-fold increased potency at the MC3R.[178] At the MC1R, the stereochemical inversion of the Nal(1') and Dip amino acids resulted in equipotent compounds. The Phe, Nal(2') and Bip stereochemical inversions resulted in 3- to 5-fold differences in MC1R potency with the L-configuration being the more potent. The most significant difference in MC1R potency was the Tic to DTic modification that resulted in a 38-fold change in potency. At the MC3R, inversion of chirality of the Phe, Nal(2'), Dip, and Bib amino acids resulted in equipotent derivatives, whereas the Nal(1') analogues resulted in a 6-fold difference in potency. At the MC4R, only the Nal(2') and Bip residues resulted in equipotency upon stereochemical inversion. Inversion in chirality of the Phe, Nal(1'), Tic, and Dip residues resulting in 4- to 20-fold changes in potency. These data suggest that, unlike the general increase in potency observed for $DPhe^7$ (α-MSH numbering) containing compounds, potency of the melanocortin ligand depends upon the chirality and particular amino acid substitution at the Trp^9 position in addition to the melanocortin receptor isoform.

Melanocortin receptor selectivity.

The melanocortin pathway consists of five known receptor isoforms, located in a variety of tissues, and involved in a variety of physiological functions.[22] The melanocortin receptor knock out mice have provided valuable information attributing some of the melanocortin receptors to a particular phenotype, but not all the physiological functions attributed to the melanocortin pathway have been linked to a specific

melanocortin receptor(s). Therefore, the search for novel melanocortin receptor selective ligands with unique pharmacology is actively being pursued in many laboratories.[22,88,133-139,143,158,162,179,180] Herein, comparison of tetrapeptide potencies at the cloned MC receptors identifies position nine modifications that result in receptor subtype selectivity. The DNal(1')^9 containing tetrapeptide possessed 46-fold MC4R versus MC3R selectivity. The DNal(2')^9 tetrapeptide possessed 35-fold MC4R versus MC3R selectivity. The 3Bal^9 tetrapeptide possessed 26-fold MC4R versus MC3R selectivity. The most notable results from this Trp^9 substitution study is the identification of the Tic and Bip substitutions that resulted in nM agonist activity at the peripherally expressed MC1R and MC5R, but possessed μM agonist potencies at the centrally expressed MC3 and MC4 receptors (Figure 3-19). The Tic^9 tetrapeptide was 540- and 197-fold selective for the MC1R versus the MC3R and MC4R, respectively, and 12- to 33-fold selective for the MC5R versus the MC4R and MC3R, respectively. The Bip^9 tetrapeptide was 257- and 52-fold selective for the MC1R versus the MC3R and MC4R, respectively, and 130- to 26-fold selective for the MC5R versus the MC3R and MC4R, respectively. These data provide experimental evidence that the Trp^9 position of melanocortin ligands may be further explored for the design of melanocortin ligands that are potent MC1R and MC5R molecules with little or no activity at the central MC3 and MC4 receptors.

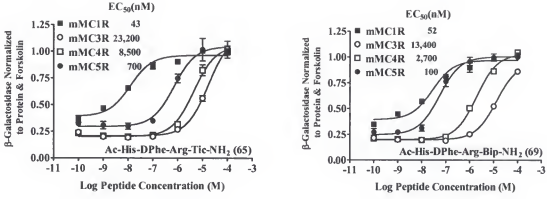

Figure 3-19. Comparison of the Tic[9] **(65)** and Bip[9] **(69)** containing tetrapeptide EC_{50} values at the mMC1 and mMC3-5 receptors. These tetrapeptides are selective for the MC1R and MC5R versus the MC3 and MC4 receptors.

Summary

We have designed, synthesized and characterized a tetrapeptide library of over 100 members, of which 75 have been presented herein. The peptides were each purified to homogeneity and verified for structural integrity by various analytical means. The peptides where analyzed for agonist and antagonist functional activity at the cloned mouse MC1, MC3-MC5 receptors to identify structure-activity relationship trends and receptor selectivity characteristics, with the hope of identifying compounds that exhibited novel and useful pharmacology. These types of information are important in the development of lead compounds for utilization in the rational drug design process and also to provide insights into the types of interactions that are required for molecular recognition and stimulation of the melanocortin receptor isoforms. As discussed in this chapter, we have identified several key modifications that can be incorporated into the core His-Phe-Arg-Trp sequence to result in functional activity that is both novel and synthetically useful.

CHAPTER 4
CONFORMATIONAL ANALYSIS OF CYCLIC MELANOCORTIN LIGANDS

Two of the peptides presented in this chapter, MTII and SHU9119, are two of the most common ligands used to characterize the melanocortin receptors. The design, synthesis, and functional activity was originally reported by the laboratory of Dr. Victor Hruby.[87,88,132] The design and pharmacology of Analogues 1 and 2 presented in this chapter have been previously reported by our laboratory.[124,131] These four peptides, in addition to Analogue 3 presented herein, were synthesized in our laboratory for additional characterization studies reported in this dissertation. SHU9119 and Analogue 1 were synthesized by Miss Fernanda Marques, a previous University of Florida Research Scholar (2001-2002) learning peptide synthesis under the supervision of Jerry Ryan Holder and Dr. Haskell-Luevano. MTII, Analogue 2 and Analogue 3 were synthesized by Jerry Ryan Holder. All peptides were purified and analytically characterized by Jerry Ryan Holder. All NMR data was obtained by Jerry Ryan Holder at the Advanced Magnetic Resonance Imaging and Spectroscopy (AMRIS) facility in the McKnight Brain Institute of the University of Florida with guidance from Mr. Jim Rocca and Dr. Arthur Edison. Molecular modeling and molecular dynamics simulations were carried out by Jerry Ryan Holder with kind assistance from Dr. Arthur Edison (AMRIS) and Dr. Andrzej Wilczynski, a postdoctoral fellow in the laboratory of Dr. Haskell-Luevano. The pharmacology studies were carried out by Rayna Bauzo, Joseph Scott and Dr. Zhimin Xiang, all previous or current members of the Haskell-Luevano laboratory group. Pharmacology data calculations were performed by Dr. Carrie Haskell-Luevano.

Introduction

Cyclic Constraints

Many endogenous peptides are small and often conformationally flexible, which makes correlating conformation with activity difficult. Spectroscopic analysis of a flexible peptide with many conformational states may not provide the actual conformational parameters of one conformation but rather an average of many conformational populations of the peptide.[181] The rationale behind using cyclic constraints is the idea that flexible peptides have many accessible backbone conformations, and thus in solution the bioactive conformation may only be present in low concentrations.[181] Introduction of cyclic restraint can restrict conformational movement and result in either: 1) a conformational geometry suitable for receptor binding, leading to no change in or an increase in affinity; or 2) a geometry ill suited for binding to the receptor, leading to a decrease in or loss of affinity. Additionally, since a proper cyclic restraint may rigidify the peptide backbone it can aid in biophysical analysis and construction of a conformational model.

The Benchmark Melanocortin Agonist MTII

It was noted in some of the initial SAR studies of α-MSH that potency was increased when $DPhe^7$ was substituted for the Phe^7 residue.[86] This observation led to a proposed conformation of α–MSH that consisted of a reverse turn around the Phe^7 residue, since D-amino acids are known to stabilize reverse turn conformations.[182,183] The cyclic analogue Ac-[Cys^4,Cys^{10}]-α-MSH was designed to stabilize the bioactive conformation and to test the hypothesis that a reverse turn existed in the peptide.[182] Molecular dynamics studies revealed that a reverse turn did occur in the cyclic analogue as expected. There have been many studies designed to determine the bioactive

conformation of α-MSH since the work of Sawyer *et al.*, and the majority of these studies have provided additional experimental evidence to suggest a reverse turn occurs around the core His-Phe-Arg-Trp sequence.[184-191] Studies by Sugg *et al.* have suggested a bioactive conformational model that contains a β-turn around the core tetrapeptide sequence, which is stabilized by the presence of the $DPhe^7$ residue, with the His, DPhe, and Trp side chains in close proximity on one surface of the peptide and the Arg side chain on the opposite surface of the molecule.[186] These initial studies attempted to relate conformation of melanocortin peptides with activity. Molecular dynamics simulations in conjunction with molecular mechanics calculations led to the design of the highly potent and enzymatically stabile cyclic analogue of α-MSH, Ac-Nle-c[Asp^6, $DPhe^7$, Lys^{10}]-MSH_{4-10}-NH_2 (MTII, Figure 4-1).[132] MTII is a 23 membered ring formed from lactam cyclization through the Lys and Asp side chains. It was suggested from NMR and quenched molecular dynamics studies on MTII that a type II β-turn occurs in the His-DPhe-Arg-Trp region as compared with a type III β-turn of the linear analogue.[187] As previously suggested,[186] this study also indicated that the His, DPhe, and Trp side chains are located on one surface of the peptide while the Arg side chain was on the opposite face.[187] Theoretical studies of Prabhu *et al.* provided additional evidence to support a bioactive conformation of melanocortin peptides that consist of a stable β-turn.[184,185] These data indicate that the solution conformation involves a β-turn around the core His-DPhe-Arg-Trp region of the melanocortin peptides and that the three hydrophobic aromatic rings are in a stacked orientation opposite the hydrophilic side chain of arginine. These above data illustrate how cyclization of a peptide can rigidify the structure and aid in conformational analysis. These data also support a bioactive conformational model for

melanocortin peptides that consist of a reverse turn centered around the core His-Phe-Arg-Trp motif; however, the exact nature of the turn and the orientation of the side chains are still debated.

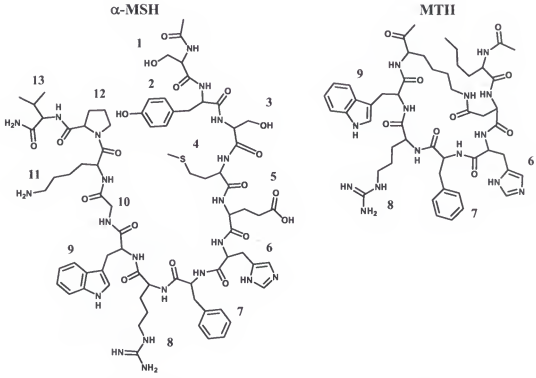

Figure 4-1. Structural comparison of the endogenous melanocortin agonist α-MSH and the highly potent and enzymatically stable synthetic analogue MTII.

The Benchmark Melanocortin Antagonist SHU9119

Prior to 1995 the melanocortin receptors had mainly been characterized by peptide agonists, such as the highly potent linear peptide NDP-MSH and the cyclic lactam analogue MTII (Figure 4-1). The cloning of the remaining MC receptors made the need for potent and selective antagonists for *in vitro* and *in vivo* characterization evident, but at that time only a few reports of melanocortin antagonists had been made.[192-195] Using the MTII cyclic template as a starting point, Hruby *et al.* made various stereoelectronic modifications of the $DPhe^7$ residue that resulted in some interesting and exciting discoveries.[88] These investigations involved modification of the $DPhe^7$ residue and were

based on previous suggestions that the His^6, Phe^7, Arg^8, and Trp^9 residues are critical for receptor binding and activation.[75,76] The authors postulated that modification of the $DPhe^7$ residue may disrupt the bioactive conformation of the peptide.[88] The theory behind the modifications was that disruption of the bioactive conformation may prevent signal transduction from occurring, but still permit ligand binding to the "inactive" state of the receptor. Thus, the DPhe amino acid was substituted with a variety of "bulky" aromatic amino acids. This study led to the discovery of the potent and selective (for the MC3R and MC4R) melanocortin receptor antagonist SHU9119 (Ac-Nle-c[Asp^6, DNal(2')^7, Lys^{10}]-MSH_{4-10}-NH_2). Substitution with DNal(2') at the Phe^7 position resulted in agonist activity at the hMC1R and the mMC5R, potent antagonist activity at the hMC3R with minimal agonist activity, and potent competitive antagonist activity at the hMC4R. Modification of the phenyl ring in the para position with halogen substituents resulted in interesting pharmacology as well. Para substitution of the phenyl ring with either fluorine or chlorine retained agonist activity at all the cloned melanocortin receptors. Replacement of DPhe with D-p-iodophenylalanine [(pI)DPhe] resulted in full agonist activity at the hMC1R, partial agonist activity at the mMC5R, partial agonist, as well as, potent antagonist activity at the hMC3R and hMC4R. The data from this study led to the hypothesis that bulky aromatic amino acid substitutions at position seven are responsible for differentiating agonist versus antagonist activities of melanocortin ligands.[88]

Additional Aromatic Modifications of Position Seven

Since the discovery of SHU9119 there have been various melanocortin peptides synthesized with DNal(2') at the seven position, and this generally results in ligands with partial agonist and/or antagonist activity at the MC4R.[124,131,136,140,158,162,179,196-198] Recently our lab characterized the mouse MC4R using a combined approach of *in vitro* receptor

mutagenesis and characterization of the receptor mutants with several melanocortin based ligands, many of which contained naphthyl substituents at position seven similar to SHU9119.[124] SHU9119 was a potent antagonist (pA_2=9.7); [DNal(1')]-MTII was a partial agonist (EC_{50}=0.12 nM); and [Nal(2')]-MTII was a full agonist (EC_{50}=0.89 nM) at the wildtype MC4R. Using the naphthyl based peptides to characterize the wildtype and mutant mMC4 receptors has led to a revision of the original hypothesis regarding the ability of bulky aromatic groups at position seven to impart antagonistic activity to melanocortin peptides. The experimental evidence from the mutagenesis study suggests that not only was the bulky aromatic moiety required for antagonism of the MC4R, but the stereochemistry of the α-carbon and the position of the naphthyl ring (1' versus 2') were equally important.[124] The SAR study presented in chapter 3 herein provides additional evidence to support this revised hypothesis, since the only tetrapeptide derivative that resulted in an MC4R antagonist contained a DNal(2') naphthyl moiety. The DNal(1') tetrapeptide derivative is an agonist and the Nal(1') and Nal(2') analogues are inactive at the mMC4R.[196]

It has been suggested that the topographical orientation of the arginine residue of SHU9119 may be modified by the presence of an adjacent naphthalene ring, compared to the topography of the arginine side chain of MTII.[124] This hypothesis was the result of the different pharmacological profiles observed from MTII, SHU9119, [DNal(1')]-MTII, and [Nal(2')]-MTII at mutant mouse MC4 receptors.[124] Several studies have suggested that acidic residues present in TM2 and TM3 of the melanocortin receptors interact with the basic arginine residue of melanocortin ligands.[124,141,159,160,171] The putative arginine-MC4R interactions are illustrated in Figure 3-13. Using site-directed mutagenesis, the

acidic residues in TM2 and TM3 of the MC4R were systematically exchanged with basic residues to test this hypothesis.[124] The pharmacological results varied for each of the naphthyl derivatives tested at the MC4 receptor. For instance, at the Asp114Arg mutant MC4 receptor there was a 30-fold difference in potency between [DNal(1')]-MTII and [Nal(2')]-MTII, and a 17-fold difference between MTII and [Nal(2')]-MTII. Additionally, SHU9119 had only a 3-fold decrease in binding affinity whereas MTII had a 74-fold decrease at the Glu92Lys mutant. Furthermore, SHU9119 was the only peptide that retained binding ability to the Asp118Lys mutant. These data indicated that the different ligands, each with a different aromatic functionality at the seven position, potentially interacted with the Asp114, Asp118, and Glu92 receptor residues in a differential manner. These data also suggested that the topographical arrangement of the arginine side chain in 3-dimensional space may be different in each of the peptides, and thus have different interactions with MC4R acidic residues. In this regard, these interactions may be responsible for the different pharmacological profiles of the naphthyl ligands and the antagonistic activity of SHU9119 at the MC4R.

The studies presented above demonstrate how introduction of cyclic constraints can lead to the discovery of ligands with increased potency, as seen with cyclic MTII compared with the linear precursor NDP-MSH. Introduction of cyclic constraints has also been shown to restrict flexibility and facilitate the conformational analysis of peptidic ligands. Additionally, the above studies indicate that bulky aromatic modifications of the Phe^7 residue can result in significant modulation in functional activity. The studies presented in this chapter were initiated to: 1) test the hypothesis that the bioactive conformation of MTII consist of a type II β–turn; 2) test the hypothesis that the aromatic

ring structures are indeed modifying the three-dimensional structure of the cyclic melanocortin ligands; and 3) determine if conformational differences can be identified between MTII and the naphthyl-analogues that can be attributed to the observed functional activity at the MC4R.

Results

The peptides analyzed in this study are based on the 23-membered MTII cyclic template (Figure 4-1). MTII and SHU9119 have been used extensively to characterize the melanocortin receptors for both *in vitro* and *in vivo* biological activity. In addition to MTII and SHU9119, our lab has previously reported the synthesis and pharmacological evaluation of Analogues 1 and 2.[124,131] Analogue 3 was designed, synthesized and included herein to complement the other four peptides and provide a complete analysis of ligands modified at position seven with naphthyl amino acid derivatives.

Peptide Synthesis

The five cyclic peptides presented herein were synthesized using a suitable Boc protection group strategy,[132] the detail of which is discussed in chapter 5. All amino acids, solvents and reagents were commercially available and used without further purification. Purified peptides had the correct molecular weight as determined by MALDI-TOF mass-spectrometry (data obtained by Jerry Ryan Holder at the University of Florida Protein Chemistry Core Facility) and were ≥95% pure as determined by analytical RP-HPLC in two diverse solvent systems (Table 4-1). Additionally, structural integrity was verified by 1D (Appendix B) and 2D ^{1}H-NMR (Appendix C) analysis.

Pharmacology

The peptides examined in this study are cyclic analogues of the endogenous melanocortin agonist α-MSH (Figure 4-1). The cyclic peptides were evaluated at the

mouse MC4R for agonist and antagonist activity (Table 4-2). The peptides were also characterized at the MC1R, MC3R and MC5R (data not shown).

Table 4-1. Analytical data for the five peptides presented in this chapter.

Peptide	Position Seven Amino Acid	HPLC k' (System 1)	HPLC k' (System 2)	M+1 (Calculated)	(M+1) (Experimental)	Purity
MTII	DPhe	5.93	10.58	1024.2	1024.6	>98%
SHU9119	DNal(2')	6.58	11.76	1074.2	1073.6	>98%
Analogue 1	DNal(1')	6.61	11.93	1074.2	1073.7	>98%
Analogue 2	Nal(2')	6.43	11.36	1074.2	1073.2	>98%
Analogue 3	Nal(1')	6.4	11.44	1074.2	1073.6	>98%

HPLC k' = [(peptide retention time - sovent retention time) / solvent retention time] in solvent system 1 (10% acetonitrile in 0.1% trifluoroacetic acid/ water and a gradient to 90% acetonitrile over 35 min) or solvent system 2 (10% methanol in 0.1% trifluoroacetic acid/ water and a gradient to 90% methanol over 35 min). An analytical Vydac C18 column (Vydac 218TP104) was used with a flow rate of 1.5 mL/min. The peptide purity was determined by HPLC at a wavelength of 214nM.

Each of the five peptides have 23-membered rings formed by side-chain to side-chain lactam bridge formation and differ only by subtle modifications of the Phe^7 residue; however these small modifications resulted in significant changes in biological activity at the mouse MC4R. Figure 4-2 summarizes the structures and pharmacology of the five peptides at the MC4R. MTII was one of the first highly potent cyclic analogues of α-MSH reported in the literature[132] and resulted in an EC_{50} value of 0.033nM reported herein. SHU9119 is another benchmark ligand used extensively to characterize the melanocortin receptors.[88] SHUI9119 is a potent antagonist at the MC4R and possessed a pA_2 value of 10 (K_i=0.072nM) in this study. Analogue **1** has a DNal(1') residue rather than the DPhe residue found in MTII and resulted in a potent agonist at the MC4R (EC_{50}=0.34nM), however the peptide was only able to elicit a 48% maximal response in the functional bioassay. Analogue **2** has a Nal(2') residue at position seven. The stereochemistry has been inverted in Analogue **2**, compared with SHU9119, which resulted in a ligand with both agonist and antagonist functional activities. This peptide had an EC_{50} of 48nM with a maximal dose response of 61%, and interestingly had an

antagonist pA_2 value of 7.4 (Ki=40nM), providing a useful ligand to aid in characterization of the MC4R. Analogue **3** contains a Nal(1') residue at position seven, resulting in an agonist with an EC_{50} of 110nM. Although substitution of $DPhe^7$ with $Nal(1')^7$ in Analogue 3 resulted in a full agonist at the MC4R, it was 3300-fold less potent than MTII.

Table 4-2. Functional activity of MTII, SHU9119, and the three analogues at the mMC4R

		mMC4R		
Peptide	Position Seven Amino Acid	EC_{50} (nM)	Emax(%)	pA_2
MTII	DPhe	0.033 ± 0.001	100	-
SHU9119	DNal(2')	-	0	10
Analogue 1	DNal(1')	0.34 ± 0.002	48	-
Analogue 2	Nal(2')	48 ± 0.15	61	7.4
Analogue 3	Nal(1')	110 ± 1.8	89	-

The indicated errors represent the standard error of the mean determined from at least four independent experiments. Emax is based on maximal MC4R stimulation by MTII.

NMR

Chemical shift assignments

The chemical shifts of each peptide in this study (Table 4-3) were assigned using standard TOCSY and ROESY ^{1}H-NMR strategies.[113] Using this approach, intraresidue resonances of each amino acid residue were assigned from the TOCSY spectra and ROESY spectra were used to correlate one amino acid with the next through interactions of the α-proton of residue *i* with the amide proton of residue *i*+1. This approach allowed the complete assignment of all amino acids as well as the lactam bridges. The aliphatic fingerprint regions of the 500MHz TOCSY and ROESY spectra for each peptide are shown in Figure 4-3 and Figure 4-4, respectively (enlarged views shown in Appendix C).

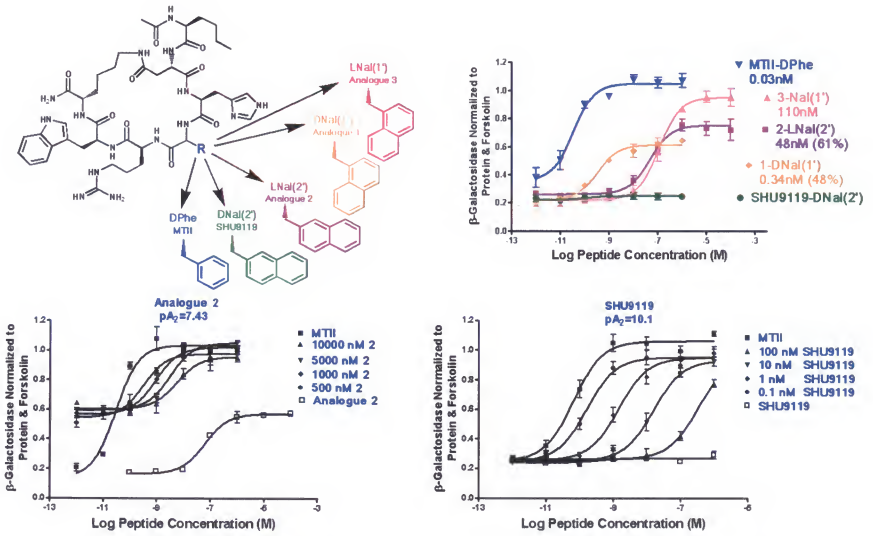

Figure 4-2. Summary of the primary chemical structures and MC4R functional activity of the five peptides presented in this chapter.

Table 4-3. ^{1}H-NMR Chemical Shifts (ppm) for the five peptides at 5°C in H_2O pH 3.6.

Residue	Proton	MTII DPhe	SHU9119 DNal(2')	Analogue 1 DNal(1')	Analogue 2 LNal(2')	Analogue 3 LNal(1')
CH_3CO	CH_3	1.97	1.96	1.97	1.96	1.93
Nle	NH	8.38	8.33	8.35	8.29	8.29
	Hα	4.19	4.14	4.19	4.08	4.11
	H$\beta\gamma$	1.61	1.60	1.60	1.53	1.49
	Hδ	1.21	1.21	1.21	1.19, 1.12	1.11
	Hϵ	0.82	0.81	0.80	0.79	0.77
Asp	NH	8.68	8.58	8.66	8.40	8.47
	Hα	4.60	4.62	4.60	4.49	4.54
	Hβ	2.89, 2.67	2.83, 2.64	2.88, 2.66	2.83, 2.59	2.81, 2.56
His	NH	8.61	8.51	8.66	8.47	8.50
	Hα	4.37	4.45	4.41	4.54	4.38
	Hβ	3.19, 3.04	3.14, 2.95	3.17, 3.00	3.16, 2.89	3.07, 2.91
	H2	8.48	8.03	8.46	8.33	8.45
	H4	7.07	6.93	7.07	6.97	6.97
Xaa	NH	8.56	8.71	8.63	8.49	8.40
	Hα	4.55	4.72	4.73	4.70	4.68
	Hβ	3.16, 2.86	3.3, 3.05	3.61, 3.37	2.89, 2.79	3.37, 3.26
	H1	NA	7.66	NA	7.69	NA
	H2	7.21	NA	7.37	NA	7.38
	H3	7.34	7.40	7.46	7.47	7.53
	H4	7.34	7.86	7.86	8.00	7.94
	H5	7.34	7.91	7.96	8.00	8.03
	H6	7.21	7.55	7.58	7.60	7.66
	H7	NA	7.55	7.58	7.60	7.66
	H8	NA	7.86	8.07	7.91	8.09
Arg	NH	7.97	8.08	7.87	8.70	8.49
	Hα	4.28	4.16	4.01	4.10	4.21
	Hβ	1.62, 1.56	1.46, 1.37	1.43, 1.33	1.60, 1.37	1.69
	Hγ	1.29	0.98	0.97	1.68, 1.38	1.42
	Hδ	3.06	2.84	2.93	3.06	3.10
	NHδ	7.14	6.93	7.07	7.13	7.18
Trp	NH	8.61	8.53	8.55	7.22	7.88
	Hα	4.63	4.63	4.64	4.64	4.66
	Hβ	3.29	3.29	3.28	3.22, 3.04	3.30
	H2	7.26	7.25	7.26	7.13	7.26
	H4	7.67	7.66	7.66	7.44	7.51
	H5	7.15	7.15	7.15	7.14	7.10
	H6	7.23	7.23	7.22	7.14	7.10
	H7	7.48	7.47	7.47	7.14	7.20
	NH_{indole}	10.22	10.21	10.23	10.16	10.08
Lys	NH	8.16	8.07	8.11	7.48	7.78
	Hα	4.18	4.20	4.18	4.16	4.14
	Hβ	1.71, 1.55	1.72, 1.58	1.71, 1.57	1.73, 1.59	1.71, 1.55
	Hγ	1.28, 1.21	1.27, 1.18	1.29, 1.21	1.28, 1.21	1.29, 1.19
	Hδ	1.50, 1.38	1.49, 1.37	1.49, 1.34	1.59, 1.40	1.55, 1.39
	Hϵ	3.20, 3.14	3.20, 3.15	3.18	3.37, 3.06	3.32, 3.01
	NHϵ	8.07	8.08	8.10	8.05	8.03
	$CONH_2$	6.91, 6.60	6.93, 6.72	6.92, 6.62	7.44, 7.14	7.09, 6.95

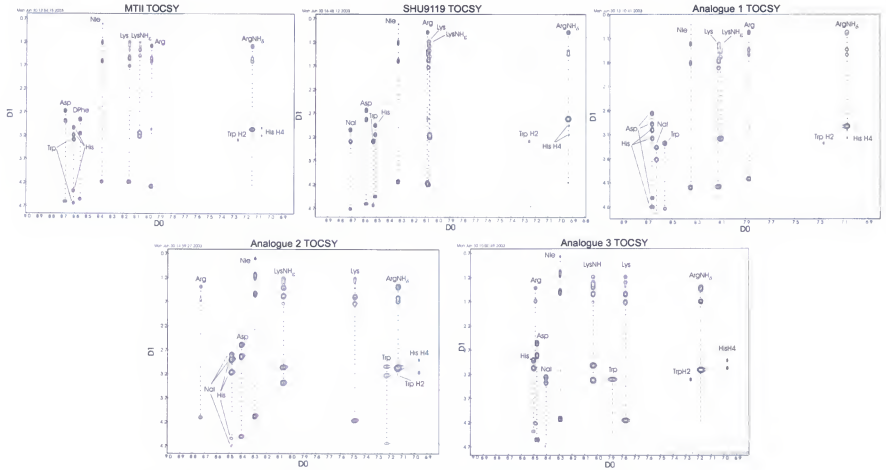

Figure 4-3. Aliphatic fingerprint region of TOCSY spectra of the five peptides presented in this chapter.

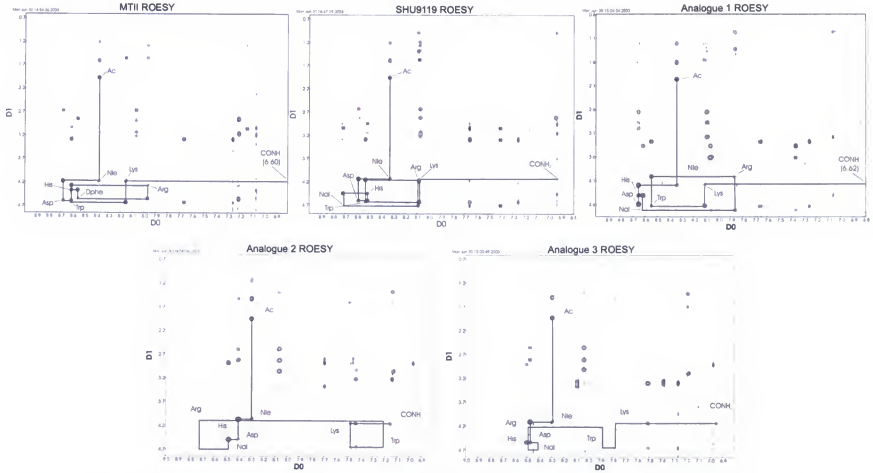

Figure 4-4. Aliphatic fingerprint region of ROESY spectra of the five peptides presented in this chapter.

Quantitative analysis of chemical shifts remains difficult for small, flexible peptides because they represent a populated weighted average of rapidly interconverting structures with different chemical shifts.[181] Although quantitative analysis of chemical shift values is difficult, we can use chemical shift values for a qualitative comparison between a related set of compounds. Chemical shifts are extremely sensitive to the electronic environment and thus provide useful probes into changes in molecular structure. Differences in chemical shift values between peptides with similar chemical structures, as with the peptides presented herein, are a good indicator that the peptides do indeed have structural differences. The five peptides in this study are similar in primary chemical structure (Figure 4-2), however the NMR spectra (Figure 4-3), and thus chemical shift values (Table 4-3), show significant differences. The chemical shift differences indicate that the conformational properties of the peptides may also be different. Overhauser effects derived from the ROESY spectra were not identical for each peptide (Figure 4-4), which also suggested structural dissimilarities between MTII and the four analogues.

Chemical shift deviations

In addition to using ^{1}H chemical shifts to compare and contrast a series of peptides, we can use backbone ^{1}H chemical shift values as an indicator of well ordered structure.[199] Random coil chemical shift values are what one would expect to observe for backbone protons in the absence of secondary structure formation. Therefore, deviations of backbone ^{1}H shifts from random coil values may indicate a certain degree of well ordered structure.[199] Figure 4-5 is a histogram of differences between experimental and aqueous random coil amide and α proton chemical shifts for the five peptides. The chemical shift

deviations (CSDs) were calculated for 5°C. Random coil NH reference values are for 25°C and were adjusted for temperature by applying a correction of -7.6 ppb/°C prior to calculating the CSD.[199] As shown in Figure 4-5, there are significant deviations from backbone random coil values for each of the five peptides. These deviations away from random coil values suggest that the peptides may possess a high degree of well ordered structure. Additionally, it can be seen in Figure 4-5 that the CSDs differ between the five peptides, which indicates that conformational dissimilarities are present among the peptides.

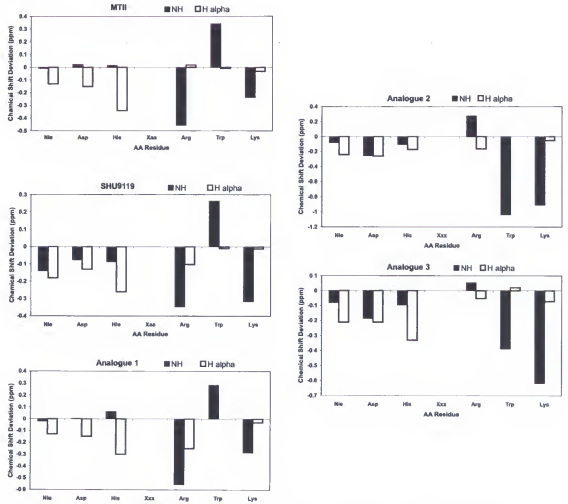

Figure 4-5. Histogram of the difference between the random coil and experimental chemical shifts. The amide and α-protons are represented by black bars and white bars, respectively.

Temperature coefficients

In our attempt to differentiate structural properties among the five peptides, we next quantitatively determined amide proton temperature coefficients ($\Delta\delta/\Delta T$, ppb/K).[190,200] The temperature coefficient values (Table 4-4) were determined over a range of 5°C to 50°C in 5°C increments (described in detail in the experimental section). Stacked plots of the 1D ^{1}H-NMR spectra used to calculate the temperature coefficients are shown in Appendix B. Amide proton temperature coefficients are complicated and not completely understood, but are known to be sensitive to structural changes.[200] Relatively small temperature coefficients are indicative of either reduced solvent accessibility or hydrogen bonding.[201,202] It has been reported that random coil peptides will have temperature coefficient values in the range of -6 to -10 ppb/K, and values between -2 and -6 may indicate that the amide protons are involved in hydrogen bonding or have reduced solvent accessibility.[190] Low values are highlighted in bold in Table 4-4. The values for MTII amide protons all fell into the range of random coil, suggesting a lack of strong hydrogen bonding or reduced solvent accessibility. Analogue 1, the other potent agonist of the set, had values very similar to that of MTII, with the exception of the low value for the Lys amide proton. SHU9119 and Analogue 3 had two residues with low temperature coefficients, and Analogue 2 had three residues with low values. The low values of the amide protons may be the result of their involvement in hydrogen bonding, possibly stabilizing turn formations. These data suggest that solvent accessibility is not the same for each peptide, indicating structural differences between them.

Table 4-4. Temperature coefficients for the Amide Protons of MTII, SHU9119, and Analogues 1-3.

	$\Delta\delta/\Delta T$ (ppb/K)				
Residue	MTII	SHU9119	Analogue 1	Analogue 2	Analogue 3
Nle	-9.33	-8.44	-8.40	-7.76	-8.36
Asp	-8.51	-7.76	-7.01	-7.67	-8.00
His	-6.14	**-4.84**	-6.25	-7.78	-8.67
Xaa	-8.29	-9.04	-7.30	**-4.58**	**-5.06**
Arg	-6.38	-7.62	-6.19	-7.15	-6.23
Trp	-9.48	-8.41	-8.14	**-3.66**	-9.28
Lys	-6.29	**-5.21**	**-5.17**	**-2.82**	**-4.70**
LysNHε	-8.55	-8.62	-8.23	-6.56	-7.00

Temperature coefficients were determined from temperature titration data collected from 5°C to 50°C in 5°C increments. All peptides were at a concentration of 1mM in 95% H_2O/ D_2O pH 3.6.

Restrained Molecular Dynamics Simulations

We concluded from the NMR data presented above that the peptides possess a certain degree of well ordered structure and there are differences in the structural features between the peptides. Based on the hypothesis that the conformational properties of the peptides are responsible for biological activity, molecular modeling and molecular dynamics simulations were carried out with the goal of identifying structural features that may account for the differences in biological activity. NMR NOE derived interatomic distances were used as pseudo potentials in restrained molecular dynamics (RMD) simulations. Interatomic distances derived from ROESY spectra were interpreted as a 3.5Å distance between protons for a strong signal, 4.5Å between protons for a medium signal, and 5.0Å between protons for a strong signal.

The first step in molecular modeling strategy is model building, followed by structure refinement and analysis. Molecular modeling and dynamics simulations of linear peptides were accomplished using the Insight II molecular modeling software suite (Accelrys, San Diego,CA). Linear peptides were built and energy minimized, pseudo cyclized by placing a pseudo potential of 1.4Å between the side chain $LysNH_\epsilon$ and the carbonyl carbon of Asp to mimic lactam bridges, energy minimized a second time, and

then RMD simulations were run for 5ns at 500K. Structures from 51 equally spaced time points along the trajectory were recorded and energy minimized. The 51 structures were then analyzed for each of the five peptides (255 total) and four structures that satisfied the NMR data for each peptide were chosen for further analysis (20 total). Next, the pseudo potentials were added to each of the 20 RMD derived structures and energy minimized. The lowest energy structure was then chosen for the final round of RMD simulations. Final RMD simulations were done for 20ns at 500K in attempts to sample all accessible conformations and compensate for conformational averaging. Following the RMD simulations, structures from 201 equally spaced points along the dynamics trajectory were energy minimized, with all pseudo potentials included, for subsequent analysis.

For each analogue a superposition of all 201 energy minimized conformations was not distinguishable, suggesting that the simulations each contained multiple conformations. However, when only the backbone atoms were superimposed a relatively ordered conformation was observed. This indicated that although the side chains are conformationally flexible, there is some degree of rigidity in the structures of backbone atoms. To simplify conformational analyses, the ten lowest energy structures from the dynamics trajectory were used for further examination. Although a superposition of all 201 energy minimized structures was not distinguishable, the 10 lowest energy structures had a high degree of similarity. RMSD values for the backbone torsional angles and superpositions of the 10 lowest energy structures are shown in Figure 4-6 and 4-7. The modeling and NMR analysis suggested conformational preferences for the peptide backbones, but neither indicated that any of the five existed in any "classical" turn structures. These findings are in agreement with the NMR solution structure of a closely

related MTII analogue, Ac-Nle-cyclo[Asp-Pro-DPhe-Arg-Trp-Lys]-NH_2, recently reported by Fotsch and co-workers at Amgen.[203] MTII, SHU9119 and Analogue 1 had turn structures that displayed similarities to both type I and type II β-turns composing the His-Xaa-Arg-Trp residues in MTII and SHU9119 and centered around the Nle-His-Xaa-Arg residues in Analogue 1. Analogues 2 and 3 had β-like turns in the Nle-His-Xaa-Arg residues and Analogue 2 also had a γ-like turn comprising the His-Xaa-Arg-Trp residues.

Discussion

The five peptides presented herein are all based on the MTII 23-membered ring system and differ only by subtle modifications of the Phe^7 position (Figure 4-2). Although similar in primary chemical structure, the peptides have significant differences in functional activity at the mouse MC4R. It is interesting that only slight modifications of the Phe^7 residue significantly alters the functional activity of the ligands, prompting one to speculate that the Phe^7 modifications may be effecting the conformational properties of the peptides. Indeed, previous data from MC4R mutagenesis studies using four of the five peptides presented herein indicated that the four peptides did not interact with the acidic residues (Asp114, Asp118, Glu92) in the putative binding pocket of the MC4R in an identical manner.[124] These data had led to the hypothesis that structural dissimilarities may exist between the peptides as a result of the bulky aromatic groups at position seven that are responsible for affecting these ligand-receptor interactions.[124] The studies presented in this chapter were initiated to test this hypothesis that the aromatic ring structures are indeed modifying the three-dimensional structure of the cyclic melanocortin ligands and to determine if conformational differences can be identified between MTII and the naphthyl-analogues that can be attributed to the observed functional activity at the MC4R. To this end, we employed the combination of various

^{1}H-NMR based strategies together with molecular modeling and restrained molecular dynamics simulations described above.

Chemical Shifts

The first step in our analyses was assignment of chemical shifts for each proton of each of the five peptides in aqueous solution (Table 4-3). This was accomplished in a straight forward manner using standard TOCSY and NOESY ^{1}H-NMR strategies.[113] Chemical shifts are extremely sensitive to the electronic environment, and thus provide useful probes into changes in structural features when comparing a closely related set of compounds, like the five peptides presented herein. We also used chemical shift deviations between experimental and random coil shift values of backbone protons as an assessment of ordered structure, as well as a means of comparing the five peptides.[199] As shown in Figure 4-5, there are differences in the experimental chemical shift values and reported random coil values, as well as variations in the degree of chemical shift deviation within the five peptides. These data not only suggest some degree of ordered structure, but also suggest the structures of the peptides are not equivalent. In addition to the backbone protons, variations in the chemical shifts in several of side chain protons were observed (Table 4-3). The Hβ protons of the naphthylalanine residue in Analogue 1 were shifted downfield, whereas the Hβ protons of Analogue 2 were shifted upfield, compared with the remaining three peptides. In Analogue 2 the Trp Hβ protons are non-equivalent and the H2, H6 and H7 protons of the indole ring are shifted upfield, compared with the Hβ and ring protons of the other four peptides. The C-terminal is amidated in all five of the peptides presented in this chapter, and the two C-terminal NH protons are shifted far downfield in Analogue 2 compared with the remaining four peptides.

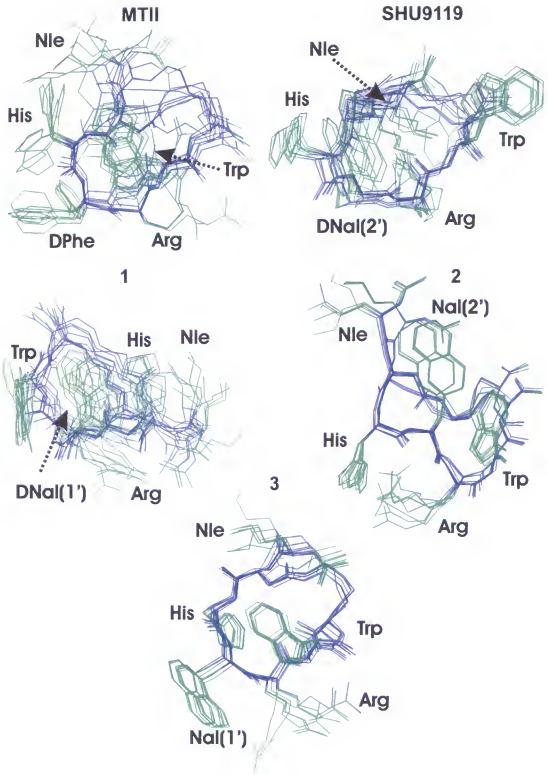

Figure 4-6. Superpositions of the 10 lowest energy conformations obtained from the RMD simulations. Backbone atoms and the side chains of Asp and Lys are in purple, side chains are in green, and hydrogen atoms have been removed for clarity.

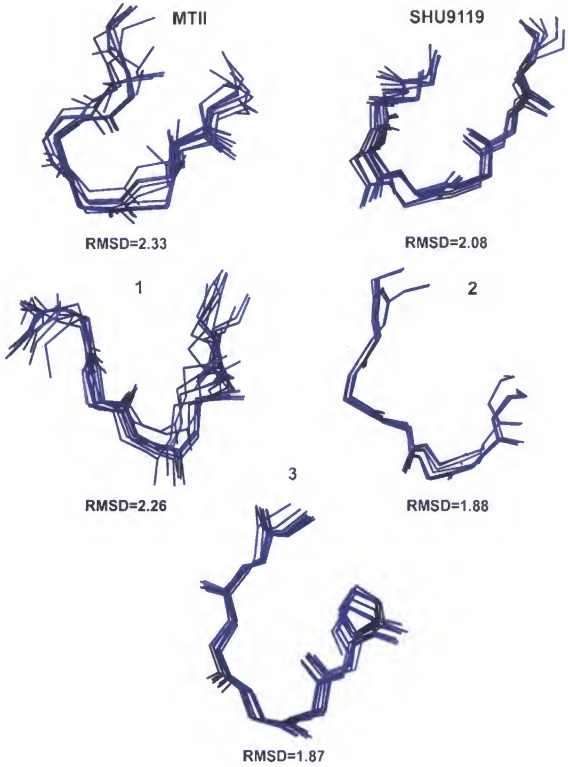

Figure 4-7. Superpositions of only the backbone atoms for 10 lowest energy conformations obtained from the RMD simulations. Backbone atoms are displayed in stick form. RMSD values, given in angstroms, are calculated from backbone torsional angles.

The most significant dissimilarities among the five peptides occurr in the chemical shifts of the Arg residues. Histograms of the differences between random coil and experimental chemical shift values for the side chain protons of the arginine residues are shown in Figure 4-8. Comparing the Arg Hβ protons: in SHU9119 and Analogue 1 the Hβ occur at the same frequency but are shifted upfield compared with MTII, Analogue 2 and Analogue 3; the two Hβ are equivalent in Analogue 3 and shifted slightly downfield compared with MTII; the Hβ are at approximately the same frequency in MTII and Analogue 2, although the two Hβ are more non-equivalent in Analogue 2. Comapring the Arg Hγ protons: there is a large upfield shift in SHU9119 and Analogue 1, whereas there is a large downfield shift in Analogues 2 and 3 as compared with MTII ; the Arg Hγ protons are equivalent in MTII, SHU9119, Analogue 1, and Analogue 3 but are non-equivalent in Analogue 2. These findings are in contrast to the chemical shifts of the Arg Hγ protons of MTII and SHU9119 recently reported by Silva-Elipe and co-workers.[190] They reported that the Arg Hγ protons of MTII and SHU9119 occurred at the same resonance frequency, although they reported that for two closely related analogues the Arg Hγ protons had upfield chemical shifts similar to the values we observed from SHU9119 and Analogue 1. In our studies presented herein the chemical shifts were determined at 5°C in aqueous solution rather than in CD_3OH at 25°C used for their assignments, which could account for the differing observations. The differences in these chemical shifts discussed above indicate differences in the electronic environments between the peptides, which may be a result of dissimilarities in shielding effects. This was a good indication to us that there may indeed be some conformational variations between the five peptides. Additionally, the significant deviations in the chemical shifts

of the protons in the Arg residues adds experimental support to the hypothesis previously put forward by our lab that the topographical orientation of this residue may be altered as a result of the adjacent bulky naphthylalanine residue.[124]

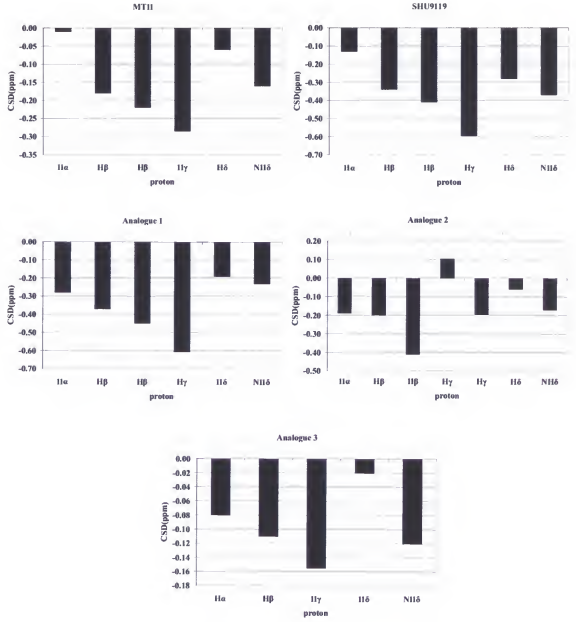

Figure 4-8. Histogram of the difference between random coil and experimental chemical shift values for the side chain protons of the arginine residues. The histogram plots illustrate the significant dissimilarities between chemical shift values for the arginine side chain protons of the five peptides, which may indicate differences in shielding effects.

Temperature Dependence of Amide Protons

Further evidence of backbone rigidity and secondary structure formation can be deduced from the behavior of amide proton chemical shifts during changes in temperature.[181] In an aqueous environment amide protons that are assessable to the solvent H-bond with it, which results in a downfield shift due to deshielding effects of the H-bond acceptor. Increasing the temperature typically breaks these bonds between solvent and amide protons and leads to an upfield shift of the amide proton. Amide protons that are not assessable to the solvent or are involved in intramolecular H-bonding tend to be less sensitive to temperature changes and will have low temperature coefficient values. To determine this relationship, we next calculated the amide temperature coefficients over a range of 5°C to 50°C in 5°C increments (Table 4-4). As shown in Table 4-4, the temperature coefficient values are not identical for the five peptides. The absence of any low values for MTII amides suggest that this highly potent agonist may be fairly flexible and may exist in several conformations rather than one rigid structure, which is consistent with the structures of MTII derived from the molecular dynamics analysis. The other potent agonist, Analogue 1, also lacked any low temperature coefficient values other than the low value of the Lys NH proton, suggesting that it also may be somewhat flexible and only has rigidity around the Lys residue. The remaining three peptides are either antagonists or have low potency at the MC4R, and it is interesting to note that these three peptides have more residues with low temperature coefficients. This data may be interpreted to indicate that these peptides have a more rigid structure than the two potent agonists MTII and Analogue 1. These data suggested that the accessibility of the solvent was different for each peptide, indicating some structural differences between them. This is similar to the conclusions drawn in another ^{1}H-NMR

study of MTII, SHU9119 and related analogues in which the authors concluded from their temperature studies that the accessibility of the solvent was different for each peptide.[190]

Molecular Modeling and Restrained Molecular Dynamics Simulations

One of the fundamental hypotheses in biochemical research is that the information possessed by chemical messengers, which are involved in information transduction processes that result in an subsequent functional biological response(s), is directly related to their conformational properties.[204] Likewise we hypothesized that the conformational properties of the five peptides presented herein were responsible for their pharamacology at the mouse MC4R. Moreover, since each of the peptides have variations in their functional activity, their conformational properties may also vary. ^{1}H-NMR analysis of the five peptides suggested to us that there are dissimilarities in structural features. To aid in identifying and understanding these features, molecular modeling studies were undertaken.

Molecular modeling based on NMR data of MTII, SHU9119, Analogues 1, 2 and 3 was carried out with the goal to identify structural features that affect the functional activity of the peptides at the mouse MC4R. A superposition of the 10 lowest energy structures for each peptide is shown in Figures 4-6 and 4-7. Although no classical turn structures could be identified by NMR data or modeling analysis, both of the analyses indicated some conformational preferences, in particular preferences in the backbone structures. This is in agreement with the recently published solution structure of a related MTII analogue, [Pro^{6}]-MTII, by Fotsch et al.[203] However, this is in contrast with two other published solution structures of MTII.[139,187] Al-Obeidi and colleagues used a combination of 1D ^{1}H-NMR and molecular dynamics studies to conclude that the

solution conformation of MTII consisted of a type II β-turn in the His-DPhe-Arg-Trp region, with hydrogen bonding between Arg NH and Asp CO.[187] As mentioned previously, there was no well defined reverse turn in the solution structure of MTII in our study, although there was a reverse turn with some similarities to several classical β-turns. Additionally, neither our NMR data nor modeling analysis revealed strong H-bonding for any of the amide protons in MTII. Bednarek and coworkers have also analyzed MTII by NMR and molecular dynamics studies, but concluded that MTII neither existed in any classical turn structure or in any preferred conformation.[139] Although we did not identify any classical reverse turns, NOE and molecular dynamics data indicated that MTII did appear to have some conformational preferences in the backbone structure (Figure 4-7). One way to account for these contradictions is that our analyses and those of Fotsch et al. were carried out in aqueous solutions at 5°C, whereas the other two studies used DMSO-d_6 or CD_3OH at 25°C. Thus, the solution conformations of the peptides may differ between aqueous and organic solvents.

Hydrogen bonding of the amide protons was consistent between the temperature coefficient data and the peptide structures obtained from the molecular modeling studies. MTII, which did not have any low temperature coefficient values, did not have any hydrogen bonds between amide protons and carbonyl groups in any of the ten lowest energy structures from the dynamics trajectory. Representative structures of SHU9119 and the other three analogues only have hydrogen bonds between carbonyl groups and the amide protons that have low temperature coefficients. However, some of the amide protons that have low temperature coefficients are not hydrogen bonded in the RMD derived representative structures. Although not all of the hydrogen bonding could be

accounted for in the representative structures, the amides with low temperature coefficients were found to be hydrogen bonded at various time points in the dynamics trajectory. These observations suggest that although the ten lowest energy structures do not display a large deviation when superimposed, there is still a significant amount of conformational flexibility of the peptide backbones. Therefore, conformational averaging of these peptides must be taken into consideration if these RMD derived structures presented herein are to be used as templates for the design of melanocortin ligands in the future.

Molecular models serve as convenient utilities for viewing and analyzing compounds, which are invaluable when attempting to correlate structure with activity. In this regard, we initiated the molecular modeling and dynamics studies for the five peptides presented herein to try and identify structural similarities or differences that may account for the wide ranged of functional activity of the compounds at the mouse MC4R. It is interesting that we were not able to identify any significant structural differences between MTII and SHU9119 that may account for the antagonist activity of SHU9119 at the MC4 receptor. A superposition of the representative structures of MTII and SHU9119 is shown in Figure 4-9, which illustrates the lack of dissimilarity between the two peptides. Due to this, we *hypothesize* that the antagonist activity of SHU9119 is a result of interactions of the bulky naphthylalanine[7] residue with the receptor rather than a result of conformational differences between the two ligands. These interactions putatively involve the ligand naphthylalanine residue with the receptor Phe254 and Phe259 residues located in TM6 of the mouse MC4R, since mutation of either of these Phe residues converted SHU9119 into an agonist (Figure 4-10).[120]

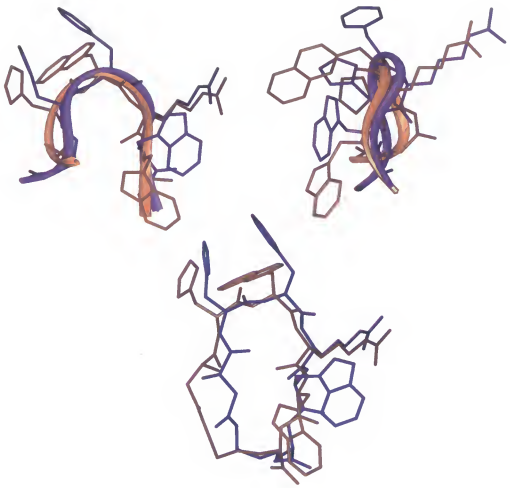

Figure 4-9. Superpositions of MTII and SHU9119 illustrating the similar structural features between the two peptides. The MC4R agonist MTII is shown in purple and the MC4R antagonist SHU9119 is shown in orange.

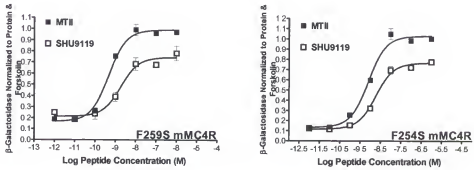

Figure 4-10. Dose response curves for SHU9119 at two mutated MC4 receptors. Modification of either of these two Phe residues converts SHU9119 into an agonist with almost full efficacy.

Although we did not identify any significant structural differences between the agonist MTII and the antagonist SHU9119, a number of similarities were found to exist between the MC4R agonists. A superposition of MTII and Analogue 3 is shown in Figure 4-11. Both of these compounds are full agonists at the mouse MC4R, although Analogue 3 is ca 3000-fold less potent than MTII. A significant amount of similarities between the two peptides can be seen in Figure 4-11. It was intriguing to observe the remarkable similarities in the solution structures of these two agonists, especially considering the stereochemistry of the position seven residue is inverted in Analogue 3, compared with MTII. The backbone atoms have related conformations, as apparent when looking at the two ribbon diagrams that represent the backbone secondary structure formations. Additionally, the $DPhe^{7}$/$Nal(2')^{7}$, Arg^{8}, and Trp^{9} residues in both of the agonists have the same topographical arrangement in 3-dimensional space. The major difference in the two structures is the placement of the imidazole ring, which sits on opposite sides of the turn regions. It is our *hypothesis* that the full agonist activity of these two ligands is a result of topographical arrangement of the position seven, eight, and nine residues. Apparently these residues are arranged in a manner that permits all of the interactions with the MC4 receptor required for the receptor conformational changes to take place that permits signal transduction to occur in full efficacy. Also, we hypothesize that the 3000-fold difference in potency is a result of the placement of the His^{6} residues. The His^{6} residue of Analogue 3 appears to be placed in an orientation that reduces potency, compared with MTII.

Figure 4-11. Superposition of the agonists MTII (purple) and Analogue 3 (red). Both of these ligands are full agonist at the mouse MC4 receptor.

We also identified similarities between MTII and the potent, albeit partial (48% maximal response), agonist Analogue 1. A superposition of these two MC4R agonists is shown in Figure 4-12. In this superposition the peptides were aligned in an inverted manner, i.e. the N-terminus of MTII aligned with the C-terminus of Analogue 1. The turn regions of the two peptides were fairly analogous in structure, which aligns the hydrophilic Arg^8 and the aromatic residues in a similar fashion in 3-dimensional space. The main differences are: the space occupied by the His^6 and $DPhe^7$ side chains of MTII was occupied by the Trp^9 side chain of Analogue 1; and the space occupied by the Trp^9 residue of MTII was occupied by the Nal^7 and His^6 residues of Analogue 1. It is *hypothesized* that this arrangement of side chains provides all of the key ligand interactions, i.e. the hydrophilic and aromatic functionalities, needed for potent agonist

activity at the mouse MC4R. However, it is hypothesized that the addition of the naphthyl and imidazole rings of Analogue 1 into the receptor binding pocket that is occupied by the MTII indole ring, and likewise, the addition of the indole ring of Analogue 1 into the receptor binding pocket where the phenyl ring and perhaps the imidazole ring of MTII presumably reside results in the inability of the receptor to undergo the conformational changes required for full efficacy.

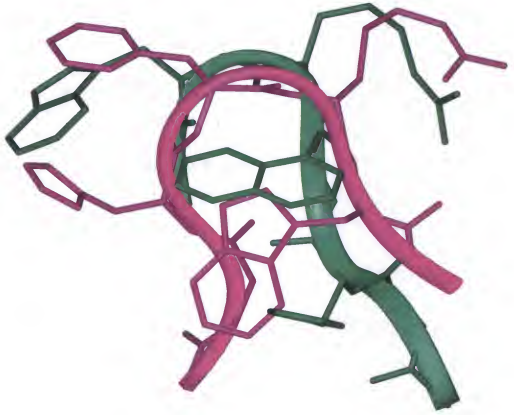

Figure 4-12. Superposition of the agonists MTII (purple) and Analogue 1 (green). Both of these ligands are potent agonist at the mouse MC4 receptor, however Analogue 1 is a partial agonists with an Emax=48%.

Summary

We have synthesized and characterized a series of five closely related cyclic peptides, each with differences in functional activity at the MC4R. ^{1}H-NMR methodologies and molecular dynamics were utilized in attempts to identify and correlate

structural features that may account for the observed MC4R activity. ^{1}H-NMR data indicated that the peptides may have some degree of conformational preferences and that there was some dissimilarity in the structures of the five compounds. Neither NMR nor molecular dynamics data indicated that any of the peptides exist in a classical turn formation, although there appeared to be some rigidity in the backbone conformations. In addition to differences in NMR parameters, different structural properties were observed in the modeling and dynamics study. We also were able to identify a significant amount of structural similarities between the full and partial agonists that may account for their functional activities at the mouse MC4R. We must use caution when using the information presented herein to correlate the functional activities of the five peptides with their structures, considering that their solution conformation may not be the conformation of the peptides in their receptor bound states. However, these studies are useful in identifying structural features that may contribute to MC4R activity and therefore are a useful means of developing a three-dimensional pharmacophore for interactions with the mouse MC4 receptor.

CHAPTER 5
EXPERIMENTAL

Peptide Synthesis

Peptides 1-75

Peptides **1-75** were synthesized using standard Fmoc methodology[97,98] on an automated synthesizer shown in Figure 5-1 (Advanced ChemTech 440MOS, Louisville, KY). The amino acids Fmoc-Tyr(tBu), Fmoc-DTyr(tBu), Fmoc-His(Trt), Fmoc-DHis(Trt), Fmoc-Arg(Pbf), Fmoc-DArg(Pbf), Fmoc-Trp(Boc), Fmoc-Pro, Fmoc-Ala, Fmoc-Phe, Fmoc-DPhe, Fmoc-3-(2-naphthyl)-alanine [Nal(2')], Fmoc-3-(2-naphthyl)-D-alanine [DNal(2')], Fmoc-phenylglycine (Phg), Fmoc-D-phenylglycine (DPhg), Fmoc-3-(1-naphthyl)-alanine [Nal(1')], Fmoc-3-(1-naphthyl)-D-alanine [DNal(1')], N^{α}-Fmoc-N^{δ}-Boc-ornithine (Orn), Fmoc-Lys(Boc), Fmoc-Asp(OtBu), Fmoc-Glu(OtBu), Fmoc-3,3-diphenyl-alanine (Dip), and Fmoc-D-3,3-diphenyl-alanine (DDip), and N^{α}-Fmoc-N^{β}-Boc-2,4-diaminobutyric acid (Dab) were purchased from Peptides International (Louisville, KY). Fmoc-DTrp(Boc), Fmoc-citruline (Cit) and Fmoc-homoArg(Pbf) (homoArg) was purchased from Advanced ChemTech (Louisville, KY). Fmoc-β-(3-benzothienyl)-alanine (3Bal), Fmoc-D-homo-phenylalanine (hDPhe), Fmoc-homo-phenylalanine (hPhe), Fmoc-3-(2-thienyl)alanine (2-Thi), Fmoc-aminoadipic acid(OtBu) (Aaa), Fmoc-3-(3-pyridinyl)alanine (3-Pal), and Fmoc-3-(4-pyridinyl)alanine (4-Pal) were purchased from Bachem (Torrance, CA). Fmoc-4-phenyl-phenylalanine (Bip), Fmoc-4-phenyl-D-phenylalanine (DBip), Fmoc-4-Iodo-D-phenylalanine (p-I-DPhe), Fmoc-1,2,3,4-tetrahydroisoquinoline-3-carboxylic acid (Tic) and Fmoc-D-1,2,3,4-

tetrahydroisoquinoline-3-carboxylic acid (DTic) were purchased from Synthetech (Albany, OR). Fmoc-(racemic)-amino-tetrahydro-2-napthyl carboxylic acid (Atc) and Fmoc-amino-2-napthyl carboxylic acid (Anc) were purchased from Pharma Core (High Point, NC). The coupling reagents 2-(1-H-benzotriazol-1-yl)-1,1,3,3-tetramethyluronium hexafluorophosphate (HBTU) and 1-hydroxybenzotriazole (HOBt) were purchased from Peptides International. Glacial acetic acid (HOAc), dichloromethane (DCM), methanol (MeOH), acetonitrile (ACN), and anhydrous ethyl ether were purchased from Fisher (Fair Lawn, NJ, USA). N,N-dimethylformamide (DMF) was purchased from Burdick and Jackson (McGaw Park, IL, USA). Trifluoroacetic acid (TFA), 1,3-diisopropylcarbodiimide (DIC), pyridine, piperidine and acetic anhydride were purchased from Sigma (St. Louis, MO, USA). N-N-diisopropylethylamine (DIEA) and triisopropylsilane (Tis) were purchased from Aldrich (Milwaukee, WI, USA). All reagents and chemicals were ACS grade or better and were used without further purification.

Figure 5-1. Picture of the Advanced ChemTech 440 MOS synthesizer used in this study to prepare peptides **1-75**.

The peptides were assembled on Rink-amide-MBHA resin (0.44 meq/g substitution), purchased from Peptides International. The synthesis was performed using a 40 well Teflon reaction block with a course Teflon frit. Approximately 100 mg resin (0.044mmole) was added to each reaction block well. The resin was allowed to solvate for 2 hr in DMF. The Fmoc group was removed using 25% piperidine in DMF for 5 min at 450 rpm followed by a 20 min 25% piperidine incubation at 450 rpm. A positive Kaiser[110] test resulted indicating free amine groups on the resin. The growing peptide chain was added to the amide-resin using the general amino acid cycle as follows: 500 μM DMF was added to each reaction well to "wet the frit", 3-fold excess amino acid starting from the C-terminus was added (275 μL of 0.5M amino acid solution containing 0.5M HOBt in DMF) followed by the addition of 275 μL 0.5M DIC in DMF and the reaction well volume was brought up to 3mL using DMF. The coupling reaction was mixed for lhr at 450 rpm, followed by emptying of the reaction block by positive nitrogen gas pressure. A second coupling reaction iwa performed by the addition of 500 μL DMF to each reaction vessel, followed by the addition of 275 μL of the respective amino acid (3-fold excess), 275 μL 0.5M HBTU, and 225 μL 1M DIEA. The reaction well volume was brought up to 3 mL with DMF and mixed at 450 rpm for 1hr. After the second coupling cycle, the reaction block was emptied and the Nα-Fmoc-protected peptide-resin was washed with DMF (4.5 mL, 4 times). Nα-Fmoc deprotection was performed by the addition of 4 mL 25% piperidine in DMF and mixed for 5 min at 450 rpm followed by a 20 min deprotection at 450 rpm. The reaction well was washed with DMF (4.5 mL, 4 times) and the next coupling cycle was performed as described above. Following Nα-Fmoc deprotection of the final amino acid, acetylation of the Nα-amine was performed

by addition of 2 mL acetic anhydride, 1 mL pyridine and 1 mL DMF to the reaction block wells and mixed for 30 min at 450 rpm. The acetylated peptide-resin was washed with DCM (4 mL, 5 times) and dried thoroughly prior to cleavage from the resin. Deprotection of the amino acid side chains and cleavage of the acetylated-peptide from the resin was performed by incubating the peptide-resin with 3mL cleavage cocktail (95% TFA, 2.5% water, 2.5% Tis) for 3 hr at 450 rpms. The cleavage product was emptied from the reaction block into a cleavage block containing 7 mL collection vials under positive nitrogen gas pressure. The resin was washed with 1.5 mL cleavage cocktail for 5 min and 450 rpm and added to the previous cleavage solution. The peptides were transferred to pre-weighed 50 mL conical tubes and precipitated with cold (4°C) anhydrous ethyl ether (up to 50 mL). The flocculent peptide was pelleted by centrifugation (Sorval Super T21 high speed centrifuge using the swinging bucket rotor) at 4000 rpm for 5 min, the ether was decanted off, and the peptide was washed one time with cold anhydrous ethyl ether and again pelleted. The crude peptide was dried *in vacuo* for 48 hrs. The crude peptide yields ranged from 60% to 90% of the theoretical yields. A 15 to 30 mg sample of crude peptide was purified by RP-HPLC using a Shimadzu chromatography system with a photodiode array detector and a semi-preparative RP-HPLC C18 bonded silica column (Vydac 218TP1010, 1.0 x 25 cm) and lyophilized. The purified peptides were at least >95% pure as determined by analytical RP-HPLC and had the correct molecular mass (University of Florida protein core facility).

MTII, SHU9119, and Analogues 1-3

Peptides **MTII, SHU9119, and Analogues 1-3** were synthesized using standard Boc methodology on a semi-automated synthesizer shown in Figure 5-2 (Advanced

ChemTech *Labtech*, Louisville, KY). The amino acids Boc-norleucine (Nle), Boc-Lys(Fmoc), Boc-Asp(OFm), Boc-His(Bom), Boc-DPhe, Boc-Arg(Tos), Boc-Trp(For), Boc-β-(1-naphthyl)-L-alanine [Nal(1')], Boc-β-(1-naphthyl)-D-alanine [DNal(1')], Boc-β-(2-naphthyl)-L-alanine [Nal(2')]and Boc-β-(2-naphthyl)-D-alanine [DNal(2')]were purchased from Bachem. The peptides were assembled on para methyl-benzhydrylamine resin (*p*MBHA) (0.28meq/g substitution), purchased from Peptides International (Louisville, KY). All reagents were ACS grade or better and used without further purification. The synthesis was performed using a 16 well Teflon reaction block with a course Teflon frit. Approximately 200mg of resin (0.056mmol) was added to each reaction block well. The resin was allowed to swell for 2hr in 5mL of dimethylformamide (DMF) and deprotected using 4mL of 50% trifluroacetic acid (TFA) and 2% anisole in dichloromethane (DCM) for 3 min followed by a 20 min incubation at 325 rpm, and washed with DCM (4.5mL, 2 min, 325 rpm 3 times). The peptide-resin trifluoracetate salt was neutralized by the addition of 4mL of 10% diisopropylethylamine (DIEA) in DCM (3 min, 325 rpm, 2 times) followed by a DCM wash (4.5mL, 2 min, 325 rpm 4 times). A positive Kaiser[110] test resulted, indicating free amine groups on the resin. The growing peptide chain was added to the amide-resin using the general amino acid cycle as follows: 500μL of DMF was added to each reaction well to "wet the frit," pre-activated amino acid starting from the C-terminus was added [3-fold excess amino acid, 3-fold excess diisopropycarbodiimide (DIC), and 3-fold excess N-hydroxybenzotriazole (HOBt) in DMF], and the reaction well volume was brought up to 4mL using DMF. The coupling reaction is mixed for 2hr at 325 rpm, followed by emptying of the reaction block by vacuum. After the coupling cycle, the peptide-resin is washed with DCM (4.5mL 4

times). Nα-Boc deprotection was performed by the addition of 4mL of 50% TFA and 2% anisole in DCM and mixed for 5 min at 325 rpm followed by a 20 min deprotection at 325 rpm. The peptide-resin trifluoroacetate salt was washed with 4.5mL of DCM (4 times), neutralized with 10% DIEA (3 min, 325 rpm, 2 times) followed by a DCM wash (4.5mL, 2 min, 325 rpms 4 times), and the next coupling cycle was performed as described above. The side chain lactam bridge was formed between the side chain carboxyl moiety of Asp and the side chain N^{ε} amino group of Lys. The Fmoc and OFm protecting groups are removed from Lys and Asp, respectively, by treatment with 4.5mL of 25% piperidine in DMF for 5 min at 325 rpm followed by a 20 min incubation at 325 rpm, with a positive Kaiser test resulting. The lactam bridge between the Asp and Dpr amino acids was formed using 5-fold excess benziotriazolyloxytris(dimethylamino) phosphonium hexafluorophosphate (BOP) and 6-fold excess DIEA as coupling agents and mixing at 325 rpms. The lactam bridges were formed (negative Kaiser test) after approximately 2-5 days at room temperature. Deprotection of the remaining amino acid side chains and cleavage of the amide-peptide from the resin was performed by incubation the peptide-resin with anhydrous hydrogen fluoride (HF, 5 mL, 0 °C, 1hr) and 5% m-cresol, 5% thioanisole as scavengers. After the reaction is complete and the HF has been distilled off, the peptide was ether precipitated by addition of cold (4°C) ethyl ether. The precipitated peptide was filtered over a course frit glass filter and washed with an additional 50 mL cold (4°) anhydrous ethyl ether. The precipitated peptide was dissolved in glacial acetic acid, collected in a 250mL round-bottomed flask, frozen, and lyophilized. The crude peptide yields ranged from 60 to 90% of the theoretical yields. Approximately 30mg of crude peptide was purified by RP-HPLC using a Shimadzu

chromatography system with a photodiode array detector and a semipreparative reversed-phase high-performance liquid chromatography (RP-HPLC) C18 bonded silica column (Vydac 218TP1010, 1.0 x 25 cm) and lyophilized. The purified peptide was >95% pure as determined by analytical RP-HPLC and had the correct molecular mass (University of Florida protein core facility).

Figure 5-2. Picture of the Advanced ChemTech 440 MOS synthesizer used in this study to prepare MTII, SHU9119, and Analogues 1-3.

Cell Culture and Transfection

Briefly, HEK-293 cells were maintained in Dulbecco's modified Eagle's medium (DMEM) with 10% fetal calf serum and seeded 1 day prior to transfection at 1 to 2 $x10^6$ cell/100-mm dish. Melanocortin receptor DNA in the $pCDNA_3$ expression vector (20 μg)

were transfected using the calcium phosphate method. Stable receptor populations were generated using G418 selection (1mg/mL) for subsequent bioassay analysis.

Bioassays

HEK-293 cells stably expressing the melanocortin receptors were transfected with 4μg CRE/β-galactosidase reporter gene as previously described.[205] Briefly, 5,000 to 15,000 post transfection cells were plated into 96 well Primera plates (Falcon) and incubated overnight. Forty-eight hours post-transfection the cells were stimulated with 100μL peptide (10^{-4} - 10^{-12} M) or forskolin (10^{-4} M) control in assay medium (DMEM containing 0.1 mg/mL BSA and 0.1 mM isobutylmethylxanthine) for 6 hr. The assay media was aspirated and 50μL of lysis buffer (250 mM Tris-HCl pH=8.0 and 0.1% Triton X-100) was added. The plates were stored at –80°C overnight. The plates containing the cell lysates were thawed the following day. Aliquots of 10 μL were taken from each well and transferred to another 96-well plate for relative protein determination. To the cell lysate plates, 40 μL phosphate-buffered saline with 0.5% BSA was added to each well. Subsequently, 150 μL substrate buffer (60 mM sodium phosphate, 1 mM $MgCl_2$, 10 mM KCl, 5 mM β-mercaptoethanol, 200 mg ONPG) was added to each well and the plates were incubated at 37°C. The sample absorbance, OD_{405}, was measured using a 96 well plate reader (Molecular Devices). The relative protein was determined by adding 200 μL 1:5 dilution Bio Rad G250 protein dye:water to the 10 μL cell lysate sample taken previously, and the OD_{595} was measured on a 96 well plate reader (Molecular Devices). Data points were normalized both to the relative protein content and non-receptor dependent forskolin stimulation. The antagonistic properties of these compounds were evaluated by the ability of these ligands to competitively displace the

MTII agonist (Bachem) in a dose-dependent manner, at up to 10μM concentrations. The pA_2 values were generated using the Schild analysis method.[206]

Data Analysis

EC_{50} and pA_2 values represent the mean of duplicate experiments performed in quadruplet or more independent experiments. EC_{50} and pA_2 estimates, and their associated standard errors, were determined by fitting the data to a nonlinear least-squares analysis using the PRISM program (v3.0, GraphPad Inc.). The results are not corrected for peptide content, although all the peptides examined in this study were determined to have approximately equal peptide content as determined by using Beers Law.

One-dimensional ^{1}H Nuclear Magnetic Resonance Spectroscopy (1D-NMR) Peptides 1-18 and 45-75

Peptides 1-18 and 45-75 were analyzed for purity and structural integrity by nuclear magnetic resonance (NMR). Peptides 19-44 were not analyzed by NMR due to budget limitations of the project. The 1D ^{1}H-NMR spectra are shown in appendix A. Peptides were dissolved in 600 μL DMSO-d_6 that contained 0.1% TMS, with an approximate final concentration of 2mM. ^{1}H NMR spectra were obtained at 27°C on a Bruker Avance 500 MHz spectrometer in the Advanced Magnetic Resonance Imaging and Spectroscopy facility at the McKnight Brain Institute, University of Florida. One dimensional ^{1}H data were collected using the decoupler coil of a Bruker 5mm BBO probe with 128 scans, 26,684 total time domain points, a tip angle of 45°, an acquisition time of 2 seconds and a delay time of 3 seconds. The spectral widths were 12 ppm and TMS was referenced to 0.0 ppm. In order to correctly determine the integral values of peaks that occasionally occurred in the region around 3.3 ppm, a standard presaturation procedure

(Bruker zgf2pr) for H_2O in DMSO was used. Prior to Fourier transformation the FID was apodized with an exponential line broadening of 0.5Hz and transformed with minimal zero-filling to 16K data points. The data were processed and analyzed using Bruker XWINNMR and XWINPLOT software.

MTII, SHU9119, and Analogues 1-3

NMR samples were prepared by dissolving approximately 1.7mg of the purified peptides in a 550μL solution of 95% (v/v) H_2O and 5% D_2O (Cambridge Isotope Labs, 99%) with a pH of 3.6. NMR data were collected using a Bruker Avance spectrometer operating at 500 MHz at the Advanced Magnetic Resonance and Imaging and Spectroscopy (AMRIS) Facility in the McKnight Brain Institute at the University of Florida. The 1D ^{1}H-NMR spectra are shown in appendix B. Data were collected using a Bruker 5mm TXI probe with 32 scans, 32768 total time domain points, a tip angle of 45°, an acquisition time of 2.5 seconds and a delay time of 3 seconds. The spectral widths were 12 ppm and DSS was referenced to 0.0 ppm. The water signal was reduced using a standard presaturation procedure (Bruker zgf2pr) during the relaxation delay. Prior to Fourier transformation the FID was apodized with an exponential line broadening of 0.5Hz and transformed with minimal zero-filling to 16K data points. Temperature titration data were recorded from 5°C to 50°C in 5°C increments. The temperature dependence of each amide peak was determined by plotting the measured frequencies as a function of temperature and amide temperature coefficients were determined from the slopes of the best fit lines. Data were processed and analyzed with Bruker XWIN-NMR and XWIN-PLOT software.

Two-dimensional ^{1}H Nuclear Magnetic Resonance Spectroscopy (2D-NMR)

The same 2mM NMR samples of MTII, SHU9119, and Analogues 1-3 prepared for 1D-NMR experiments were used in the 2D-NMR experiments. Chemical shifts were assigned using standard TOCSY and NOESY based methodologies.[113] Data were collected using a Bruker Avance spectrometer operating at 500 MHz at the Advanced Magnetic Resonance and Imaging and Spectroscopy (AMRIS) Facility in theMcKnight Brain Institute at the University of Florida. The 2D ^{1}H-NMR spectra are shown in appendix C. NMR data were collected at 5°C and 35°C. The water signal was reduced by presaturation during the relaxation delay. Data were referenced to internal DSS (0.0 ppm). Total correlation spectroscopy (TOCSY) data were recorded with a 70 ms mixing time using the MLEV-17 spin-lock sequence. Rotating frame Nuclear overhauser effect spectroscopy (ROESY) data were recorded with 250ms mixing times. Data were processed in XWIN-NMR. Data were analyzed with the interactive computer program NMRView.[207]

Molecular Dynamics Simulations

All conformational modeling was performed using InsightII software (Molecular Simulations Inc, San Diego, CA). Linear structures for the five peptides were initially energy minimized with a pseudo-potential between the side chains of Lys and Asp and restrained molecular dynamics (RMD) simulations for each peptide were run for 5ns in a vacuum with a dielectric constant of 4.0 and 500 K using the cvff force field with cross-terms, Morse potentials, and no cutoff distances. Fifty-one structures from the history file were energy minimized using 2000 steps of steepest decent followed by conjugate gradients and Newton-Raphson until a convergence of 0.1 was reached. Following analysis of the 51 structures; the lowest energy conformer that best satisfied NMR

derived restraints was chosen, NMR derived restraints were included and a 20ns RMD simulation was started. Following the 20ns RMD simulation, 201 structures from the history file were energy minimized with NMR restraints using 2000 steps of steepest decent followed by conjugate gradients and Newton-Raphson until a convergence of 0.1 was reached. The ten lowest energy structures for each peptide were used for subsequent analysis.

CHAPTER 6
CONCLUSIONS

Successful treatment of obesity and the obesity syndrome dictates that the complex pathways involved in weight homeostasis and feeding behavior must be understood. Remarkable new insights into the mechanisms that control body weight are providing an increasingly detailed framework for a better understanding of obesity pathogenesis. The central regulators of food intake and body weight, such as POMC, AGRP, Leptin, Grehlin, PYY and NPY receptors have been identified.[13-21] Key peripheral signals, such as leptin, insulin, and ghrelin, have been linked to these hypothalamic neuropeptide systems, and the networks that integrate these systems have begun to be elucidated.[14]

Over the last ten years compelling genetic and pharmacological evidence has emerged that supports a role of the melanocortin receptor system in weight homeostasis.[22,23] The current data suggest that central MC3 and MC4 receptors, along with their endogenous agonists and antagonist, are key components responsible for the regulation of body weight via the modulation of both food intake and energy expenditure.[23]

As mentioned above, the melanocortin system is intricately linked in the complex pathways of feeding behavior and weight homeostasis, and thus have become viable targets for therapeutic treatment of obesity and related diseases. There are two primary methods of drug discovery: random screening of diverse collections of compounds, such as natural products mainly derived from plants and microorganisms; and rational drug design. Rather than screening random compounds against a variety of disease states, the

rational design approach relies on knowledge of the mechanistic basis for the disease and the molecular characteristics of compounds that interact with the disease target.[121] The costs associated with random screening combined with the low yield of new and useful lead compounds have led to a decrease in popularity of the former method.

The rational design approach relies on identification of a disease target and understanding the fundamental physiologic and biochemical processes involved in the disease state. Once a disease target has been selected, a lead compound needs to be established. Lead compounds serve as a starting point in the rational drug design process. Often these compounds are the natural ligand for a receptor or a substrate for an enzyme. Once a lead is identified, it is necessary to determine what key structural features of the compound are responsible for activity. In the case of a peptide ligand, this information can be obtained by a set of experiments carefully designed to provide information regarding ligand-receptor interactions. These experiments are referred to as structure-activity relationship studies, and in the case of peptides and proteins often begin with two important experiments: 1) an alanine scan to determine the specific side chains involved in binding and functional activity; and 2) truncation studies to determine the minimal fragments needed to retain activity and binding, as well as potency equal to that of the lead peptide. Once the above studies are completed, one can generally determine the pharmacophore of the lead compound. Following the establishment of the peptidic pharmacophore, one can begin to assess how structural changes will affect activity. This structural knowledge is then used in the design of new ligands with improved properties. Structure-activity studies are designed to provide insight into the types of interactions that occur in the formation of the ligand-receptor complex. One would like to know both the

favorable and unfavorable processes that occur in ligand-receptor interactions that result in receptor stimulation (or inhibition). One objective of structure-activity studies is to aid in the design of ligands, with specific function, *a priori* for a given receptor or receptor system.

Structure-Activity Relationships of Melanocortin Tetrapeptides

In our efforts to characterize the melanocortin system, we recently have carried out truncation studies of NDP-MSH at the cloned central and peripheral mouse melanocortin receptors.[78] The Ac-His-DPhe-Arg-Trp-NH_2 tetrapeptide was identified as possessing an EC_{50} value of 10 nM at the murine MC4 receptor, which is similar to the 8 nM results published by Yang et al. for the tetrapeptide at the human MC4 receptor.[141] This tetrapeptide exhibits full agonist efficacy at all the mouse MC receptors and is equipotent to the endogenous hormone α-MSH (within experimental error), and only 30-fold less potent than NDP-MSH at the mouse MC4R. Due to the small size and potency of this peptide, relative to the tridecapeptide α-MSH, it was used as a starting point in a study aimed at improving the potency and receptor selectivity of the ligand at the melanocortin receptors. In a series of extensive structure-activity relationship (SAR) studies presented in chapter 3 of this dissertation, modifications were systematically made at each of the four amino acid residues, with subsequent pharmacological evaluation at the mouse MC1R, MC3R-MC5R.[196,208-211]

We have synthesized, purified to homogeneity, analytically and pharmacologically characterized over 75 modified melanocortin tetrapeptides to evaluate structure-activity trends and to identify peptides with novel and useful pharmacology. We have identified modifications that increase potency and receptor selectivity, as well as identified

chemically non-reactive moieties that can used to replace reactive indole and imidazole groups in the design of future melanocortin ligands. Two peptides have been discovered with very interesting pharmacological profiles, JRH 322-18 (peptide **20** herein) and JRH 420-12 (peptide **16** herein), that are currently being characterized for the *in vivo* properties in our animal models.

Conformational Analysis of Cyclic Melanocortin Ligands

The five peptides presented in chapter 4 of this dissertation are all based on the MTII 23-membered ring system and differ only by subtle modifications at the Phe^7 position. Although similar in primary chemical structure, the peptides have significant differences in functional activity at the mouse MC4R. It is interesting that slight modifications of the Phe^7 residue significantly alters the functional activity of the ligands, prompting one to speculate that the Phe^7 modifications may be effecting the conformational properties of the peptides. Indeed, previous data from MC4R mutagenesis studies using four of the five peptides presented herein indicated that the four peptides do not interact with the acidic residues in the putative binding pocket of the MC4R in an identical manner. These data have led to the hypothesis that structural dissimilarities may exist between the peptides as a result of the bulky aromatic groups at position seven that are responsible for affecting these ligand-receptor interactions.[124] The studies presented in chapter 3 were initiated to test this hypothesis that the aromatic ring structures are indeed modifying the three-dimensional structure of the cyclic melanocortin ligands and determine if conformational differences can be identified between MTII and the naphthyl-analogues that can be attributed to the observed functional activity at the MC4R. To this end, we employed the combination of various ^{1}H-NMR based strategies

together with molecular modeling and restrained molecular dynamics simulations described in chapter 4.

The first step in our analyses was assignment of chemical shifts for each proton of each of the five peptides in aqueous solution. This was accomplished in a straight forward manner using standard TOCSY and NOESY ^{1}H-NMR strategies.[113] Chemical shifts are extremely sensitive to the electronic environment, and thus provide useful probes into changes in structural features when comparing a closely related set of compounds, like the five peptides presented herein. We also used chemical shift deviations between experimental and random coil shift values of backbone protons as an assessment of ordered structure, as well as a means of comparing the five peptides.[199] As discussed in chapter 4, there are differences in the experimental chemical shift values and reported random coil values, as well as variations in the degree of chemical shift deviation within the five peptides. These data not only suggest some degree of ordered structure, but also suggest the structures of the peptides are not equivalent. In addition to the backbone protons, variations in the chemical shifts in several of side chain protons were observed. The NMR data prompted us to further investigate the conformational properties of the five peptides.

One of the fundamental hypotheses in biochemical research is that the information possessed by chemical messengers involved in information transduction processes and subsequent functional behavior is directly related to their conformational properties.[204] Likewise we hypothesized that the conformational properties of the five peptides presented herein were responsible for their pharmacology at the mouse MC4R, and since each of the peptides have variations in their functional activity their conformational

properties may also vary. ^{1}H-NMR analysis of the five peptides suggested to us that there are dissimilarities in structural features. To aid in identifying and understanding these features, modeling studies were undertaken.

Molecular modeling based on NMR data in MTII, SHU9119, analogues 1, 2 and 3 was carried out with the goal to identify structural features that affect the functional activity at the mouse MC4R. Although no classical turn structures could be identified by NMR data or modeling analysis, both of the analyses indicated some conformational preferences, in particular preferences in the backbone structures. This is in agreement with the recently published solution structure of a related MTII analogue by Fotsch et al.[203] However, this is in contrast with two other published solution structures of MTII.[139,187] Al-Obeidi and colleagues used a combination of 1D ^{1}H-NMR and molecular dynamics studies to conclude that the solution conformation of MTII consisted of a type II β-turn in the His-DPhe-Arg-Trp region, with hydrogen bonding between Arg NH and Asp CO.[187] As mentioned previously, there was no well defined reverse turns in the solution structure of MTII in our study, although there was a reverse turn with similarities to several classical β-turns. Additionally, neither our NMR data nor modeling analysis revealed strong H-bonding for any of the amide protons in MTII. Bednarek and coworkers have also analyzed MTII by NMR and molecular dynamics studies, but concluded that MTII did not exist in any classical turn structure or in any preferred conformation.[139] Although we did not identify any classical turn, NOE and molecular dynamics data indicated that MTII did appear to have some conformational preferences in the backbone structure. Conformational differences were observed in the ligands that may be attributed to the variation in MC4R functional activity. Additionally, similarities

in structural features were identified between the cyclic agonists that may account for their functional activity at the MC4R.

APPENDIX A
1-DIMENSIONAL (1D) ^{1}H-NMR SPECTRA OF LINEAR TETRAPEPTIDES

The 1-dimensional (1D) ^{1}H-NMR spectra of the linear tetrapeptides discussed in chapter three are presented herein appendix A. The peptides were dissolved in DMSO-d_6 at a concentration of 2mM. Data were collected at 27°C on a Bruker Avance spectrometer operating at 500MHz in the Advanced Magnetic Resonance Imaging and Spectroscopy (AMRIS) facility at the McKnight Brain Institute, University of Florida. The spectra are presented for peptides 1-18 and 45-75. The 1D data sets were not collected for peptides 19-44 due to budget restrictions of the project.

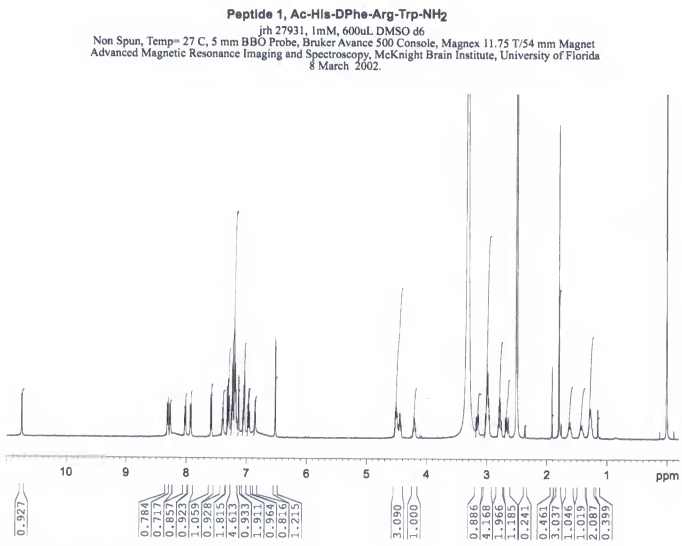

Figure A-1. Peptide 1 one-dimensional (1D) ^{1}H-NMR spectrum.

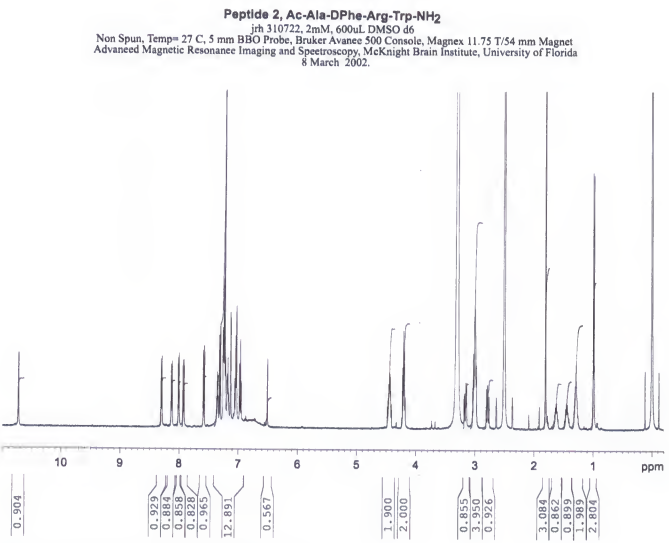

Figure A-2. Peptide 2 one-dimensional (1D) ^{1}H-NMR spectrum.

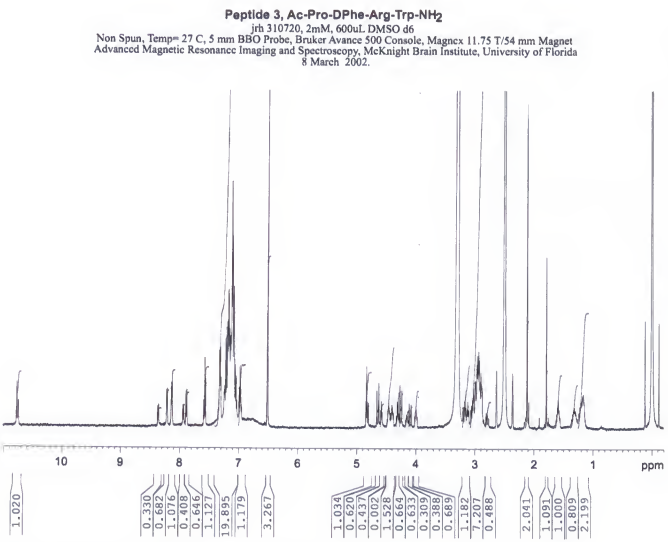

Figure A-3. Peptide 3 one-dimensional (1D) ^{1}H-NMR spectrum.

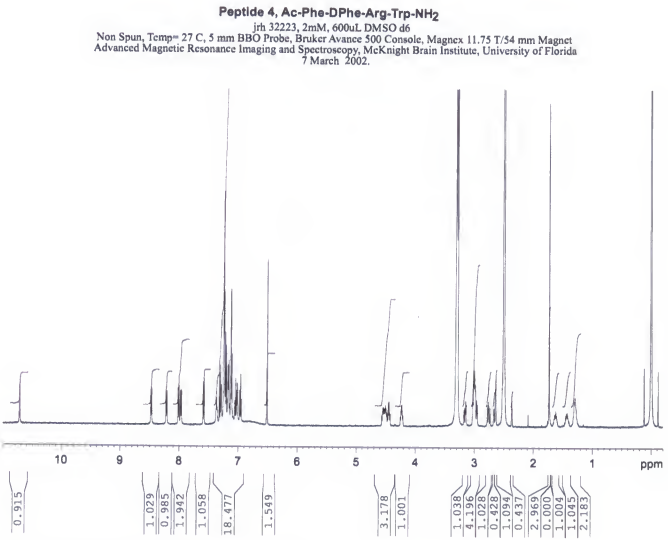

Figure A-4. Peptide 4 one-dimensional (1D) ^{1}H-NMR spectrum.

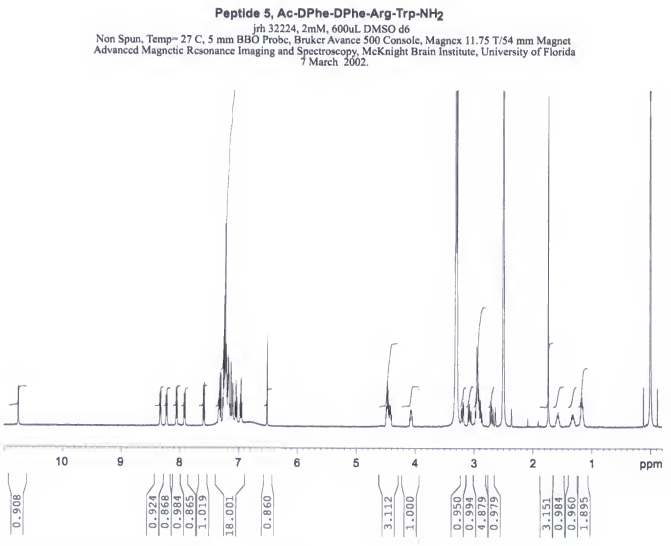

Figure A-5. Peptide 5 one-dimensional (1D) ^{1}H-NMR spectrum.

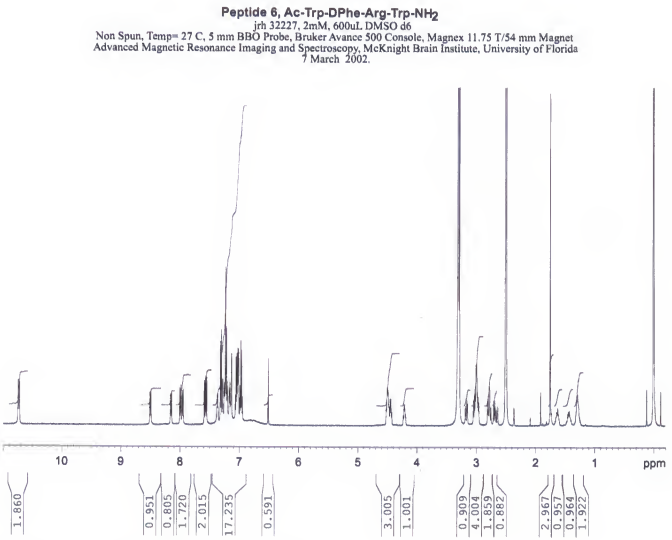

Figure A-6. Peptide 6 one-dimensional (1D) ^{1}H-NMR spectrum.

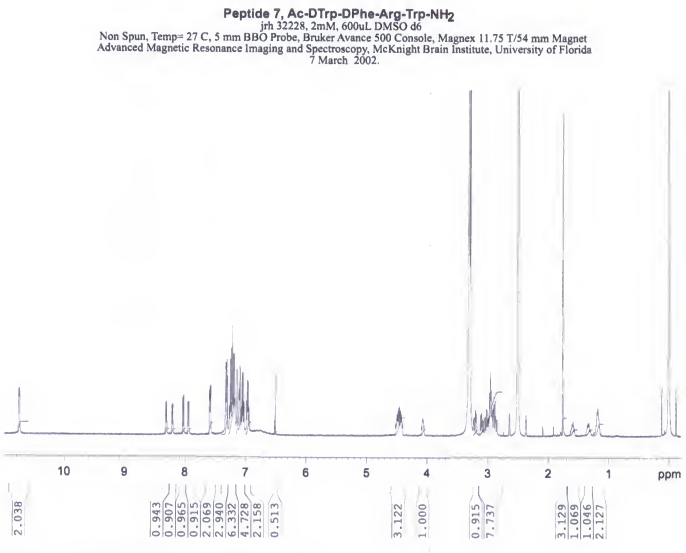

Figure A-7. Peptide 7 one-dimensional (1D) ^{1}H-NMR spectrum.

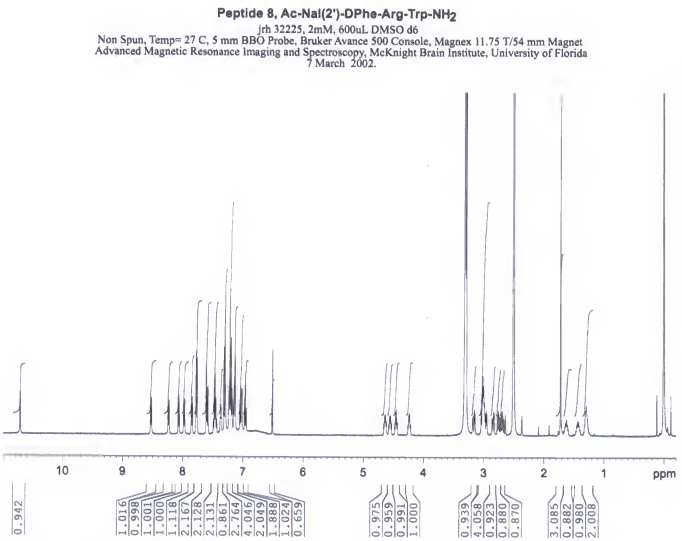

Figure A-8. Peptide 8 one-dimensional (1D) ^{1}H-NMR spectrum.

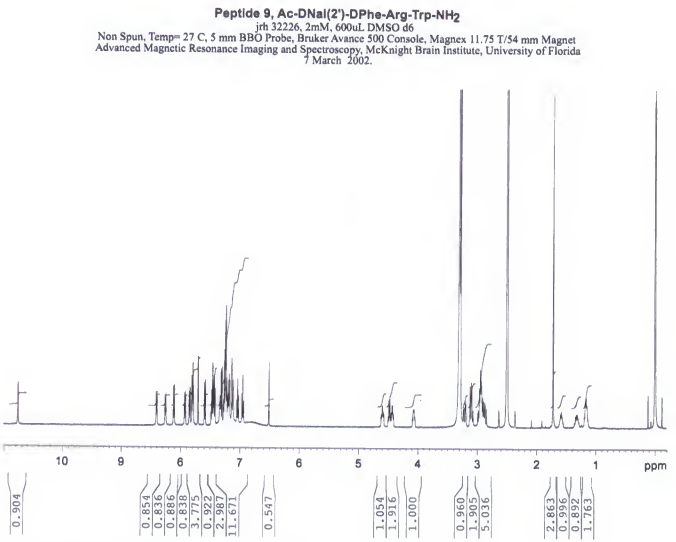

Figure A-9. Peptide 9 one-dimensional (1D) ^{1}H-NMR spectrum.

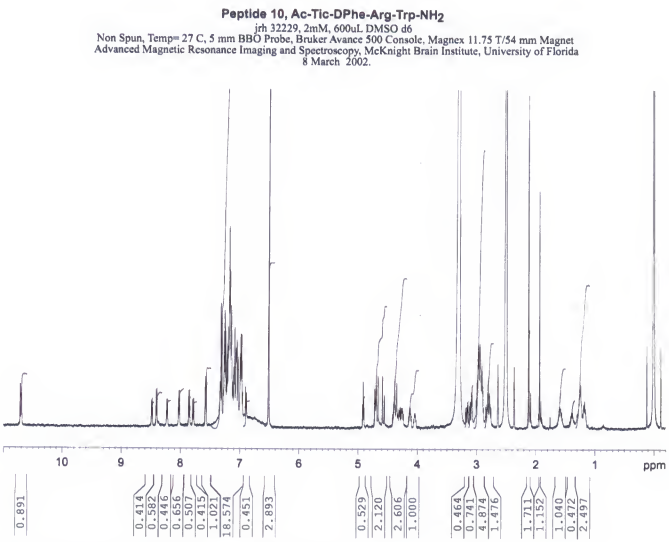

Figure A-10. Peptide 10 one-dimensional (1D) ^{1}H-NMR spectrum.

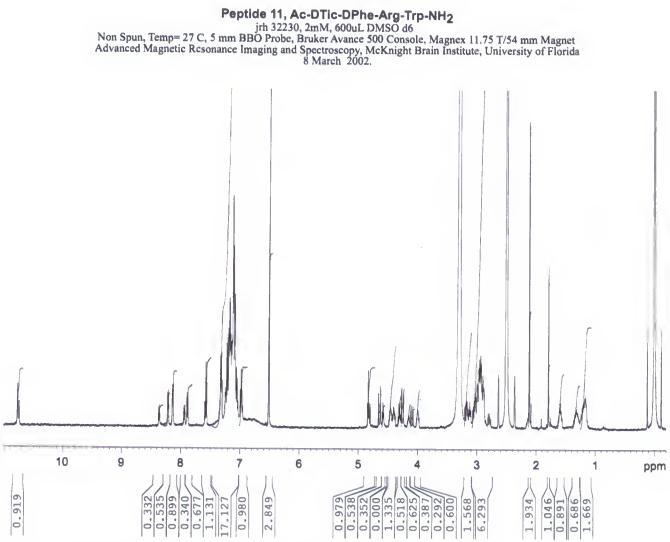

Figure A-11. Peptide 11 one-dimensional (1D) ^{1}H-NMR spectrum.

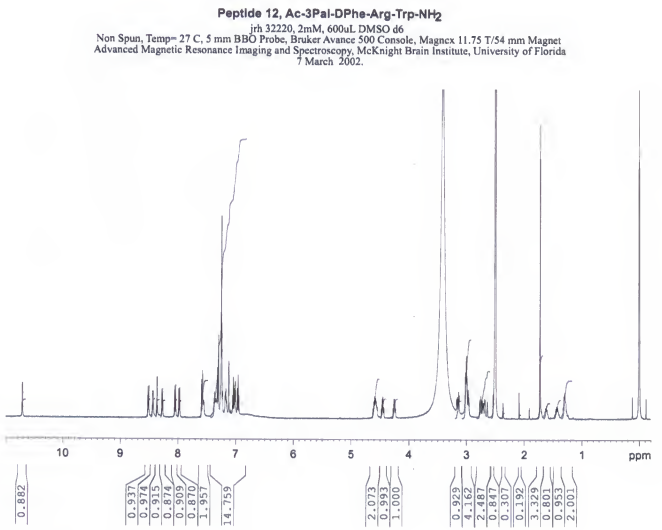

Figure A-12. Peptide 12 one-dimensional (1D) ^{1}H-NMR spectrum.

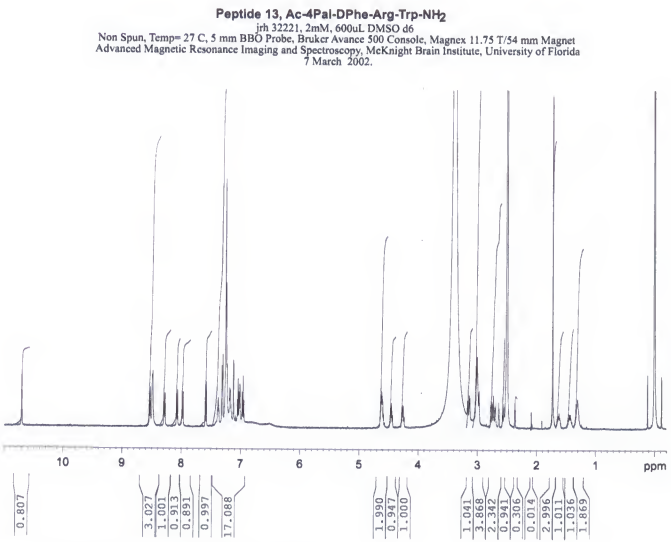

Figure A-13. Peptide 13 one-dimensional (1D) ^{1}H-NMR spectrum.

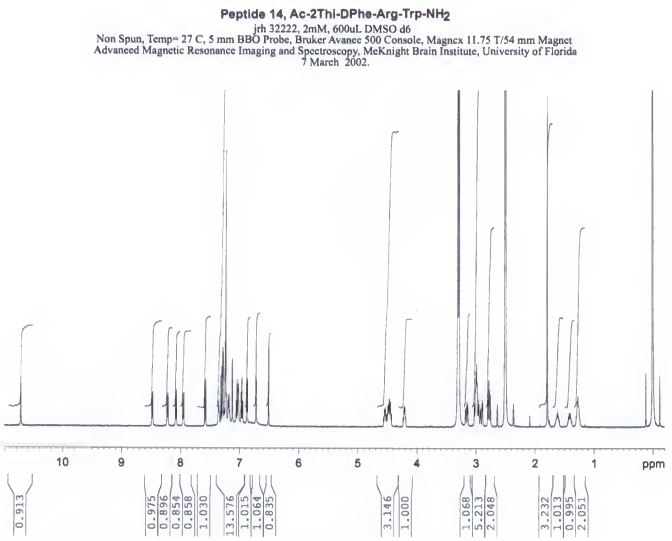

Figure A-14. Peptide 14 one-dimensional (1D) ^{1}H-NMR spectrum.

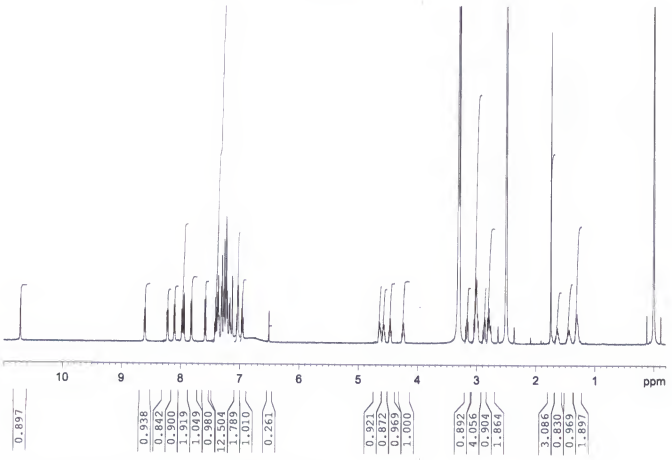

Figure A-15. Peptide 15 one-dimensional (1D) ^{1}H-NMR spectrum.

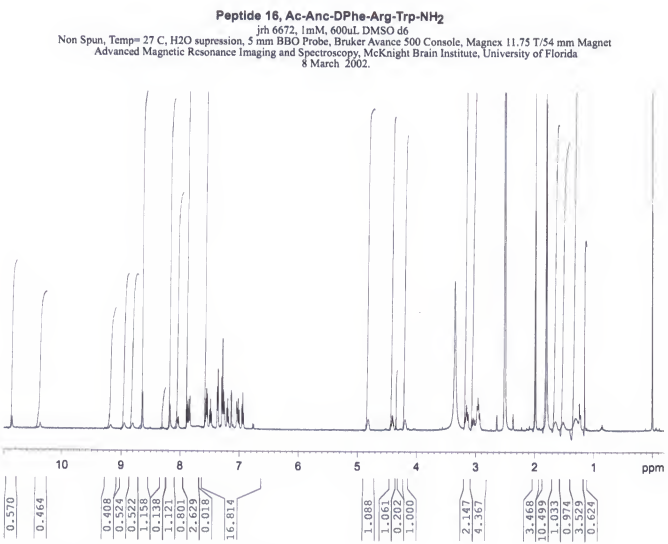

Figure A-16. Peptide 16 one-dimensional (1D) ^{1}H-NMR spectrum.

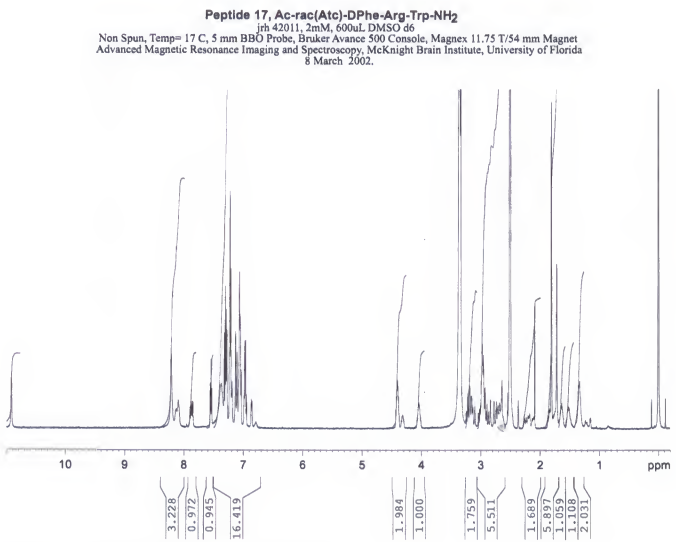

Figure A-17. Peptide 17 one-dimensional (1D) ^{1}H-NMR spectrum.

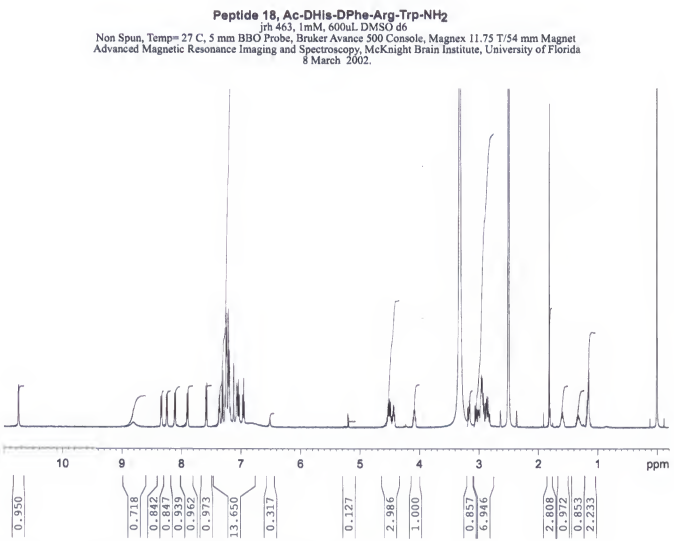

Figure A-18. Peptide 18 one-dimensional (1D) ^{1}H-NMR spectrum.

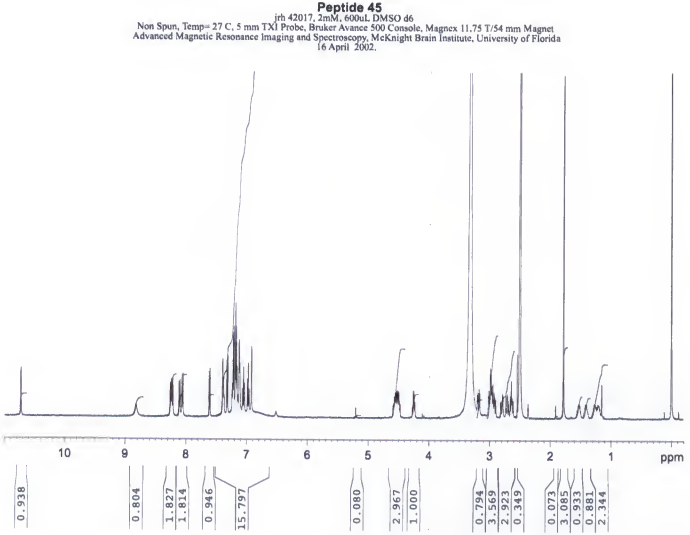

Figure A-19. Peptide 45 one-dimensional (1D) ^{1}H-NMR spectrum.

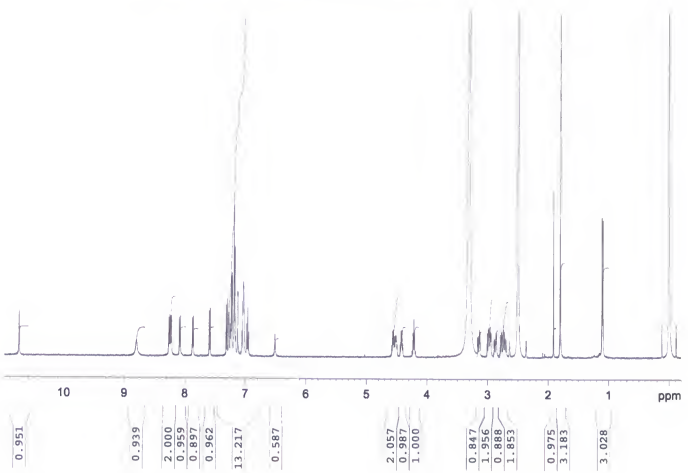

Figure A-20. Peptide 46 one-dimensional (1D) ^{1}H-NMR spectrum.

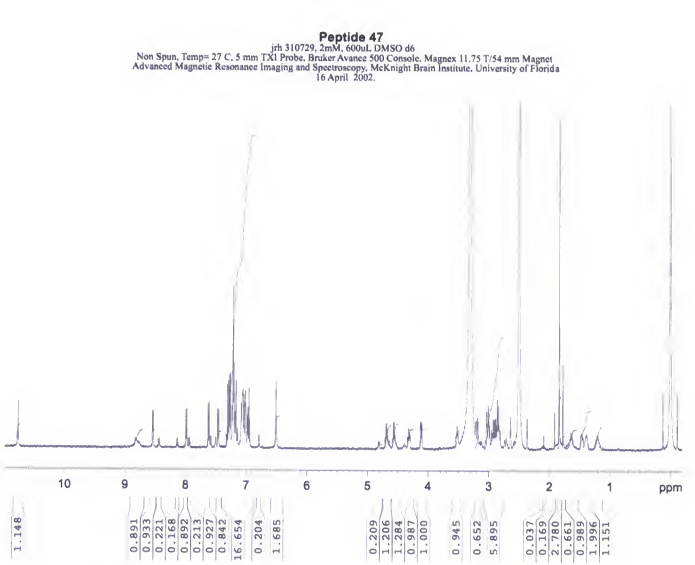

Figure A-21. Peptide 47 one-dimensional (1D) ^{1}H-NMR spectrum.

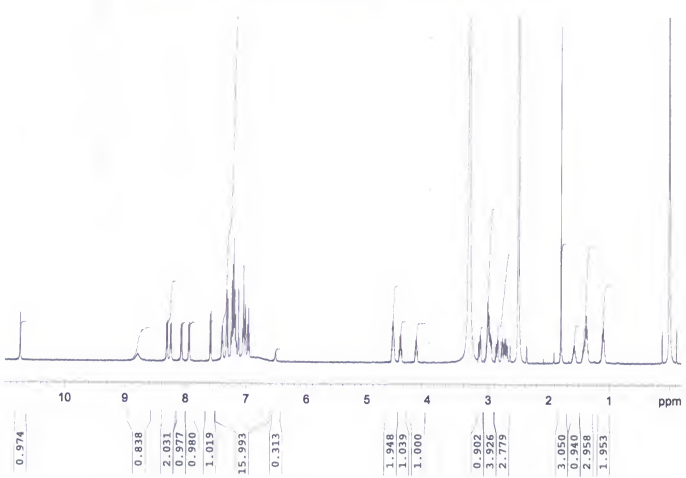

Figure A-22. Peptide 48 one-dimensional (1D) ^{1}H-NMR spectrum.

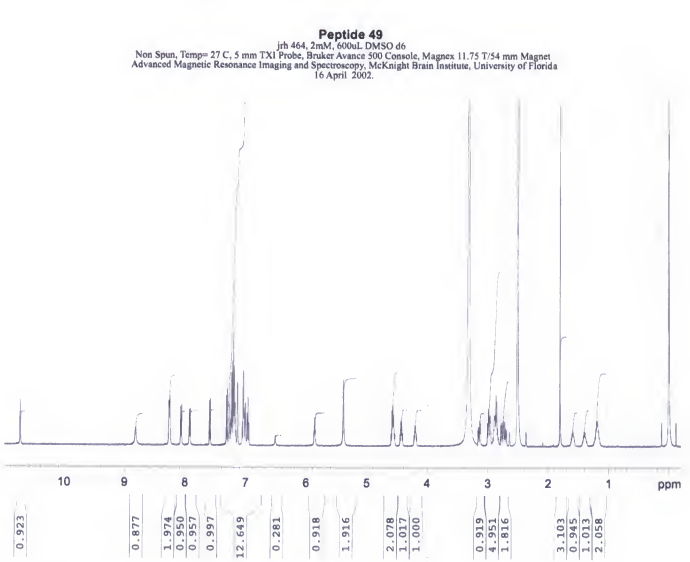

Figure A-23. Peptide 49 one-dimensional (1D) ^{1}H-NMR spectrum.

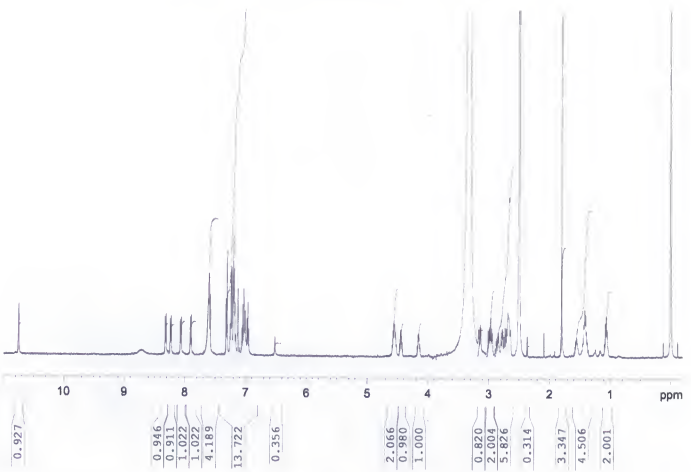

Figure A-24. Peptide 50 one-dimensional (1D) ^{1}H-NMR spectrum.

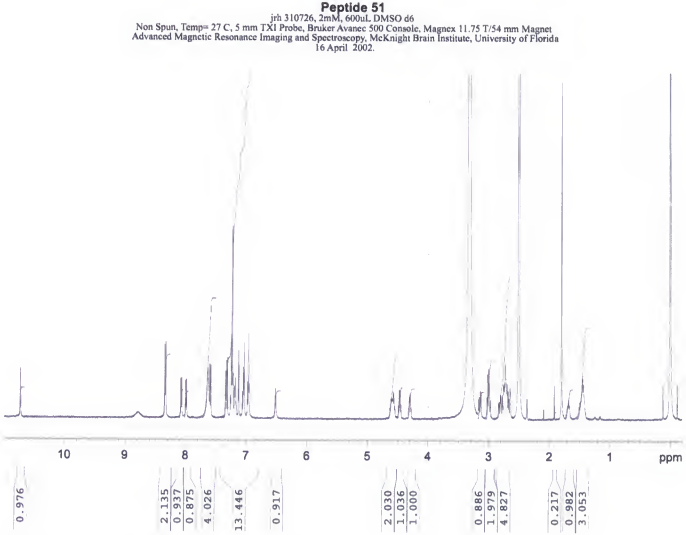

Figure A-25. Peptide 51 one-dimensional (1D) ^{1}H-NMR spectrum.

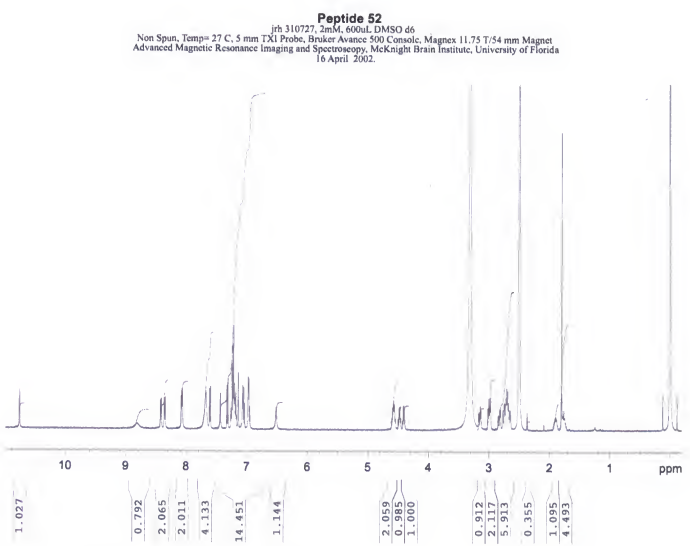

Figure A-26. Peptide 52 one-dimensional (1D) ^{1}H-NMR spectrum.

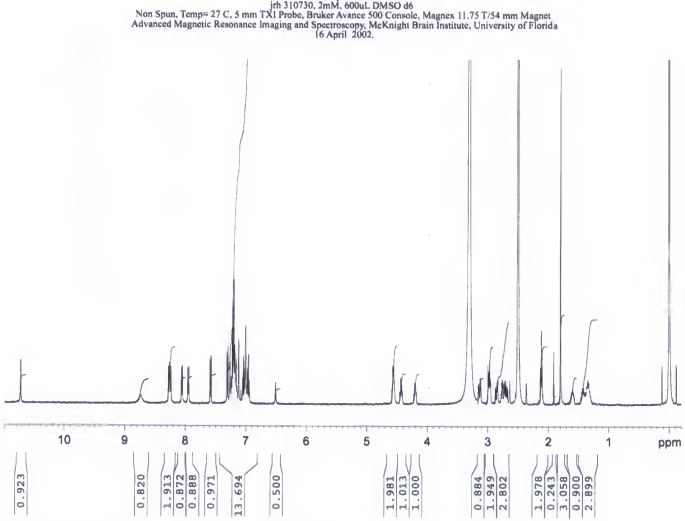

Figure A-27. Peptide 53 one-dimensional (1D) ^{1}H-NMR spectrum.

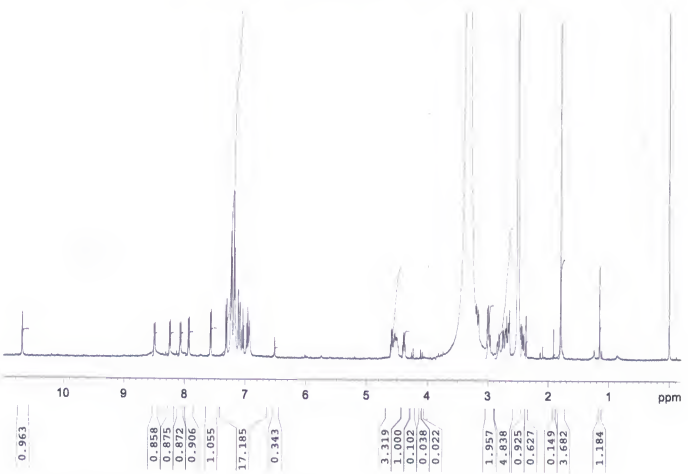

Figure A-28. Peptide 54 one-dimensional (1D) ^{1}H-NMR spectrum.

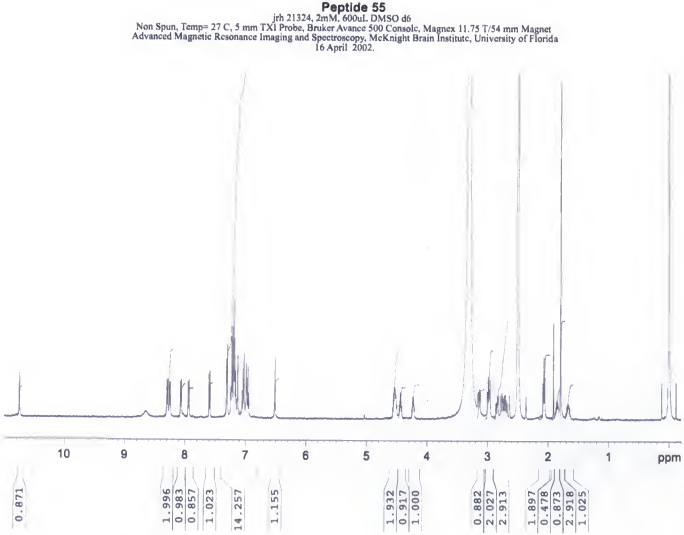

Figure A-29. Peptide 55 one-dimensional (1D) ^{1}H-NMR spectrum.

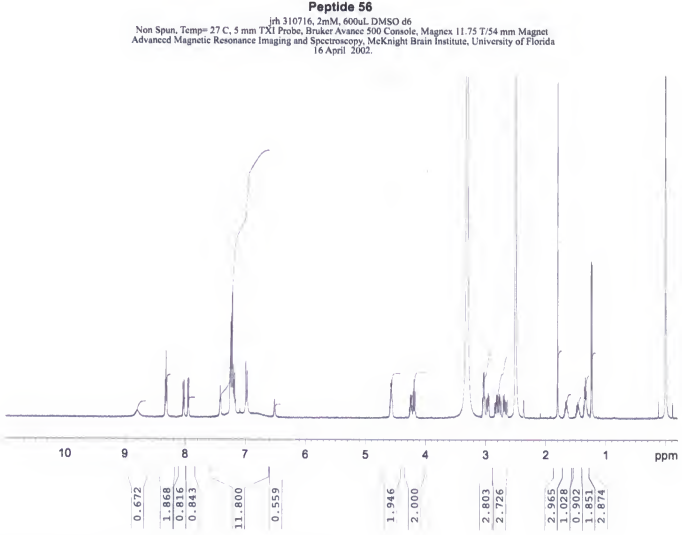

Figure A-30. Peptide 56 one-dimensional (1D) ^{1}H-NMR spectrum.

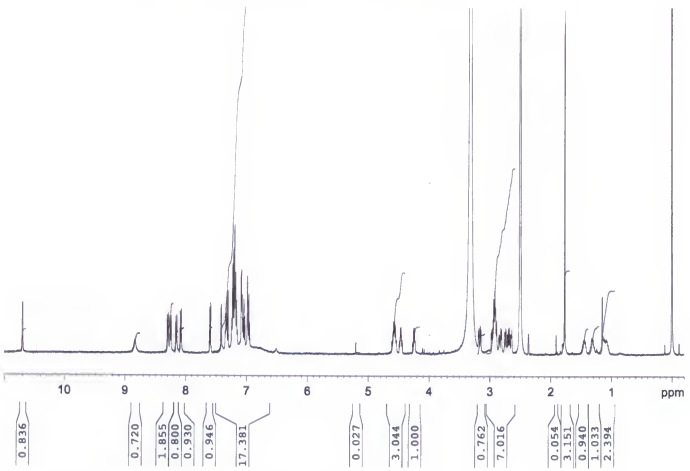

Figure A-31. Peptide 57 one-dimensional (1D) ^{1}H-NMR spectrum.

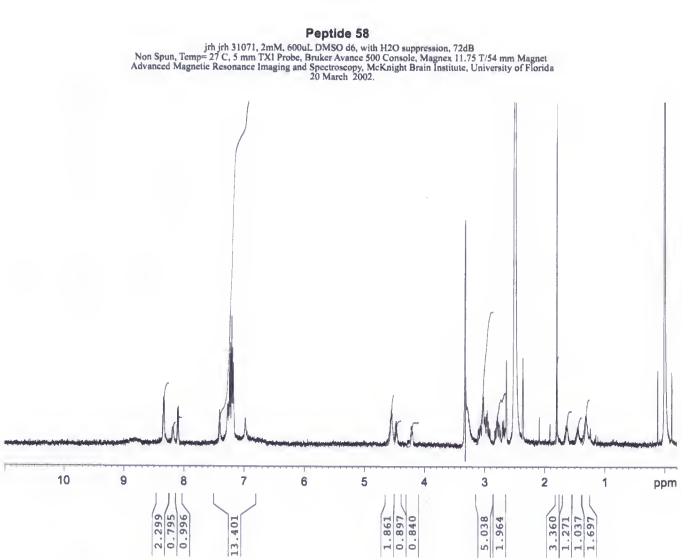

Figure A-32. Peptide 58 one-dimensional (1D) ^{1}H-NMR spectrum.

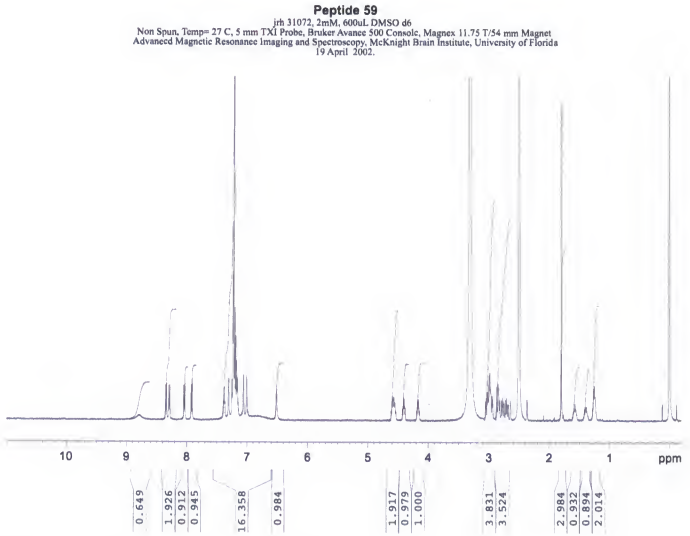

Figure A-33. Peptide 59 one-dimensional (1D) ^{1}H-NMR spectrum.

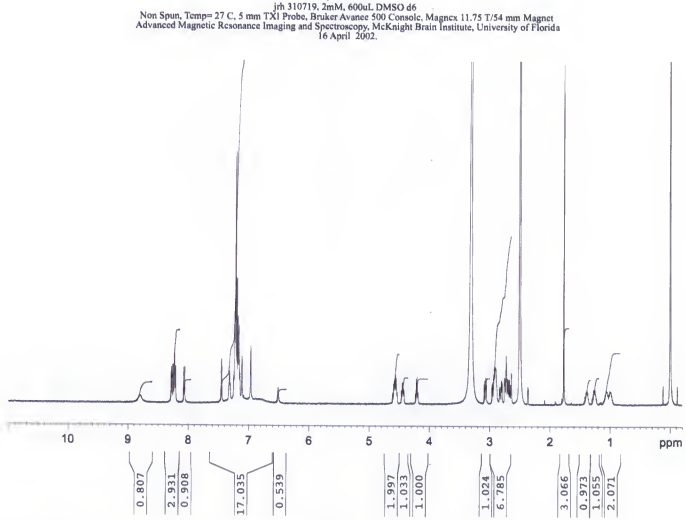

Figure A-34. Peptide 60 one-dimensional (1D) ^{1}H-NMR spectrum.

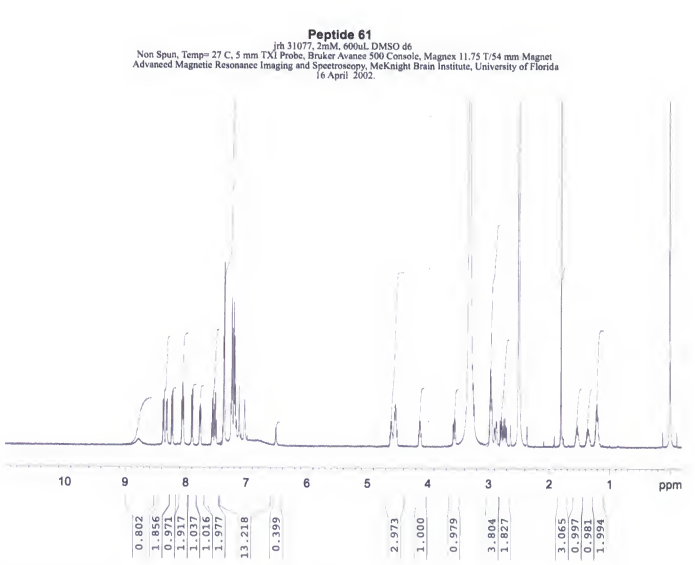

Figure A-35. Peptide 61 one-dimensional (1D) ^{1}H-NMR spectrum.

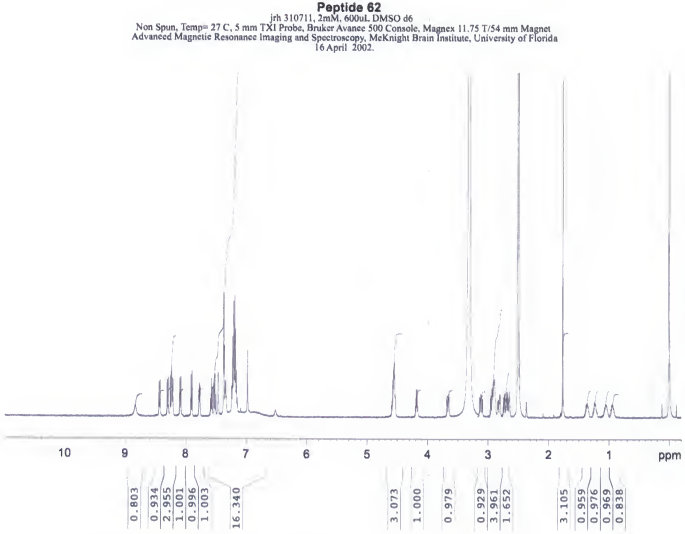

Figure A-36. Peptide 62 one-dimensional (1D) ^{1}H-NMR spectrum.

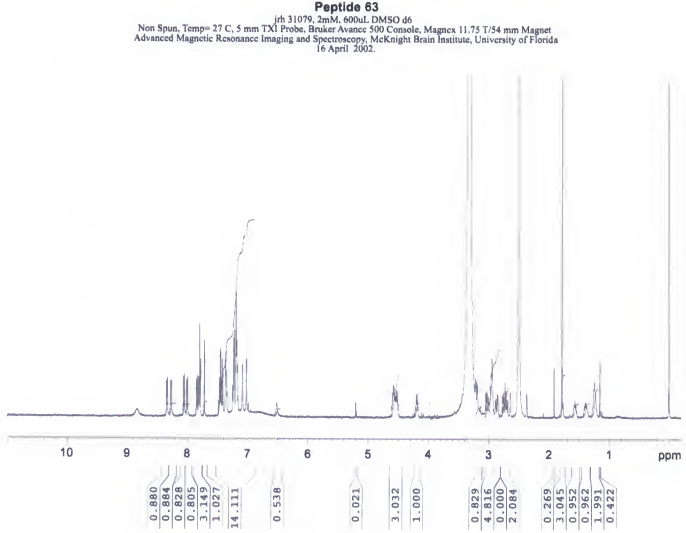

Figure A-37. Peptide 63 one-dimensional (1D) ^{1}H-NMR spectrum.

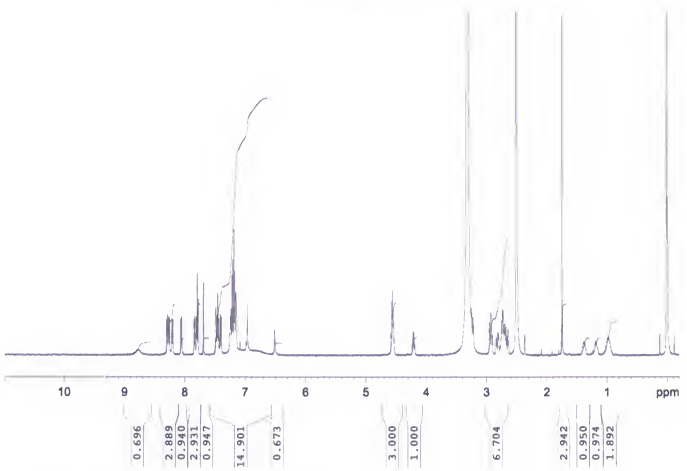

Figure A-38. Peptide 64 one-dimensional (1D) ^{1}H-NMR spectrum.

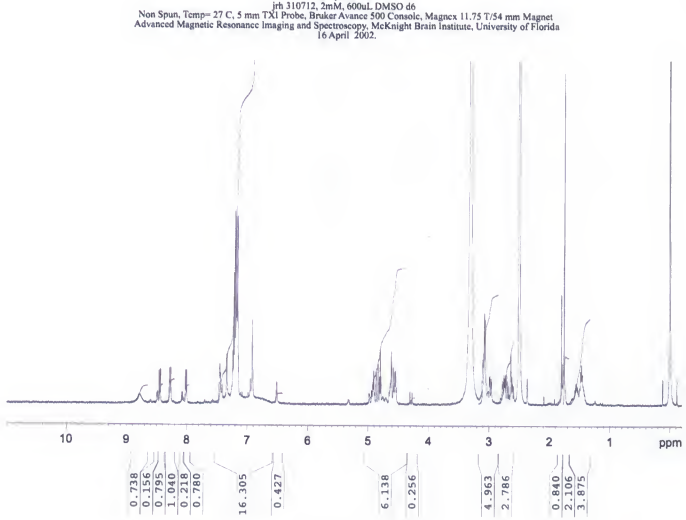

Figure A-39. Peptide 65 one-dimensional (1D) ^{1}H-NMR spectrum.

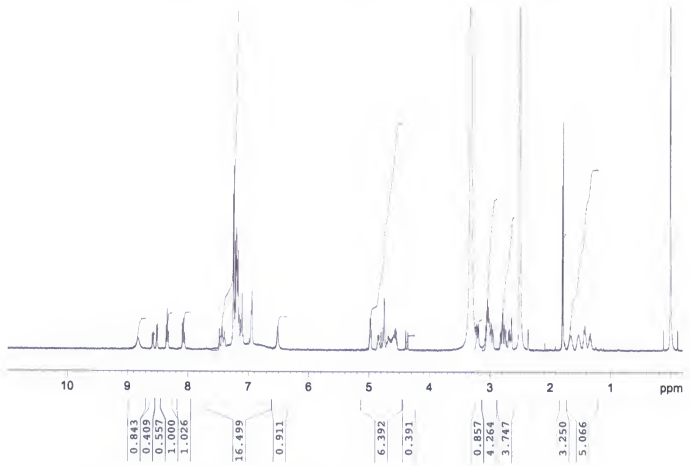

Figure A-40. Peptide 66 one-dimensional (1D) ^{1}H-NMR spectrum.

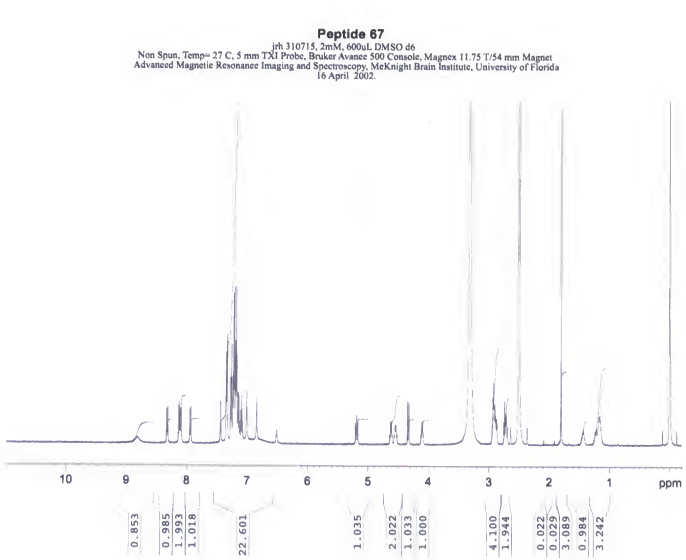

Figure A-41. Peptide 67 one-dimensional (1D) ^{1}H-NMR spectrum.

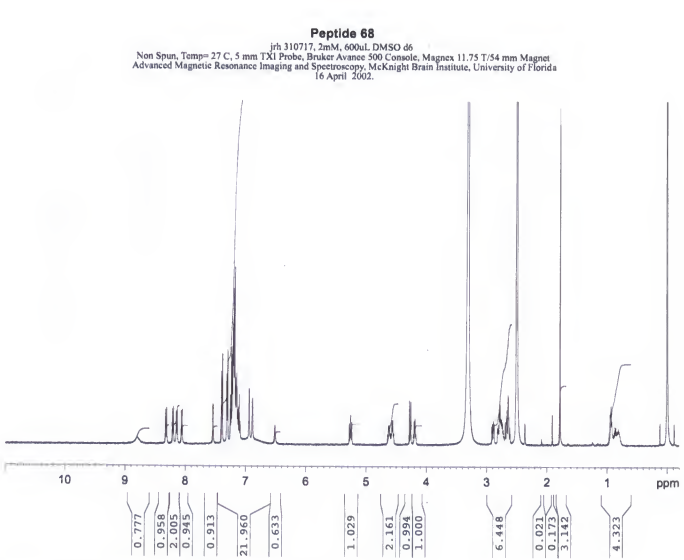

Figure A-42. Peptide 68 one-dimensional (1D) ^{1}H-NMR spectrum.

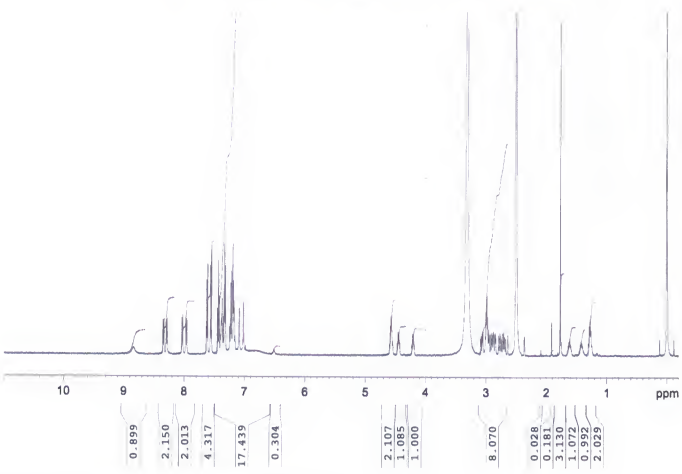

Figure A-43. Peptide 69 one-dimensional (1D) ^{1}H-NMR spectrum.

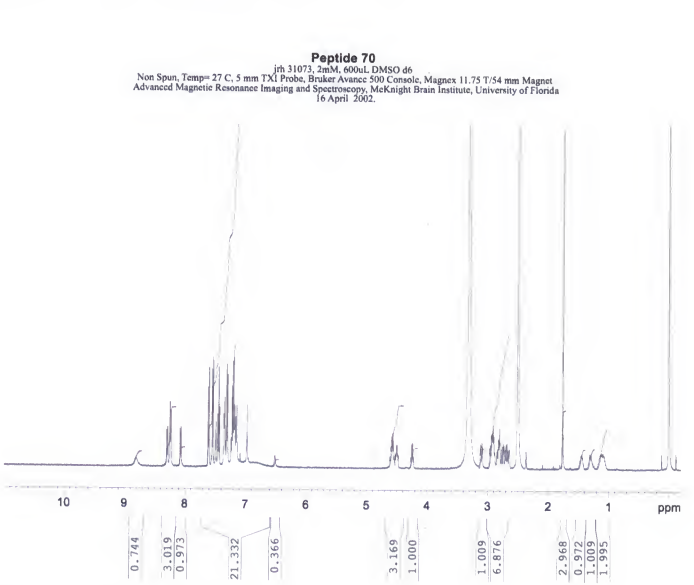

Figure A-44. Peptide 70 one-dimensional (1D) ^{1}H-NMR spectrum.

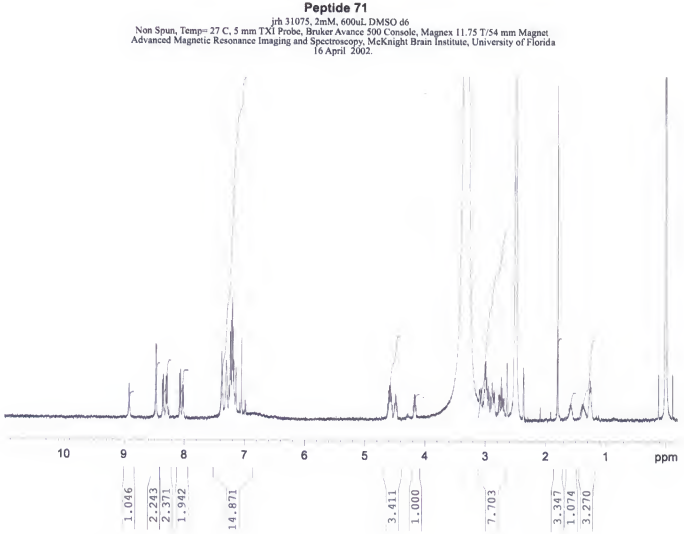

Figure A-45. Peptide 71 one-dimensional (1D) ^{1}H-NMR spectrum.

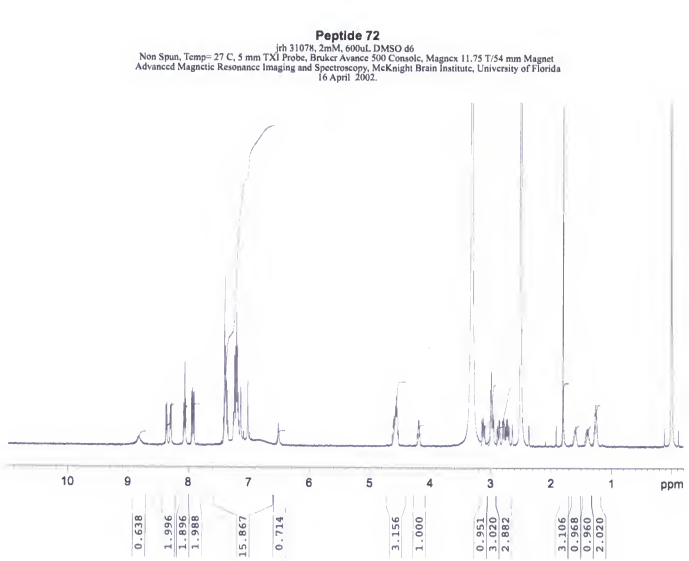

Figure A-46. Peptide 72 one-dimensional (1D) ^{1}H-NMR spectrum.

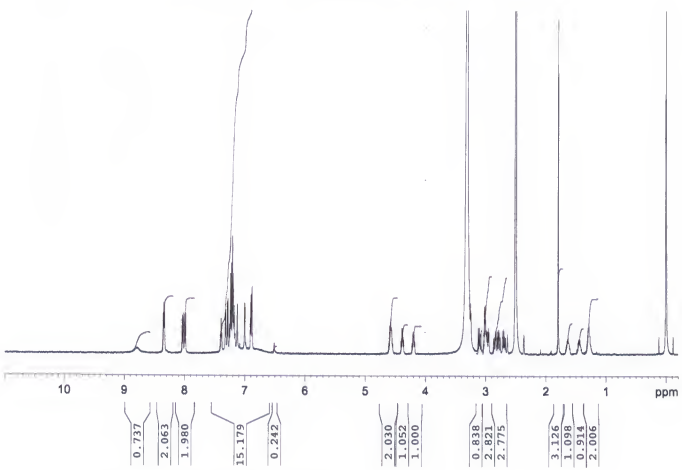

Figure A-47. Peptide 73 one-dimensional (1D) ^{1}H-NMR spectrum.

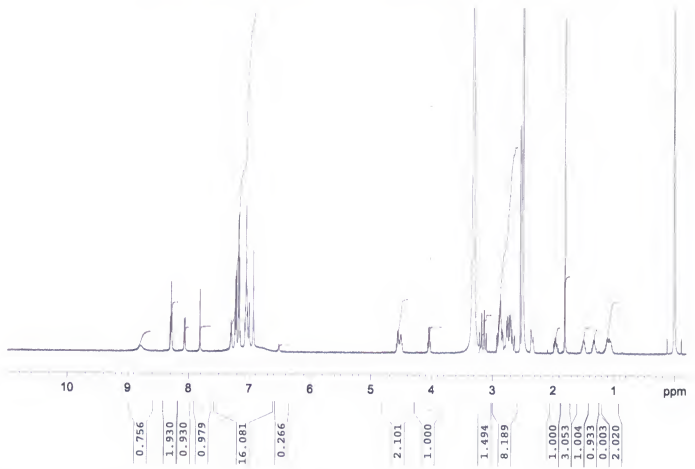

Figure A-48. Peptide 74 one-dimensional (1D) ^{1}H-NMR spectrum.

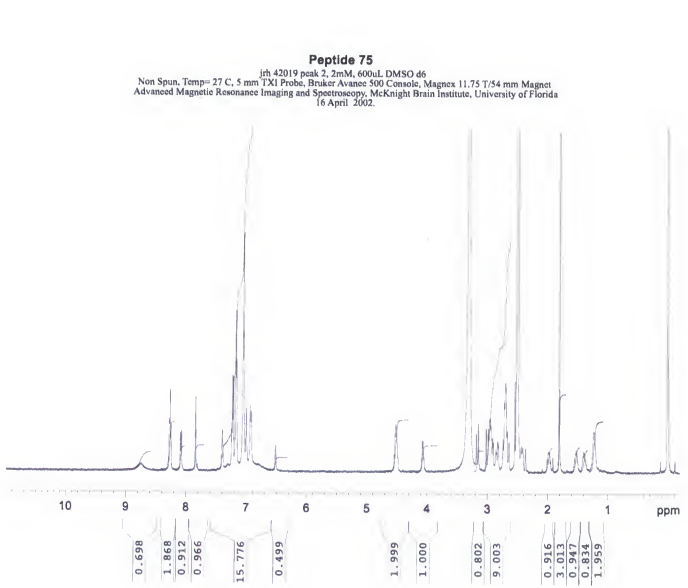

Figure A-49. Peptide 75 one-dimensional (1D) ^{1}H-NMR spectrum.

APPENDIX B
1-DIMENSIONAL (1D) ^{1}H-NMR SPECTRA OF CYCLIC HEPTAPEPTIDES

The 1-dimensional (1D) ^{1}H-NMR spectra of the cyclic heptapeptides discussed in chapter four are presented herein appendix B. The spectral widths were 12ppm with DSS referenced to 0.0ppm. The peptides were dissolved in 95%$H_2$0/5%D_2O at a concentration of 1mM. Data were collected at 5°C on a Bruker Avance spectrometer operating at 500MHz in the Advanced Magnetic Resonance Imaging and Spectroscopy (AMRIS) facility at the McKnight Brain Institute, University of Florida.

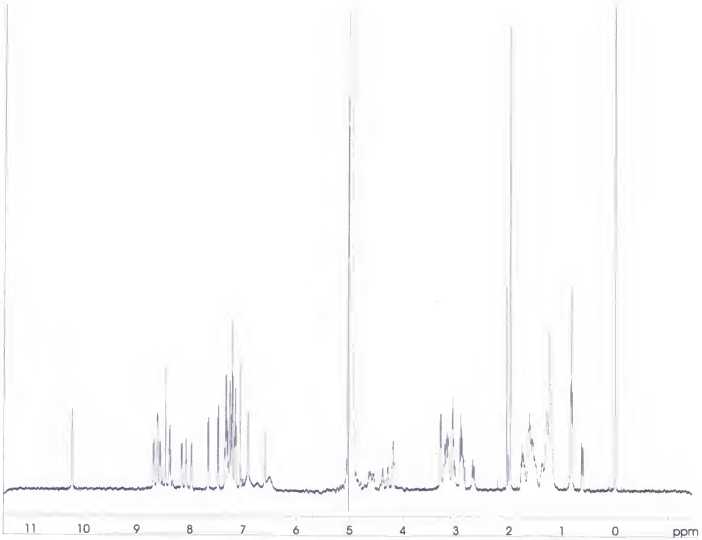

Figure B-1. One-dimensional (1D) ^{1}H-NMR spectrum of MTII collected at 5°C on a 500MHz spectrometer.

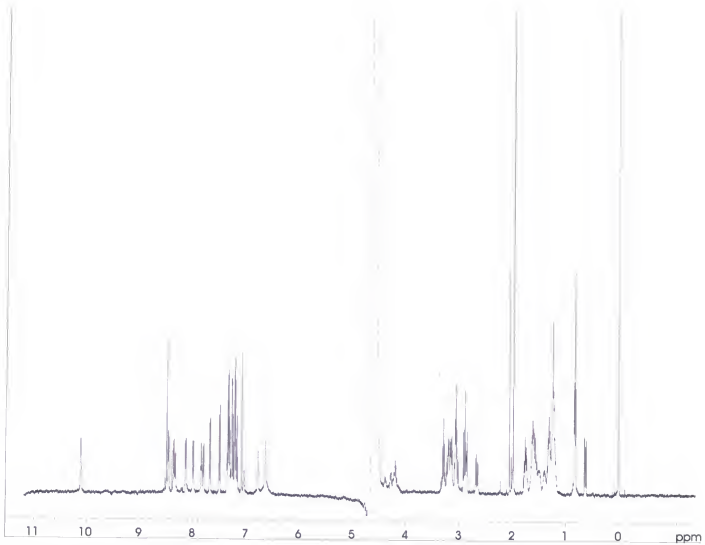

Figure B-2. One-dimensional (1D) ^{1}H-NMR spectrum of MTII collected at 35°C on a 500MHz spectrometer.

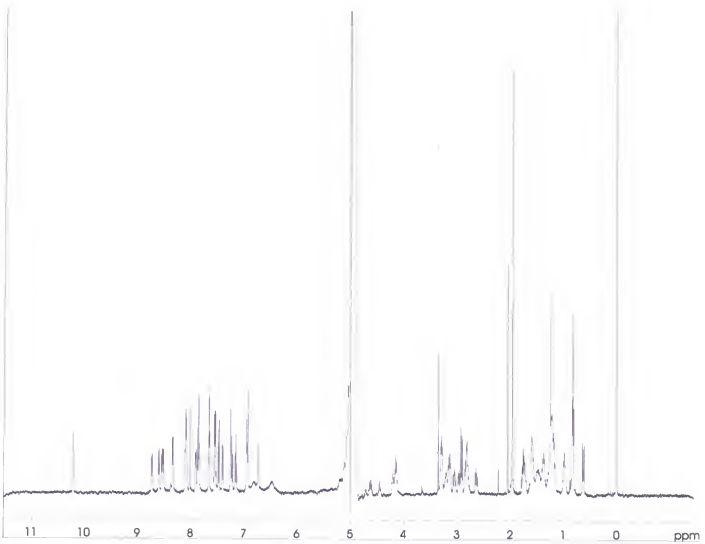

Figure B-3. One-dimensional (1D) ^{1}H-NMR spectrum of SHU9119 collected at 5°C on a 500MHz spectrometer.

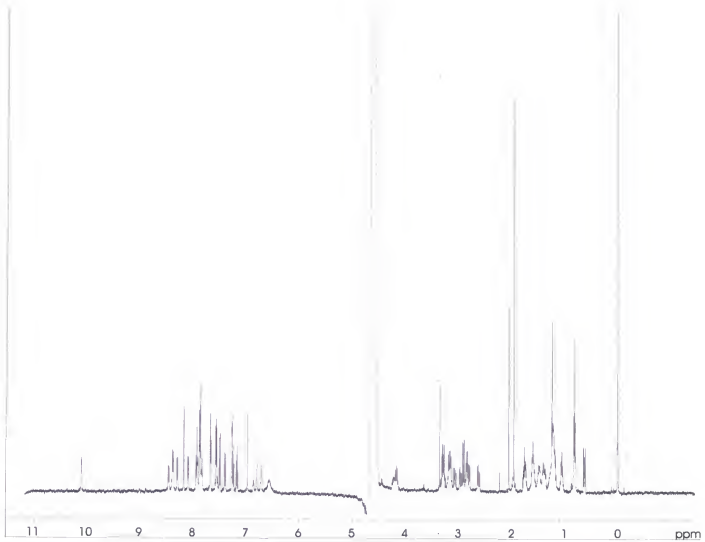

Figure B-4. One-dimensional (1D) ^{1}H-NMR spectrum of SHU9119 collected at 35°C on a 500MHz spectrometer.

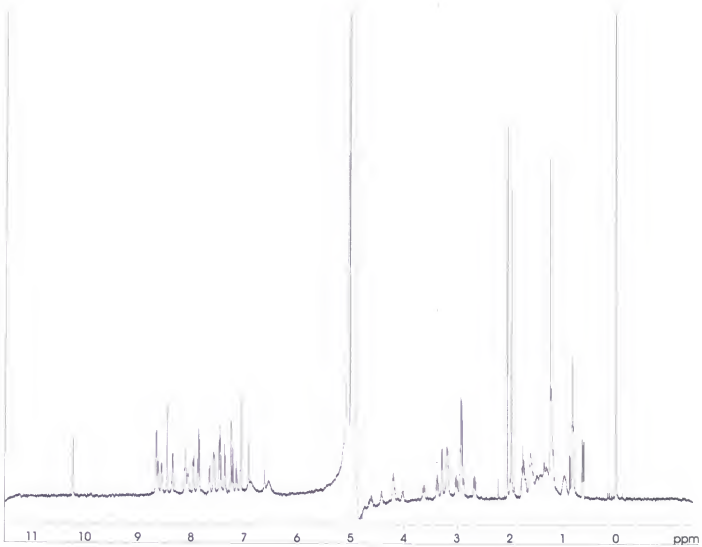

Figure B-5. One-dimensional (1D) ^{1}H-NMR spectrum of Analogue 1 collected at 5°C on a 500MHz spectrometer.

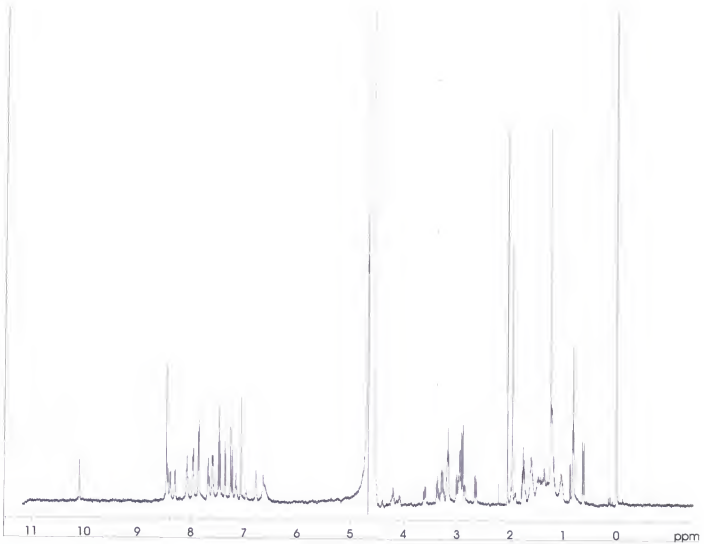

Figure B-6. One-dimensional (1D) ^{1}H-NMR spectrum of Analogue 1 collected at 35°C on a 500MHz spectrometer.

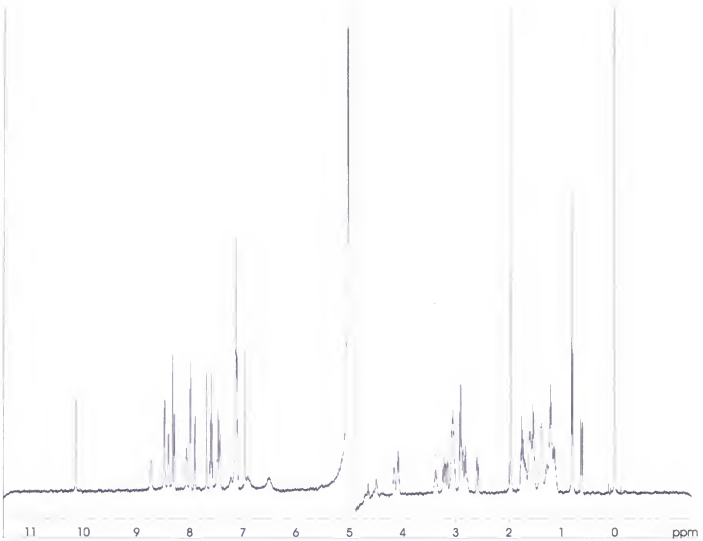

Figure B-7. One-dimensional (1D) ^{1}H-NMR spectrum of Analogue 2 collected at 5°C on a 500MHz spectrometer.

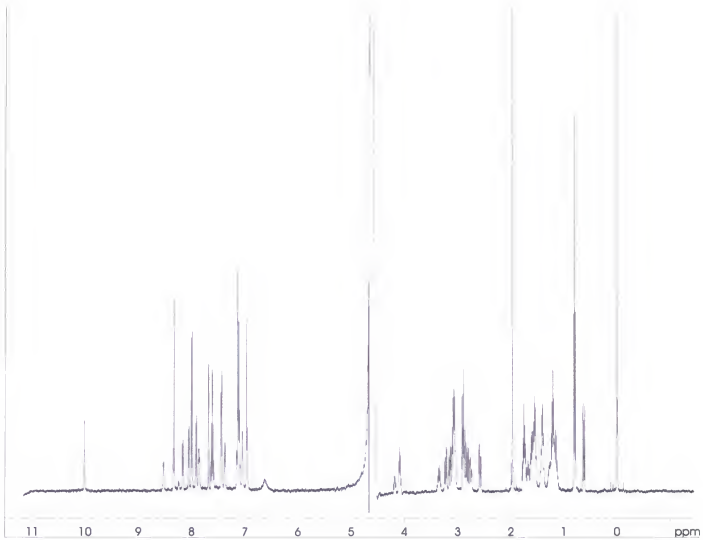

Figure B-8. One-dimensional (1D) ^{1}H-NMR spectrum of Analogue 2 collected at 35°C on a 500MHz spectrometer.

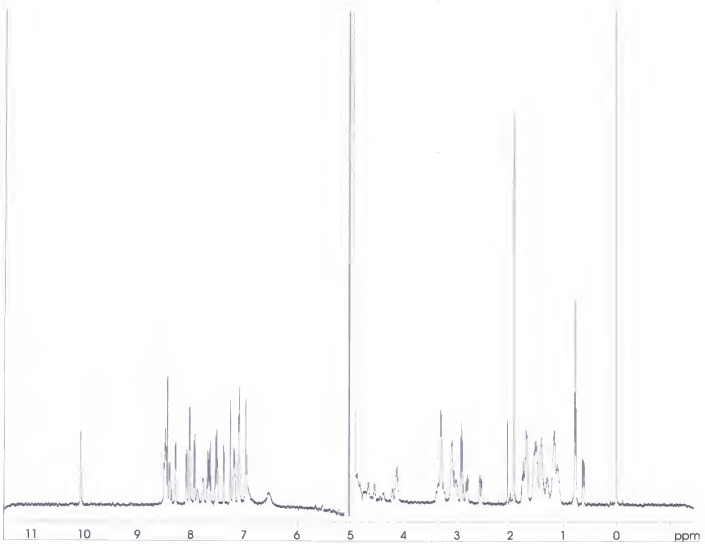

Figure B-9. One-dimensional (1D) ^{1}H-NMR spectrum of Analogue 3 collected at 5°C on a 500MHz spectrometer.

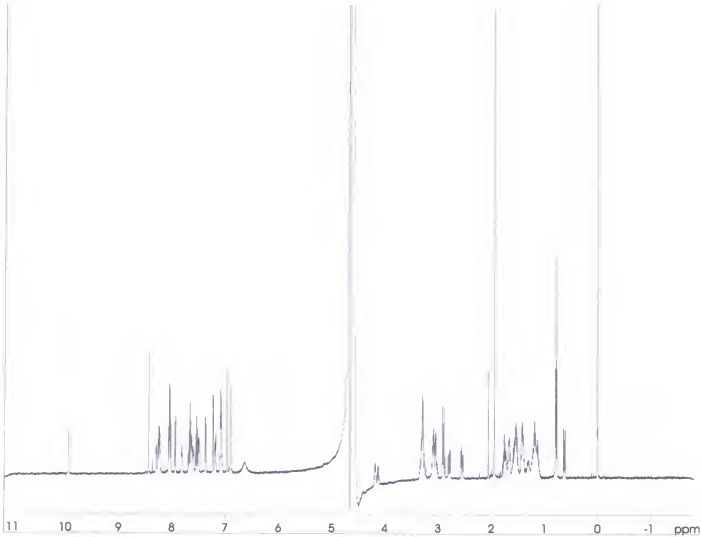

Figure B-10. One-dimensional (1D) ^{1}H-NMR spectrum of Analogue 3 collected at 35°C on a 500MHz spectrometer.

APPENDIX C
2-DIMENSIONAL (2D) ^{1}H-NMR SPECTRA OF CYCLIC HEPTAPEPTIDES

The 2-dimensional (2D) ^{1}H-NMR spectra of the cyclic heptapeptides discussed in chapter four are presented herein appendix C. The spectral widths are shown from -0.2-10.5ppm with DSS referenced to 0.0ppm. The peptides were dissolved in 95%$H_2$0/5%D_2O at a concentration of 1mM. Data were collected at 5°C on a Bruker Avance spectrometer operating at 500MHz in the Advanced Magnetic Resonance Imaging and Spectroscopy (AMRIS) facility at the McKnight Brain Institute, University of Florida.

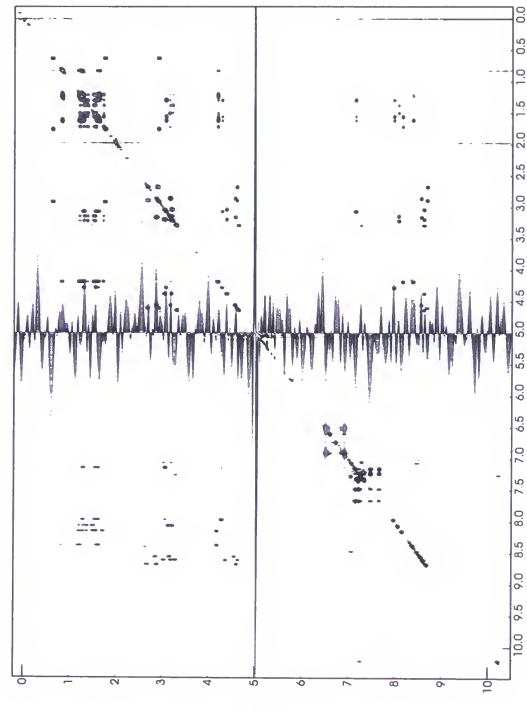

Figure C-1. TOCSY spectra of MTII collected at 5°C on a 500MHz spectrometer.

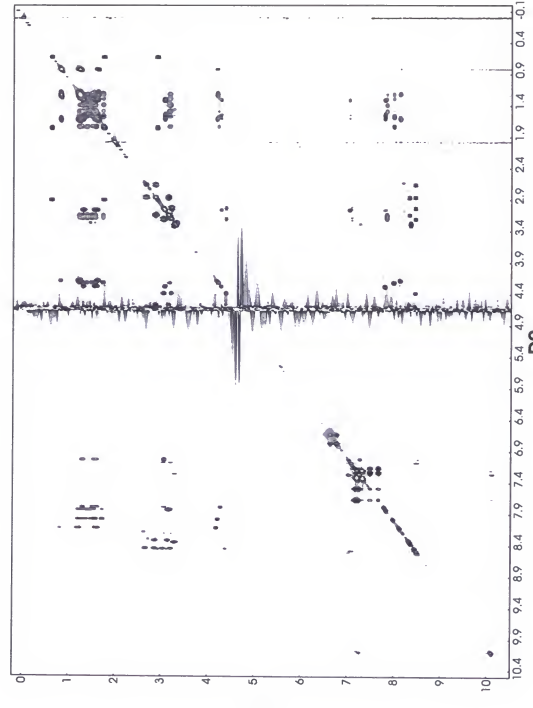

Figure C-2. TOCSY spectra of MTII collected at 35°C on a 500MHz spectrometer.

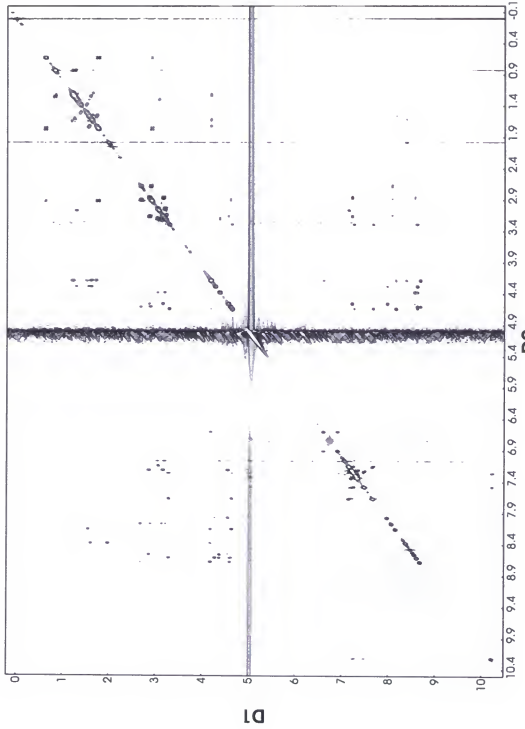

Figure C-3. ROESY spectra of MTII collected at 5°C on a 500MHz spectrometer.

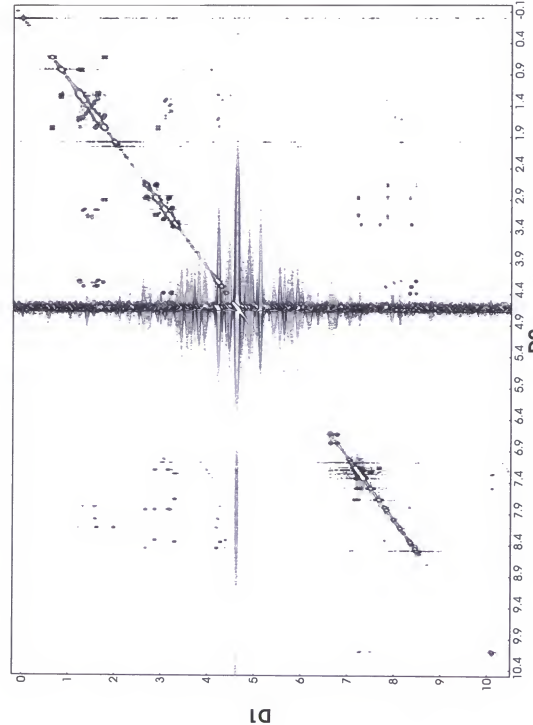

Figure C-4. ROESY spectra of MTII collected at 35°C on a 500MHz spectrometer.

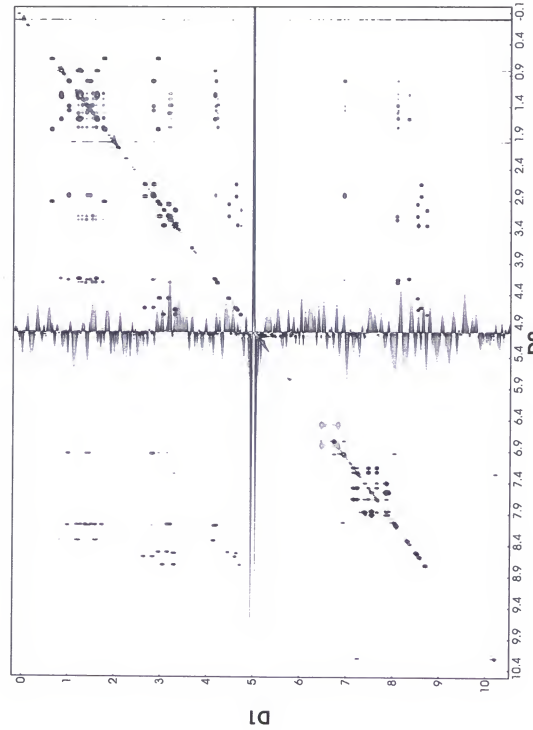

Figure C-5. TOCSY spectra of SHU9119 collected at 5°C on a 500MHz spectrometer.

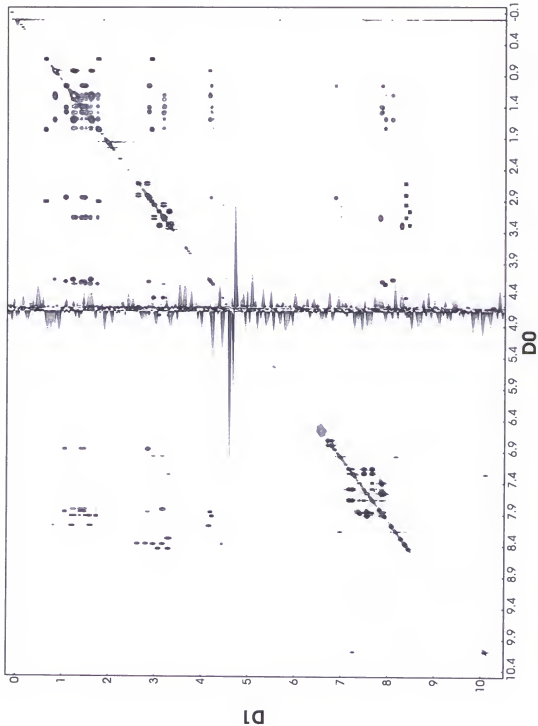

Figure C-6. TOCSY spectra of SHU9119 collected at 35°C on a 500MHz spectrometer.

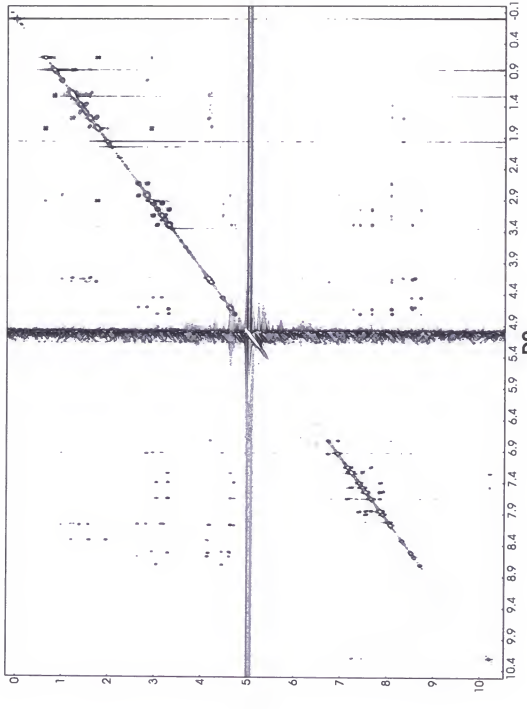

Figure C-7. ROESY spectra of SHU9119 collected at 5°C on a 500MHz spectrometer.

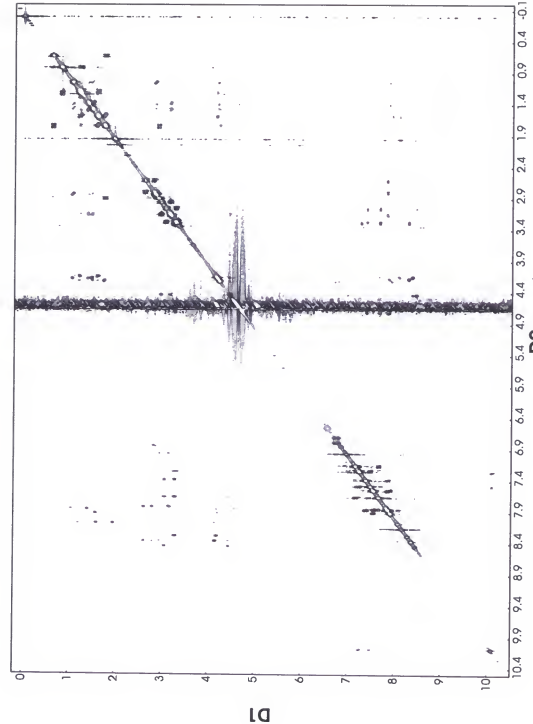

Figure C-8. ROESY spectra of SHU9119 collected at 35°C on a 500MHz spectrometer.

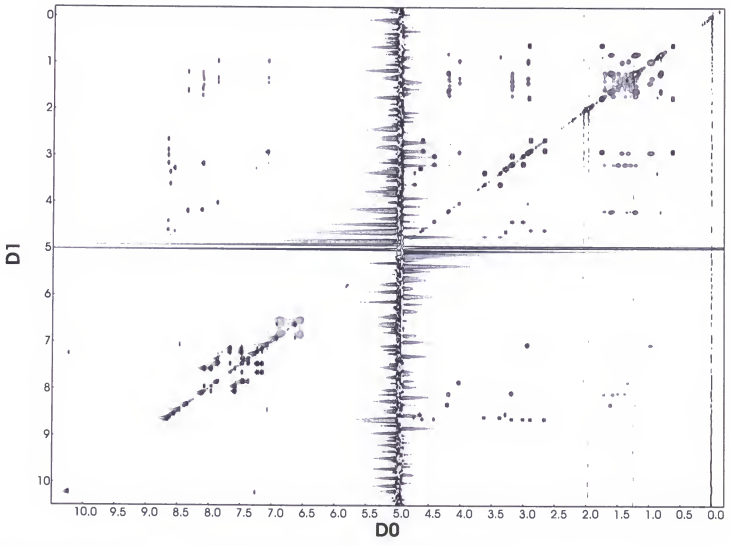

Figure C-9. TOCSY spectra of Analogue 1 collected at 5°C on a 500MHz spectrometer.

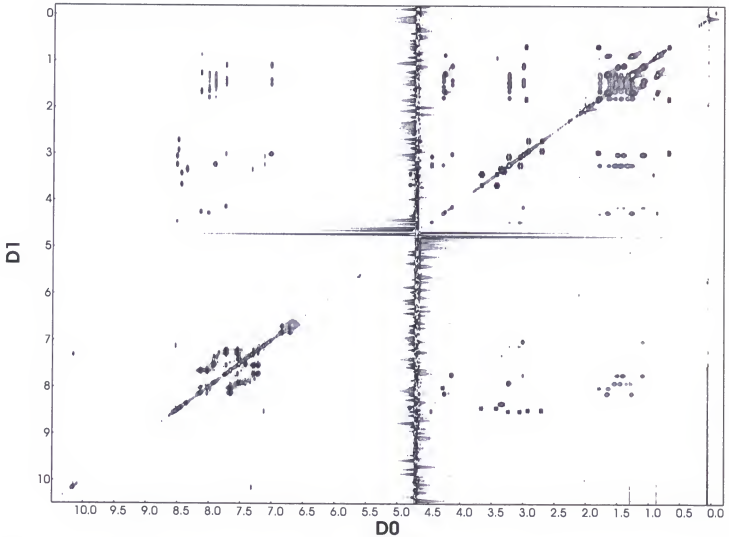

Figure C-10. TOCSY spectra of Analogue 1 collected at 35°C on a 500MHz spectrometer.

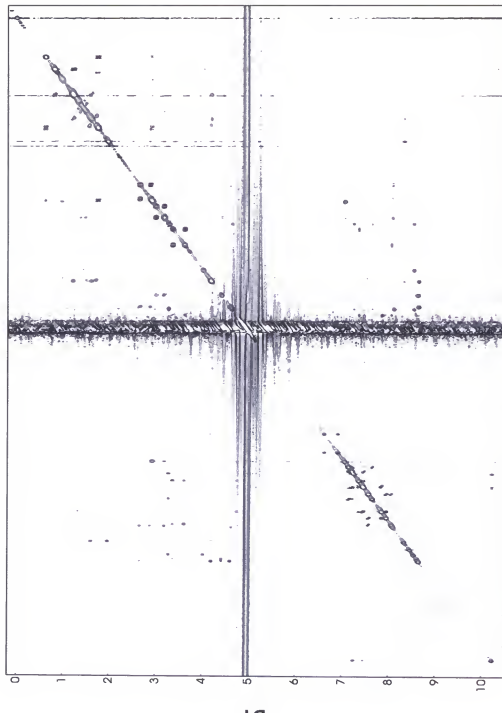

Figure C-11. ROESY spectra of Analogue 1 collected at 5°C on a 500MHz spectrometer.

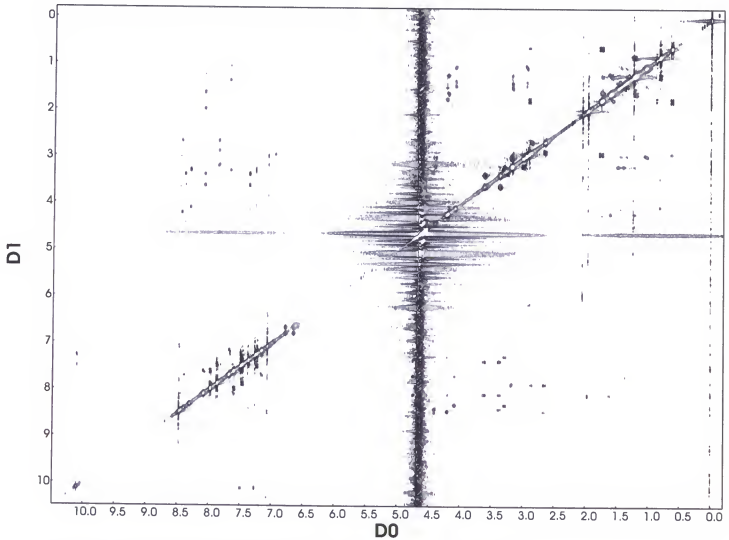

Figure C-12. ROESY spectra of Analogue 1 collected at 35°C on a 500MHz spectrometer.

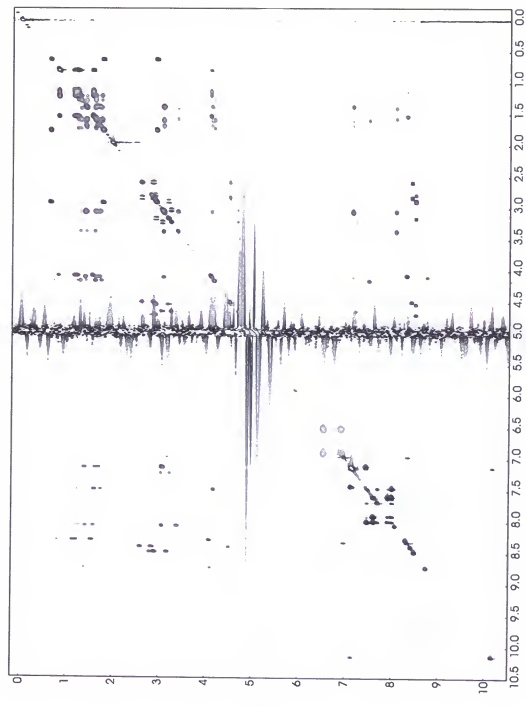

Figure C-13. TOCSY spectra of Analogue 2 collected at 5°C on a 500MHz spectrometer.

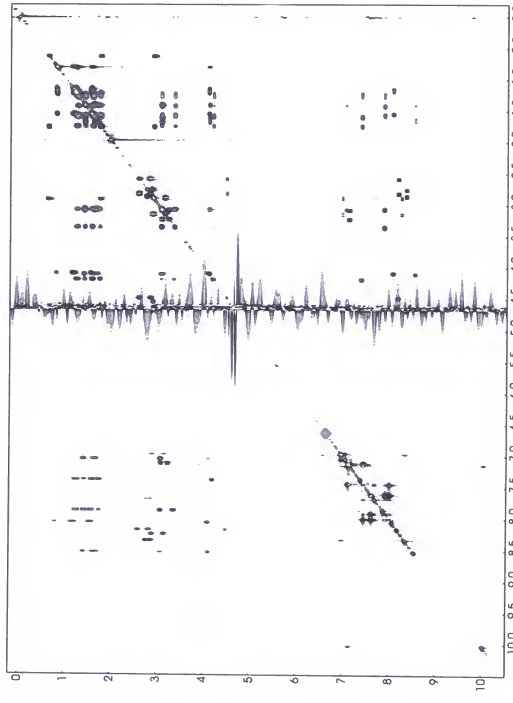

Figure C-14. TOCSY spectra of Analogue 2 collected at 35°C on a 500MHz spectrometer.

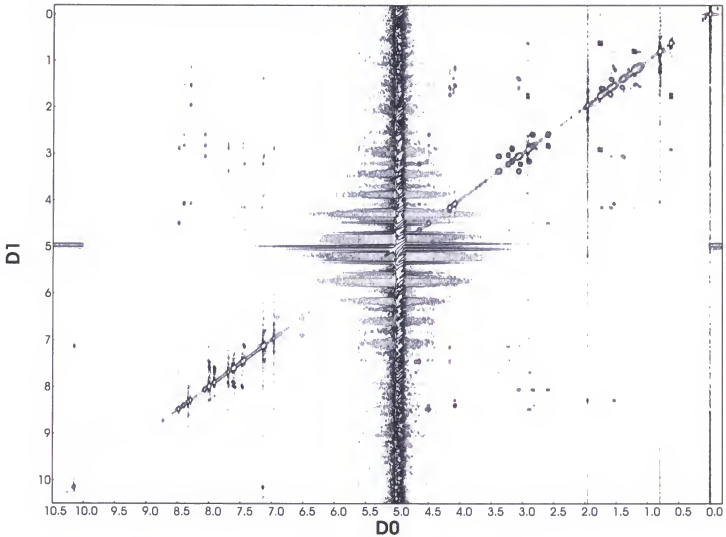

Figure C-15. ROESY spectra of Analogue 2 collected at 5°C on a 500MHz spectrometer.

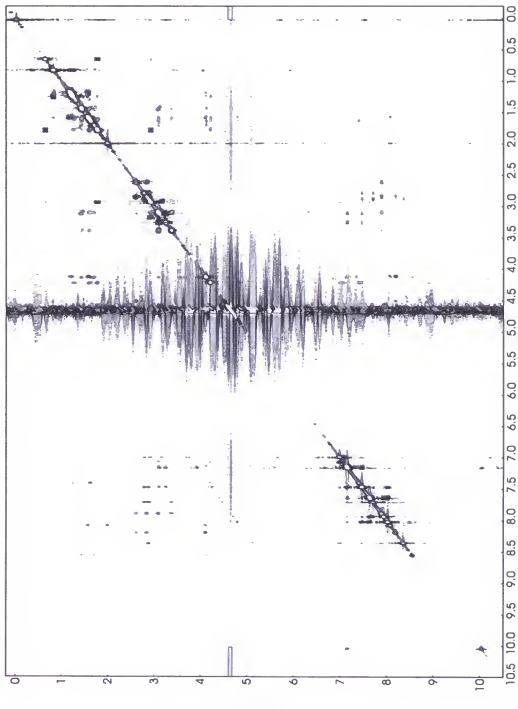

Figure C-16. ROESY spectra of Analogue 2 collected at 35°C on a 500MHz spectrometer.

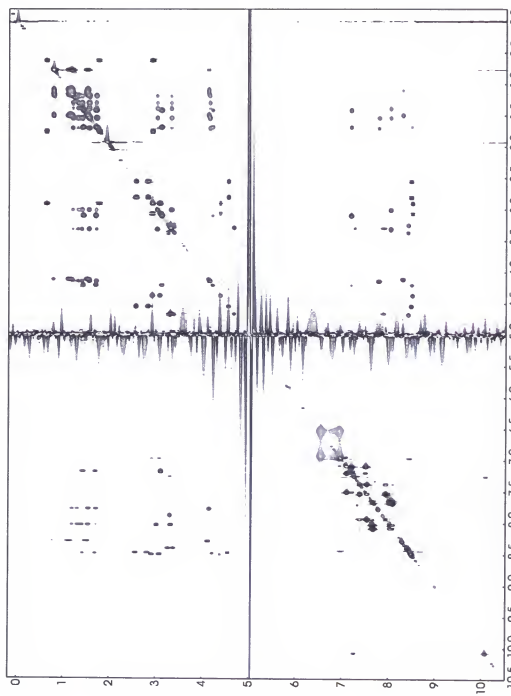

Figure C-17. TOCSY spectra of Analogue 3 collected at 5°C on a 500MHz spectrometer.

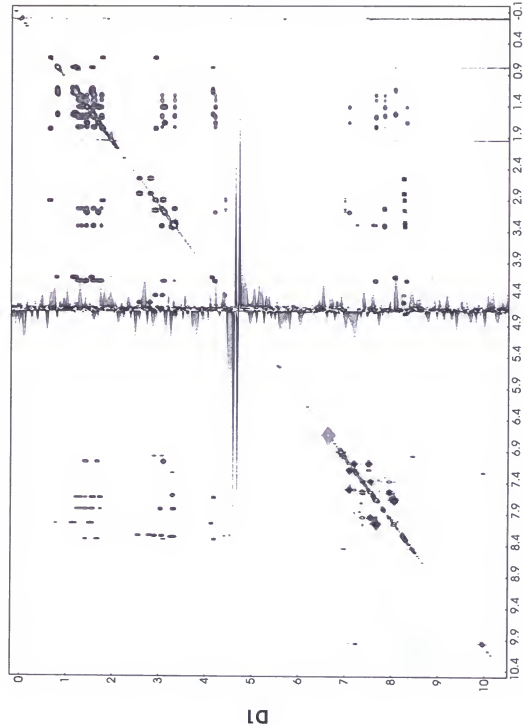

Figure C-18. TOCSY spectra of Analogue 3 collected at 35°C on a 500MHz spectrometer.

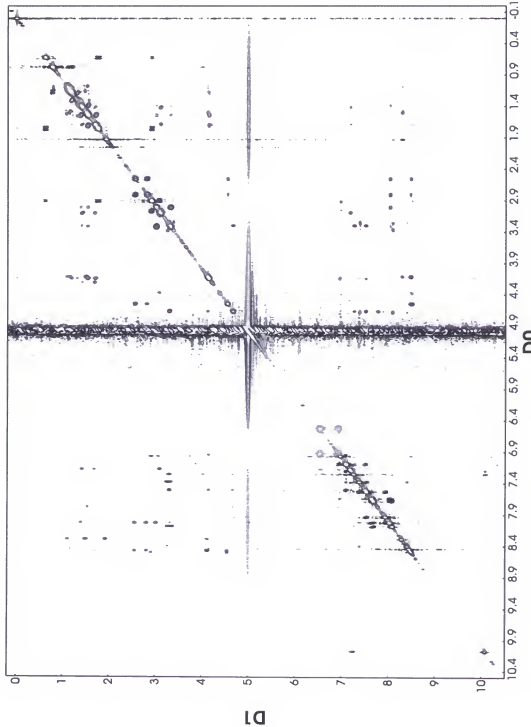

Figure C-19. ROESY spectra of Analogue 3 collected at 5°C on a 500MHz spectrometer.

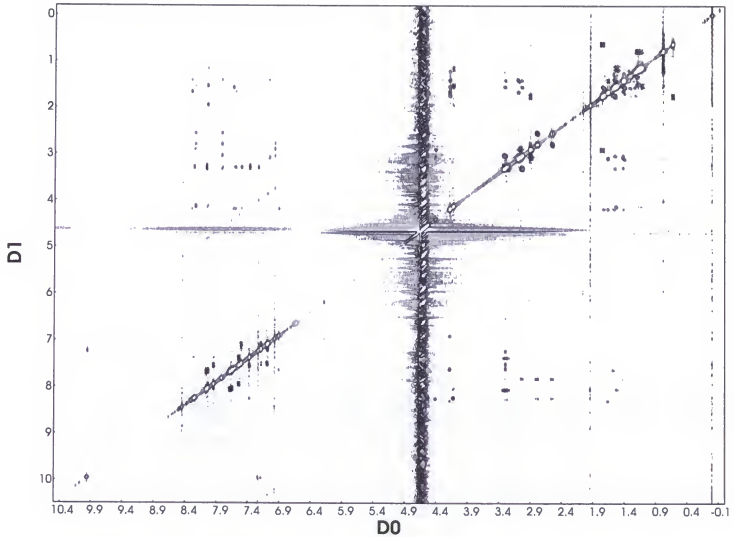

Figure C-20. ROESY spectra of Analogue 3 collected at 35°C on a 500MHz spectromete

APPENDIX D
TEMPERATURE TITRATION FREQUENCY SPECTRA

The 1-dimensional (1D) ^{1}H-NMR spectra used to calculate temperature coefficients of backbone amide protons of the cyclic heptapeptides presented in chapter four are presented herein appendix D. The data were collected from 5°C to 50°C in 5°C increments. The 1D ^{1}H-NMR spectra for each temperature point are shown stacked. Only amide and aromatic protons are shown in the spectra. Backbone amide protons are labeled at 5°C and 50°C for clarity. The peptides were dissolved in 95%$H_2$0/5%D_2O at a concentration of 1mM. Data were collected on a Bruker Avance spectrometer operating at 500MHz in the Advanced Magnetic Resonance Imaging and Spectroscopy (AMRIS) facility at the McKnight Brain Institute, University of Florida.

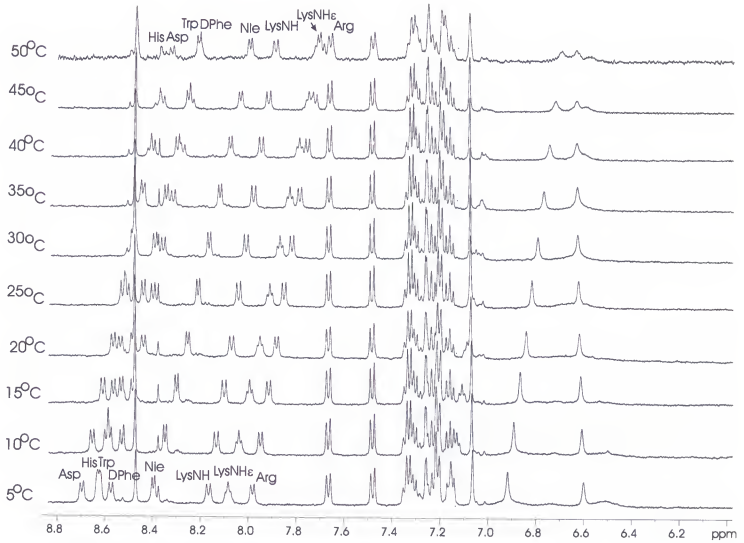

One-dimensional ^{1}H-NMR temperature titration stack plots of MTII amide protons.

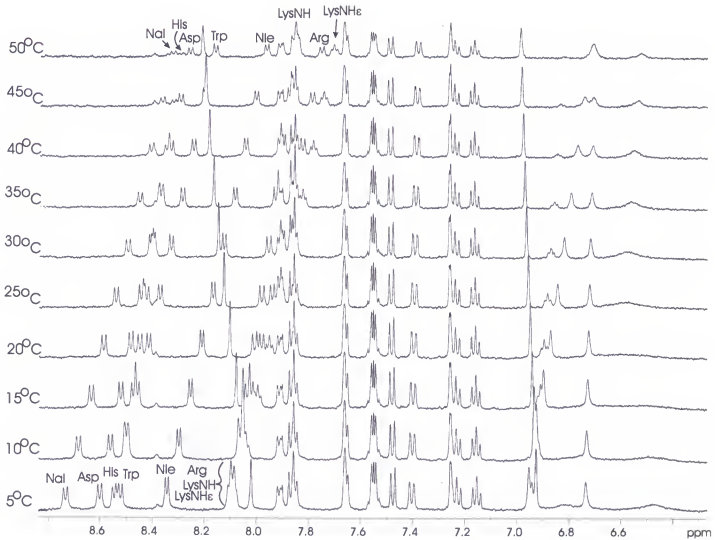

One-dimensional ^{1}H-NMR temperature titration stack plots of SHU9119 amide protons.

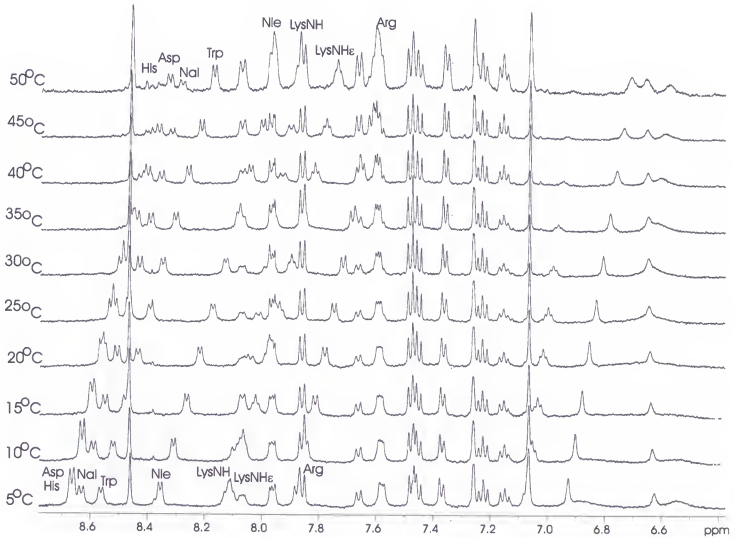

One-dimensional ^{1}H-NMR temperature titration stack plots of Analogue 1 amide protons.

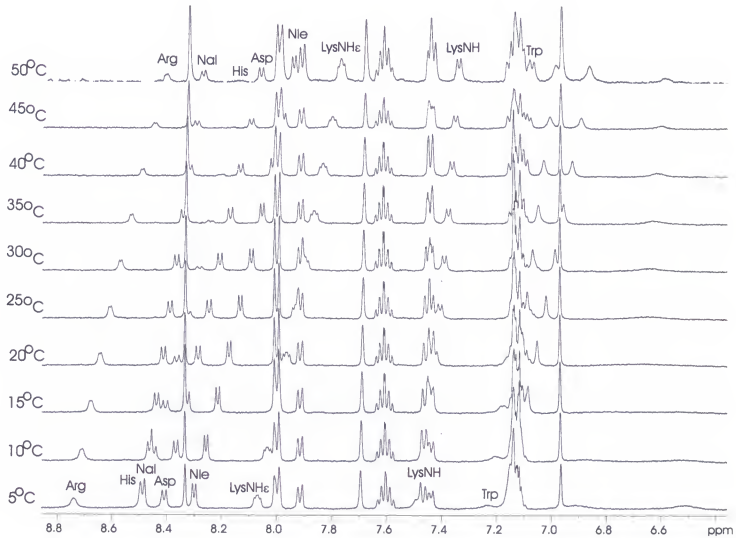

One-dimensional ^{1}H-NMR temperature titration stack plots of Analogue 2 amide protons.

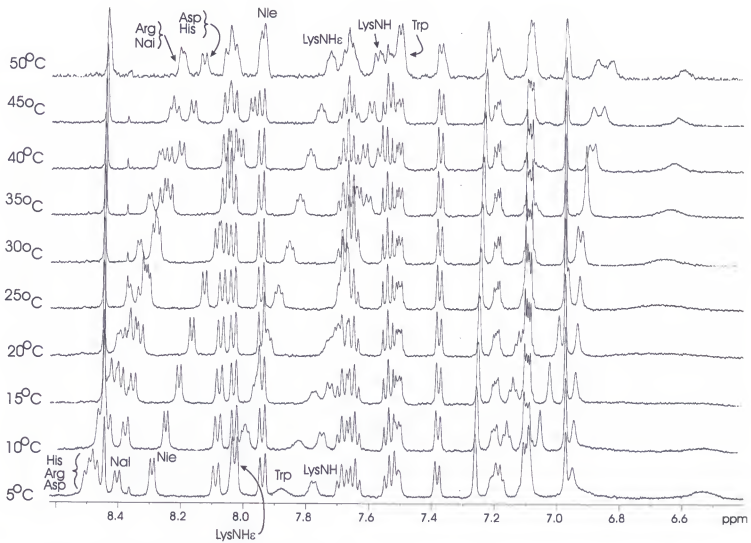

One-dimensional ^{1}H-NMR temperature titration stack plots of Analogue 3 amide protons.

REFERENCES

(1) Mokdad, A. H.; Ford, E. S.; Bowman, B. A.; Dietz, W. H.; Vinicor, F.; Bales, V. S.; Marks, J. S. Prevalence of Obesity, Diabetes, and Obesity-Related Health Risk Factors, 2001. *JAMA* **2003**, *289*, 76-79.

(2) Mokdad, A. H.; Bowman, B. A.; Ford, E. S.; Vinicor, F.; Marks, J. S.; Koplan, J. P. The Continuing Epidemics of Obesity and Diabetes in the United States. *JAMA* **2001**, *286*, 1195-1200.

(3) Mokdad, A. H.; Serdula, M. K.; Dietz, W. H.; Bowman, B. A.; Marks, J. S.; Koplan, J. P. The Spread of the Obesity Epidemic in the United States, 1991-1998. *JAMA* **1999**, *282*, 1519-1522.

(4) Mokdad, A. H.; Serdula, M. K.; Dietz, W. H.; Bowman, B. A.; Marks, J. S.; Koplan, J. P. The Continuing Epidemic of Obesity in the United States. *JAMA* **2000**, *284*, 1650-1651.

(5) Flegal, K. M.; Carroll, M. D.; Ogden, C. L.; Johnson, C. L. Prevalence and Trends in Obesity among Us Adults, 1999-2000. *JAMA* **2002**, *288*, 1723-1727.

(6) U. S. Department of Health and Human Services, Clinical Guidelines on the Identification, Evaluation, and Treatment of Overweight and Obesity in Adults, **1998**, 262, NIH Publication No. 98-4083

(7) U.S. Department of Health and Human Services, Office of the Surgeon General, The Surgeon General's Call to Action to Prevent and Decrease Overweight and Obesity, U.S. Government Printing Office: Washington D.C., **2001**.

(8) Ogden, C. L.; Flegal, K. M.; Carroll, M. D.; Johnson, C. L. Prevalence and Trends in Overweight among Us Children and Adolescents, 1999-2000. *JAMA* **2002**, *288*, 1728-1732.

(9) Mokdad, A. H.; Ford, E. S.; Bowman, B. A.; Nelson, D. E.; Engelgau, M. M.; Vinicor, F.; Marks, J. S. The Continuing Increase of Diabetes in the U.S. *Diabetes Care* **2001**, *24*, 412.

(10) Ford, E. S.; Giles, W. H.; Dietz, W. H. Prevalence of the Metabolic Syndrome among Us Adults: Findings from the Third National Health and Nutrition Examination Survey. *JAMA* **2002**, *287*, 356-359.

(11) Wolf, A. M.; Colditz, G. A. Current Estimates of the Economic Cost of Obesity in the United States. *Obes Res* **1998**, *6*, 97-106.

(12) Wolf, A. M. What Is the Economic Case for Treating Obesity? *Obes Res* **1998**, *6 Suppl 1*, 2S-7S.

(13) Schwartz, M. W.; Woods, S. C.; Seeley, R. J.; Barsh, G. S.; Baskin, D. G.; Leibel, R. L. Is the Energy Homeostasis System Inherently Biased toward Weight Gain? *Diabetes* **2003**, *52*, 232-238.

(14) Cummings, D. E.; Schwartz, M. W. Genetics and Pathophysiology of Human Obesity. *Annu Rev Med* **2003**, *54*, 453-471.

(15) Schwartz, M. W.; Morton, G. J. Obesity: Keeping Hunger at Bay. *Nature* **2002**, *418*, 595-597.

(16) Barsh, G. S.; Schwartz, M. W. Genetic Approaches to Studying Energy Balance: Perception and Integration. *Nat Rev Genet* **2002**, *3*, 589-600.

(17) McMinn, J. E.; Baskin, D. G.; Schwartz, M. W. Neuroendocrine Mechanisms Regulating Food Intake and Body Weight. *Obes Rev* **2000**, *1*, 37-46.

(18) Blevins, J. E.; Schwartz, M. W.; Baskin, D. G. Peptide Signals Regulating Food Intake and Energy Homeostasis. *Can J Physiol Pharmacol* **2002**, *80*, 396-406.

(19) Schwartz, M. W. Neuronal Pathways Regulating Food Intake and Body Adiposity. *Ann Endocrinol (Paris)* **2002**, *63*, 117-120.

(20) Morton, G. J.; Schwartz, M. W. The NPY/AGRP Neuron and Energy Homeostasis. *Int J Obes Relat Metab Disord* **2001**, *25 Suppl 5*, S56-62.

(21) Baskin, D. G.; Blevins, J. E.; Schwartz, M. W. How the Brain Regulates Food Intake and Body Weight: The Role of Leptin. *J Pediatr Endocrinol Metab* **2001**, *14 Suppl 6*, 1417-1429

(22) The Melanocortin Receptors; Cone, R.D., Ed., The Humana Press Inc.: New Jersey, **2000**.

(23) MacNeil, D. J.; Howard, A. D.; Guan, X. M.; Fong, T. M.; Nargund, R. P.; Bednarek, M. A.; Goulet, M. T.; Weinberg, D. H.; Strack, A. M.; Marsh, D. J.; Chen, H. Y.; Shen, C. P.; Chen, A. R. S.; Rosenblum, C. I.; MacNeil, T.; Tota, M.; MacIntyre, E. D.; Van der Ploeg, L. H. T. The Role of Melanocortins in Body Weight Regulation: Opportunities for the Treatment of Obesity. *Eur J Pharmacol* **2002**, *440*, 141-157.

(24) Muller, G. Towards 3D Structures of G Protein-Coupled Receptors: A Multidisciplinary Approach. *Curr Med Chem* **2000**, *7*, 861-888.

(25) Palczewski, K.; Kumasaka, T.; Hori, T.; Behnke, C. A.; Motoshima, H.; Fox, B. A.; Le Trong, I.; Teller, D. C.; Okada, T.; Stenkamp, R. E.; Yamamoto, M.; Miyano, M. Crystal Structure of Rhodopsin: A G Protein-Coupled Receptor. *Science* **2000**, *289*, 739-745.

(26) Mountjoy, K. G.; Robbins, L. S.; Mortrud, M. T.; Cone, R. D. The Cloning of a Family of Genes That Encode the Melanocortin Receptors. *Science* **1992**, *257*, 1248-1251.

(27) Chhajlani, V.; Wikberg, J. E. S. Molecular-Cloning and Expression of the Human Melanocyte Stimulating Hormone Receptor Cdna. *FEBS Lett* **1992**, *309*, 417-420.

(28) Chhajlani, V.; Muceniece, R.; Wikberg, J. E. S. Molecular-Cloning of a Novel Human Melanocortin Receptor. *Biochem Biophys Res Commun* **1993**, *195*, 866-873.

(29) Gantz, I.; Miwa, H.; Konda, Y.; Shimoto, Y.; Tashiro, T.; Watson, S. J.; Delvalle, J.; Yamada, T. Molecular-Cloning, Expression, and Gene Localization of a 4th Melanocortin Receptor. *J Biol Chem* **1993**, *268*, 15174-15179.

(30) Gantz, I.; Tashiro, T.; Barcroft, C.; Konda, Y.; Shimoto, Y.; Miwa, H.; Glover, T.; Munzert, G.; Yamada, T. Localization of the Genes Encoding the Melanocortin-2 (Adrenocorticotropic Hormone) and Melanocortin-3 Receptors to Chromosomes 18P11.2 and 20Q13.2-Q13.3 by Fluorescence *in situ* Hybridization. *Genomics* **1993**, *18*, 166-167.

(31) Gantz, I.; Konda, Y.; Tashiro, T.; Shimoto, Y.; Miwa, H.; Munzert, G.; Watson, S. J.; Delvalle, J.; Yamada, T. Molecular-Cloning of a Novel Melanocortin Receptor. *J Biol Chem* **1993**, *268*, 8246-8250.

(32) Roselliirehfuss, L.; Mountjoy, K. G.; Robbins, L. S.; Mortrud, M. T.; Low, M. J.; Tatro, J. B.; Entwistle, M. L.; Simerly, R. B.; Cone, R. D. Identification of a Receptor for Gamma-Melanotropin and Other Proopiomelanocortin Peptides in the Hypothalamus and Limbic System. *Proc Natl Acad Sci U S A* **1993**, *90*, 8856-8860.

(33) Labbe, O.; Desarnaud, F.; Eggerickx, D.; Vassart, G.; Parmentier, M. Molecular-Cloning of a Mouse Melanocortin-5 Receptor Gene Widely Expressed in Peripheral-Tissues. *Biochemistry* **1994**, *33*, 4543-4549.

(34) Ringholm, A.; Fredriksson, R.; Poliakova, N.; Yan, Y. L.; Postlethwait, J. H.; Larhammar, D.; Schioth, H. B. One Melanocortin 4 and Two Melanocortin 5 Receptors from Zebrafish Show Remarkable Conservation in Structure and Pharmacology. *J Neurochem* **2002**, *82*, 6-18.

(35) Hruby, V. J.; Krstenansky, J. L.; Cody, W. L. Recent Progress in the Rational Design of Peptide-Hormones and Neurotransmitters. *Ann Rep in Med Chem* **1984**, *19*, 303-312.

(36) Tsatmali, M.; Ancans, J.; Thody, A. J. Melanocyte Function and Its Control by Melanocortin Peptides. *J Histochem Cytochem* **2002**, *50*, 125-133.

(37) Stockfleth, E.; Sterry, W. New Treatment Modalities for Basal Cell Carcinoma. *Recent Results Cancer Res* **2002**, *160*, 259-268.

(38) Stander, S.; Bohm, M.; Brzoska, T.; Zimmer, K. P.; Luger, T.; Metze, D. Expression of Melanocortin-1 Receptor in Normal, Malformed and Neoplastic Skin Glands and Hair Follicles. *Exp Dermatol* **2002**, *11*, 42-51.

(39) Ha, T.; Rees, J. L. Melanocortin 1 Receptor: What's Red Got to Do with It? *J Am Acad Dermatol* **2001**, *45*, 961-964

(40) Abdel-Malek, Z. A. Melanocortin Receptors: Their Functions and Regulation by Physiological Agonists and Antagonists. *Cell Mol Life Sci* **2001**, *58*, 434-441.

(41) Luger, T. A.; Brzoska, T.; Scholzen, T. E.; Kalden, D. H.; Sunderkotter, C.; Armstrong, C.; Ansel, J. The Role of Alpha-MSH as a Modulator of Cutaneous Inflammation. *Ann N Y Acad Sci* **2000**, *917*, 232-238.

(42) Ichiyama, T.; Sato, S.; Okada, K.; Catania, A.; Lipton, J. M. The Neuroimmunomodulatory Peptide Alpha-MSH. *Ann N Y Acad Sci* **2000**, *917*, 221-226.

(43) Bohm, M.; Luger, T. A. The Role of Melanocortins in Skin Homeostasis. *Horm Res* **2000**, *54*, 287-293.

(44) Scott, M. C.; Wakamatsu, K.; Ito, S.; Kadekaro, A. L.; Kobayashi, N.; Groden, J.; Kavanagh, R.; Takakuwa, T.; Virador, V.; Hearing, V. J.; Abdel-Malek, Z. A. Human Melanocortin 1 Receptor Variants, Receptor Function and Melanocyte Response to UV Radiation. *J Cell Sci* **2002**, *115*, 2349-2355.

(45) Hassoun, H. T.; Zou, L.; Moore, F. A.; Kozar, R. A.; Weisbrodt, N. W.; Kone, B. C. Alpha-Melanocyte-Stimulating Hormone Protects against Mesenteric Ischemia-Reperfusion Injury. *Am J Physiol Gastrointest Liver Physiol* **2002**, *282*, G1059-1068.

(46) Gibbs, P.; Brady, B. M.; Robinson, W. A. The Genes and Genetics of Malignant Melanoma. *J Cutan Med Surg* **2002**, *6*, 229-235.

(47) Schaffer, J. V.; Bolognia, J. L. The Melanocortin-1 Receptor: Red Hair and Beyond. *Arch Dermatol* **2001**, *137*, 1477-1485.

(48) Schioth, H. B. The Physiological Role of Melanocortin Receptors. *Vitam Horm* **2001**, *63*, 195-232.

(49) Bohm, M.; Schiller, M.; Stander, S.; Seltmann, H.; Li, Z.; Brzoska, T.; Metze, D.; Schioth, H. B.; Skottner, A.; Seiffert, K.; Zouboulis, C. C.; Luger, T. A. Evidence for Expression of Melanocortin-1 Receptor in Human Sebocytes in vitro and in situ. *J Invest Dermatol* **2002**, *118*, 533-539.

(50) Herpin, T. F.; Yu, G.; Carlson, K. E.; Morton, G. C.; Wu, X.; Kang, L.; Tuerdi, H.; Khanna, A.; Tokarski, J. S.; Lawrence, R. M.; Macor, J. E. Discovery of Tyrosine-Based Potent and Selective Melanocortin-1 Receptor Small-Molecule Agonists with Anti-Inflammatory Properties. *J Med Chem* **2003**, *46*, 1123-1126.

(51) Hruby, V. J.; Han, G. The Molecular Pharmacology of Alpha-Melanocyte Stimulating Hormone. in *The Melanocortin Receptors*; Cone, R.D., Ed., The Humana Press Inc.: Totowa:New Jersey, 2000; 239-261.

(52) Halkerston, I. D. Cyclic Amp and Adrenocortical Function. *Adv Cyclic Nucleotide Res* **1975**, *6*, 99-136.

(53) Boston, B. A.; Cone, R. D. Characterization of Melanocortin Receptor Subtype Expression in Murine Adipose Tissues and in the 3T3-L1 Cell Line. *Endocrinology* **1996**, *137*, 2043-2050.

(54) Grunfeld, C.; Hagman, J.; Sabin, E. A.; Buckley, D. I.; Jones, D. S.; Ramachandran, J. Characterization of Adrenocorticotropin Receptors That Appear When 3T3- L1 Cells Differentiate into Adipocytes. *Endocrinology* **1985**, *116*, 113-117.

(55) Slominski, A.; Ermak, G.; Mihm, M. Acth Receptor, CYP11A1, CYP17 and CYP21A2 Genes Are Expressed in Skin. *J Clin Endocrinol Metab* **1996**, *81*, 2746-2749.

(56) Low, M. J.; Simerly, R. B.; R.D., C. Receptors for the Melanocortin Peptides in the Central Nervous System. *Curr Opin Endocrinol Diabetes* **1994**, *1*, 1068-1097.

(57) Daniels, D.; Patten, C. S.; Roth, J. D.; Yee, D. K.; Fluharty, S. J. Melanocortin Receptor Signaling through Mitogen-Activated Protein Kinase in vitro and in Rat Hypothalamus. *Brain Res* **2003**, *986*, 1-11.

(58) Chen, A. S.; Marsh, D. J.; Trumbauer, M. E.; Frazier, E. G.; Guan, X. M.; Yu, H.; Rosenblum, C. I.; Vongs, A.; Feng, Y.; Cao, L. H.; Metzger, J. M.; Strack, A. M.; Camacho, R. E.; Mellin, T. N.; Nunes, C. N.; Min, W.; Fisher, J.; Gopal-Truter, S.; MacIntyre, D. E.; Chen, H. Y.; Van der Ploeg, L. H. T. Inactivation of the Mouse Melanocortin-3 Receptor Results in Increased Fat Mass and Reduced Lean Body Mass. *Nature Genet* **2000**, *26*, 97-102.

(59) Butler, A. A.; Kesterson, R. A.; Khong, K.; Cullen, M. J.; Pelleymounter, M. A.; Dekoning, J.; Baetscher, M.; Cone, R. D. A Unique Metabolic Syndrome Causes Obesity in the Melanocortin- 3 Receptor-Deficient Mouse. *Endocrinology* **2000**, *141*, 3518-3521.

(60) Mountjoy, K. G.; Mortrud, M. T.; Low, M. J.; Simerly, R. B.; Cone, R. D. Localization of the Melanocortin-4 Receptor (MC4-R) in Neuroendocrine and Autonomic Control-Circuits in the Brain. *Mol Endocrinol* **1994**, *8*, 1298-1308.

(61) Gantz, I.; Konda, Y.; Tashiro, T.; Shimoto, Y.; Munzert, G.; Miwa, H.; Delvalle, J.; Yamada, T. Molecular-Cloning and Expression of a Novel Melanocortin Receptor Present in the Brain and Gut. *Gastroenterology* **1993**, *104*, A826-A826.

(62) Van der Ploeg, L. H.; Martin, W. J.; Howard, A. D.; Nargund, R. P.; Austin, C. P.; Guan, X.; Drisko, J.; Cashen, D.; Sebhat, I.; Patchett, A. A.; Figueroa, D. J.; DiLella, A. G.; Connolly, B. M.; Weinberg, D. H.; Tan, C. P.; Palyha, O. C.; Pong, S. S.; MacNeil, T.; Rosenblum, C.; Vongs, A.; Tang, R.; Yu, H.; Sailer, A. W.; Fong, T. M.; Huang, C.; Tota, M. R.; Chang, R. S.; Stearns, R.; Tamvakopoulos, C.; Christ, G.; Drazen, D. L.; Spar, B. D.; Nelson, R. J.; MacIntyre, D. E. A Role for the Melanocortin 4 Receptor in Sexual Function. *Proc Natl Acad Sci U S A* **2002**, *99*, 11381-11386.

(63) Huszar, D.; Lynch, C. A.; FairchildHuntress, V.; Dunmore, J. H.; Fang, Q.; Berkemeier, L. R.; Gu, W.; Kesterson, R. A.; Boston, B. A.; Cone, R. D.; Smith, F. J.; Campfield, L. A.; Burn, P.; Lee, F. Targeted Disruption of the Melanocortin-4 Receptor Results in Obesity in Mice. *Cell* **1997**, *88*, 131-141.

(64) Krude, H.; Biebermann, H.; Luck, W.; Horn, R.; Brabant, G.; Gruters, A. Severe Early-Onset Obesity, Adrenal Insufficiency and Red Hair Pigmentation Caused by Pomc Mutations in Humans. *Nature Genet* **1998**, *19*, 155-157.

(65) Yeo, G. S. H.; Farooqi, I. S.; Aminian, S.; Halsall, D. J.; Stanhope, R. C.; O'Rahilly, S. A Frameshift Mutation in MC4R Associated with Dominantly Inherited Human Obesity. *Nature Genet* **1998**, *20*, 111-112.

(66) Hinney, A.; Remschmidt, H.; Hebebrand, J. Candidate Gene Polymorphisms in Eating Disorders. *Eur J Pharmacol* **2000**, *410*, 147-159.

(67) Vaisse, C.; Clement, K.; Durand, E.; Hercberg, S.; Guy-Grand, B.; Froguel, P. Melanocortin-4 Receptor Mutations Are a Frequent and Heterogeneous Cause of Morbid Obesity. *J Clin Invest* **2000**, *106*, 253-262.

(68) Lubrano-Berthelier, C.; Clement, K.; Le Stunff, C.; Dubern, B.; Froguel, P.; Bougneres, P.; Vaisse, C. Functional Characterization of Obesity Associated MC4R Mutations. *Obes Res* **2001**, *9*, 53S-53S.

(69) Hoogduijn, M. J.; McGurk, S.; Smit, N. P.; Nibbering, P. H.; Ancans, J.; van der Laarse, A.; Thody, A. J. Ligand-Dependent Activation of the Melanocortin 5 Receptor: Camp Production and Ryanodine Receptor-Dependent Elevations of [Ca(2+)](I). *Biochem Biophys Res Commun* **2002**, *290*, 844-850.

(70) Chhajlani, V. Distribution of Cdna for Melanocortin Receptor Subtypes in Human Tissues. *Biochem Mol Biol Int* **1996**, *38*, 73-80.

(71) Chen, W. B.; Kelly, M. A.; OpitzAraya, X.; Thomas, R. E.; Low, M. J.; Cone, R. D. Exocrine Gland Dysfunction in Mc5-R-Deficient Mice: Evidence for Coordinated Regulation of Exocrine Gland Function by Melanocortin Peptides. *Cell* **1997**, *91*, 789-798.

(72) van der Kraan, M.; Adan, R. A. H.; Entwistle, M. L.; Gispen, W. H.; Burbach, J. P. H.; Tatro, J. B. Expression of Melanocortin-5 Receptor in Secretory Epithelia Supports a Functional Role in Exocrine and Endocrine Glands. *Endocrinology* **1998**, *139*, 2348-2355.

(73) Adan, R. A. H.; Gispen, W. H. Melanocortins and the Brain: From Effects Via Receptors to Drug Targets. *Eur J Pharmacol* **2000**, *405*, 13-24.

(74) Vergoni, A. V.; Bertolini, A. Role of Melanocortins in the Central Control of Feeding. *Eur J Pharmacol* **2000**, *405*, 25-32.

(75) Hruby, V. J.; Wilkes, B. C.; Hadley, M. E.; Alobeidi, F.; Sawyer, T. K.; Staples, D. J.; Devaux, A. E.; Dym, O.; Castrucci, A. M. D.; Hintz, M. F.; Riehm, J. P.; Rao, K. R. Alpha-Melanotropin - the Minimal Active Sequence in the Frog- Skin Bioassay. *J Med Chem* **1987**, *30*, 2126-2130.

(76) Castrucci, A. M. L.; Hadley, M. E.; Sawyer, T. K.; Wilkes, B. C.; Alobeidi, F.; Staples, D. J.; Devaux, A. E.; Dym, O.; Hintz, M. F.; Riehm, J. P.; Rao, K. R.; Hruby, V. J. Alpha-Melanotropin - the Minimal Active Sequence in the Lizard Skin Bioassay. *Gen Comp Endocrinol* **1989**, *73*, 157-163.

(77) Haskell-Luevano, C.; Sawyer, T. K.; Hendrata, S.; North, C.; Panahinia, L.; Stum, M.; Staples, D. J.; Castrucci, A. M. D.; Hadley, M. E.; Hruby, V. J. Truncation Studies of Alpha-Melanotropin Peptides Identify Tripeptide Analogues Exhibiting Prolonged Agonist Bioactivity. *Peptides* **1996**, *17*, 995-1002.

(78) Haskell-Luevano, C.; Holder, J. R.; Monck, E. K.; Bauzo, R. M. Characterization of Melanocortin Ndp-Msh Agonist Peptide Fragments at the Mouse Central and Peripheral Melanocortin Receptors. *J Med Chem* **2001**, *44*, 2247-2252.

(79) Lu, D. S.; Willard, D.; Patel, I. R.; Kadwell, S.; Overton, L.; Kost, T.; Luther, M.; Chen, W. B.; Woychik, R. P.; Wilkison, W. O.; Cone, R. D. Agouti Protein Is an Antagonist of the Melanocyte-Stimulating- Hormone Receptor. *Nature* **1994**, *371*, 799-802.

(80) Willard, D. H.; Bodnar, W.; Harris, C.; Kiefer, L.; Nichols, J. S.; Blanchard, S.; Hoffman, C.; Moyer, M.; Burkhart, W.; Weiel, J.; Luther, M. A.; Wilkison, W. O.; Rocque, W. J. Agouti Structure and Function - Characterization of a Potent Alpha-Melanocyte Stimulating Hormone Receptor Antagonist. *Biochemistry* **1995**, *34*, 12341-12346.

(81) Fong, T. M.; Mao, C.; MacNeil, T.; Kalyani, R.; Smith, T.; Weinberg, D.; Tota, M. R.; VanderPloeg, L. H. T. ART (Protein Product of Agouti-Related Transcript) as an Antagonist of MC-3 and MC-4 Receptors. *Biochem Biophys Res Commun* **1997**, *237*, 629-631.

(82) Graham, M.; Shutter, J. R.; Sarmiento, U.; Sarosi, I.; Stark, K. L. Overexpression of AGRT Leads to Obesity in Transgenic Mice. *Nature Genet* **1997**, *17*, 273-274.

(83) Ollmann, M. M.; Wilson, B. D.; Yang, Y. K.; Kerns, J. A.; Chen, Y.; Gantz, I.; Barsh, G. S. Antagonism of Central Melanocortin Receptors in vitro and in vivo by Agouti-Related Protein. *Science* **1997**, *278*, 135-138.

(84) Shutter, J. R.; Graham, M.; Kinsey, A. C.; Scully, S.; Luthy, R.; Stark, K. L. Hypothalamic Expression of ART, a Novel Gene Related to Agouti, Is up-Regulated in Obese and Diabetic Mutant Mice. *Genes Dev* **1997**, *11*, 593-602.

(85) Yang, Y. K.; Ollmann, M. M.; Wilson, B. D.; Dickinson, C.; Yamada, T.; Barsh, G. S.; Gantz, I. Effects of Recombinant Agouti-Signaling Protein on Melanocortin Action. *Mol Endocrinol* **1997**, *11*, 274-280.

(86) Sawyer, T. K.; Sanfilippo, P. J.; Hruby, V. J.; Engel, M. H.; Heward, C. B.; Burnett, J. B.; Hadley, M. E. 4-Norleucine, 7-D-Phenylalanine-Alpha-Melanocyte-Stimulating Hormone—A Highly Potent Alpha-Melanotropin with Ultralong Biological Activity. *Proceedings of the National Academy of Sciences of the United States of America-Biological Sciences* **1980**, *77*, 5754-5758.

(87) Al-Obeidi, F.; Hruby, V. J.; Castrucci, A. M.; Hadley, M. E. Design of Potent Linear Alpha-Melanotropin 4-10 Analogues Modified in Positions 5 and 10. *J Med Chem* **1989**, *32*, 174-179.

(88) Hruby, V. J.; Lu, D.; Sharma, S. D.; Castrucci, A. L.; Kesterson, R. A.; Al-Obeidi, F. A.; Hadley, M. E.; Cone, R. D. Cyclic Lactam Alpha-Melanotropin Analogues of Ac-Nle4-Cyclo[Asp5, D- Phe7,Lys10] Alpha-Melanocyte-Stimulating Hormone-(4-10)-NH_2 with Bulky Aromatic Amino Acids at Position 7 Show High Antagonist Potency and Selectivity at Specific Melanocortin Receptors. *J Med Chem* **1995**, *38*, 3454-3461.

(89) Tatro, J. B. Receptor Biology of the Melanocortins, a Family of Neuroimmunomodulatory Peptides. *Neuroimmunomodulation* **1996**, *3*, 259-284.

(90) Fan, W.; Boston, B. A.; Kesterson, R. A.; Hruby, V. J.; Cone, R. D. Role of Melanocortinergic Neurons in Feeding and the Agouti Obesity Syndrome. *Nature* **1997**, *385*, 165-168.

(91) Hagan, M. M.; Rushing, P. A.; Pritchard, L. M.; Schwartz, M. W.; Strack, A. M.; Van Der Ploeg, L. H.; Woods, S. C.; Seeley, R. J. Long-Term Orexigenic Effects of AGRP-(83-132) Involve Mechanisms Other Than Melanocortin Receptor Blockade. *Am J Physiol Regul Integr Comp Physiol* **2000**, *279*, R47-52.

(92) Lu, X. Y.; Nicholson, J. R.; Akil, H.; Watson, S. J. Time Course of Short-Term and Long-Term Orexigenic Effects of Agouti- Related Protein (86-132). *Neuroreport* **2001**, *12*, 1281-1284.

(93) Merrifield, R. B. Solid Phase Peptide Synthesis .1. Synthesis of a Tetrapeptide. *J Am Chem Soc* **1963**, *85*, 2149-2154.

(94) Merrifield, R. B. Solid-Phase Peptide Synthesis .3. Improved Synthesis of Bradykinin. *Biochemistry* **1964**, *3*, 1385-1390.

(95) Merrifield, R. B. Solid Phase Peptide Synthesis .2. Synthesis of Bradykinin. *J Am Chem Soc* **1964**, *86*, 304-305.

(96) Merrifield, R. B. Solid Phase Peptide Synthesis .4. Synthesis of Methionyl-Lysyl-Bradykinin. *J Org Chem* **1964**, *29*, 3100-3102.

(97) Carpino, L. A.; Han, G. Y. 9-Fluorenylmethoxycarbonyl Function, a New Base-Sensitive Amino-Protecting Group. *J Am Chem Soc* **1970**, *92*, 5748-5749.

(98) Carpino, L. A.; Han, G. Y. 9-Fluorenylmethoxycarbonyl Amino-Protecting Group. *J Org Chem* **1972**, *37*, 3404-3405.

(99) *Solid-Phase Synthsis: A Practical Guide*Kates, S. A., Albericio, F., Eds.; Marcel Dekker: New York, 2000.

(100) Bates, H. S.; Jones, J. H.; Witty, M. J. Direct Observation of an Alkoxycarbonylamino Acid O-Acylisourea. *J Chem Soc-Chem Commun* **1980**, 773-774.

(101) Bates, H. S.; Jones, J. H.; Ramage, W. I.; Witty, M. Some Observations on the Activation of Alkoxycarbonylamino Acids by Diisopropylcarbodiimide. in *Peptides, Proceedings of the 16th European Peptide Symposium*; Brunfeldt, K., Ed., Scriptor: Copenhagen, 1981; pp 185-190.

(102) Beyermann, M.; Henklein, P.; Klose, A.; Sohr, R.; Bienert, M. Effect of Tertiary Amine on the Carbodiimide-Mediated Peptide-Synthesis. *Int J Pept Protein Res* **1991**, *37*, 252-256.

(103) Coste, J.; Campagne, J. M. Esterification of Carboxylic-Acids Using BOP or PyBOP. *Tetrahedron Lett* **1995**, *36*, 4253-4256.

(104) Bates, A. J.; Galpin, I. J.; Hallett, A.; Hudson, D.; Kenner, G. W.; Ramage, R.; Sheppard, R. C. New Reagent for Polypeptide-Synthesis - Mu-Oxo-Bis- Tris-(Dimethylamino)-Phosphonium -Bis-Tetrafluoroborate. *Helv Chim Acta* **1975**, *58*, 688-696.

(105) Castro, B.; Dormoy, J. R. Chlorotrisdimethylaminophosphonium Perchlorate - a New Reagent for Peptide Coupling. *Tetrahedron Lett* **1972**, 4747-&.

(106) Yamada, S.; Takeuchi, Y. New Method for Synthesis of Peptides Using Adducts of Phosphorus Compounds and Tetrahalomethanes. *Tetrahedron Lett* **1971**, 3595-&.

(107) Barstow, L. E.; Hruby, V. J. Simple Method for Synthesis of Amides. *J Org Chem* **1971**, *36*, 1305-&.

(108) Gawne, G.; Kenner, G. W.; Sheppard, R. C. Acyloxyphosphonium Salts as Acylating Agents, a New Synthesis of Peptides. *J Am Chem Soc* **1969**, *91*, 5669-&.

(109) Schnolzer, M.; Alewood, P.; Jones, A.; Alewood, D.; Kent, S. B. In Situ Neutralization in Boc-Chemistry Solid Phase Peptide Synthesis. Rapid, High Yield Assembly of Difficult Sequences. *Int J Pept Protein Res* **1992**, *40*, 180-193.

(110) Kaiser, E.; Colescot.Rl; Bossinge.Cd; Cook, P. I. Color Test for Detection of Free Terminal Amino Groups in Solid-Phase Synthesis of Peptides. *Anal Biochem* **1970**, *34*, 595-598.

(111) Sarin, V. K.; Kent, S. B.; Tam, J. P.; Merrifield, R. B. Quantitative Monitoring of Solid-Phase Peptide Synthesis by the Ninhydrin Reaction. *Anal Biochem* **1981**, *117*, 147-157.

(112) Christensen, T. Qualitative Test for Monitoring Coupling Completeness in Solid-Phase Peptide-Synthesis Using Chloranil. *Acta Chem Scand B -Organic Chemistry and Biochemistry* **1979**, *33*, 763-766.

(113) Wüthrich, K. *NMR of Proteins and Nucleic Acids,* John Wiley and Sons: New York, **1986**.

(114) Saunders, M.; Wishnia, A.; Kirkwood, J. G. The Nuclear Magnetic Resonance Spectrum of Ribonuclease. *J Am Chem Soc* **1957**, *79*, 3289-3290.

(115) Crews, P.; Rodríguez, J.; Jaspars, M. *Organic Structure Analysis,* Oxford University Press: New York, **1998**; 552.

(116) Bloch, F. Nuclear Induction. *Phys Rev* **1946**, *70*, 460-477.

(117) *Modern Techniques in Protein NMR,* Krishna, N. R., Berliner, L. J.Eds.; Kluwer Academic / Plenum Publishers: New York, 1999.

(118) Braunschweiler, L.; Ernst, R. R. Coherence Transfer by Isotropic Mixing - Application to Proton Correlation Spectroscopy. *J Magn Reson* **1983**, *53*, 521-528.

(119) Kumar, A.; Ernst, R. R.; Wuthrich, K. A Two-Dimensional Nuclear Overhauser Enhancement (2d Noe) Experiment for the Elucidation of Complete Proton-Proton Cross-Relaxation Networks in Biological Macromolecules. *Biochem Biophys Res Commun* **1980**, *95*, 1-6.

(120) Accelrys., www.accelrys.com.

(121) *Principles of Medicinal Chemistry*; 4th ed.;Foye, W. O., Lemke, T. L., Williams, D. A., Eds.; Williams and Wilkins: Media, **1995**.

(122) Sahm, U. G.; Olivier, G. W. J.; Branch, S. K.; Moss, S. H.; Pouton, C. W. Influence of Alpha-MSH Terminal Amino-Acids on Binding-Affinity and Biological-Activity in Melanoma-Cells. *Peptides* **1994**, *15*, 441-446.

(123) Sawyer, T. K.; Castrucci, A. M.; Staples, D. J.; Affholter, J. A.; De Vaux, A.; Hruby, V. J.; Hadley, M. E. Structure-Activity Relationships of [Nle4, D-Phe7]Alpha-Msh. Discovery of a Tripeptidyl Agonist Exhibiting Sustained Bioactivity. *Ann N Y Acad Sci* **1993**, *680*, 597-599.

(124) Haskell-Luevano, C.; Cone, R. D.; Monck, E. K.; Wan, Y. P. Structure Activity Studies of the Melanocortin-4 Receptor by *in Vitro* Mutagenesis: Identification of Agouti-Related Protein (AGRP), Melanocortin Agonist and Synthetic Peptide Antagonist Interaction Determinants. *Biochemistry* **2001**, *40*, 6164-6179.

(125) Haskell-Luevano, C.; Hendrata, S.; North, C.; Sawyer, T. K.; Hadley, M. E.; Hruby, V. J.; Dickinson, C.; Gantz, I. Discovery of Prototype Peptidomimetic Agonists at the Human Melanocortin Receptors MC1R and MC4R. *J MedChem* **1997**, *40*, 2133-2139.

(126) Peeters, T. L.; Macielag, M. J.; Depoortere, I.; Konteatis, Z. D.; Florance, J. R.; Lessor, R. A.; Galdes, A. D-Amino Acid and Alanine Scans of the Bioactive Portion of Porcine Motilin. *Peptides* **1992**, *13*, 1103-1107.

(127) Beck-Sickinger, A. G.; Gaida, W.; Schnorrenberg, G.; Lang, R.; Jung, G. Neuropeptide Y: Identification of the Binding Site. *Int J Pept Protein Res* **1990**, *36*, 522-530.

(128) Sahm, U. G.; Olivier, G. W. J.; Branch, S. K.; Moss, S. H.; Pouton, C. W. Synthesis and Biological Evaluation of Alpha-MSH Analogs Substituted with Alanine. *Peptides* **1994**, *15*, 1297-1302.

(129) Grieco, P.; Balse-Srinivasan, P.; Han, G.; Weinberg, D.; MacNeil, T.; Van der Ploeg, L. H. T.; Hruby, V. J. Synthesis and Biological Evaluation on hMC(3), hMC(4) and hMC(5) Receptors of Gamma-MSH Analogs Substituted with L-Alanine. *J Pept Res* **2002**, *59*, 203-210.

(130) Chen, L.; Cheung, A. W.-H.; Chu, X.-J.; Danho, W.; Swistok, J.; Yagaloff, K. A. *World Intellectual Property Organization* **2001**, *F.Hoffmann-La Roche AG*, 265.

(131) Haskell-Luevano, C.; Lim, S.; Yuan, W.; Cone, R. D.; Hruby, V. J. Structure Activity Studies of the Melanocortin Antagonist SHU9119 Modified at the 6, 7, 8, and 9 Positions. *Peptides* **2000**, *21*, 49-57.

(132) Al-Obeidi, F.; Castrucci, A. M. D.; Hadley, M. E.; Hruby, V. J. Potent and Prolonged Acting Cyclic Lactam Analogs of Alpha- Melanotropin - Design Based on Molecular Dynamics. *J Med Chem* **1989**, *32*, 2555-2561.

(133) Bednarek, M. A.; Macneil, T.; Kalyani, R. N.; Tang, R.; Van der Ploeg, L. H. T.; Weinberg, D. H. Analogs of MTII, Lactam Derivatives of Alpha-Melanotropin, Modified at the N-Terminus, and their Selectivity at Human Melanocortin Receptors 3, 4, and 5. *Biochem Biophys Res Commun* **1999**, *261*, 209-213.

(134) Grieco, P.; Han, G.; Hruby, V. J. New Dimensions in the Design of Potent and Receptor Selective Melanotropin Analogues. *Peptides for the New Millenium, Proceedings of the 16th American Peptide Symposium*; Fields, G. B., Tam, J.P., and Barany, G., Eds., Kluwer: The Netherlands, **2000**; pp 541-542.

(135) Kavarana, M. J.; Han, G.; Cai, M.; Trivedi, D.; Hruby, V. J. The Design and Evaluation of a Novel Selective and Potent Agonist of the Human Melanocortin Receptor 4. *Peptides:The Wave of Teh Future, Proceedings of the 2nd International/17th American Peptide Symposium*; Lebl, M. and Houghten, R. A., Eds., Kluwer Academic Publishers: The Netherlands, **2001**; pp 708-709.

(136) Kavarana, M. J.; Trivedi, D.; Cai, M.; Ying, J.; Hammer, M.; Cabello, C.; Grieco, P.; Han, G.; Hruby, V. J. Novel Cyclic Templates of Alpha-MSH Give Highly Selective and Potent Antagonists/Agonists for Human Melanocortin-3/4 Receptors. *J Med Chem* **2002**, *45*, 2644-2650.

(137) Bednarek, M. A.; MacNeil, T.; Tang, R.; Kalyani, R. N.; Van der Ploeg, L. H.; Weinberg, D. H. Potent and Selective Peptide Agonists of Alpha-Melanotropin Action at Human Melanocortin Receptor 4: Their Synthesis and Biological Evaluation in Vitro. *Biochem Biophys Res Commun* **2001**, *286*, 641-645.

(138) Danho, W.; Swistok, J.; Cheung, A.; Chu, X.-J.; Wang, Y.; Chen, L.; Bartkovitz, D.; Gore, V.; Qi, L.; Fry, D.; Greeley, D.; Sun, H.; Guenot, J.; Franco, L.; Kurylko, G.; Rumennik, L.; Yagaloff, K. Highly Selective Cyclic Peptides for Human Melanocortin-4 Receptor: Design, Synthesis, Bioactive Conformation, and Pharmacological Evaluation as an Anti-Obesity Agent. *Peptides: The Wave of the Future: Proceedings of the Second International and the Seventeenth American Peptide Symposium*; Lebl, M. and Houghten, R. A., Eds., Kluwer Academic Publishers: The Netherlands, **2001**; p 701-704.

(139) Bednarek, M. A.; Silva, M. V.; Arison, B.; MacNeil, T.; Kalyani, R. N.; Huang, R. R. C.; Weinberg, D. H. Structure-Function Studies on the Cyclic Peptide MTII, Lactam Derivative of Alpha-Melanotropin. *Peptides* **1999**, *20*, 401-409.

(140) Skuladottir, G. V.; Jonsson, L.; Skarphedinsson, J. O.; Mutulis, F.; Muceniece, R.; Raine, A.; Mutule, I.; Helgason, J.; Prusis, P.; Wikberg, J. E. S.; Schioth, H. B. Long Term Orexigenic Effect of a Novel Melanocortin 4 Receptor Selective Antagonist. *Br J Pharmacol* **1999**, *126*, 27-34.

(141) Yang, Y. K.; Fong, T. M.; Dickinson, C. J.; Mao, C.; Li, J. Y.; Tota, M. R.; Mosley, R.; Van Der Ploeg, L. H.; Gantz, I. Molecular Determinants of Ligand Binding to the Human Melanocortin-4 Receptor. *Biochemistry* **2000**, *39*, 14900-14911.

(142) Lu, D.; Väge, D. I.; Cone, R. D. A Ligand-Mimetic Model for Constitutive Activation of the Melanocortin-1 Receptor. *Mol Endocrinol* **1998**, *12*, 592-604.

(143) Bednarek, M. A.; MacNeil, T.; Kalyani, R. N.; Tang, R.; Van der Ploeg, L. H.; Weinberg, D. H. Analogs of Lactam Derivatives of Alpha-Melanotropin with Basic and Acidic Residues. *Biochem Biophys Res Commun* **2000**, *272*, 23-28.

(144) Sina, M.; Hinney, A.; Ziegler, A.; Neupert, T.; Mayer, H.; Siegfried, W.; Blum, W. F.; Remschmidt, H.; Hebebrand, J. Phenotypes in Three Pedigrees with Autosomal Dominant Obesity Caused by Haploinsufficiency Mutations in the Melanocortin-4 Receptor Gene. *Am J Hum Genet* **1999**, *65*, 1501-1507.

(145) Farooqi, I. S.; Yeo, G. S.; Keogh, J. M.; Aminian, S.; Jebb, S. A.; Butler, G.; Cheetham, T.; O'Rahilly, S. Dominant and Recessive Inheritance of Morbid Obesity Associated with Melanocortin 4 Receptor Deficiency. *J Clin Invest* **2000**, *106*, 271-279.

(146) Barsh, G. S.; Farooqi, I. S.; O'Rahilly, S. Genetics of Body-Weight Regulation. *Nature* **2000**, *404*, 644-651.

(147) Vaisse, C.; Clement, K.; Guy-Grand, B.; Froguel, P. A Frameshift Mutation in Human Mc4r Is Associated with a Dominant Form of Obesity. *Nat Genet* **1998**, *20*, 113-114.

(148) Mergen, M.; Mergen, H.; Ozata, M.; Oner, R.; Oner, C. A Novel Melanocortin 4 Receptor (MC4R) Gene Mutation Associated with Morbid Obesity. *J Clin Endocrinol Metab* **2001**, *86*, 3448.

(149) Gantz, I.; Shimoto, Y.; Konda, Y.; Miwa, H.; Dickinson, C. J.; Yamada, T. Molecular-Cloning, Expression, and Characterization of a 5th Melanocortin Receptor. *Biochem Biophys Res Commun* **1994**, *200*, 1214-1220.

(150) Cone, R. D.; Lu, D.; Koppula, S.; Vage, D. I.; Klungland, H.; Boston, B.; Chen, W.; Orth, D. N.; Pouton, C.; Kesterson, R. A. The Melanocortin Receptors: Agonists, Antagonists, and the Hormonal Control of Pigmentation. *Recent Prog Horm Res* **1996**, *51*, 287-317; discussion 318.

(151) Kazmierski, W. M.; Yamamura, H. I.; Hruby, V. J. Topographic Design of Peptide Neurotransmitters and Hormones on Stable Backbone Templates - Relation of Conformation and Dynamics to Bioactivity. *J Am Chem Soc* **1991**, *113*, 2275-2283.

(152) Kazmierski, W.; Hruby, V. J. A New Approach to Receptor Ligand Design - Synthesis and Conformation of a New Class of Potent and Highly Selective Mu-Opioid Antagonists Utilizing Tetrahydroisoquinoline Carboxylic-Acid. *Tetrahedron* **1988**, *44*, 697-710.

(153) Butler, A. A.; Cone, R. D. Knockout Models Resulting in the Development of Obesity. *Trends Genet* **2001**, *17*, S50-54.

(154) Butler, A. A.; Marks, D. L.; Fan, W.; Kuhn, C. M.; Bartolome, M.; Cone, R. D. Melanocortin-4 Receptor Is Required for Acute Homeostatic Responses to Increased Dietary Fat. *Nat Neurosci* **2001**, *4*, 605-611.

(155) Cowley, M. A.; Smart, J. L.; Rubinstein, M.; Cerdan, M. G.; Diano, S.; Horvath, T. L.; Cone, R. D.; Low, M. J. Leptin Activates Anorexigenic POMC Neurons through a Neural Network in the Arcuate Nucleus. *Nature* **2001**, *411*, 480-484.

(156) Kask, A.; Mutulis, F.; Muceniece, R.; Pahkla, R.; Mutule, I.; Wikberg, J. E.; Rago, L.; Schioth, H. B. Discovery of a Novel Superpotent and Selective Melanocortin-4 Receptor Antagonist (HS024): Evaluation in Vitro and in Vivo. *Endocrinology* **1998**, *139*, 5006-5014.

(157) Kask, A.; Pahkla, R.; Irs, A.; Rago, L.; Wikberg, J. E. S.; Schioth, H. B. Long-Term Administration of MC4 Receptor Antagonist HS014 Causes Hyperphagia and Obesity in Rats. *Neuroreport* **1999**, *10*, 707-711.

(158) Benoit, S. C.; Schwartz, M. W.; Lachey, J. L.; Hagan, M. M.; Rushing, P. A.; Blake, K. A.; Yagaloff, K. A.; Kurylko, G.; Franco, L.; Danhoo, W.; Seeley, R. J. A Novel Selective Melanocortin-4 Receptor Agonist Reduces Food Intake in Rats and Mice without Producing Aversive Consequences. *J Neurosci* **2000**, *20*, 3442-3448.

(159) Haskell-Luevano, C.; Sawyer, T. K.; Trumpp-Kallmeyer, S.; Bikker, J. A.; Humblet, C.; Gantz, I.; Hruby, V. J. Three-Dimensional Molecular Models of the hMC1 Melanocortin Receptor: Complexes with Melanotropin Peptide Agonists. *Drug Des Discov* **1996**, *14*, 197-211.

(160) Yang, Y.; Dickinson, C.; Haskell-Luevano, C.; Gantz, I. Molecular Basis for the Interaction of [Nle4,D-Phe7]Melanocyte Stimulating Hormone with the Human Melanocortin-1 Receptor. *J Biol Chem* **1997**, *272*, 23000-23010.

(161) Haskell-Luevano, C. In Vitro Mutagenesis Studies of Melanocortin Receptor Coupling and Ligand Binding. in *The Melanocortin Receptors*; Cone, R.D., Ed., The Humana Press Inc.: New Jersey, **2000**; pp 263-306.

(162) Bednarek, M. A.; MacNeil, T.; Kalyani, R. N.; Tang, R.; Van der Ploeg, L. H.; Weinberg, D. H. Selective, High Affinity Peptide Antagonists of Alpha-Melanotropin Action at Human Melanocortin Receptor 4: Their Synthesis and Biological Evaluation in Vitro. *J Med Chem* **2001**, *44*, 3665-3672.

(163) Mercer, J. G.; Moar, K. M.; Ross, A. W.; Hoggard, N.; Morgan, P. J. Photoperiod Regulates Arcuate Nucleus Pomc, AGRP, and Leptin Receptor mRNA in Siberian Hamster Hypothalamus. *Am J Physiol Regul Integr Comp Physiol* **2000**, *278*, R271-281.

(164) Hinney, A.; Schmidt, A.; Nottebom, K.; Heibult, O.; Becker, I.; Ziegler, A.; Gerber, G.; Sina, M.; Gorg, T.; Mayer, H.; Siegfried, W.; Fichter, M.; Remschmidt, H.; Hebebrand, J. Several Mutations in the Melanocortin-4 Receptor Gene Including a Nonsense and a Frameshift Mutation Associated with Dominantly Inherited Obesity in Humans. *J Clin Endocrinol Metab* **1999**, *84*, 1483-1486.

(165) Hruby, V. J. Design of Peptide Superagonists and Antagonists - Conformational and Dynamic Considerations. *Acs Symposium Series* **1984**, *251*, 9-27.

(166) *The Melanotropins: Chemistry, Physiology, and Mechanism of Action.* Eberle, A. N.,Ed. Karger: Basel, 1988.

(167) Haskell-Luevano, C.; Miwa, H.; Dickinson, C.; Hadley, M. E.; Hruby, V. J.; Yamada, T.; Gantz, I. Characterizations of the Unusual Dissociation Properties of Melanotropin Peptides from the Melanocortin Receptor, hMC1R. *J Med Chem* **1996**, *39*, 432-435.

(168) Robbins, L. S.; Nadeau, J. H.; Johnson, K. R.; Kelly, M. A.; Roselli-Rehfuss, L.; Baack, E.; Mountjoy, K. G.; Cone, R. D. Pigmentation Phenotypes of Variant Extension Locus Alleles Result from Point Mutations That Alter MSH Receptor Function. *Cell* **1993**, *72*, 827-834.

(169) Haskell-Luevano, C.; Rosenquist, A.; Souers, A.; Khong, K. C.; Ellman, J. A.; Cone, R. D. Compounds That Activate the Mouse Melanocortin-1 Receptor Identified by Screening a Small Molecule Library Based Upon the Beta-Turn. *J Med Chem* **1999**, *42*, 4380-4387.

(170) Haskell-Luevano, C.; Nikiforovich, G.; Sharma, S. D.; Yang, Y. K.; Dickinson, C.; Hruby, V. J.; Gantz, I. Biological and Conformational Examination of Stereochemical Modifications Using the Template Melanotropin Peptide, Ac-Nle-C[Asp-His- Phe-Arg-Trp-Ala-Lys]-NH_2, on Human Melanocortin Receptors. *J Med Chem* **1997**, *40*, 1738-1748.

(171) Yang, Y.; Chen, M.; Lai, Y.; Gantz, I.; Georgeson, K. E.; Harmon, C. M. Molecular Determinants of Human Melanocortin-4 Receptor Responsible for Antagonist SHU9119 Selective Activity. *J Biol Chem* **2002**, *277*, 20328-20335.

(172) Bondebjerg, J.; Xiang, Z.; Bauzo, R. M.; Haskell-Luevano, C.; Meldal, M. A Solid-Phase Approach to Mouse Melanocortin Receptor Agonists Derived from a Novel Thioether Cyclized Peptidomimetic Scaffold. *J Am Chem Soc* **2002**, *124*, 11046-11055.

(173) Sebhat, I. K.; Martin, W. J.; Ye, Z.; Barakat, K.; Mosley, R. T.; Johnston, D. B.; Bakshi, R.; Palucki, B.; Weinberg, D. H.; MacNeil, T.; Kalyani, R. N.; Tang, R.; Stearns, R. A.; Miller, R. R.; Tamvakopoulos, C.; Strack, A. M.; McGowan, E.; Cashen, D. E.; Drisko, J. E.; Hom, G. J.; Howard, A. D.; MacIntyre, D. E.; van der Ploeg, L. H.; Patchett, A. A.; Nargund, R. P. Design and Pharmacology of N-[(3R)-1,2,3,4-tetrahydroisoquinolinium- 3-yl-carbonyl]-(1R)-1-(4-chlorobenzyl)-2-[4-cyclohexyl-4-(1H-1,2,4-triazol- 1-yl-methyl)piperidin-1-yl]-2-oxoethylamine (1), a Potent, Selective, Melanocortin Subtype-4 Receptor Agonist. *J Med Chem* **2002**, *45*, 4589-4593.

(174) Martin, W. J.; McGowan, E.; Cashen, D. E.; Gantert, L. T.; Drisko, J. E.; Hom, G. J.; Nargund, R.; Sebhat, I.; Howard, A. D.; Van der Ploeg, L. H.; MacIntyre, D. E. Activation of Melanocortin MC(4) Receptors Increases Erectile Activity in Rats Ex Copula. *Eur J Pharmacol* **2002**, *454*, 71-79.

(175) Haskell-Luevano, C.; Toth, K.; Boteju, L.; Job, C.; Castrucci, A. M.; Hadley, M. E.; Hruby, V. J. Beta-Methylation of the Phe7 and Trp9 Melanotropin Side Chain Pharmacophores Affects Ligand-Receptor Interactions and Prolonged Biological Activity. *J Med Chem* **1997**, *40*, 2740-2749.

(176) Haskell-Luevano, C.; Boteju, L. W.; Miwa, H.; Dickinson, C.; Gantz, I.; Yamada, T.; Hadley, M. E.; Hruby, V. J. Topographical Modification of Melanotropin Peptide Analogues with Beta-Methyltryptophan Isomers at Position 9 Leads to Differential Potencies and Prolonged Biological Activities. *J Med Chem* **1995**, *38*, 4720-4729.

(177) Hruby, V. J.; Li, G.; Haskell-Luevano, C.; Shenderovich, M. Design of Peptides, Proteins, and Peptidomimetics in Chi Space. *Biopolymers* **1997**, *43*, 219-266.

(178) Grieco, P.; Balse, P. M.; Weinberg, D.; MacNeil, T.; Hruby, V. J. D-Amino Acid Scan of Gamma-Melanocyte-Stimulating Hormone: Importance of Trp(8) on Human MC3 Receptor Selectivity. *J Med Chem* **2000**, *43*, 4998-5002.

(179) Grieco, P.; Han, G. X.; Weinberg, D.; MacNeil, T.; Van der Ploeg, L. H. T.; Hruby, V. J. Design and Synthesis of Highly Potent and Selective Melanotropin Analogues of SHU9119 Modified at Position 6. *Biochem Biophys Res Commun* **2002**, *292*, 1075-1080.

(180) Grieco, P.; Lavecchia, A.; Cai, M.; Trivedi, D.; Weinberg, D.; MacNeil, T.; Van der Ploeg, L. H.; Hruby, V. J. Structure-Activity Studies of the Melanocortin Peptides: Discovery of Potent and Selective Affinity Antagonists for the hMC3 and hMC4 Receptors. *J Med Chem* **2002**, *45*, 5287-5294.

(181) Hruby, V. J.; Mosberg, H. I. Conformational and Dynamic Considerations in Peptide Structure-Function Studies. *Peptides* **1982**, *3*, 329-336.

(182) Sawyer, T. K.; Hruby, V. J.; Darman, P. S.; Hadley, M. E. [Half-Cys4,Half-Cys10]-Alpha-Melanocyte-Stimulating Hormone - a Cyclic Alpha-Melanotropin Exhibiting Superagonist Biological- Activity. *Proc Natl Acad Sci USA* **1982**, *79*, 1751-1755.

(183) Hruby, V. J.; Sharma, S. D.; Toth, K.; Jaw, J. Y.; al-Obeidi, F.; Sawyer, T. K.; Hadley, M. E. Design, Synthesis, and Conformation of Superpotent and Prolonged Acting Melanotropins. *Ann N Y Acad Sci* **1993**, *680*, 51-63.

(184) Prabhu, N. V.; Perkyns, J. S.; Pettitt, B. M.; Hruby, V. J. Structure and Dynamics of Alpha-MSH Using Drism Integral Equation Theory and Stochastic Dynamics. *Biopolymers* **1999**, *50*, 255-272.

(185) Prabhu, N. V.; Perkyns, J. S.; Pettitt, B. M. Modeling of Alpha-MSH Conformations with Implicit Solvent. *J Pept Res* **1999**, *54*, 394-407.

(186) Sugg, E. E.; Castrucci, A. M.; Hadley, M. E.; van Binst, G.; Hruby, V. J. Cyclic Lactam Analogues of Ac-[Nle4]Alpha-Msh4-11-NH_2. *Biochemistry* **1988**, *27*, 8181-8188.

(187) Al-Obeidi, F.; O'Connor, S. D.; Job, C.; Hruby, V. J.; Pettitt, B. M. Nmr and Quenched Molecular Dynamics Studies of Superpotent Linear and Cyclic Alpha-Melanotropins. *J Pept Res* **1998**, *51*, 420-431.

(188) Lee, J. H.; Lim, S. K.; Huh, S. H.; Lee, D.; Lee, W. Solution Structures of the Melanocyte-Stimulating Hormones by Two-Dimensional NMR Spectroscopy and Dynamical Simulated-Annealing Calculations. *Eur J Biochem* **1998**, *257*, 31-40.

(189) Li, S. Z.; Lee, J. H.; Lee, W.; Yoon, C. J.; Baik, J. H.; Lim, S. K. Type I Beta-Turn Conformation Is Important for Biological Activity of the Melanocyte-Stimulating Hormone Analogues. *Eur J Biochem* **1999**, *265*, 430-440.

(190) Victoria Silva Elipe, M.; Mosley, R. T.; Bednarek, M. A.; Arison, B. H. 1h-Nmr Studies on a Potent and Selective Antagonist at Human Melanocortin Receptor 4 (hMC-4R). *Biopolymers* **2003**, *68*, 512-527.

(191) Prachand, M. S.; Dhingra, M. M.; Saran, A.; Coutinho, E.; Bodi, J.; Suli-Vargha, H.; Medzihardszky, K. Comparative Conformational Studies on Cyclic Hexapeptides Corresponding to Message Sequence His-Phe-Arg-Trp of Alpha-Melanotropin by NMR. *J Pept Res* **1998**, *51*, 251-265.

(192) Jayawickreme, C. K.; Quillan, J. M.; Graminski, G. F.; Lerner, M. R. Discovery and Structure-Function Analysis of Alpha-Melanocyte- Stimulating Hormone Antagonists. *J Biol Chem* **1994**, *269*, 29846-29854.

(193) Sawyer, T. K.; Staples, D. J.; Castrucci, A. M.; Hadley, M. E.; al-Obeidi, F. A.; Cody, W. L.; Hruby, V. J. Alpha-Melanocyte Stimulating Hormone Message and Inhibitory Sequences: Comparative Structure-Activity Studies on Melanocytes. *Peptides* **1990**, *11*, 351-357.

(194) Al-Obeidi, F.; Hruby, V. J.; Hadley, M. E.; Sawyer, T. K.; Castrucci, A. M. Design, Synthesis, and Biological Activities of a Potent and Selective Alpha-Melanotropin Antagonist. *Int J Pept Protein Res* **1990**, *35*, 228-234.

(195) Sawyer, T. K.; Staples, D. J.; de Lauro Castrucci, A. M.; Hadley, M. E. Discovery and Structure-Activity Relationships of Novel Alpha- Melanocyte-Stimulating Hormone Inhibitors. *Pept Res* **1989**, *2*, 140-146.

(196) Holder, J. R.; Bauzo, R. M.; Xiang, Z.; Haskell-Luevano, C. Structure-Activity Relationships of the Melanocortin Tetrapeptide Ac-His-DPhe-Arg-Trp-NH_2 at the Mouse Melanocortin Receptors: Part 2 Modification at the Phe Position. *J Med Chem* **2002**, *45*, 3073-3081.

(197) Schioth, H. B.; Muceniece, R.; Mutulis, F.; Prusis, P.; Lindeberg, G.; Sharma, S. D.; Hruby, V. J.; Wikberg, J. E. S. Selectivity of Cyclic [Dnal7] and [Dphe7] Substituted MSH Analogues for the Melanocortin Receptor Subtypes. *Peptides* **1997**, *18*, 1009-1013.

(198) Schioth, H. B.; Mutulis, F.; Muceniece, R.; Prusis, P.; Wikberg, J. E. Discovery of Novel Melanocortin4 Receptor Selective MSH Analogues. *Br J Pharmacol* **1998**, *124*, 75-82.

(199) Andersen, N. H.; Neidigh, J. W.; Harris, S. M.; Lee, G. M.; Liu, Z. H.; Tong, H. Extracting Information from the Temperature Gradients of Polypeptide Nh Chemical Shifts .1. The Importance of Conformational Averaging. *J Am Chem Soc* **1997**, *119*, 8547-8561.

(200) Ohnishi, M.; Urry, D. W. Temperature Dependence of Amide Proton Chemical Shifts - Secondary Structures of Gramicidin S and Valinomycin. *Biochem Biophys Res Commun* **1969**, *36*, 194-&.

(201) Troganis, A.; Gerothanassis, I. P.; Athanassiou, Z.; Mavromoustakos, T.; Hawkes, G. E.; Sakarellos, C. Thermodynamic Origin of Cis/Trans Isomers of a Proline-Containing Beta-Turn Model Dipeptide in Aqueous Solution: A Combined Variable Temperature H-1-NMR, Two-Dimensional H-1,H-1 Gradient Enhanced Nuclear Overhauser Effect Spectroscopy (NOESY), One-Dimensional Steady-State Intermolecular C-13,H-1 NOE, and Molecular Dynamics Study. *Biopolymers* **2000**, *53*, 72-83.

(202) Higashijima, T.; Tasumi, M.; Miyazawa, T. H-1 Nuclear Magnetic-Resonance Studies of Melanostatin - Dependence of Chemical-Shifts of NH Protons on Temperature and Concentration. *FEBS Lett* **1975**, *57*, 175-178.

(203) Fotsch, C.; Smith, D. M.; Adams, J. A.; Cheetham, J.; Croghan, M.; Doherty, E. M.; Hale, C.; Jarosinski, M. A.; Kelly, M. G.; Norman, M. H.; Tamayo, N. A.; Xi, N.; Baumgartner, J. W. Design of a New Peptidomimetic Agonist for the Melanocortin Receptors Based on the Solution Structure of the Peptide Ligand, Ac-Nle-Cyclo[Asp-Pro-Dphe-Arg-Trp-Lys]-NH_2. *Bioorg Med Chem Lett* **2003**, *13*, 2337-2340.

(204) Hruby, V. J. Design in Topographical Space of Peptide and Peptidomimetic Ligands That Affect Behavior. A Chemist's Glimpse at the Mind--Body Problem. *Acc Chem Res* **2001**, *34*, 389-397.

(205) Chen, W.; Shields, T. S.; Stork, P. J.; Cone, R. D. A Colorimetric Assay for Measuring Activation of Gs- and Gq-Coupled Signaling Pathways. *Anal Biochem* **1995**, *226*, 349-354.

(206) Schild, H. O. Pa, a New Scale for the Measurement of Drug Antagonism. *British Journal of Pharmacology and Chemotherapy* **1947**, *2*, 189-206.

(207) Johnson, B. A.; Blevins, R. A., NMR View-A Computer Program for the Visualization and Analysis of NMR Data. *J Biomol NMR* **1994**, *4*, 603-614.

(208) Holder, J. R.; Bauzo, R. M.; Xiang, Z.; Haskell-Luevano, C. Structure-Activity Relationships of the Melanocortin Tetrapeptide Ac-His-DPhe-Arg-Trp-NH_2 at the Mouse Melanocortin Receptors: Part 1 Modification at the His Position. *J Med Chem* **2002**, *45*, 2801-2810.

(209) Holder, J. R.; Bauzo, R. M.; Xiang, Z.; Haskell-Luevano, C. Structure-Activity Relationships of the Melanocortin Tetrapeptide Ac-His-DPhe-Arg-Trp-NH_2 at the Mouse Melanocortin Receptors: Part 4modification at the Trp Position. *J Med Chem* **2002**, *45*, 5736-5744.

(210) Holder, J. R.; Bauzo, R. M.; Xiang, Z.; Haskell-Luevano, C. Structure-Activity Relationships of the Melanocortin Tetrapeptide Ac-His-DPhe-Arg-Trp-NH_2 at the Mouse Melanocortin Receptors. Part 3: Modifications at the Arg Position. *Peptides* **2003**, *24*, 73-82.

(211) Holder, J. R.; Marques, F. F.; Bauzo, R. M.; Xiang, Z.; Haskell-Luevano, C. Characterization of Aliphatic, Cyclic, and Aromatic N-Terminally "Capped" His-DPhe-Arg-Trp-NH_2 Tetrapeptides at the Melanocortin Receptors. *Eur J Pharmacol* **2003**, *462*, 41-52.

BIOGRAPHICAL SKETCH

Jerry Ryan Holder was born on June 8, 1972, in Gainesville, Florida, to Jerry Don Holder and Patricia Ann Rogers (formally Holder). He spent his childhood years in the rural communities of Newberry and Trenton, Florida, frequently visiting the beautiful Suwannee River and surrounding natural springs. He graduated from Trenton High School in June 1990. At his parents' request, Ryan enrolled in classes at Santa Fe Community College in Gainesville the fall semester of 1991, only to quickly withdraw in only his third semester. Ryan spent the next two years working in the construction industry before realizing that a college education offered far more opportunity than manual labor. Ryan enrolled again at Santa Fe Community College in the fall of 1994, where he soon found an admiration of both biology and organic chemistry. Ryan received his AA degree in the spring of 1997 prior to enrolling at the University of Florida in the fall of 1997. Ryan graduated with honors from the University of Florida in August 1999 with a BS in microbiology and a minor in chemistry. He joined the Medicinal Chemistry Department of the University of Florida in August 1999 where he pursued his doctoral studies under the supervision of Dr. Carrie Haskell-Luevano. Ryan married Carmen Taylor, his girlfriend of six years, in March 2003. Future plans for the Holders involve relocating for Ryan to further advance his scientific career as a research scientist at Amgen in Thousand Oaks California, his wife Carmen to continue teaching elementary school once they are relocated to beautiful Thousand Oaks, and starting a family.

I certify that I have read this study and that in my opinion it conforms to acceptable standards of scholarly presentation and is fully adequate, in scope and quality, as a dissertation for the degree of Doctor of Philosophy.

Carrie Haskell-Luevano, Chair
Assistant Professor of Medicinal Chemistry

I certify that I have read this study and that in my opinion it conforms to acceptable standards of scholarly presentation and is fully adequate, in scope and quality, as a dissertation for the degree of Doctor of Philosophy.

Margaret O. James
Professor of Medicinal Chemistry

I certify that I have read this study and that in my opinion it conforms to acceptable standards of scholarly presentation and is fully adequate, in scope and quality, as a dissertation for the degree of Doctor of Philosophy.

Kenneth B. Sloan
Professor of Medicinal Chemistry

I certify that I have read this study and that in my opinion it conforms to acceptable standards of scholarly presentation and is fully adequate, in scope and quality, as a dissertation for the degree of Doctor of Philosophy.

Dong-Hai Wu
Assistant Professor of Medicinal Chemistry

I certify that I have read this study and that in my opinion it conforms to acceptable standards of scholarly presentation and is fully adequate, in scope and quality, as a dissertation for the degree of Doctor of Philosophy.

Arthur S. Edison,
Associate Professor of Biochemistry and
Molecular Biology

This dissertation was submitted to the Graduate Faculty of the College of Pharmacy and to the Graduate School and was accepted as partial fulfillment of the requirements for the degree of Doctor of Philosophy.

December 2003

Dean, College of Pharmacy

Dean, Graduate School